

ROADMAP FOR SCALING UP THERMOPHILIC CO₂ BIOREDUCTION TO ACETATE : SHEDDING LIGHT ON USING SURPLUS RENEWABLE ENERGY AND INDUSTRIAL OFF GASES

Laura Rovira Alsina

ADVERTIMENT. L'accés als continguts d'aquesta tesi doctoral i la seva utilització ha de respectar els drets de la persona autora. Pot ser utilitzada per a consulta o estudi personal, així com en activitats o materials d'investigació i docència en els termes establerts a l'art. 32 del Text Refós de la Llei de Propietat Intel·lectual (RDL 1/1996). Per altres utilitzacions es requereix l'autorització prèvia i expressa de la persona autora. En qualsevol cas, en la utilització dels seus continguts caldrà indicar de forma clara el nom i cognoms de la persona autora i el títol de la tesi doctoral. No s'autoritza la seva reproducció o altres formes d'explotació efectuades amb finalitats de lucre ni la seva comunicació pública des d'un lloc aliè al servei TDX. Tampoc s'autoritza la presentació del seu contingut en una finestra o marc aliè a TDX (framing). Aquesta reserva de drets afecta tant als continguts de la tesi com als seus resums i índexs.

ADVERTENCIA. El acceso a los contenidos de esta tesis doctoral y su utilización debe respetar los derechos de la persona autora. Puede ser utilizada para consulta o estudio personal, así como en actividades o materiales de investigación y docencia en los términos establecidos en el art. 32 del Texto Refundido de la Ley de Propiedad Intelectual (RDL 1/1996). Para otros usos se requiere la autorización previa y expresa de la persona autora. En cualquier caso, en la utilización de sus contenidos se deberá indicar de forma clara el nombre y apellidos de la persona autora y el título de la tesis doctoral. No se autoriza su reproducción u otras formas de explotación efectuadas con fines lucrativos ni su comunicación pública desde un sitio ajeno al servicio TDR. Tampoco se autoriza la presentación de su contenido en una ventana o marco ajeno a TDR (framing). Esta reserva de derechos afecta tanto al contenido de la tesis como a sus resúmenes e índices.

WARNING. Access to the contents of this doctoral thesis and its use must respect the rights of the author. It can be used for reference or private study, as well as research and learning activities or materials in the terms established by the 32nd article of the Spanish Consolidated Copyright Act (RDL 1/1996). Express and previous authorization of the author is required for any other uses. In any case, when using its content, full name of the author and title of the thesis must be clearly indicated. Reproduction or other forms of for profit use or public communication from outside TDX service is not allowed. Presentation of its content in a window or frame external to TDX (framing) is not authorized either. These rights affect both the content of the thesis and its abstracts and indexes.



DOCTORAL THESIS

**ROADMAP FOR SCALING UP THERMOPHILIC CO₂ BIOREDUCTION TO
ACETATE: SHEDDING LIGHT ON USING SURPLUS RENEWABLE
ENERGY AND INDUSTRIAL OFF-GASES**

LAURA ROVIRA-ALSINA

2022



DOCTORAL THESIS

**Roadmap for scaling up thermophilic CO₂ bioreduction
to acetate: shedding light on using surplus renewable
energy and industrial off-gases**

Laura Rovira-Alsina

2022

Doctoral programme in **Water Science and Technology**

Supervised by: Dra. Maria Dolors Balaguer Condom and Dr. Sebastià Puig Broch

Tutor: Dr. Sebastià Puig Broch

Presented to obtain the degree of PhD at the
University of Girona

Certificate of thesis direction



Dr. Maria Dolors Balaguer Condom and Dr. Sebastià Puig of the Laboratory of Chemical and Environmental Engineering (LQUIA) of the University of Girona,

WE DECLARE:

That the thesis titled "Roadmap for scaling up thermophilic CO₂ bioreduction to acetate: shedding light on using surplus renewable energy and industrial off-gases", presented by Laura Rovira-Alsina to obtain a doctoral degree, has been completed under my supervision and meets the requirements to opt for an International Doctorate.

For all intents and purposes, we hereby sign this document.

Les coses no canvien fins que algú les fa canviar.

Ritme bisó, fins a l'horitzó!

Agraïments

Com a Hippie, Penny i radical que se m'ha ben etiquetat, ara sí que em permeto aprofitar aquest espai per compartir sense cap filtre el que vull deixar anar, segurament de forma poc convencional. No posaré noms ni cares, m'agradaria que tothom qui ho llegeixi es senti identificat d'alguna manera amb aquestes paraules i que cadascú connecti amb els records que li transmeten.

Primer de tot, dono les gracies per la casualitat de les coses, pel fet de que m'hagin portat aquí, sense triar, sense forçar, com m'agrada dir, fluïnt. Suposo que si ens deixem portar acabem fent el que realment volem i si més no, puc dir que tinc la gran sort de valorar tantes coses, que sigui com sigui, les gaudeixo.

Agreixo també els moments viscuts, amb uns i altres, els gestos simples per demostrar-nos que hi som i ens ajudem, els detalls que ens alegren el dia (això em fa venir gana!), el voler saber de veritat com estem, i si podem millorar. Escric això per tots els matins productius en què ens proposàvem no deixar de mirar la pantalla durant una bona estona, i em quedava mòbils per evitar temptacions. Per les hores "perdudes" al laboratori que ens hem passat muntant reactors, ajuntant tubs que no encaixaven ni amb calçador, buscant solucions impossibles i enginyant alternatives; vida al teflón i que no falti silicona! Per les hores intempestives en què treballava en solitari, amb la música estrepitosament alta i la motivació necessària per estar contenta de ser-hi. Per les desmantellades que hem fet als tallers perquè fos un lloc més agradable, organitzat i funcional. Per qui venia i feia, perquè així ho creia. Per les birres que alegraven les tardes de divendres, pels dies que ens hem quedat sense aigua i per tots els licors estranys que ens han fet provar els de fora. Per trobar sempre un racó de pluja i perquè som els de la taula de càmping. Per les incomptables corregudes a les Gavarres i les escapades de desconexió que em permetien tornar amb les idees més clares. Pels moments d'alegria i de frustració a les reunions, al despatx i encara més al lab. Per poder fer la croqueta pel terra amb normalitat, per anar descalça o vestir de qualsevol manera sense que ningú em mirés gaire estrany. Per poder ser jo, per mostrar-me tal com sóc, per desenvolupar-me una mica més com a persona i per aprendre dels altres. Pels que semblen durs però no ho són tant i pels que no s'ho creuen, però arribaran lluny. Per tots els que han compartit un trosset de mi, aquí i quan vaig marxar un temps a treure el cap a terra estrangera. Pels que m'han acompanyat a trobar camins, muntanyes i sensació de pertànyer allà on fos. Per venir i marxar quan volia, per quedar-me quan no hi havia ningú.

També podria demanar perdó, perdó per sempre sortir tard a dinar, per fer pel meu compte sense preguntar, per no escoltar, pels sermons de reciclatge i estil de vida. Però en comptes d'això, prefereixo continuar donant les gràcies, gràcies per esperar-me, per donar-me la confiança i l'espai, per repetir-m'ho quan era necessari i agafar idees que per mi eren rellevants. Per toots els moments, pels que ja no recordo, pels que guardaré per sempre i pels que encara em queda viure abans no em podeu trobar. Per la gent de dins, la de fora, la que s'ha unit i la que no té res a veure. Per les idees, que no paren i a vegades no em deixen dormir. Per l'habilitat que tenim de raonar, les inquietuds que ens fan moure i per la bona sort de poder fer, de tenir capacitat, recursos i estar en el lloc adequat.

I finalment m'agradaria fer una petita reflexió, com no. Que tot el que fem tingui sentit, sobretot per nosaltres. Quan deixes de creure en el que fas, deixa de tenir valor i en conseqüència, utilitat. Demano que no ens perdem pel camí, que defensem les nostres idees, que lluitem pel que creiem i que ho fem de la millor manera possible. He de dir que en aquest món veig lluita, una lluita molt poderosa, però malauradament, en molts àmbits va dirigida a mantenir-se individualment a dalt, en lloc de permetre'ns a tots surar a la superfície. També crec en la força de les petites accions i de l'activisme casolà. Tots tenim un potencial brutal per avançar i ajudar a millorar, només cal saber enfocar aquesta potència a construir, en comptes de destruir.

A tots els que us sentiu amb ganes, perquè siguem on siguem i fem el que fem, continuem compartint. M'emportut una molt bona experiència, gràciis!

Pd. Ha sigut el 7b més difícil que he encadenat fins al moment, ha costat molts pegues i encara més saques, però com la sensació d'arribar a dalt, és indescriptible! Ara tinc ganes de volar.

Gaaaaaaaaaaaaaaaaaaaaaaaaaaaaas!

Acknowledgments

This thesis was financially supported by the Catalan Government (2018 FI-B 00347) in the European FSE program (CCI 2014ES05SFOP007) and the European Union's Horizon 2020 research and innovation program under the grant agreement no. 760431 (BioReCO2ver; <http://bioreco2ver.eu/>). LEQUIA has been recognised as consolidated Research group by the Catalan Government with code 2017-SGR-1552.

List of contents

List of peer reviewed publications presented as chapters of PhD thesis.....	i
List of abbreviations	ii
List of tables.....	v
List of figures	vi
Summary.....	vii
Resum.....	ix
Resumen.....	xi
1. Introduction	1
1.1. Background.....	1
1.2. Harvesting energy from renewable sources	3
1.3. Bio-electro interactive communication systems.....	4
1.3.1. Microbial electrosynthesis (MES).....	5
1.3.1.1. Electroactive microorganisms acting as catalysts	6
1.3.1.2. Niches of applications for MES	9
1.3.1.3. Production parameters influencing efficiency	10
1.3.1.4. Thermophilic MES.....	12
1.4. Scalability: main challenges and digitalisation	14
2. Research questions and objectives.....	18
3. Materials and methods	23
3.1. Chemicals and media.....	23
3.2. Inoculum source and growth conditions	23
3.3. Reactors set-up and operation	24
3.3.1. H-type reactors	24
3.3.2. Penicillin bottles fermenters.....	26
3.3.3. ECell reactors	27
3.3.4. Flat-plate reactor	30
3.4. Analytic methodologies	30
3.4.1. Photometric measurements	31
3.4.2. Physicochemical analyses	31
3.4.3. Gas-chromatography analysis for gas samples	31
3.4.4. Gas-chromatography analysis for liquid samples	31
3.5. Electrochemical analyses	32
3.5.1. Cyclic voltammetry (CV).....	32
3.5.2. Coulombic and carbon conversion efficiencies.....	32
3.6. Calculations.....	33
3.6.1. Production of gases	33
3.6.2. Production of organics in the liquid phase	34

3.6.3. Thermodynamics	34
3.7. Microbial community analyses	36
3.7.1. Microscopy observation techniques	36
3.7.2. DNA extraction and microbial analyses	36
3.7.3. Quantitative analysis through qPCR.....	36
4. Results.....	38
4.1. Thermophilic bio-electro CO ₂ recycling into organic compounds.....	39
4.1.1. Introduction	40
4.1.2. Materials and methods.....	41
4.1.3. Results and discussion	43
4.1.4. Conclusions.....	47
Supporting Information	49
4.2. Thermophilic bio-electro carbon dioxide recycling harnessing renewable energy surplus	51
4.2.1. Introduction	52
4.2.2. Materials and methods.....	53
4.2.3. Results and discussion	54
4.2.4. Conclusions.....	58
Supporting Information	60
4.3. Thermodynamic approach to foresee experimental CO ₂ reduction to organic compounds	63
4.3.1. Introduction	64
4.3.2. Materials and methods.....	65
4.3.3. Results and discussion	66
4.3.4. Conclusions.....	71
Supporting Information	73
4.4. Transition roadmap for thermophilic CO ₂ microbial electrosynthesis: from lab to pilot plant	77
4.4.1. Introduction	79
4.4.2. Materials and methods.....	80
4.4.3. Results and discussion	84
4.4.4. Conclusions.....	92
5. General discussion.....	99
5.1. Current state of the art of HA production from CO ₂	99
5.1.1. Acetate production relative to energy consumption.....	101
5.2. Perspectives for MES evolution to higher technology readiness levels (TRLs)	103
5.2.1. Moving towards a digital transformation	105
5.3. MES as a sustainable energy battery	106
5.3.1. Challenging options and prospects.....	108

6. Conclusions	112
6.1. Outlook	113
7. References	115

List of peer reviewed publications presented as chapters of PhD thesis

Rovira-Alsina, L., Perona-Vico, E., Bañeras, L., Colprim, J., Balaguer, M.D., Puig, S., 2020. Thermophilic bio-electro CO₂ recycling into organic compounds. *Green Chem.* 22, 2947–2955.
<https://doi.org/10.1039/d0gc00320d>

Rovira-Alsina, L., Balaguer, M.D., Puig, S., 2021. Thermophilic bio-electro carbon dioxide recycling harnessing renewable energy surplus. *Bioresour. Technol.* 321.
<https://doi.org/10.1016/j.biortech.2020.124423>

Rovira-Alsina, L., Romans-Casas, M., Balaguer, M.D., Puig, S., 2022. Thermodynamic approach to foresee experimental CO₂ reduction to organic compounds. *Bioresour. Technol.* 354.
<https://doi.org/10.1016/j.biortech.2022.127181>

Other publications

Batlle-Vilanova, P., **Rovira-Alsina, L.**, Puig, S., Balaguer, M.D., Icaran, P., Monsalvo, V.M., Rogalla, F., Colprim, J., 2019. Biogas upgrading, CO₂ valorisation and economic revaluation of bioelectrochemical systems through anodic chlorine production in the framework of wastewater treatment plants. *Sci. Total Environ.* 690.
<https://doi.org/10.1016/j.scitotenv.2019.06.361>

Osset-Álvarez, M., **Rovira-Alsina, L.**, Pous, N., Blasco-Gómez, R., Colprim, J., Balaguer, M.D., Puig, S., 2019. Niches for bioelectrochemical systems on the recovery of water, carbon and nitrogen in wastewater treatment plants. *Biomass and Bioenergy* 130.
<https://doi.org/10.1016/j.biombioe.2019.105380>

Dessi, P., **Rovira-Alsina, L.**, Sánchez, C., Dinesh, G.K., Tong, W., Chatterjee, P., Tedesco, M., Farràs, P., Hamelers, H.M.V., Puig, S., 2020. Microbial electrosynthesis: Towards sustainable biorefineries for production of green chemicals from CO₂ emissions. *Biotechnol. Adv.* 107675.
<https://doi.org/10.1016/j.biotechadv.2020.107675>

Velvizhi, G., Sarkar, O., **Rovira-Alsina, L.**, Puig, S., Mohan, S.V., 2022. Conversion of carbon dioxide to value added products through anaerobic fermentation and electro fermentation: A comparative approach. *Int. J. Hydrogen Energy.* <https://doi.org/10.1016/j.ijhydene.2021.12.205>

List of abbreviations

AD	Anaerobic digestion
AF	Anaerobic fermentation
BES	Bioelectrochemical system
C	Carbon
CA	Chronoamperometry
CCE	Carbon conversion efficiency
CCS	Carbon capture and storage
CCU	Carbon capture and utilisation
CE	Coulombic efficiency
CEM	Cation exchange membrane
CH ₄	Methane
CIET	Conductive interspecies electron transfer
CO	Carbon monoxide
CO ₂	Carbon dioxide
CV	Cyclic voltammetry
DCW	Dry cell weight
DET	Direct electron transfer
DIET	Direct interspecies electron transfer
E _{an}	Anode potential
EC	Electric conductivity
E _{cat}	Cathode potential
E _{cell}	Cell voltage
ECell	Electro-cell
EET	Extracellular electron transfer
EF	Electro fermentation
E' _o	Standard electrode potential
EWA	Electrode working area
F	Faraday constant

FP	Flat Plate
GA	Galvanostatic
GC	Gas chromatography
GHG	Greenhouse gas
H ⁺	Protons
H ₂	Hydrogen gas
HA	Acetic acid
HRT	Hydraulic retention time
HT	H-type
MW	Molecular weight
MEC	Microbial electrolysis cell
MES	Microbial electrosynthesis
MET	Mediated electron transfer
MFC	Microbial fuel cell
mMC	Milimolar of carbon
N ₂	Nitrogen gas
NCC	Net cathode compartment
O ₂	Oxygen gas
OCV	Open circuit voltage
OD	Optical density
P	Pressure
PCR	Polymerase chain reaction
PEM	Proton exchange membrane
PV	Photovoltaics
PVC	Polyvinyl chloride
Q	Production rate
qPCR	Quantitative polymerase chain reaction
QS	Quorum sensing
RE	Reference electrode
RQ	Research questions

SDG	Sustainable development goal
SEM	Scanning electron microscopy
SHE	Standard hydrogen electrode
T	Temperature
TRL	Technology readiness levels
VFA	Volatile fatty acid
WE	Working electrode
WWTP	Wastewater treatment plant
ΔG	Gibbs free energy variation

List of tables

Table 1. Advantages and disadvantages of pure, mixed, and genetically modified electrotroph cultures.....	7
Table 2. Advantages and disadvantages of working under mesophilic and thermophilic conditions and the main associated genera.....	13
Table 3. Reactor type, inoculum and operating conditions used in each study related to the corresponding results chapter.....	24
Table 4. Comparison of the state of the art of microbial electrosynthesis of acetate from CO ₂ using enriched mixed consortia. In many cases, concentration and production rates have been calculated according to the data provided by the authors.....	100

List of figures

Figure 1. Diagram of the industrial carbon dioxide storage vs. utilisation chain.....	3
Figure 2. Schematic representation of a potential strategy for CO ₂ reduction to bio-commodities through microbial electrosynthesis (MES).....	6
Figure 3. Derivatives and end uses of acetic acid. Data adapted from Cision (Software platform and marketing solutions).	10
Figure 4. Technology readiness levels (TRLs) described by the work programme of Horizon 2020.	14
Figure 5. Schematic representation of the steps to progressively fine-tune the operating parameters and optimise the bioproduction of acetic acid from CO ₂	18
Figure 6. Photograph (A) and schematic (B) representation of the assembly and operation of the H-types reactors.	25
Figure 7. Photograph (A) and schematic (B) representation of the assembly and operation of the serum bottles set-ups.	26
Figure 8. Photograph (A) and schematic (B) representation of the assembly and operation of the ECell reactor set-ups.....	27
Figure 9. Photograph (A) and schematic (B) representation of the ECell reactor operating circuit	28
Figure 10. Schematic diagram of the ECell reactor programmable commands.....	29
Figure 11. Photographs (A) and schematic (B) representation of the assembly and operation of the Flat-plate reactor set-up.....	30
Figure 12. Acetic acid production rate vs. energy consumption of microbial electrosynthesis studies from CO ₂ using different electrodes. The energy consumption <i>via</i> methanol carbonylation (3.5 kWh kg ⁻¹) and the theoretical production threshold of 4100 g m ⁻² d ⁻¹ were considered targets to be attained for MECs implementation.	102
Figure 13. Schematic proposal for the digitalisation of microbial acetate electrosynthesis from renewable energy surplus and CO ₂ . While electricity input is intermittent, acetate (HA) and CO ₂ are produced and consumed continuously at different rates, depending on the availability of H ₂ . H ₂ is produced when electricity is available and consumed when it is not, combining electrochemical and anaerobic fermentation processes.....	106
Figure 14. Summarising outline including the roadmap from the objectives set to the results achieved.	108
Figure 15. Options for solar-driven chemical processes	110

Summary

Carbon dioxide (CO₂) is largely emitted in the ignition of fossil fuels for transport, electricity generation or other industrial processes. CO₂ is an inorganic compound that exists naturally on Earth, but its concentration has increased exponentially since the industrial revolution, causing the acceleration of global warming. Bioelectrochemical systems (BES) and more specifically, the **microbial electrosynthesis** (MES) platform is one of the several technologies that have been proposed to capture and convert it. What gives added value to MES is the use of microorganisms to catalyse the reduction of CO₂ to target compounds, without the need for expensive and scarce materials. However, additional research is still needed for its commercialisation. In this sense, this PhD thesis addresses the challenges of scaling up thermophilic microbial electrosynthesis of **acetate** (HA) from CO₂, using a mixed microbial culture, renewable energy and industrial gas emissions.

Taking into account that the industrial sector emits CO₂ at high temperatures, all experiments were carried out under **thermophilic conditions** (50 °C), which enhanced the kinetics of the reactions as well as the selectivity of the final product. To address one of the main challenges of the technology linked to the electricity utilisation as the main operational cost, **renewable energy** use was considered, and operation was simulated with only the **surplus** without battery storage, resulting in intermittent power supply. This reduced energy consumption by a factor of three and resulted in the combination of bioelectrochemical and microbial fermentation processes, achieving continuous HA production (43 g m⁻² d⁻¹) and promising carbon conversion rates (2.2 kg CO₂ kg HA⁻¹). In terms of the intensification of the process, a developed **thermodynamic model** allowed to determine the most favourable operating conditions depending on the desired end product. Analysis of the results showed that under thermophilic conditions, the chain elongation of HA to longer carboxylates was not spontaneous, rendering its conversion in successive anaerobic fermentation steps under mesophilic conditions as the most viable option.

To bring the technology one step closer to field application, the systems were tested with **real industrial off-gases** containing impurities and a lower percentage of CO₂ (from 100 to 14 %). The microbial community proved to be robust enough to maintain similar productivities compared to the operation with synthetic gas (2.5 % of difference) and to adapt to the new conditions, developing synergies to mitigate the impacts derived from the use of real gas with the presence of 12 % of oxygen. Finally, the **first pilot plant** for microbial electrosynthesis from CO₂ with digital **monitoring and control** of the key operational variables was designed, built and launched. This allowed to define control ranges with different levels of variability and immediate signal-response

actions for the proper use and exploitation of the resources, achieving the best product/energy ratio obtained to date (483 g HA kWh⁻¹).

This PhD thesis contributes to the development of a technology that converts a harmful waste into a platform product by making the best use of available resources. However, many unknowns remain to be solved to scale up the technology, such as finding electrodes with biocompatible, cheap and efficient materials, along with the constraints that limit production rates.

Resum

El **diòxid de carboni** (CO_2) s'emet en la seva major part en la ignició de combustibles fòssils per al transport, la generació d'electricitat o altres processos industrials. El CO_2 és un compost inorgànic que es dona de manera natural en la Terra, però la seva concentració ha augmentat exponencialment des de la revolució industrial, provocant l'acceleració de l'escalfament global. Els sistemes bioelectroquímics (BES) i, més concretament, la plataforma d'**electrosíntesis microbiana** (MES) és una de les diverses tecnologies que s'han proposat per a la seva captura i conversió. El que dona valor afegit a la MES és l'ús de microorganismes per a catalitzar la reducció del CO_2 a compostos útils, sense necessitat de materials cars ni escassos. No obstant això, encara és necessari investigar més per a la seva comercialització. En aquest sentit, aquesta tesi doctoral aborda els reptes de l'escalatge de l'electrosíntesis microbiana d'**acetat** (HA) a partir de CO_2 en condicions termòfiles, utilitzant un cultiu microbià mixt, energies renovables i emissions de gasos industrials.

Tenint en compte que el sector industrial emet CO_2 a altes temperatures, tots els experiments es van realitzar en **condicions termòfiles** ($50\text{ }^\circ\text{C}$), fet que va millorar la cinètica de les reaccions, així com la selectivitat del producte final. Per a abordar un dels principals reptes de la tecnologia relacionat amb la utilització de l'electricitat com a principal cost operatiu, es va considerar l'ús d'**energia renovable**, i es va simular el funcionament només amb l'**excedent** sense emmagatzematge en bateries, donant lloc a un subministrament d'energia intermitent. Això va reduir per tres el consum d'energia i va promoure la combinació de processos bioelectroquímics i de fermentació microbiana, aconseguint una producció contínua de HA ($43\text{ g m}^{-2}\text{ d}^{-1}$) i unes taxes de conversió de carboni prometedores ($2.2\text{ kg CO}_2\text{ kg HA}^{-1}$). En quant a la intensificació del procés, es va desenvolupar un **model termodinàmic** que va permetre determinar les condicions d'operació més favorables en funció del producte final desitjat. L'anàlisi dels resultats va mostrar que, en condicions termòfiles, l'elongació de HA a carboxilats de cadena més llarga no era espontània, per la qual cosa la seva conversió en successius passos de fermentació anaeròbica en condicions mesòfiles va resultar ser l'opció més viable.

Per tal de que la tecnologia estigui un pas més prop de la seva aplicació comercial, els sistemes es van provar amb gasos industrials reals que contenien impureses i un percentatge menor de CO_2 (del 100 al 14 %). La comunitat microbiana va demostrar ser prou robusta com per a mantenir productivitats similars a l'operació amb gas sintètic (2.5 % de diferència) i adaptar-se a les noves condicions, desenvolupant sinergies per a mitigar els impactes derivats de l'ús de gas real amb presència d'un 12 % d'oxigen. Finalment, es va dissenyar, construir i posar en marxa la **primera**

planta pilot d'electrosíntesis microbiana a partir de CO₂ amb monitoratge i control digital de les principals variables operacionals. Això va permetre definir rangs de control amb diferents nivells de variabilitat i obtenir accions de senyal-resposta immediates per al correcte ús i aprofitament dels recursos, aconseguint la millor relació producte/energia obtinguda fins al moment (483 g HA kWh⁻¹).

Aquesta tesi doctoral contribueix al desenvolupament d'una tecnologia que converteix un residu nociu en un producte útil aprofitant al màxim els recursos disponibles. No obstant això, per a escalar la tecnologia encara queden moltes incògnites per resoldre, com trobar elèctrodes amb materials biocompatibles, barats i eficients, juntament amb les restriccions que limiten les taxes de producció.

Resumen

El **dióxido de carbono** (CO_2) se emite en su mayor parte en la ignición de combustibles fósiles para el transporte, la generación de electricidad u otros procesos industriales. El CO_2 es un compuesto inorgánico que se da de forma natural en la Tierra, pero su concentración ha aumentado exponencialmente desde la revolución industrial, provocando la aceleración del calentamiento global. Los sistemas bioelectroquímicos (BES) y, más concretamente, la plataforma de **electrosíntesis microbiana** (MES) es una de las varias tecnologías que se han propuesto para capturarlo y convertirlo. Lo que da valor añadido a la MES es el uso de microorganismos para catalizar la reducción del CO_2 a compuestos útiles, sin necesidad de materiales caros ni escasos. Sin embargo, todavía es necesario investigar más para su comercialización. En este sentido, esta tesis doctoral aborda los retos del escalado de la electrosíntesis microbiana de **acetato** (HA) a partir de CO_2 en condiciones termófilas, utilizando un cultivo microbiano mixto, energías renovables y emisiones de gases industriales.

Teniendo en cuenta que el sector industrial emite CO_2 a altas temperaturas, todos los experimentos se realizaron en **condiciones termófilas** ($50\text{ }^\circ\text{C}$), lo que aumentó la cinética de las reacciones, así como la selectividad del producto final. Para abordar uno de los principales retos de la tecnología relacionado con la utilización de la electricidad como principal coste operativo, se consideró el uso de **energía renovable**, y se simuló el funcionamiento sólo con el **excedente** sin almacenamiento en baterías, dando lugar a un suministro de energía intermitente. Esto redujo en tres el consumo de energía y promovió la combinación de procesos bioelectroquímicos y de fermentación microbiana, logrando una producción continua de HA ($43\text{ g m}^{-2}\text{ d}^{-1}$) y unas tasas de conversión de carbono prometedoras ($2.2\text{ kg CO}_2\text{ kg HA}^{-1}$). En cuanto a la intensificación del proceso, se desarrolló un **modelo termodinámico** que permitió determinar las condiciones de operación más favorables en función del producto final deseado. El análisis de los resultados mostró que, en condiciones termófilas, la elongación de HA a carboxilatos de cadena más larga no era espontánea, por lo que su conversión en sucesivos pasos de fermentación anaeróbica en condiciones mesófilas resultó ser la opción más viable.

Para que la tecnología esté un paso más cerca de su aplicación comercial, los sistemas se probaron con **gases industriales reales** que contenían impurezas y un porcentaje menor de CO_2 (del 100 al 14 %). La comunidad microbiana demostró ser lo suficientemente robusta como para mantener productividades similares a la operación con gas sintético (2.5 % de diferencia) y adaptarse a las nuevas condiciones, desarrollando sinergias para mitigar los impactos derivados del uso de gas real con presencia de un 12 % de oxígeno. Por último, se diseñó, construyó y puso

en marcha la **primera planta piloto** de electrosíntesis microbiana a partir de CO₂ con monitorización y control digital de las principales variables operativas. Esto permitió definir rangos de control con diferentes niveles de variabilidad y obtener acciones de señal-respuesta inmediatas para el correcto uso y aprovechamiento de los recursos, logrando la mejor relación producto/energía obtenida hasta la fecha (483 g HA kWh⁻¹).

Esta tesis doctoral contribuye al desarrollo de una tecnología que convierte un residuo nocivo en un producto útil aprovechando al máximo los recursos disponibles. Sin embargo, para escalar la tecnología aún quedan muchas incógnitas por resolver, como encontrar electrodos con materiales biocompatibles, baratos y eficientes, junto con las restricciones que limitan las tasas de producción.

Chapter 1. Introduction



1. Introduction

1.1. Background

We trust that we are on the face of the earth to make big changes. We are constantly focused on innovation, and we assume we must own and control the technologies behind the products we create. **Electricity** is one of the greatest inventions. However, we have been making this happen for many years without considering the consequences for the environment. Now is the time to reverse it. Since we began facing relentless population growth and improving wealth worldwide, electrical energy consumption has risen from 6000 TWh in the pre-industrial period to more than 160000 TWh in 2019 (Ritchie and Roser, 2020). The global pandemic braked the usage, but the year 2021 started again with exceptional demands, pushing the electricity production by 6 % (1500 TWh); the largest increase since the recovery from the financial crisis in 2010 (IEA, 2022). The rapid recovery in the global energy demand squeezed electricity supply chains, driving up wholesale prices by more than four times compared to the 2015-2020 period. Despite the impressive 6 % growth in renewables, electricity generation from coal and gas reached a growth of 9 and 2 %, respectively. To provide the required electricity, **fossil fuels** have been burned on a massive scale, leading to a relentless increase in carbon dioxide (**CO₂**) concentration in the atmosphere and reaching a new record high: 420 mg L⁻¹ (NOAA, 2022). In addition, non-treated exhaust gases emitted by the abundant diesel-cycle engines and chemical industries are usually released at **temperatures** between 400 and 600 °C (Nolan, 2017), whereas if treated, they are emitted at 100-200 °C (Barker et al., 2009; Mikulčić et al., 2012). This is still warm enough to threaten adjacent areas including forests, crops and villages (Samdariya et al., 2021).

Fossil fuels are unevenly distributed, making countries dependent on regions that are sometimes politically unstable. The war in Ukraine not only brings with it incalculable humanitarian problems but has also fuelled the European revolution on its energy supplies (Demedziuk, 2018). This makes fossil fuel prices even more expensive, which reinforces the need to seek alternatives. Electricity is one of the main energy carriers that can be produced from all **renewable resources**. However, according to the projection, even if renewables would meet the vast majority of the increase in global electricity demand in the coming years, this trend would only result in stagnating CO₂ levels from electricity generation. The agreements driving the European CO₂ emissions policy started 30 years ago with the United Nations Framework Convention on Climate Change (United Nations, 1992), which was the core for the Kyoto Protocol (COP 3) (United Nations, 1998) and the Paris Agreement (COP 21) (United Nations, 2015). Even the 2030 Agenda for Sustainable Development (United Nations, 2022), adopted by all United Nations Member States in 2015, provided a

blueprint for ensuring affordable and clean energy for all by improving energy efficiency along with increased deployment of renewable energy to reduce greenhouse gas (GHG) emissions (sustainable development goal (SDG) 6). Nevertheless, current policies are insufficient to reduce emissions and reach the IEA's zero-emissions scenario in 2050 (Cozzi and Gould, 2021), and long-term goals should be treated with scepticism if they are not backed up by short-term commitments that put countries on track to reach those targets in the next decade (Hausfather and Moore, 2022). This underscores the urgent call for action to achieve the huge changes needed in terms of low-carbon energy efficiency and supply for the **decarbonisation of the energy system** throughout the world.

Unfortunately, and despite the clear needs, many companies and even nations persist in relying on fossil resources as fuel and chemical feedstocks. Therefore, it is of the utmost importance that the movement from a chemical-based energy system to a mainly electricity-based energy system has to be across consumers, companies and politicians, combined with technological strategies to mitigate CO₂ emissions (IPCC, 2021). Most technical solutions have focused on CO₂ sequestration (**Figure 1**) such as carbon capture and storage (CCS). It has been already applied in different parts of the world in conjunction with power plants or other industrial processes (Bui et al., 2018). However, the costs of capturing and transporting CO₂ from emission sites to storage units, leakages and the risk to the environment and human health, are factors that need to be considered and addressed (Larsen and Petersen, 2016). On the other hand, CO₂ can also be seen as an interesting feedstock. The newer term "carbon capture and utilisation (CCU)" aims at converting the captured CO₂ into more valuable products while retaining the carbon (C) neutrality of the production processes (C2ES, 2022). Its conversion to stable gas or liquid products makes it easier to store, transport, or use when needed. Many chemical and biological technologies are under research and development for the transformation of CO₂ into a wide range of chemicals such as organic acids, alcohols, and plastics. Some of these products can be transformed back into electricity, making CO₂ not only a feedstock but also an ideal energy carrier (Van Geem et al., 2019). However, because CO₂ has a thermodynamically stable structural form, its conversion is energy-intensive. At this point, it looks like an infinite circle. Consuming energy produces CO₂ and reducing CO₂ requires energy. This is where the renewables, more sustainable and environmentally friendly, play a crucial role.

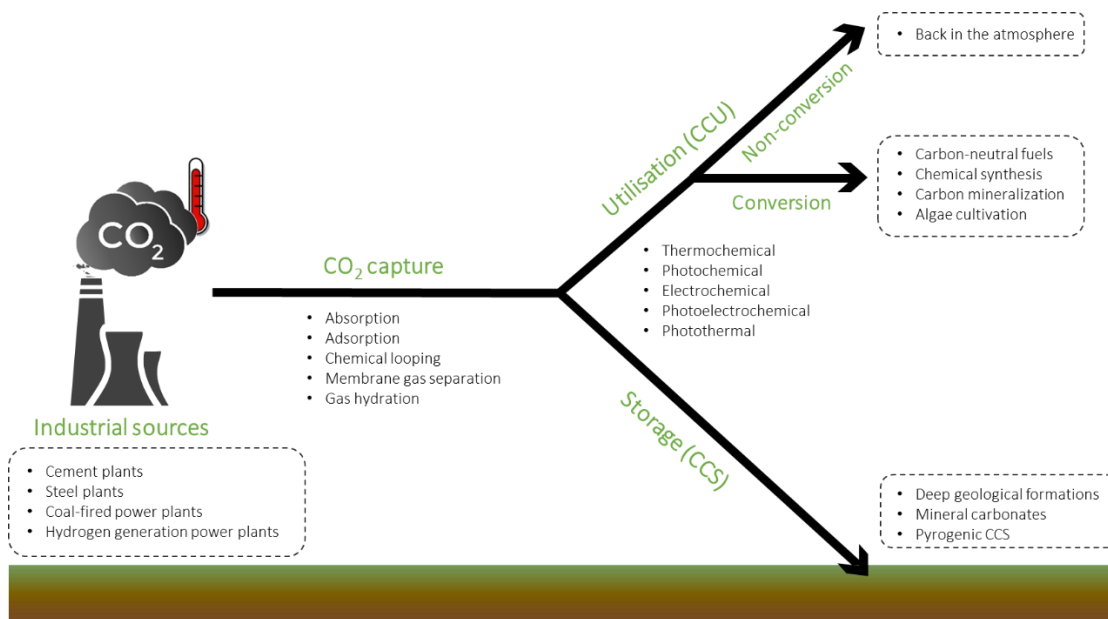


Figure 1. Diagram of the industrial carbon dioxide (CO₂) storage vs. utilisation chain.

1.2. Harvesting energy from renewable sources

Recent technological improvements and declining costs of renewable energy resources, together with the increased competitiveness of battery storage, have made renewables one of the most promising sources of energy in several fields. However, they still do not account for more than a quarter of the World's total energy consumption (GCDL, 2022). The sun can provide more energy to the earth in 1 hour than all the energy consumed by humans in a year. Despite this, technical factors such as transmission, storage and transport of electricity, as well as social, economic and political aspects limit its implementation (Groth et al., 2019). One of the challenges of using renewable electricity as the main energy carrier in a power system is that electricity from most renewable resources is produced **intermittently**. On a "good" energy day, bright sunshine and moderate wind fill our power grid with cheap, renewable energy. On a "bad" energy day, when the skies are grey and the wind is calm, we rely on the back-up of hydro-power or conventional generation. Thus, innovative and price-competitive solutions are needed to help future energy systems remain balanced across different levels of demand without additional costs. All but without adding a further constraint to cope with a change that does not favour the large companies that continue to control the energy market.

Europe and China are leading the installation of new pumped-storage hydropower plants, powered by the movement of water. Grid-scale batteries are also being built in countries such as the United States, Australia, and Germany. Mechanical energy storage is also a viable option,

which harnesses motion or gravity, and thermal energy storage is expected to triple in size by 2030 (IEA, 2022). These technologies store electrical energy by converting it into other forms of energy, such as chemical, potential, mechanical, thermal, and kinetic, and turn them back into electricity when required. However, most of them require the use of expensive catalysts, large surfaces and volumes, and are questioned due to the impact on the environment, the efficiency, the lifetime, and the limited capacity (Blanc et al., 2020). In a system with electricity as the main energy carrier, energy security must be ensured. It is therefore crucial that excess renewable energy can be stored in a sustainable way and that new alternatives are developed that are able to produce fuels without relying on biomass or expensive raw materials. Bioelectrochemical systems (BESs) are the backbone of a novel technology that has the potential to meet both criteria.

1.3. Bio-electro interactive communication systems

Records of the ability of some bacteria to exchange electrons with a solid-state electrode can be found as far back as 1911 (Potter, 1911), but it was not before 100 years after, that laboratory applications began to be identified and implemented (Arends and Verstraete, 2012). The key principle of a BES is the use of microorganisms as catalysts for a wide diversity of redox reactions, for which two electrodes are involved. The use of **microorganisms** instead of chemical catalysts makes the technology a more sustainable alternative, as they can self-regenerate, and non-noble materials and cheaper electrodes can be used (Schröder et al., 2015). BESs were initially aimed at converting organic wastes into energy, but novel applications have emerged focusing on the double benefit of C sequestration and commodity chemicals production, resulting in new hybrid technology. When bio-electricity is generated by oxidising an organic substrate (e.g. acetate), BESs are referred to as microbial fuels cells (MFCs) (Logan et al., 2006). When more complex processes such as bioremediation or the production of organic compounds by, for example, reducing CO₂ to carbohydrates (Osset-Álvarez et al., 2019), BESs are then referred to as microbial electrolysis cells (MECs). The difference between the redox potential on each reaction to convert C waste at the anode or the cathode defines the spontaneity of the reactions. MFCs are characterized by a spontaneous reaction, which exploits the electron flow between the anode and cathode electrodes for power generation (Hernández-Fernández et al., 2015), whereas MECs require an external energy supply to overcome thermodynamic constraints and enable the production or recovery of valuable compounds (Lu and Ren, 2016).

Since its implementation in 2010 (Nevin et al., 2010), microbial electrosynthesis in BESs has led to the CO₂ conversion into a wide variety of C-neutral commodities, such as methane (CH₄) (Blasco-Gómez et al., 2017), acetic acid (HA) (May et al., 2016) and longer carboxylates (Vassilev et al., 2018). At the same time, it can be seen as a sustainable alternative to storing electrical energy in the form of hydrogen (H₂) (Kadier et al., 2016) or other stable, high energy-density and C-neutral products (e.g. caproate, formate, butanol, isopropanol) that can be easily reserved, distributed and consumed on-demand (Dessi et al., 2020).

1.3.1. Microbial electrosynthesis (MES)

A MEC usually consists of an anode and a cathode separated by an ion-exchange membrane (**Figure 2**). The oxidation of an electron donor occurs in the anode compartment (e.g. water) and the opposite, the reduction of an electron acceptor at a lower electrode potential, occurs in the cathode compartment (e.g. CO₂). When a cationic exchange membrane is used, the electrons are transferred to the cathode *via* an external electrical circuit, while protons (H⁺) migrate through the membrane to maintain charge neutrality. From H⁺, H₂ can be produced either electrochemically or biologically, and together with the available electrons, it is used to catalyse the reduction of CO₂ to organic compounds (e.g. acetate, ethanol, butyrate, caproate). From the basic principle, a plethora of different choices can be applied in a MEC regarding the material and nature of the catalysts, the number of compartments, the type of membrane used, the design of the reactor, the inoculum, and the operating configuration (Muñoz-Aguilar et al., 2018). In addition, oxidative reactions other than water electrolysis could take place in the anodic chamber to improve the process feasibility, such as nitrification, oxygen production or the generation of more economically valuable compounds like chlorine (Batlle-Vilanova et al., 2019). The microorganisms in charge, can grow on the electrode (forming a biofilm) or can remain suspended in the liquid as planktonic cells (as bulk in the medium), forming a community that may also contain electrochemically inactive microorganisms very useful for other functions such as the breakdown of complex substrates.

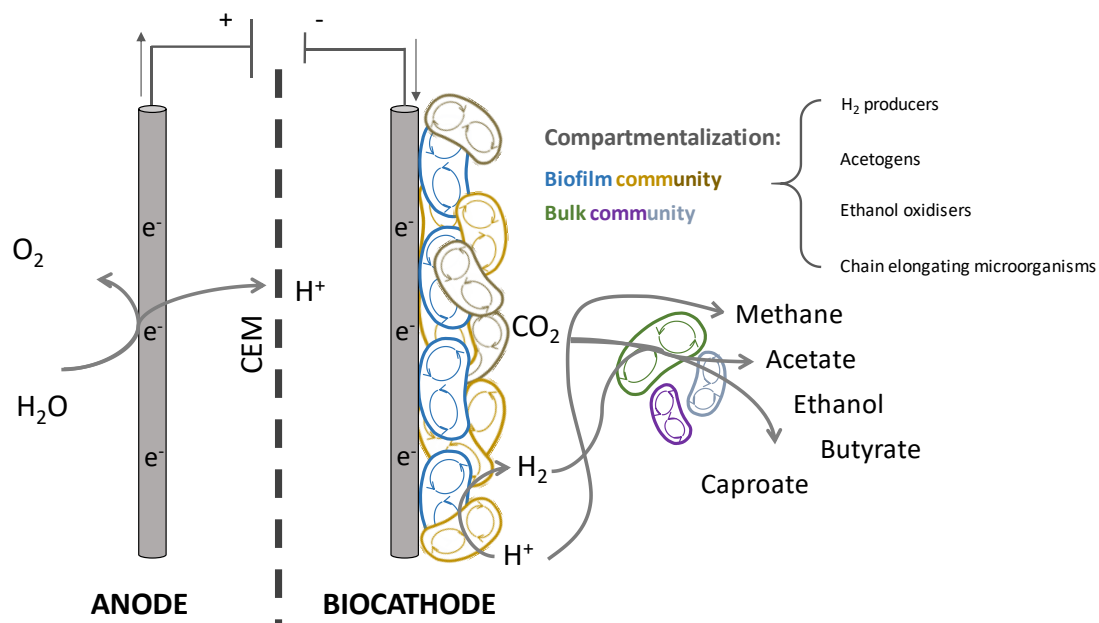


Figure 2. Schematic representation of a potential strategy for CO₂ reduction to bio-commodities through microbial electrosynthesis. CEM: cationic exchange membrane.

1.3.1.1. Electroactive microorganisms acting as catalysts

There is a vast number of microorganisms capable of CO₂ fixation (e.g. algae, cyanobacteria, β -proteobacteria, *Clostridia* and *Archaea*) through different metabolic pathways, being the Wood-Ljungdahl (also known as the reductive acetyl-CoA pathway) one of the most ancient pathways for CO₂ reduction to valuable compounds (Martin, 2012). Electroactive microorganisms though, are able to exchange electrons with other cells or conductive interfaces in their extracellular environment (Paquete et al., 2022). These comprise the core of MES and open the way to a broad variety of novel cathode-driven reactions, enabling a wide range of practical biotechnological applications. Pure cultures and mixed microbial consortia, either natural or genetically modified, have been used for different purposes presenting their specific advantages and disadvantages (**Table 1**). Although pure culture-based processes often allow high selectivity and productivity, maintaining sterile conditions implies the use of specific and purified substrates. These problems have redirected many research efforts towards the use of mixed microbial cultures that are simpler to operate and require cheap, non-sterile substrates as raw material, favouring the economic viability and sustainability of the technology (Virdis et al., 2022).

Table 1. Advantages and disadvantages of pure, mixed, and genetically modified electrotoph cultures.

Biocatalyst	Advantage	Disadvantages
Pure microbial culture	<ul style="list-style-type: none"> High production rates High selectivity Low competitiveness High stability 	<ul style="list-style-type: none"> Severe sterilization Vulnerability to fluctuations Specific growth medium and start-up procedure Strict anaerobes
Mixed microbial culture	<ul style="list-style-type: none"> Widely available Resilient to fluctuations Easy to start-up and operate Synergic inter-relations 	<ul style="list-style-type: none"> Low selectivity Prone to membrane biofouling Risk of competitiveness between species Low predictability
Genetically modified microorganisms	<ul style="list-style-type: none"> Wider product spectrum High selectivity High-value products High resistibility to fluctuations 	<ul style="list-style-type: none"> Expensive and laborious start-up procedure Questionable societal acceptance Requires approval from the government Requires specific waste treatment

The first example of a bio-cathode driven CO₂ fixation was to stimulate methanogenesis (Clauwaert et al., 2008) while HA was first demonstrated to be produced in 2010 by a pure culture of *Sporomusa ovata* (Nevin et al., 2010). Bacterial communities of *Desulfovibrio spp.* have been widely used to enhance H₂ production (Aulenta et al., 2012; Cheng and Logan, 2007; Rozendal et al., 2008), but later, electro-acetogenesis was also demonstrated with other pure cultures of *S. sphaeroides*, *S. silvacetica*, *Clostridium ljungdahlii*, *Clostridium aceticum* and *Moorella thermoacetica*. Indeed, *Clostridium spp.* has been reported to be a key CO₂ reducer (Emerson et al., 2018) and the use of thermophilic communities of *Moorella spp.* has reported to enhance HA production rates (Yu et al., 2017). Meanwhile, the possibility to produce HA from CO₂ using **mixed cultures** (open cultures) was presented more recently by different authors (Min et al., 2013; Patil et al., 2015), which also resulted in the diversification of products (Jiang et al., 2013; Marshall et al., 2012). Since the use of mixed cultures allows the simultaneous production of different compounds, it can also result in the conflict between species for the same feedstock. For instance, hydrogenophilic methanogens are capable of CO₂ reduction to CH₄, competing with acetogens to produce HA from the same substrate, whereas acetoclastic methanogens convert HA to CH₄ (Breznak and Switzer, 1986), reducing HA accumulation as a final product. Some strategies to decrease methanogens competition are the use of expensive chemicals such as sodium 2-bromoethanesulfonic acid to inhibit metabolic activity, while operational pH and the enrichment of the community before the inoculation has been proposed as an effective alternative (Gavilanes et al., 2019).

On the other hand, understanding how microorganisms interact with electrodes **transporting electrons** extracellularly (EET) into and out of the cells is still a challenge. Direct electron transfer (DET) was reported in 2004 (Gregory et al., 2004), which is usually performed through membrane redox proteins, such as c-type cytochromes or hydrogenases (Rosenbaum et al., 2011), and physical cellular structures known as the nanowires (Gorby et al., 2006). It does not require the diffusion of any mobile component for electron transport, while the mediated electron transfer (MET) involves key electron shuttles as transporters between the electrode surface and microorganisms (Rabaey and Rozendal, 2010). Even though H₂ is considered the main electron donor for the bio-electro conversion of CO₂ (Perona-Vico, 2021), other intermediate soluble redox compounds such as phenazines and flavines can also be used as mediators (Marsili et al., 2008; Rabaey et al., 2005). The common activation of certain biosynthetic pathways is often controlled by quorum sensing (QS), which can influence bacterial electro-activity by conditioning the formation of biofilms necessary for DET or by regulating the production of redox compounds necessary for MET (Patil et al., 2012). In addition, there can exist **syntrophic relationships** between microbial species for direct and mediated transfer of electrons to the final products, especially in biocathodes with mixed cultures (Lovley, 2011). Normally, syntrophic associations rely on the transfer of electrons from one bacterium that oxidises an organic substrate to another that reduces an available electron acceptor (e.g. CO₂). The exchange of electrons usually occurs *via* diffusible intermediates (e.g. H₂) or by direct electron exchange between physically connected cells (Rotaru et al., 2021). Physical cell-to-cell connections can transfer electrons *via* direct interspecies electron transfer (DIET) or by conductive particle mediated interspecies electron transfer (CIET), boosting EET in mixed cultures (Paquete et al., 2022).

Usually, microorganisms can maximise their energy gain by selecting the electron acceptor with the highest potential available. Nevertheless, when soluble electron acceptors are scarce in the microbial environment, microorganisms may then make use of a solid electron acceptor (e.g. electrode) or resort to fermentation processes. An alternative to MES is the anaerobic gas fermentation (AF), a biological process that can produce a valuable carboxylate platform using CO₂ as a C source. However, in this case H₂ has to be added externally to be used as a source of electrons. Even though AF processes have long been applied for HA formation (Poston et al., 1966), they are limited by the relatively low solubility of H₂ (Stoll et al., 2018). This makes the gas-liquid mass transfer a drawback in this technology compared to MES, in which H₂ is produced *in situ* and directly used. Recently, the concept of **electro-fermentation** (EF) has emerged to use electrochemistry to steer and control fermentative process (Chandrasekhar et al., 2021) and enhance the generation of reduced products. In an open culture MEC, microorganisms attached

to the electrode can uptake electrons and H^+ to produce bio- H_2 for use by other bacteria in the bulk liquid, while other compounds act as intermediates (e.g. acetate or ethanol) for the production of longer-chain carboxylates (Puig et al., 2017) (**Figure 2**). However, it is still uncertain if EET is involved in EF or whether the polarised electrode merely acts as a means to control the oxidation-reduction potential of the fermentation broth (Virdis et al., 2022).

1.3.1.2. Niches of applications for MES

The rising costs of CO_2 emissions and environmental incentives are pushing industries towards the use of C conversion technologies. In this sense, MECs have the potential to be part of the gradual replacement of existing chemical production facilities, producing a revenue stream that can compensate for operating costs (Grim et al., 2020). MES is a technology-independent of arable land utilization and freshwater resources with several market entry opportunities to a nearly unlimited substrate revalorisation. It can be applied hand in hand with industry (Osset-Álvarez et al., 2019; Sadhukhan et al., 2016) decreasing the costs of transportation, though depending on the off-gases composition, a previous purification will be required. For example, MECs could be installed in the paper, food, oil refineries, chemical and metallurgical industries, which are considered to be major CO_2 emitters. In addition, since power input is needed to drive the thermodynamically unfavourable cathodic reactions, the generated products must be more valuable than the power invested for viable and practical implementation. In this sense, MES can be seen as a suitable option for off-peak renewable energy storage, harvesting intermittent energy into covalent C bonds.

MES has many promising applications starting from the catalysis of H_2 evolution (Ambler and Logan, 2011) to the production of a wide range of C-neutral chemicals when coupled with renewable resources. The resulting products (carboxylates and alcohols) can be applied in food packaging, preservatives, rubber, metallurgy, pharmaceuticals, polymers, and chemical and renewable energy industries (ElMekawy et al., 2016). Over the past two decades, the global market for these products has increased steadily, valued at 122 billion € in 2013, and projected to exceed 200 billion € by 2023 (Wood et al., 2021). The recent improvements in the design of reactors and operation control have led to the production of more complex and specific molecules such as bioplastics, polysaccharides and proteins *via* multi-step bioconversions (Haas et al., 2018), or even in the same MEC (Vassilev et al., 2019). However, HA is one of the few products obtained with selectivity of over 90 %, high reaction rates (over $200\text{ g m}^{-2}\text{ d}^{-1}$ of working cathode area), coulombic efficiency (CE) exceeding 85 %, and rising decarbonisation potential (Jiang et al., 2019; Nevin et al., 2010).

Even though HA is a short-chain volatile fatty acid with low market value, it has a huge market size. It can be useful as an end product (e.g. for denitrification or biological phosphorus removal) or as an intermediate compound for further chemical transformations and derivatives (**Figure 3**). About 13 MT of HA are used as a precursor every year (Christodoulou et al., 2017). Its production has been demonstrated on a laboratory scale using either pure cultures (Nevin et al., 2011) or mixed microbial cultures (Batlle-Vilanova et al., 2016), and novel reactor designs allowed to carry out simultaneous bioprocesses (Van Eerten-Jansen et al., 2013) or to couple other secondary fermentative reactions as in conventional anaerobic fermenters (Romans-Casas et al., 2021). In this sense, CO₂-rich gaseous waste streams are considered potential inlets for combined MES and AD systems. However, significant research efforts are required to improve production performance, selectivity and management of operational variables.

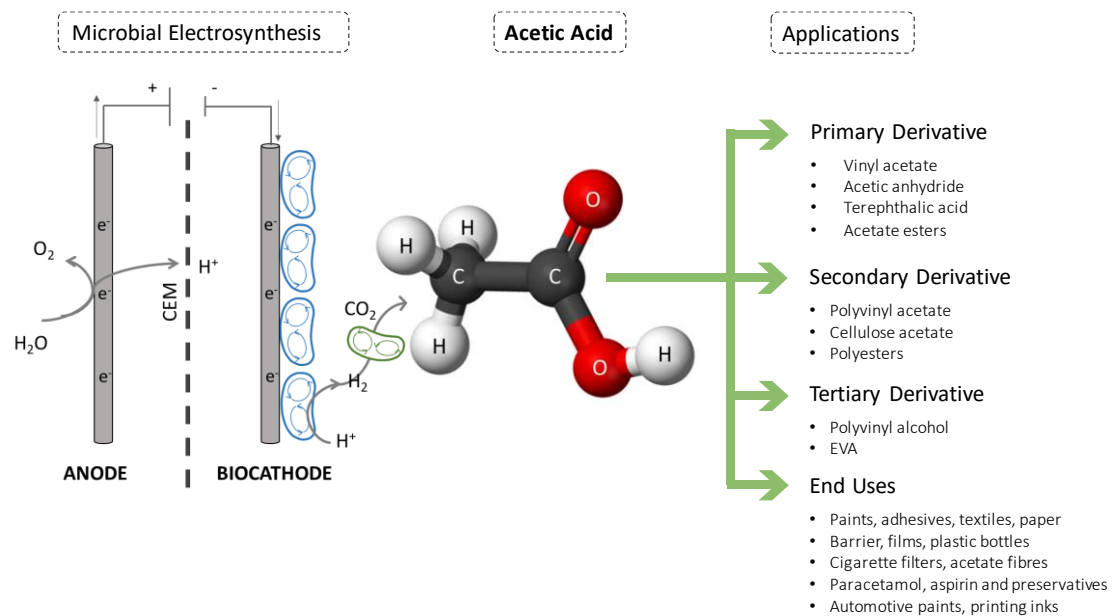


Figure 3. Derivatives and end uses of acetic acid. CEM: cationic exchange membrane. Data adapted from Cision (Software platform and marketing solutions).

1.3.1.3. Production parameters influencing efficiency

Jourdin et al. (2020) identified 28 key parameters and their impact on the techno-economic feasibility of MES. The main capital and operating costs were the electrode material, accounting for 59 %, and the electricity consumption (up to 69 %). However, CE, cell voltage and product selectivity also showed a significant impact on costs. In studies focusing on CO₂ bio-electro recycling into HA (Bajracharya et al., 2015; Jourdin et al., 2015b; Min et al., 2013), operating parameters and reactor start-up and configuration were reported to be largely involved in production rates and product selectivity (Jiang et al., 2013). Patil et al. (2015) proved the performance and reproducibility of the results following a selective enrichment strategy to

develop a microbial community to produce HA ($19 \pm 2 \text{ g m}^{-2} \text{ d}^{-1}$) using unmodified C-based cathodes. However, the HA production rate in MECs is often limited by low current densities ($< 200 \text{ A m}^{-2}$), which results in potential differences close to 3 V when conventional C electrodes are used (Bian et al., 2020). Using reticulated vitreous C modified with C nanotubes, HA production rate and current density increased by a factor of 2.6 and 1.7 times, respectively, compared to a C plate control (Jourdin et al., 2014). Meanwhile, Zhang et al. (2013) studied the electrode-microbe electron transfer in HA production by growing *Sporomusa ovata* on different cathode materials. Modification of the carbon cloth with 3-aminopropyltriethoxysilane, chitosan, or cyanuric chloride to provide positively charged surfaces increased HA production by 3, 6 and 7 times more than with untreated controls. Coating the carbon cloth with metal (nickel, palladium or gold) also provided electrosynthesis rates that were 4.5, 4.7 and 6.0 times faster than the untreated control, while the recovery of electrons consumed in HA was around 80 % for all materials (Zhang et al., 2013). Alternatively, gas diffusion electrodes were used to double the mass transfer rate in the feeding of gaseous CO_2 compared to the supply *via* conventional spargers at the submerged electrode, though maximum production rate was below $3.8 \text{ g m}^{-2} \text{ d}^{-1}$ (Bajracharya et al., 2016).

MES reactions, similar to chemical ones, obey the laws of thermodynamics (Von Stockar et al., 2006) and consequently, the energetic limits for microbial life (Korth et al., 2016). However, the development of a mature biofilm and bulk community is crucial to drive CO_2 reduction to the desired compound. The growth rate of a microorganism as a function of the limiting substrate concentration follows the Monod kinetics described in 1949 (Monod, 1949), which also depends on environmental conditions such as temperature. Liu (2007) provided an extensive discussion of the Monod equation and various derivations, leading to an accurate prediction of the response of a bioelectrochemical reaction to operating variables, and allowing broad applications in cell biology, bioreactor design, and performance improvement (Maggi et al., 2018). More in depth, Korth and Harnisch, (2019) used it to model MES and estimate the direct EET mechanisms in addition to substrate and redox mediators uptake. On the other hand, a computational modelling indicated that for biofilm-driven reactors, continuous CO_2 supply enhanced microbial growth, denser biofilm formation and higher current densities (Cabau-Peinado et al., 2021).

Since MES requires **an external input of power**, a MEC is either operated at a poised cathode potential (potentiostatic mode), or with a fixed current supply (galvanostatic (GA) mode). CE, calculated as the ratio of the real vs. the theoretical compounds produced based on the current, is a key parameter to evaluate the performance of MES. This can be optimised by changing operating parameters such as substrate concentration to boost growth kinetics (Sleutels et al., 2011) or by adding redox mediators (Chen et al., 2021; Ying et al., 2022). Theoretically, the totality

of electrons passing through the external circuit should be consumed for production. However, a higher amount is usually added to the system to overcome ohmic losses due to the overpotential on the cathode and ensure microbial growth (Call et al., 2009). Here, operating conditions such as temperature can modify the thermodynamic properties, kinetic performance and stability of the process.

1.3.1.4. Thermophilic MES

Temperature is a key parameter in MES since it can severally affect the composition and productivity of the microbial communities (Karadag and Puhakka, 2010). Up to now, most of the MECs have been operated at temperatures below 36 °C due to the wide diversity of mesophilic electrotroths, the facility to operate, and the slightly more favourable thermodynamics (Foglia et al., 2011) (**Table 2**). However, working at higher temperatures is beneficial for the kinetics of the reactions and it can assist in the energy input for the endothermic reaction of H₂ production in the cathode, resulting in a lower voltage input (Fu, 2013). Moreover, it increases the metabolic activity of microorganisms and reduces the competitiveness between them since, for instance, many H₂ consuming bacteria and pathogens cannot survive at high temperatures, which brings an advantage for acetogens (Hasyim et al., 2011). On the other hand, the main drawbacks are the decreased solubility of gases, the restricted temperature range for most commercial probes, and the underexplored thermophilic exoelectrogens, which have been limited to Gram-positive species affiliated to the phylum *Firmicutes*. The energy required for heating the bioreactors is also a concern, though the technology could use high-temperature industrial off-gases on-site with a minimum or without further energy addition.

The range of possibilities for thermophilic consortia was first evaluated in 2016 by Dopson et al. (2016) who reviewed the microbial catalysis advances under extreme conditions and showed possible new routes open for microbial electrochemical systems. However, most of them were operated under MFC configuration, using mainly HA as electron donor and obtaining electricity as the main product. For instance, a MFC inoculated with a mixed culture from a methanogenic anaerobic digester at 55 °C showed stability for 100 days with a CE of 89 % (Wrighton et al., 2008). A pure culture of ferric iron-reducing Gram-positive thermophile, *Thermincola ferriacetica*, was also able to oxidise acetate at the anode at 60 °C, keeping a stable current of 0.4 A m⁻² for over 3 months with 97 % CE (Marshall and May, 2009). Subsequent studies used thermophilic inocula as well (Fu et al., 2013a, 2013b; Ha et al., 2012; Hussain et al., 2012), either with communities dominated by strains related to Gram-negative nitrate-reducing species, electrogenic thermophiles, or from conventional anaerobic digesters. The work was followed by Shrestha et al. (2018), who highlighted the need to identify the underpinning mechanisms that define the

exceptional electro-catalytic performance of extremophiles in MECs. Later, Faraghiparapari and Zengler, (2017) determined the optimal temperature range (55-60 °C) for acetate generation from CO₂ using two different *Moorella* strains, whereas Yu et al. (2017) immobilized *M. thermoautotrophica* on the cathode, obtaining a 14-fold higher production compared to natural biofilms. However, thermophilic MES is still in an early stage of development, which is why most researchers focus on the principles for the production of commodities compounds, underestimating their potential compared to more technologically advanced MES operated under mesophilic conditions. In this sense, further research for an effective thermophilic CO₂ conversion to HA is required to become price competitive.

Table 2. Advantages and disadvantages of working under mesophilic and thermophilic conditions and the main associated genera.

Operating conditions	Advantages	Disadvantages	Main genera
Mesophilic conditions	<ul style="list-style-type: none"> Easy operation Broad product spectrum Wide set-ups configurations More metabolic activity 	<ul style="list-style-type: none"> More competitiveness Low selectivity Energy intensive separation Low kinetics 	<ul style="list-style-type: none"> <i>Acetobacterium</i> <i>Acetoanaerobium</i> <i>Clostridium</i>
Thermophilic conditions	<ul style="list-style-type: none"> High reaction rates Less risk of contamination More product specificity High selectivity 	<ul style="list-style-type: none"> Low gas solubility Tricky operational management Limited temperature range of many sensors High thermal energy required 	<ul style="list-style-type: none"> <i>Moorella</i> <i>Acetogenium</i>

Aside from CO₂, anaerobic thermophiles have alternatively been used in fermentative reactors for HA production from substrates such as lactate. In 2000, a study was conducted using milk permeate to feed *M. thermoautotrophica* and *M. thermoacetica*, yielding approximately 0.9 g g⁻¹ (Talabardon et al., 2000a). The same authors also compared HA production by immobilising a co-culture of *M. thermoautotrophica* and *Clostridium thermolacticum* in a fibrous-bed bioreactor with a conventional one, obtaining an overall HA yield from lactose between 0.8 and 0.9 g g⁻¹ higher, and reaching concentrations up to 25.5 g L⁻¹ (Talabardon et al., 2000b). Later, Collet et al. (2003) compared a pure culture of *Cl. thermolacticum* with co-cultures of *Cl. thermolacticum* with *M. thermoautotrophica*, *Cl. thermolacticum* with *Methanothermobacter thermoautotrophicus*, and a consortium of the three species, the latter obtaining the best results although the highest HA concentration did not exceed the 3.0 g L⁻¹.

1.4. Scalability: main challenges and digitalisation

The ultimate goal of reactor and process engineering remains the improvement of yields and reaction rates to achieve higher technology readiness levels (TRLs) (Virdis et al., 2022). MES is approaching the maturity needed to finally move beyond the laboratory, but the operation of **pilot plants** under relevant industrial conditions will corroborate its techno-economic feasibility. MECs of TRLs 1-3 (**Figure 4**) have been deeply studied by different Universities worldwide in recent doctoral thesis defended since 2015 (Bajracharya, 2016; Batlle-Vilanova, 2016; Blasco-Gómez, 2020; Bolognesi, 2021; Jourdin, 2015; Mateos, 2018; Perona-Vico, 2021; Vassilev, 2019). These studies are ideal for fundamental and proof-of-concept research due to the easy control of reaction conditions, but are often poorly scalable designs with low production rates and low surface-area electrodes. The trend since 2020 shows the shift towards more practical rather than fundamental research. Several initiatives (Schievano et al., 2019) and ongoing European research projects such as INITIATE (<https://www.initiate-project.eu/>), TAKE-OFF (<https://takeoff-project.eu/>), CO₂SMOS (<https://co2smos.eu/>), VIVALDI (<https://www.vivaldi-h2020.eu/>) and IMPACTS9 (<https://www.ccus-setplan.eu/>) are dealing with bio-electro CO₂ recycling for the production of valuable biochemicals (CO₂ Value Europe, 2022), also coupling MES with fermentation-related technologies and renewable power sources. TRLs of 5-6 have the potential for higher productivity and scalability, but there is a lack of information on parameters such as design criteria and performance, and the use of real off-gases may cause undesirable cross-over effects. Reporting on MES **scaling-up** is highly limited, and to date, no pilot-scale MES systems of TRLs 7-9 are reported for CO₂ conversion.

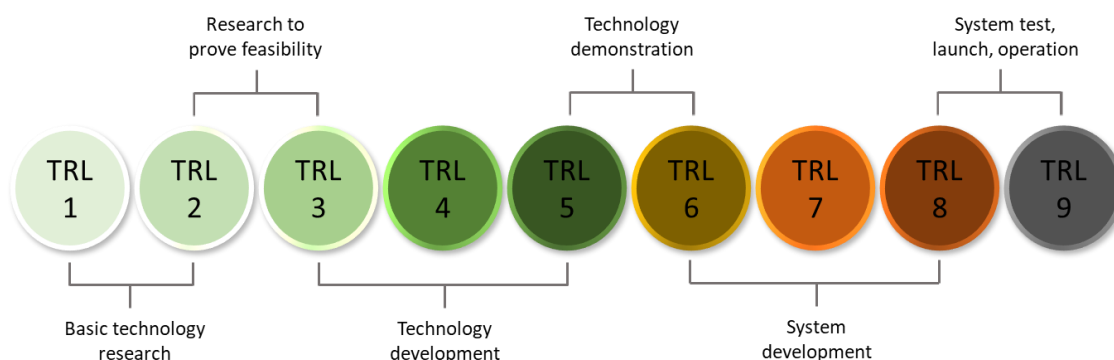


Figure 4. Technology readiness levels (TRLs) described by the work programme of Horizon 2020.

The main goals for using CO₂ as feedstock are clear, though the practical considerations to use it instead of organic substrates are less obvious. The specific mass of CO₂ to produce HA was calculated to be 0.75 kg CO₂ kg HA⁻¹, and it could avoid approximately 700 KT of CO₂, with a relative added value of about 340 % (Otto et al., 2015). Despite, less than a 1 % of the global CO₂

emissions are currently being used as a substrate. The high CO₂ oxidation state makes it energy-intensive to be reduced to organic compounds, rendering energy one of the main costs for MES. When assuming an optimistic CE of 90 % and an operational voltage of 3 V, about 12 kWh are required for the production of 1 kg of HA (PrévotEAU et al., 2020). Only considering the increased average price for current electricity of 150 € MWh⁻¹ (EEX, 2022), 1.8 € is the cost for the production of 1 kg of HA, which already exceeds its commercial value (ECHEMI, 2022). Gadkari et al., (2022) suggested a minimum threshold production rate of 4100 g m⁻² d⁻¹ that needs to be achieved before MES could be seen as a sustainable alternative to fossil-based HA production, that considering an average electrode size of 0.003 m², it accounts for 0.15 kWh d⁻¹. Estimating that a conventional electrolyser consumes 53 kWh per kg of H₂ produced (Hodges et al., 2022) and that 2 moles of H₂ are required for the production of 1 mole of HA (according to stoichiometry), the amount of energy required per kg of HA is 3.53 kWh kg⁻¹, which is still more than 3 times lower than *via* MES. Despite, if scaled-up, a case study that considered a 50 m² MEC operated at 20 A m⁻² and 1 V from CO₂, concluded that the maximum allowable investment cost could be a factor of 10 smaller compared to an organic substrate-based system (Desloover et al., 2012). Therefore, the use of renewable, low-cost (excess)energy is crucial.

A rational scale-up approach must be prioritised over empirical methods based on trial-and-error experiments, which have so far not been successful in similar processes (Cheng and Logan, 2011; Cusick et al., 2011). Scale-up reactors require simple and robust designs that allow for changes in gas and liquid streams, and operational and design parameters, so modular designs should be preferred as they avoid disturbance to the biological community. In addition, scalable electrode materials are needed with good biocompatibility, high conductivity and strong chemical stability (Logan et al., 2006), while proper mixing conditions are essential to avoid pH gradients and increase the contact time between biofilm and fresh medium (Zeppilli et al., 2021). The information available in the literature on reactor design parameters is scarce and lacks standardization in data representation (Santoro et al., 2021). However, the design of commercially available electrochemical cells such as electrolysers can be potentially applied to scale up the MECs with minor modifications, and available pilot-scale studies on other BESs, such as MFCs, can provide useful guidelines (PrévotEAU et al., 2020). Configurations of scaled-up, stacked BESs have been applied for the treatment of swine manure (Vilajeliu-Pons et al., 2017), brewery wastewater (Dong et al., 2015), and municipal wastewater (Feng et al., 2014; Liang et al., 2018; Rossi et al., 2019), as well as ammonia recovery (Zamora et al., 2017).

Commercialisation of MES still requires detailed but extensive knowledge that can be achieved through moving towards a **digital transformation**. Digitalisation of processes reduces cost and risk,

and improves operator effectiveness. In this sense, there is a potential intensification of the process by monitoring and control operational conditions to make data-informed decisions. Overall, while maintaining simplicity, optimisation of MES should rely on the enhancement of product specificity and production rates to enable large-scale applicability without compromising the affordability nor the eventuality of a needed change.

Chapter 2. Research questions and Objectives



2. Research questions and objectives

Research at both the elementary and applied levels plays a critical role in assessing the 2030 Agenda across the entire system of SDGs-related advocacy and outreach. To make this a tangible reality, broad ownership of the SDGs must translate into a strong commitment by all stakeholders to implement the global goals. A key challenge is to find a way to transform something that works on a small scale into something that can be useful for a holistic problem. With the ambitious aim of contributing to the solution of a large-scale problem, **the present PhD thesis gathered the expertise of MES with global needs, environmental opportunities and theoretical approaches to address some of the limitations of these systems and optimise the electrical use for CO₂ conversion to HA.** To achieve the main goal, more specific research questions (RQ) and sub-objectives were defined. **Figure 5** relates the RQ to the results classified in the following chapters.

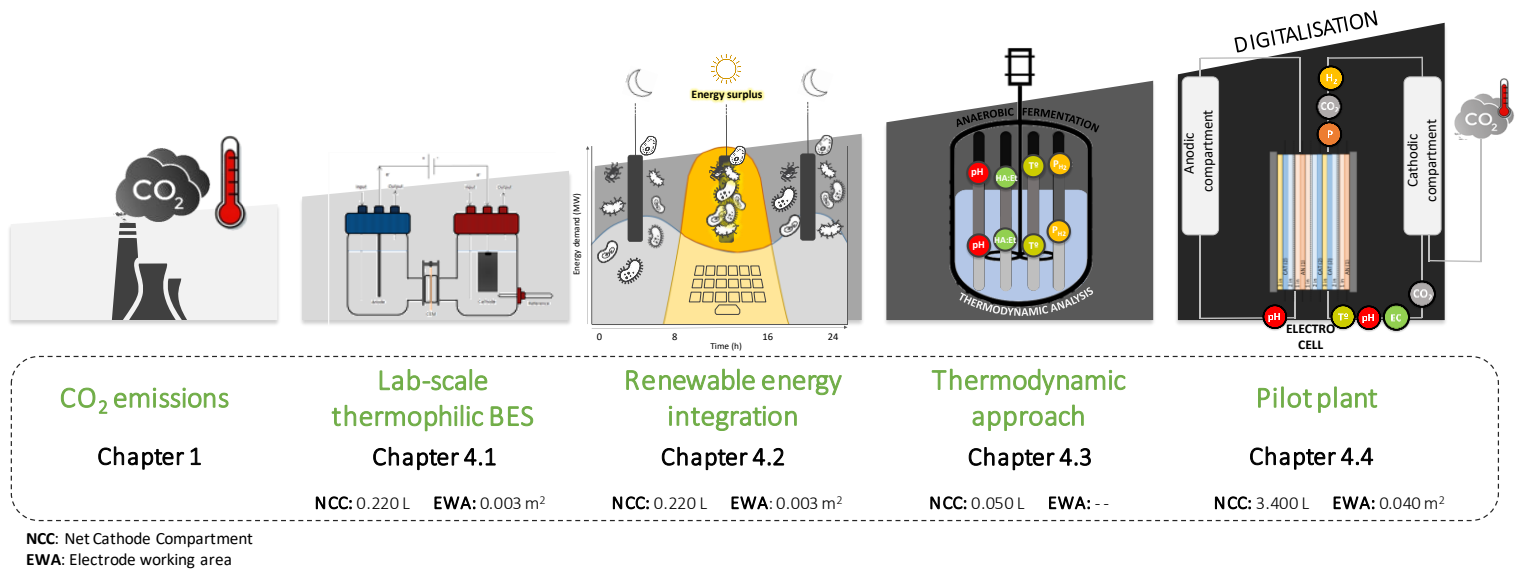


Figure 5. Schematic representation of the steps to progressively fine-tune the operating parameters and optimise the bioproduction of acetic acid from CO₂.

1. What is the potential of microbial electrosynthesis to approach a decarbonised energy system?

Complex solutions are often chosen for problems that nature has already solved in a simple way. The efficient conversion of CO₂ into added-value products relies on the performance of catalysts. Although pure cultures were initially employed and largely investigated, it was later demonstrated that mixed cultures are advantageous due to their robust and resilient communities, and their increased production rates owing to their synergistic behaviour. The use

of free and abundant open cultures facilitates the implementation of this system to generate revenue from atmospheric pollutants. It gives additional versatility to the technology and minimises the associated constraints for its acquisition and manipulation. However, the increased cost due to energy consumption for autotrophic growth and for driving non-spontaneous reactions, as well as the inadequate performance for industrial scale-up and commercialisation, are some of the bottlenecks that must be addressed.

This PhD thesis considered microbial electrochemical technologies as sustainable energy batteries that additionally contribute to decarbonise the energy system through biocatalysts, and tried to address step by step all the variables to provide a viable and effective alternative for the conversion of CO₂ into a C-neutral compound (i.e. acetate).

2. How effective is it to exploit residual heat from CO₂ point sources to boost the kinetics of biological reactions?

Until now, MES under thermophilic conditions has been rarely studied, though potential applications would not only reevaluate industrial off-gases but also overcome some of the bottlenecks exposed in the first question. Thermophilic conditions would increase the kinetics of reactions and reduce the risk of microbial contamination, although it reduces the solubility of gases, causing a two-sided effect. On the one hand, less oxygen from industrial gases or from the anodic oxygen evolution reaction would be dissolved in the solution, which is advantageous for anaerobic microorganisms. On the other hand, H₂ and CO₂ solubility would be reduced as well (0.0013 g of H₂ kg⁻¹ of H₂O at 50 °C compared to 0.0016 at 25 °C, and 0.78 g CO₂ kg⁻¹ of H₂O at 50 °C compared to 1.5 at 25 °C), which limits C and energy availability for biotic reactions. In consideration of the foregoing, operational management can become more difficult and many sensors, electrodes and membranes may not be suitable because of their limited temperature range. In addition, to make use of the waste heat from CO₂ emissions, it should be used immediately or stored in a suitable repository to conserve thermal energy.

Intensive research on thermophilic MES is lacking to evaluate its implementation in comparison with other equivalent technologies for the effective conversion of CO₂ streams generated from thermal industrial processes. In this regard, one of the purposes of the present PhD thesis was to assess MES under thermophilic conditions and its influence on the long-term performance concerning operation, production rates, energy efficiency, bacterial community distribution and product selectivity.

3. How can the deployment of renewable electricity be harnessed to boost energy efficiency?

MES relies on electricity-driven microbial reactions to transform CO₂ from a liability into an asset. Since electrical energy is needed, renewables must be used not only as a sustainable alternative but also to make this approach an economically feasible option. However, while CO₂ as the sole C source is suitable for autotrophic electroactive bacteria acting as catalysts, the intermittency of renewable energy as the only electron donor source could adversely influence the microbial community and thus, the overall performance of this technology. This becomes more relevant in off-grid systems for isolated locations without reliance on public utilities. Hence, there is a need for seeking technologies other than conventional lithium-ion batteries able to collect, transport and convert excess energy. While in the field of renewables, intermittency can be seen as an inconvenience, working with living systems can be seen as an opportunity. In the same way that plants run cyclically following the day, using the sun as energy and CO₂ as a C, MES could be combined with AF to produce H₂ when harnessing renewable energy surplus, and use it to mediate the thermophilic conversion of CO₂ to HA even when electricity is no longer provided.

Several studies have been carried out assuming the use of renewable energy in MES. Nonetheless, only a few have determined the influence that continuous power supply interruptions could suppose on the stability of the process. There is a lack of knowledge on the influence of using exclusively the renewable energy surplus and thus, the prolonged effect of the daily repetition of periods with/without electrical connection under thermophilic conditions. In this regard, this PhD thesis focused on assessing the unremitting fluctuation of renewable energy sources to prove the resilience of MES technologies and the possibility to use them connected to an off-grid photovoltaic system.

4. What features can thermodynamics provide to anticipate the outcomes and promote effective use of resources?

The CO₂ conversion to target chemicals is a relatively unknown process with still many gaps in knowledge, especially related to unravelling the optimal working conditions to achieve higher selectivity of the final product. A thermodynamic based-model could be a useful tool to elucidate the appropriate conditions for its conversion focusing on the combination of different parameters such as pH, temperature, substrates ratio, and compounds titers. However, there are only few studies that use thermodynamics beyond the explanation of the results. Experimental tests must address the limited knowledge of the co-effect of working conditions and biology, given that thermodynamics is conditioned by the enzymatic capabilities of each microorganism. However, such a theoretical framework can help conducting laboratory trials (e.g. under specific conditions)

and gaining knowledge to operate larger scale reactors, adjusting feedstock input and thus, minimising losses.

Therefore, the main challenges that hinder a competitive and efficient production should be addressed from a combined approach (theoretical and experimental). In this PhD thesis, fermentative tests were directed from a thermodynamic perspective to foresee and select the putative elongation reactions from CO₂ depending on the operating conditions, evaluating the interaction between reaction energy, kinetics and biology.

5. Tests under industrially relevant environmental conditions for process scale-up. How should a pilot plant be operated to optimise the energy/product ratio?

Flue and gasification-derived gases have been postulated as promising feedstock, containing a high percentage of CO₂ (10–30 % v/v) compared to the atmospheric concentration (0.04 % v/v). However, the usage of these C streams is limited by the high temperature and capture procedure. Because of the flexible design, these compact systems could be operated at the same location where the emissions are produced, avoiding losses and costs associated with transport. In this case, the transition from using synthetic to real CO₂ and a tight control system will determine the transformation of this technology from laboratory scale to real competence in the current market.

The optimisation of operating parameters such as CO₂ supply, pH range, H₂ concentration or electron flow can make the difference between the economic viability or technical defeat of the technology. Therefore, the last objective was to test real industrial exhaust gases and to design, construct and operate a fully automated bench-scale system (TRL 4-5) to optimise the utilisation of both energy and C feed stocks. However, what are still the limiting constraints for the application of this novel bio-based technology to convert a raw C source from flue and gasification-derived gases into value-added products at high selectivity and production rates?

All these uncertainties need clarification. Hence, the present PhD thesis strived to tackle them to help filling the current gaps of knowledge and to determine in which direction the technology should focus soon.

Chapter 3. Materials and methods



3. Materials and methods

This chapter provides an overview of the materials and methods used to conduct the experimental work aimed to address the outlined research questions. A more detailed explanation of this section is presented in each chapter of the results.

3.1. Chemicals and media

All chemicals used in this work were obtained from Sigma-Aldrich (Germany), Merck Life Science (Spain and Germany) and Scharlab S.L. (Spain). A defined low-buffered mineral medium (ATCC1754 PETC) for bacterial growth consisted of a mixture of salts (g L^{-1}): 0.1 KH_2PO_4 , 0.8 NaCl, 1 NH_4Cl , 0.2 $\text{MgCl}_2 \cdot 6\text{H}_2\text{O}$, 0.1 KCl, 0.02 $\text{CaCl}_2 \cdot 2\text{H}_2\text{O}$ and 1.95 $\text{C}_6\text{H}_{13}\text{NO}_4\text{S H}_2\text{O}$ (MES); trace metals (mg L^{-1}): 20 nitrilotriacetic acid, 10 $\text{MnSO}_4 \cdot \text{H}_2\text{O}$, 8 $\text{Fe}(\text{SO}_4)_2(\text{NH}_4)_2 \cdot 6\text{H}_2\text{O}$, 2 $\text{CoCl}_2 \cdot 6\text{H}_2\text{O}$, 0.002 $\text{Zn}_5\text{O}_4 \cdot 7\text{H}_2\text{O}$, 0.2 $\text{CuCl}_2 \cdot 2\text{H}_2\text{O}$, 0.2 $\text{NiCl} \cdot 2\text{H}_2\text{O}$ and 0.2 $\text{Na}_2\text{MoO}_4 \cdot 2\text{H}_2\text{O}$; and vitamins ($\mu\text{g L}^{-1}$): 20 biotin, 20 folic acid, 100 pyridoxine, hydrochloride, 50 thiamine hydrochloride, 50 riboflavin nicotinic acid, 50 DL-calcium pantothenate, 1 vitamin B12. Medium was prepared anaerobically and pH was adjusted to 6.

3.2. Inoculum source and growth conditions

Mixed microbial consortia from an anaerobic digestion (AD) sludge and enriched culture from previous working MECs were used to inoculate the electrochemical reactors used for this PhD thesis. The anaerobic digester inoculum was taken from a conventional wastewater treatment plant (WWTP) located in Girona (Spain), working under 34.5 °C and pH 6.9. It was kept in mild agitation and progressively incubated at higher temperatures up to 50.0 °C using an orbital incubator (SI600 Stuart, UK). During the enrichment stage, 2-bromoethanesulfonic acid (10 mM; Scharlab, Spain) was added to inhibit methanogens, and consecutive transfers to a freshly prepared medium were performed at a 20 % ratio (v/v).

Gas-tight bottles of 1 L and the ATCC1754 PETC medium were used for growth to a minimum OD_{600} of 0.1, maintenance, and pre-adaptation to the specific operational conditions for each test prior to inoculation. Cultures were flushed on a two-three days' basis with a gas mixture of H_2 and CO_2 (80:20 v/v; Praxair, Spain) for approximately 5 min, and kept at an overpressure of 0.5 atm in the dark.

3.3. Reactors set-up and operation

Four different reactor configurations were used during the experiments (**Table 3**): H-type (HT) reactors (chapters 4.1 and 4.2), penicillin bottle reactors (chapter 4.3), Electro-cell (ECell) reactors (chapter 4.4) and Flat plate (FP) reactors (chapter 4.4).

Table 3. Reactor type, inoculum and operating conditions used in each study related to the corresponding results chapter.

Study	Reactor	Inoculum	Operation
Chapter 4.1	H-Type (0.25 L)	Enriched inoculum from an anaerobic digester	Potentiostatic (-0.6 V vs. SHE) 50 °C
Chapter 4.2	H-Type (0.25 L)	Enriched anaerobic digester + from previous MEC	Intermittent power supply Potentiostatic (-0.6 V vs. SHE) Open circuit voltage 50 °C
Chapter 4.3	Penicillin bottles (0.12 L)	Enriched inoculum from fermenter and MEC	H ₂ :CO ₂ (80:20 v/v) Acetate : Ethanol (1:1, 1:3 M) pH 5, 6, 7 25, 37, 50 °C
Chapter 4.4	ECell (3.50 L) Flat-plate (3.10 L)	Enriched inoculum from an anaerobic digester	Galvanostatic (-0.5 to -5 A m ⁻²) 50 °C Real CO ₂ supply*

Real CO₂ supply*: 11.7 % O₂, 73.9 % N₂, 14.4 % CO₂ (v/v)

Most of the bioelectrochemical experiments were carried out under anaerobic conditions and at 50 °C except for chapter 4.3, in which fermentation trials were conducted at different temperatures. Three-electrode/two-chambered systems were used for chapters 4.1 and 4.2, whereas the number of chambers increased up to 5 when using ECell configuration in chapter 4.4. All experiments were carried out under dark conditions to avoid phototrophic activity and in batch mode, spot feeding with CO₂ as a C source, and following different strategies depending on the test (details specified in each chapter of results).

3.3.1. H-type reactors

The experiments presented in chapters 4.1 and 4.2 were performed in HT reactor set-ups to prove the thermophilic CO₂ reduction to HA and the possibility to operate them using only renewable energy surplus. They consisted of double-chamber glass vessels (Pyrex V-65231; Scharlab, Spain) with a total volume of 0.25 L (**Figure 6**) separated by a cationic exchange membrane (CMI – 1875 T; Membranes International, USA). The liquid volume accounted for 0.22 L and the headspace for 0.03 L. The system was operated using a cathodic electrode of commercial carbon cloth (NuVant's

ELATs LT2400W, FuelCellsEtc, USA) with a working surface area of $3 \times 10^{-3} \text{ m}^2$, an anodic electrode of graphite rod ($2 \times 10^{-6} \text{ m}^3$ of volume, Grade 2191; Mersen, Spain) acting as a counter, and a reference electrode of Ag/AgCl in saturated KCl (+0.197 V vs. the Standard Hydrogen Electrode (SHE), RE-5B, BASI, UK) placed in the cathodic chamber. The carbon cloth was connected to a stainless-steel wire functioning as an electrical conductor. The cathodic compartment had two butyl-rubber sampling ports for gas and liquid analyses and the cells were either wrapped with a coil of plastic tubing connected to a thermostatic bath (Polyscience, 8212A12E; Scharlab, Spain), or placed inside an orbital incubator to control the temperature of operation at 50 °C. A magnetic stirrer (Agimatic-ED-C; Scharlab, Spain) or the orbital incubator operating at 100 rpm ensured the mixing of the medium.

The MECs were filled with synthetic medium and in the case of cathodic chambers, with a 20 % of the inoculum. They were sparged with CO₂ (99.9 %; Praxair, Spain) at a flow rate of 0.1 L min⁻¹ for 10 min to achieve anaerobic and C-rich conditions. During the experiments, synthetic CO₂ or real exhaust gas containing 11.7 % O₂, 73.9 % N₂ and 14.4 % CO₂ was provided every one to three days by routinely sparging the catholyte or adding it up to an overpressure of 0.5 atm to avoid H₂ loss. The pH was initially adjusted at 6.0 and later followed to track the effect of H₂ and HA productions. The MECs were operated at a fixed working electrode potential (usually -0.6 V vs. SHE) using a potentiostat (Potentiostat /Galvanostat VSP; BioLogic Science Instruments, France) and other electrochemical techniques were occasionally performed (section 3.5).

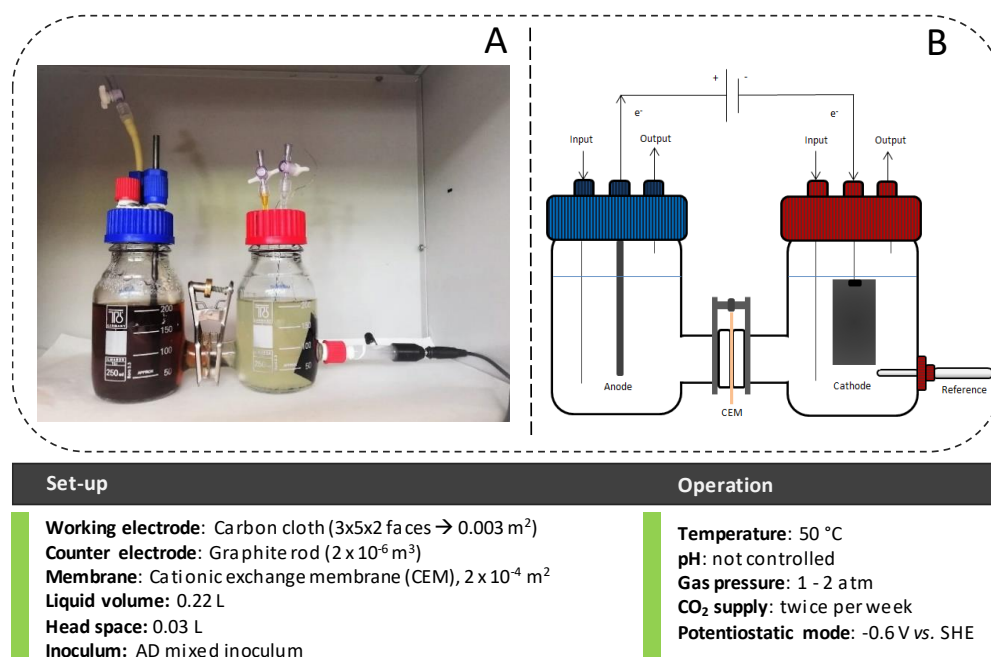


Figure 6. Photograph (A) and schematic (B) representation of the assembly and operation of the H-types reactors.

3.3.2. Penicillin bottles fermenters

The simplest configuration was used to carry out fermentative processes to study the chain elongation reactions presented in chapter 4.3. The penicillin bottles (Z114014; Merck, Spain) consisted of a single chamber of 0.12 L (**Figure 7**), with 0.05 L of the liquid phase and 0.07 L of headspace. They were hermetically closed with rubber stoppers and aluminium caps. Two needles with two-way valves were attached to the butyl rubbers to remove and add medium and gas without compromising the tightness of the stoppers.

They were filled with the synthetic medium (ATCC1754 PETC) and inoculated with a 20 % of enriched mixed culture that previously showed the ability to trigger chain elongation (Romans-Casas et al., 2021). Operational conditions were established at the beginning of each experimental test (see chapter 4.3). Three different temperatures (25, 37 and 50 °C) were applied either with an Advanced Programmable Heated Circulator thermostat bath (AP28H200A1, Spain), or with the orbital incubator. pH was set at 5.0, 6.0 or 7.0 and punctually adjusted throughout the tests by adding 1 M sodium hydroxide or 1 M hydrochloric acid (Scharlab, Spain). Ethanol (99 %; Sigma-Aldrich, Germany) was added in different concentrations to test its effectiveness as a reducing agent. Twice a week, the fermenters were sparged with a gas mixture of H₂ and CO₂ (80:20) or with pure CO₂ to an overpressure of 1 atm. They were kept in agitation (MM90E; OVAN, Spain) to keep biomass in suspension and promote mass transfer, and in the dark to avoid photosynthetic growth.

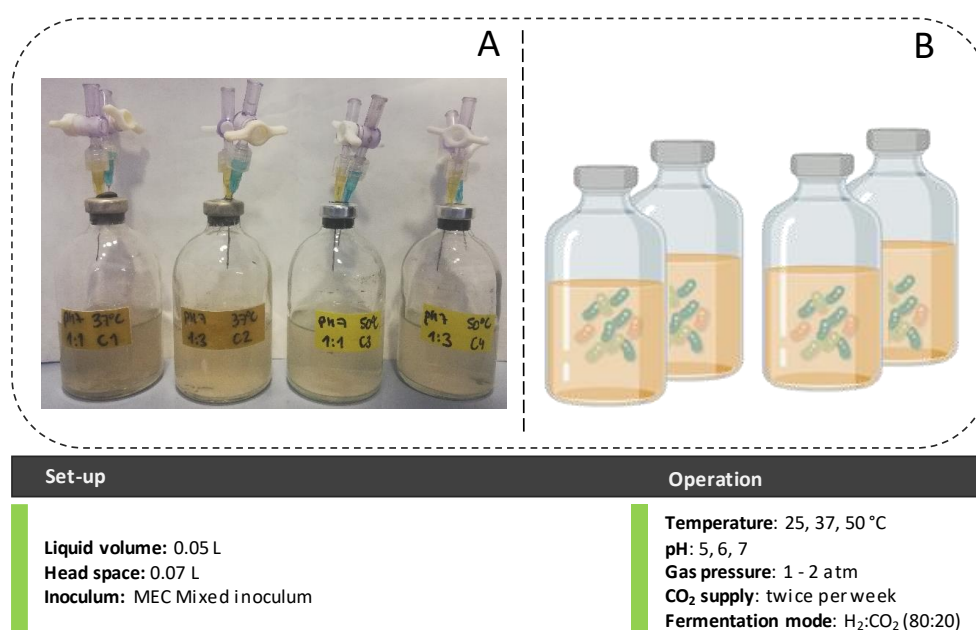


Figure 7. Photograph (A) and schematic (B) representation of the assembly and operation of the serum bottles set-ups.

3.3.3. ECell reactors

A plate-and-frame Electro MP Cell (ECell model 1735; ElectroCell A/S, Denmark) designed for process evaluation and experimental testing was used in chapter 4.4 to improve performance and bring the systems closer to full scale. It consisted of two stainless steel end plates (**Figure 8**), compacting two types of electrolyte distributor racks (PVDF frame sets) that separated two anodic compartments from three cathodic ones by cationic exchange membranes (Nafion N324). 1mm EPDM rubber gaskets were placed between the PVDF frame sets to avoid leaks. The electrodes consisted of graphite plates (SIGRAFINE® R8710; FuelCellStore). Three of them functioned as working electrodes (4 operative faces; surface area of 0.04 m²) and the two rest served as counter electrodes (4 operative faces; surface area of 0.04 m²). The ECells were operated under GA control through a programmable logic controller (Haiwell PLC - H02PW, China) connected to a power supply unit (MQR120-24F; Mibbo, China), fixing the cathodic current and tracking the cell voltage evolution over time. The cathodic and anodic compartments accounted for 0.4 L each, and the medium was injected in parallel from the bottom to the top of the cell, following a cross-flow distribution.

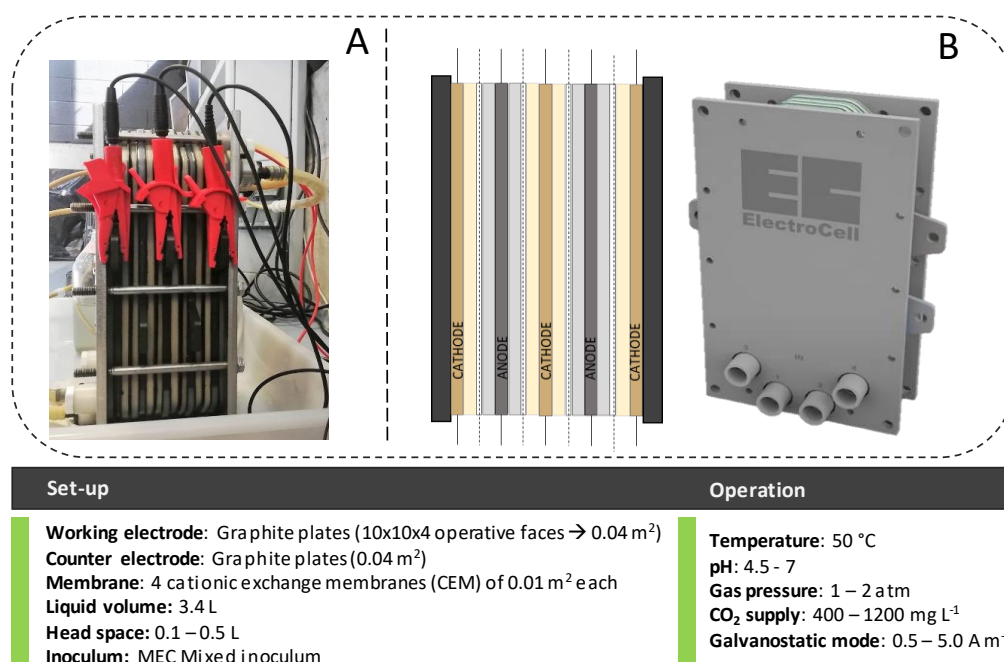


Figure 8. Photograph (A) and schematic (B) representation of the assembly and operation of the ECell reactor set-ups.

The assembly of the pilot plant and the commissioning of the electrical system were carried out by Telwesa and Casas Masgrau SA, Spain. pH (easySense pH 32; Mettler Toledo, Spain), electric conductivity (EC) (easySense Cond 77; Mettler Toledo, Spain), pressure (PA3526; ifm, Spain),

temperature and dissolved CO₂ (InPro® 5000(i); Mettler Toledo, Spain), H₂ (H2100 microsensor; UniSense, Denmark) and O₂ (easySense O₂ 21; Mettler Toledo, Spain) content were monitored by in-line probes in the recirculation loop placed in a continuous stirred (HYCC, EEUU) probe holder (Figure 9). They were controlled by actuator pumps and a multi-transmitter (Multi-parameter Transmitter M200; Mettler Toledo, Spain) that supplied the required component on demand through a remote access tool (EasyAccess 2.0) and an operation interface software (cMT Viewer) (Figure 10). An Ag/AgCl reference electrode was placed also in the recirculation loop for proper electrochemical control. A 1 L capacity buffer tank (T1) and a gas/liquid separation module (0.5 L) made of methacrylate were installed before and after the ECell respectively, and several electro-valves (Solenoid GEM-SOL PN10; Regaber, Spain) were placed in different points of the circuit to keep the total system pressure below 2 atm in the case of high H₂ production. A one-way check valve (SS-XSF4; Swagelok, Spain) was installed after the separation module to avoid a decrease of pressure below 1.5 atm every time the electro-valve opened. Two automatic air vents (70037; Genebre, Spain) and multi-layer foil gas sampling bags of 3 L capacity (22951; Restek, Spain) were disposed at the output of T1 and the separation module for gas analysis, while an exhaust valve was set at 2.1 atm as a safety measure. The level of liquid in T1 was measured with two pressure transmitters with ceramic measuring cells (PA3526; ifm, Spain). An ultrafiltration module (MO P1C; Berghof GmbH, Netherlands) downstream of the reactor ensured the retention of the biomass within the system in case of possible continuous operation, while the effluent with the final product could be collected free of microorganisms.

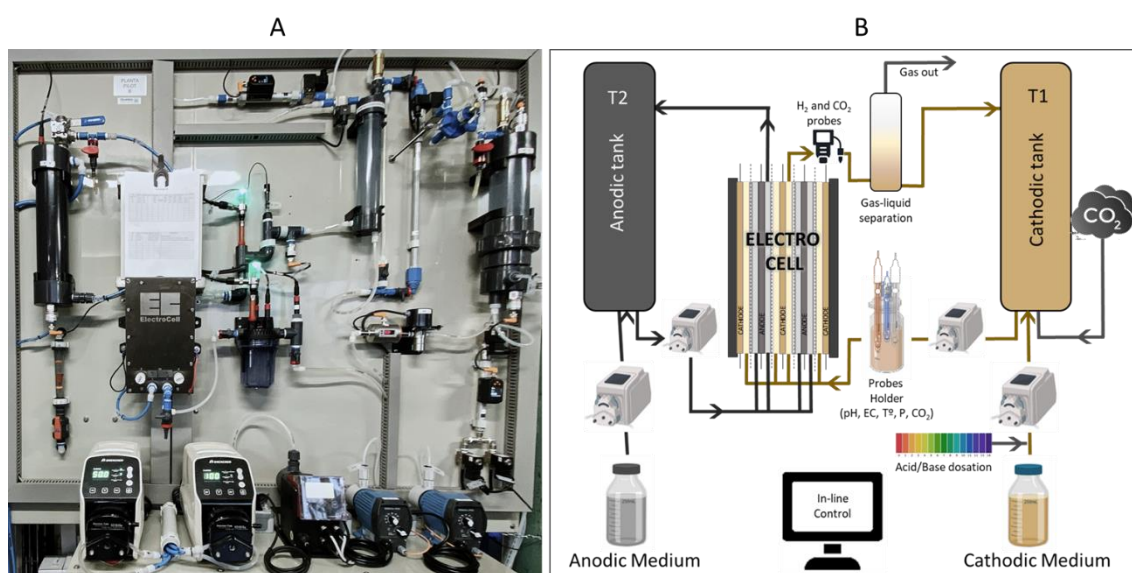


Figure 9. Photograph (A) and schematic (B) representation of the ECell reactor operating circuit

The cathodic circuit was filled with 3 L of mineral growth medium (ATCC1754 PETC) and 0.4 L of enriched inoculum with a digital dosing pump (DDC 15-4; Grundfos, Spain), and the mixture was recirculated by a micro-pump (85376; MicroPump, USA) at a flow rate of 0.1 L min⁻¹ to ensure mixing of the medium. The current of the working electrode was fixed at a range of 0.5 - 5.0 A m⁻² and the temperature at 50 °C using a circulation ultra-thermostat (Digit-cool 3001373; Selecta, Spain) and a thermal heating mat (Lerway, Spain) that surrounded T1. CO₂ concentration was kept between 400 and 1200 mg L⁻¹ by using a magneto-inductive flowmeter (SM4100; ifm, Spain) installed and connected to a gas bottle (99.9 % CO₂) to keep the set point. A pH control system pumped HCl or NaOH 5M using electromagnetic diaphragm dosing pumps (DOSATec PCO; Dosatron, Spain) to the medium when required to maintain a pH range between 4.5 and 7.0. Gas flow meters (Digital Flow Switch PF2M721; SMC, Spain) were installed in the inlet and outlet of the circuit to quantify the CO₂ conversion and H₂ production rates. The anodic circuit was filled with 2.4 L of mineral medium and recirculated at the same flow rate as the cathodic one using peristaltic pumps (M6 series; Shenchen, China). pH and liquid levels were monitored inside the buffer tank (T2) to check proper operation and it was kept open to the atmosphere to avoid overpressure due to possible O₂ production.

Gas samples were daily taken to check and recalibrate the dissolved gas sensors, while liquid samples were taken from 2 to 7 days per week, depending on the experimental period, for the quantification of volatile fatty acids. At the end of each test, 80 % and 100 % of the cathodic and anodic media, respectively, were drained and replaced by a fresh medium to start the following one.

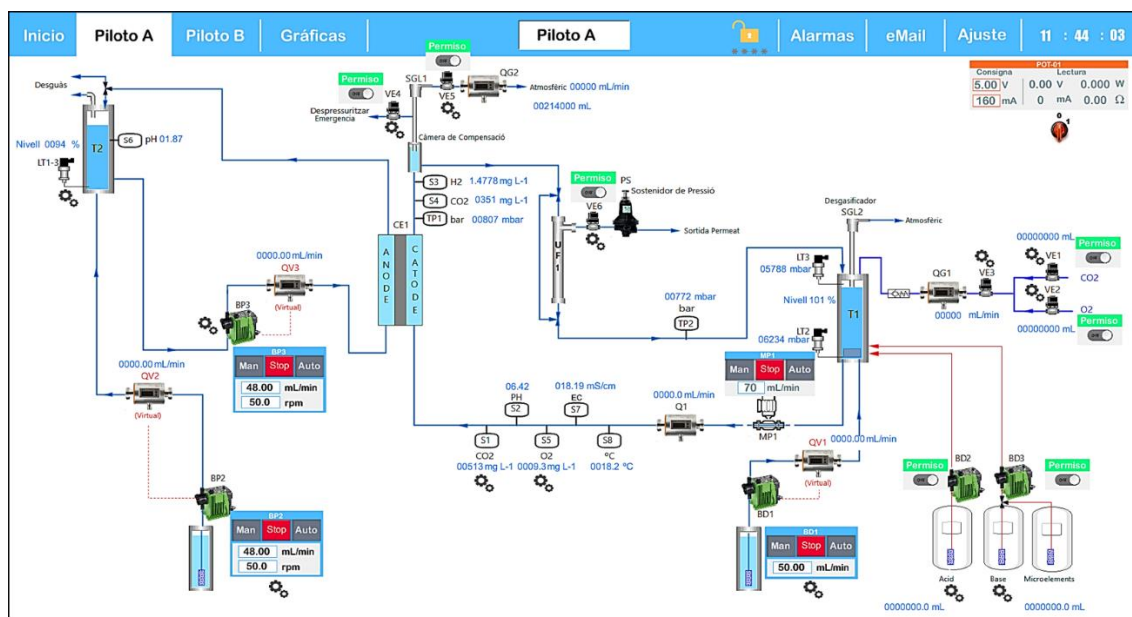


Figure 10. Schematic diagram of the ECell reactor programmable commands

3.3.4. Flat-plate reactor

A FP reactor (**Figure 11**) consisting of two methacrylate compartments of 0.19 L each separated by a cationic exchange membrane (CMI-1875T, Membranes international, USA) of 0.008 m² (4.4 cm width and 18.8 cm length) was used to test different design and materials in the pilot plant. The anode consisted of 0.013 m² (4.3 cm width and 15 cm length) of commercial carbon cloth (Thickness 490 μm; NuVant's ELAT, LT2400W, FuelCellsEtc, USA) connected to a carbon rod (0.45 cm diameter and 4.4 cm of length, Mersen Iberica, Spain) and the same, a 0.013 m² carbon cloth in contact to a carbon rod was used as cathode electrode. The reactor was operated under GA control fixing the cathodic current at 5 A m⁻² and the same temperature, mixing and control conditions as in the ECells were applied for this set-up.

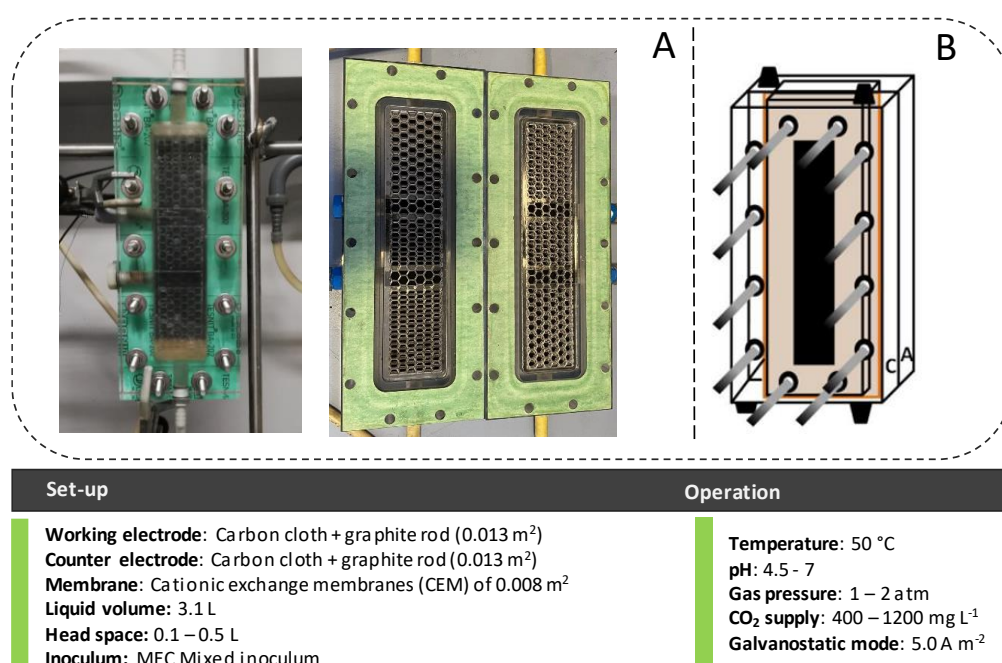


Figure 11. Photographs (A) and schematic (B) representation of the assembly and operation of the Flat-plate reactor set-up.

3.4. Analytic methodologies

Parameters such as gas pressure, gas composition in the headspace, pH, EC and optical density (OD) were measured every 2-4 days in chapters 4.1, 4.2 and 4.3, and every 5-min interval in chapter 4.4. The electric consumption (intensity demand in chapters 4.1 and 4.2, and cell voltage in chapter 4.4) was recorded every 5 min and the concentration of organic substances in the liquid phase was measured periodically at different time intervals depending on each test.

3.4.1. Photometric measurements

The cell density of the bulk liquid was measured photometrically with a spectrophotometer (Thermo Fisher Scientific, USA) at a wavelength of 660 nm (OD_{660}) using distilled water as a blank. OD measurements were converted into dry cell weight (DCW) by the following empirical determined conversion factor: $DCW (g L^{-1}) = m \times OD_{660}$; where m is $0.57 g L^{-1}$ of DCW.

3.4.2. Physicochemical analyses

Measurements for pH and EC were performed with a pH-meter (pH -meter basic 20+; Crison, Spain) and an EC meter (EC-meter basic 30+; Crison, Spain), respectively. The pressure of the gas phase in the headspace was measured with a differential manometer (Model-512; Testo, Germany) in the case of chapters 4.1, 4.2 and 4.3. In-line measurements performed in chapter 4.4 have been described in section 3.3.3.

3.4.3. Gas-chromatography analysis for gas samples

Anaerobic conditions, H_2 production, availability of CO_2 and the eventual CH_4 formation during MES experiments were determined by quantitative analysis of gas samples from the reactor headspace *via* gas chromatography (GC). Samples were collected with a glass syringe (500 μ L Samplelock; Hamilton, USA) and subsequently analysed in an Agilent 490 Micro GC (Agilent Technologies, USA) equipped with a Molesive 5 Å and PoraPLOT U columns in parallel coupled to a TCD detector. High purity argon was used as carrier gas at a flow rate of $28 ml min^{-1}$ and a pressure of 135.7 kPa. The chromatograph injection port, oven and detector were operated at 75, 45 and 100 °C, respectively.

3.4.4. Gas-chromatography analysis for liquid samples

Samples of the liquid phase were taken routinely from the anodic and cathodic broths (approximately every 2 to 4 days) and filtered immediately through a 0.22 μ m pore filter (GSWP04700; Merck, Spain) for analysis of volatile fatty acids (VFA) and their corresponding alcohols *via* GC. GC analysis was performed using an Agilent Technologies 7890A GC System (Agilent, USA) equipped with a polar capillary column (DB-FFAP 30 m x 0.53 mm x 1.0 μ m) and flame ionization detector (FID, make-up flow of $10 ml min^{-1}$ of N_2 and 250 °C). Samples were acidified with ortho-phosphoric acid (85 %; Scharlab, Spain) and an internal standard (crotonic acid $0.5 g L^{-1}$; Scharlab, Spain) was added before the analysis to ensure the results obtained. 0.2 μ L of each sample were injected in pulsed splitless at 220 °C. High purity helium gas was used as carrier gas. The analyses were performed using the following temperature programme: 2 min at

60 °C, 20 °C min⁻¹ to 240 °C, hold for 2 min. For quality control of the GC results, random samples were analysed in duplicate.

3.5. Electrochemical analyses

Two models (SP-50 and VSP) of the potentiostat (BioLogic, France) were used with a three-electrode configuration to poise the cathode potential to the desired value in chapters 4.1 and 4.2. The working electrode (WE) was always the cathode electrode and it was placed close to the reference electrode (RE) for potentiostatic control, while the counter electrode was placed in the anodic chamber. The MECs were operated in chronoamperometry (CA) mode at a poised cathode potential of -0.6 vs. SHE. The current demand, cell potential and power consumption among other parameters were monitored at a 5-min interval. In chapter 4.4, the pilot plant was operated in GA at a fixed current supply, ranging from 0.5 to 5.0 A m⁻². The rest of variables were also monitored at a 5-min interval.

3.5.1. Cyclic voltammetry (CV)

CV was used to characterize the (bio)H₂ production. Several CVs were performed under abiotic and biotic conditions to decipher what % of the total was produced biotically. The same three-electrode set-up was used as described in the prior section (3.3) for each reactor configuration. For the CV measurements, current profiles of 4 repeated cycles were recorded by scanning the cathode potential at a scan rate of 0.5 mV s⁻¹ within a potential window between -1.2 to 0.0 V vs. Ag/AgCl, sufficiently wide to detect oxidation and reduction peaks. During the measurements, the pH and temperature were set to the working conditions.

3.5.2. Coulombic and carbon conversion efficiencies

The percentage of electrons from the cathode recovered in organic C products was provided as the CE calculated per Equation 1 below:

$$CE = \frac{C_i \sum_i n_i F V_{NCC}}{\int_{t_0}^t I dt} * 100 \quad \text{Equation 1}$$

Where n_i is the molar conversion factor (2 and 8 equivalent moles⁻¹ for H₂ and HA, respectively), F is the Faraday's constant (96485 C mol e⁻¹), and I is the intensity demand of the system in A.

C conversion efficiency (CCE) was calculated as the per cent variation between the initial and final samples in a batch (Equation 2).

$$CCE = \frac{\Delta C_{CO_2} - \Delta C_{products}}{C_{CO_2 initial}} * 100 \quad \text{Equation 2}$$

Where ΔC_{CO_2} is the difference in moles of C of CO_2 in the gas plus liquid phases from the beginning to the end of a batch, and $\Delta C_{products}$ is the difference in moles of C of the organic products obtained (i.e. HA) between batches.

3.6. Calculations

3.6.1. Production of gases

Considering the volume, pressure variation and composition of the gas phase, and applying the ideal gas law (Equation 3), the gas production was quantified.

$$PV = nRT \quad \text{Equation 3}$$

Where P is the pressure in atm, V is the gas phase volume in L, n is the number of moles of a substance, R is the ideal gas constant ($0.0821 \text{ L atm mol}^{-1} \text{ K}^{-1}$) and T is the temperature in K.

The concentration of the gases in the liquid phase was calculated according to the Henry's law (Equation 4).

$$C_i = H_i P_i \quad \text{Equation 4}$$

Where C_i is the concentration of the component i in the liquid phase (mol L^{-1}), H_i is the Henry's law constant in $\text{mol L}^{-1} \text{ atm}^{-1}$ of the compound at the experimental temperature and P_i is the partial pressure of the gas component i in atm. P_i is calculated from the total pressure and the molar fraction of i in the gas phase, according to Equation 5.

$$P_i = P_t Y_i \quad \text{Equation 5}$$

Where P_t is the total pressure in atm measured in the head space of the reactor and Y_i is the molar fraction of the compound i in the gas phase.

H_i was calculated as a function of the temperature according to the experimental conditions through Equation 6.

$$H_i = K_i^\circ \exp\left[\frac{-\Delta H_{sol}}{R} \left(\frac{1}{T} - \frac{1}{T^\circ}\right)\right] \quad \text{Equation 6}$$

Where K_i° is the Henry's constant of i at the standard temperature ($T^\circ = 298.15 \text{ K}$) and ΔH_{sol} is the enthalpy of dissolution of i .

The volumetric gas (H₂) production rate (m³ m_{NCC}⁻³ d⁻¹) was calculated according to Equation 7.

$$Q_{H_2} = \frac{\int_{t_0}^t c_{H_2} V_g dt}{V_{NCC}} \quad \text{Equation 7}$$

Where V_g is the produced gas volume in m³ over a period of time (days), c_{H_2} is the composition (v/v) of H₂ in the gas, and V_{NCC} is the net cathode compartment (NCC) volume in m³.

Similarly, the utilisation of CO₂ was calculated from the pressure and composition of the gas phase according to equations 4, 5 and 6.

3.6.2. Production of organics in the liquid phase

Liquid compounds were analysed in terms of product concentration in moles per liter and were usually expressed as the concentration of C in the molecule. Therefore, the moles or millimoles of C per liter (mM C) were calculated according to its molecular weight (MW) and the number of C atoms contained on its structure, as shown in Equation 8.

$$mMC = \frac{c_i n_{c,i}}{M_i} \quad \text{Equation 8}$$

Where c_i is the concentration of the product i in the liquid phase in mg L⁻¹, $n_{c,i}$ is the number of C atoms contained in the molecular structure of i , and M_i is the MW of i in mg mmol⁻¹.

The accumulated products (mg L⁻¹) and the production rate of a compound (Q_i) in g m⁻² d⁻¹ were presented as a function of time through the integration of experimental results following Equation 9 and normalising the values depending on the working surface area (m²) and liquid volume (L) of the cathode.

$$Q_i = \int_{t_0}^t c_i dt \quad \text{Equation 9}$$

The amount of dissociated (A⁻) and undissociated (HA) carboxylic acids was calculated *via* the Henderson-Hasselbalch equation (Equation 10):

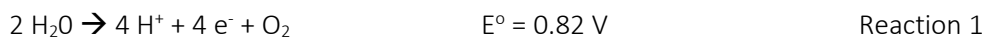
$$pH = pK_a + \log\left(\frac{[A^-]}{[HA]}\right) \quad \text{Equation 10}$$

Where pK_a is the negative of the logarithmic dissociation constant of an organic carboxylic acid HA, that dissociates into the carboxylate A⁻.

3.6.3. Thermodynamics

The reactions occurring in the MECs were analysed in terms of standard potentials for each half-cell reaction at biological conditions (pH 7, 25 °C, 1 atm, 1M) occurring in the anode and cathode,

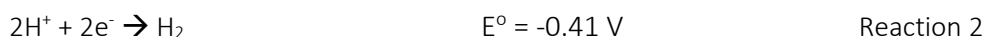
respectively (Bard et al., 1985). Assuming water oxidation in the anodic chamber, the half-redox reaction was written as:



Based on the Nernst equation, the anodic potential (E_{an}) could be calculated using Equation 11, where in the case of water oxidation, E_{an}° is 0.82 V vs. SHE, R is the ideal gas constant (8.31447 J mol⁻¹ K⁻¹), T is the operating temperature (298 K in standard conditions), n is the number of electrons transferred in the reaction (4 for water electrolysis), F is the Faraday's constant (96485 C mol⁻¹) and the *quotient* is the ratio of the products divided by the reactants' concentration in the liquid, raised to their respective stoichiometric coefficients.

$$E_{an} = E_{an}^\circ - \frac{RT}{nF} \ln\left(\frac{[\text{H}^+]^4 [\text{O}_2]}{[\text{H}_2\text{O}]}\right) \quad \text{Equation 11}$$

For the theoretical cathodic potential (E_{cat}), considering that H₂ was used as the electron acceptor and through H₂, CO₂ was converted to HA, the reactions were written as:



Similar to the anodic potential, the cathodic one could be calculated using Equation 12:

$$E_{cat} = E_{cat}^\circ - \frac{RT}{nF} \ln\left(\frac{[\text{H}_2]}{[\text{H}^+]^2}\right) \quad \text{Equation 12}$$

The cell voltage (E_{cell}) could then be calculated using the potential difference between the anode (E_{an}) and cathode (E_{cat}) electrodes (Equation 13), and it was used to determine the process spontaneity, which was calculated according to Equation 14.

$$E_{cell} = E_{cat} - E_{an} \quad \text{Equation 13}$$

$$\Delta G = -n \cdot F \cdot E_{cell} \quad \text{Equation 14}$$

Where E_{cell} units are volts (V), E_{cat} and E_{an} are the half-cell potentials (V) for cathode and anode, respectively, and ΔG is the Gibbs free energy (J) of the overall reaction. Since the equilibrium potential for the proton reduction is -0.41 V vs. SHE (Reaction 2), and the anodic potential for water oxidation is 0.82 V vs. SHE (Reaction 1), the E_{cell} of the overall water splitting reaction at biological standard conditions is -1.23 V, with a ΔG of 237 kJ. Nevertheless, if 50 °C are considered (thermophilic conditions), the ΔG value increases up to 281 kJ, pointing out the effect of temperature in redox reactions.

3.7. Microbial community analyses

Microbial analyses of the biological community in both the carbon cloth electrodes and the bulk liquids of the MECs were performed at different time points during the experiments of chapter 4.1 to follow the microbial growth and community structure.

3.7.1. Microscopy observation techniques

Scanning electron microscopy (SEM) was performed as qualitative microbial analysis in samples extracted from the bulk liquid of the cathodes. The samples were immersed in 2.5 % (w/v) glutaraldehyde in a 0.1 M cacodylate buffer at pH 7.4 for 4 hours. Next, the samples were washed and dehydrated in an ethanol series. Washes were done with cacodylate buffer and with water, both per duplicate. Dehydration with graded ethanol followed temperature steps of 50, 75, 80, 90, 95 and 3x100 °C in periods of 20 min. The fixed samples were dried with a critical-point drier (model 122 K-850 CPD, Emitech, Germany) and sputtered-coated with a 40 nm gold layer. The coated samples were examined with a SEM (model DSM-960; Zeiss, Germany) at 20 kV and images were captured digitally.

3.7.2. DNA extraction and microbial analyses

Biological communities present on the cathode and in the bulk solution were analysed through conventional polymerase chain reaction (PCR). DNA extractions were performed from (i) the pieces of carbon cloth extracted and (ii) the pellets resulting from the centrifugation of the bulk liquid. The cell lysis was achieved through bead-beating with the addition of sterilized 0.2 g of 0.1 mm diameter glass beads and 0.3 g of 0.1 mm diameter silica beads in sterilized 2 mL Eppendorf tubes. The pellets resulting from the settlement of bulk liquid community were re-suspended in 0.31 mL of lysis buffer (40 mM EDTA, 50 mM Tris-HCl; pH of 8.3) and 0.75 M of sucrose. This solution was then added to the previously mentioned Bead-Beater tubes and followed the protocol described elsewhere (Llirós et al., 2008) involving the use of hexadecyltrimethylammonium bromide. In the case of the lysis of the cells forming the biofilm attached to the carbon cloth, a 0.25 cm² piece collected during each sampling was introduced in the 2-mL Bead-beater Eppendorf tube and 0.31 mL of lysis buffer was added. The extraction was also achieved through a protocol described in the same work (Llirós et al., 2008).

3.7.3. Quantitative analysis through qPCR

The determination of the amount of biomass attached to the electrode and present in the bulk liquid was achieved through quantitative PCR (qPCR). Notwithstanding, a previous quantification

was carried out using Qubit® (Qubit® 2.0 fluorimeter; Invitrogen, USA). The qPCR was based on SYBR green technology and targeted the 16S rRNA gene. 10 µL of each sample analysed contained 6 µL of a LightCycler® 480 SYBR® Green (Roche Molecular Systems, USA) mix, 3 µL of MiliQ water and 0,5 µL of each primer (341F/534R) whose design is available elsewhere (López-Gutiérrez et al., 2004). The mixture was added to a 96 microplate and was subsequently added 2 µL of the sample (or 1 µL of the sample plus 1 µL of MiliQ water). Therefore each well contained 12 µL of solution. The microplate was introduced in a LightCycler® 96 (Roche Molecular Systems, USA) that performed a pre-incubation cycle, 40 cycles of amplification and one cycle of analysis of the formed amplicons as stated in the same paper (López-Gutiérrez et al., 2004). The fluorescent signal data was processed with LightCycler software (v.1.1.) and a pattern line resulting from the alignment of all the dilutions of the amplified 16S rRNA was used to obtain the number of copies obtained per sample.

Chapter 4. Results



4.1. Thermophilic bio-electro CO₂ recycling into organic compounds

Laura Rovira-Alsina ^a, Elisabet Perona-Vico ^b, Lluís Bañeras ^b, Jesús Colprim ^a,
M. Dolors Balaguer ^a, and Sebastià Puig ^{a*}

^a LEQUiA. Institute of the Environment, University of Girona. Campus Montilivi,
C/Maria Aurèlia Capmany, 69, E-17003 GironaCatalonia, Spain.
*E-mail: sebastia.puig@udg.edu







^b gEMM. Group of Molecular Microbial Ecology. Institute of Aquatic Ecology,
University of Girona. Campus Montilivi, C/Maria Aurèlia Capmany, 69,
E-17003 GironaCatalonia, Spain

PAPER



Cite this: *Green Chem.*, 2020, **22**, 2947

Thermophilic bio-electro CO₂ recycling into organic compounds†

Laura Rovira-Alsina, ^a Elisabet Perona-Vico, ^b Lluís Bañeras, ^b
Jesús Colprim, ^a M. Dolors Balaguer ^a and Sebastià Puig ^{*a}

Many industrial combustion processes produce carbon dioxide (CO₂) at high temperature, which may be electrically recycled into valuable chemicals using microorganisms as catalysts. However, little attention has been paid to handle the remaining heat of these processes as an alternative to increase CO₂ fixation and production rates. Thus, this study was aimed at steering electro bio-CO₂ recycling into organic compounds under thermophilic conditions. A mesophilic anaerobic sludge was adapted in lab-scale reactors at 50 °C, developing a resilient biocathode. High amounts of acetate (5250 mg L⁻¹) were accumulated during a long-term operation period (150 days). The maximum production rate was 28 g acetate per m² per d, with coulombic efficiencies over 80%. In terms of carbon (C) conversion, 0.31 kg of C as acetate were obtained per 1 kg of C as CO₂ inlet, with an energy demand of 24 kW h per 1 kg of acetate. *Thermoanaerobacterales* appeared to dominate the cathodic chambers, though they were compartmentalized by distinct bacterial communities in the electrode biofilm compared to the bulk liquid. This research delves into the sustained ability of a mixed microbial culture to electrochemically produce organic compounds at 50 °C and considers the possibility of using CO₂-saturated effluents from industrial heated point sources to bring the technology closer to its scale-up.

Received 25th January 2020,
Accepted 31st March 2020

DOI: 10.1039/d0gc00320d

rsc.li/greenchem

1. Introduction

The continuous increase of atmospheric carbon dioxide (CO₂) due to anthropogenic activities as a relevant cause of climate change is out of debate.¹ Industrial combustion processes on a large scale, *i.e.* cement industries and refineries, largely contribute to this increase and are spread all over the globe. The emitted gases from these processes also alter the air temperature in the adjacent areas to the source, whose effects have not been exposed with enough relevance despite having a clear environmental impact. On the other hand, microbial electrochemical technologies (METs) have become a hotspot for the development of a versatile platform for the synthesis of fuels and chemical building blocks from CO₂,² thus partially contributing to mitigate its emissions. Applying an external voltage, hydrogen (H₂) and acetate can be simultaneously generated, using electricity as the only electron donor and CO₂ as the only

electron acceptor. Although acetate has a relatively low economic value, until now it has been the main soluble product obtained and it has been indispensable for chain elongation in secondary fermentation processes.³

The efficient conversion of electric energy into soluble products relies on the performance of catalysts, which can be biological or not. The use of microbial catalytic systems based on CO₂ capture and fixation allows for: (i) the production of CO₂-neutral commodities, (ii) versatile operation modes and (iii) minimizing the competition with food production for high-quality land.⁴ Among the main challenges of microbial catalysts, we should consider: (i) a limited rate and efficiency in the microbial reduction of CO₂ to multi-carbon compounds, (ii) an increased cost due to energy consumption for autotrophic growth, and (iii) an inadequate performance for industrial up-scaling and commercialization.⁴ Some of these bottlenecks can be overcome when working at higher temperatures. A greater reaction activity besides a larger bioavailability of soluble compounds can be achieved under thermophilic conditions (50–65 °C).⁵ Furthermore, the increase in temperature increases the reactions' kinetic constant value, diminishing the activation energy to reach the transition state. An elevated temperature may reduce the risk of microbial contamination, while pushing the proton mass transfer rate through the electrolyte.⁶ Besides, *in situ* product separation may be aided, as intense heat triggers the volatility of organic compounds,

^aLEQUiA. Institute of the Environment, University of Girona. Campus Montilivi, C/Maria Aurèlia Capmany, 69, E-17003 GironaCatalonia, Spain.

E-mail: sebastia.puig@udg.edu

^bgEMM. Group of Molecular Microbial Ecology. Institute of Aquatic Ecology, University of Girona. Campus Montilivi, C/Maria Aurèlia Capmany, 69,

E-17003 GironaCatalonia, Spain

†Electronic supplementary information (ESI) available. See DOI: 10.1039/d0gc00320d

which alleviates the need for additional energy input and further recovery steps.⁷ High temperatures will also reduce the solubility of gases, which will cause a two-side effect. On the one hand, less oxygen will be dissolved in solution, which is advantageous for anaerobic microorganisms. On the other hand, H₂ and CO₂ solubility will be reduced as well, which limits carbon and energy availability for biotic reactions. In consideration of the foregoing, operational management becomes more difficult and many sensors, electrodes and membranes may not be suitable because of their limited temperature range.⁸

Until now, microbial electrosynthesis under thermophilic conditions has been rarely studied, though potential applications would not only reevaluate industrial off-gases but also boost the product separation procedure. The recent advances and range of possibilities for thermophilic microorganisms in METs were first reviewed by Dopson *et al.* (2016)⁴⁰ and recently by Shrestha *et al.* (2018).⁸ Initial studies confirmed H₂ production at 55 °C by a *Firmicutes* population.⁹ Later, Faraghiparapari and Zengler (2017)²² determined the optimal temperature range for acetate generation using two different *Moorella* strains, whereas Yu and colleagues studied the enhancement of applying immobilized cathodes for simultaneous acetate and formate production.⁴ Thermophilic methane (CH₄) production has also been examined by different authors,^{10,11} and the interaction between methanogens and acetogens has been recently explained comparing the microbial communities before and after electricity supply.¹² Regardless of the examples provided above, intensive research on thermophilic METs is lacking in order to evaluate their implementation in comparison with other equivalent technologies for the effective conversion of CO₂ streams generated from thermal industrial processes. In this regard, the purpose of the present work was to unveil the key operational conditions for the thermophilic bio-electro CO₂ recycling into organic compounds and investigate the key limiting factors to enhance high production rates in the long-term.

2. Materials and methods

2.1. Setup. Bioreactor construction and operational conditions

Two H-type METs (Pyrex V-65231 Scharlab, Spain) were constructed (named HT1, HT2) using two identical glass bottles of 0.25 L, separated by a cation exchange membrane (2×10^{-4} m²) (standard CMX Neosepta, Tokuyama Corp., Japan). The cathode consisted of a plain carbon cloth (Thickness 490 μm; NuVant's Elat LT2400 FuelCellsEtc, USA) of 15 cm² (working area of 30 cm²) connected to a stainless steel wire, while the anode was a graphite rod (EnViro-cell, Germany). The anode electrode was replaced every 8 weeks to maintain a stable cell potential. An Ag/AgCl electrode (+0.197 V vs. SHE, model RE-5B, BASI, UK) with an operating temperature range from 0 to 60 °C was placed in the cathode chamber and used as the reference electrode. Reactors were sealed with butyl rubber

caps to prevent gas leakage and were operated in a three-electrode configuration with a potentiostat (BioLogic, Model VSP, France), which controlled the cathode potential at -0.6 V vs. SHE and monitored the current demand. All the potentials reported in this work are relative to the standard hydrogen electrode (SHE) unless otherwise noted. To validate the reproducibility of the process, two extra reactors (HT3, HT4) were constructed using the same configuration and materials, but they were started up with a mixture of HT1 and HT2 effluents after 67 days since inoculation. All systems were operated in batch mode and kept in the dark to avoid the growth of phototrophic microorganisms. The temperature was kept constant at 50 °C either by using an orbital incubator (SI600 Stuart, UK) or externally jacketed reactors (PolyScience, Illinois), and an agitation speed of 80 rpm was fixed (SB 161 Stuart, UK) to enable mixing and facilitate mass transfer inside the cathode chambers.

2.2. Inoculum and growth media

A sample from an anaerobic digester working at 37.5 °C of Girona's wastewater treatment plant (WWTP) located in Spain was used as an inoculum. A 1 : 20 dilution was first incubated in two fermentative reactors to promote acetogenesis. During this enrichment stage, 2-bromoethanesulfonic acid (10 mM) was added to prevent methanogenesis.¹³ After 30 days, 864 ± 17 mg L⁻¹ of acetate had been accumulated, with a maximum production rate of 0.65 mg acetate per mg SSV per d. For the inoculation of the two microbial electrolysis cells (HT1 and HT2), the anaerobic sludge was again diluted 20 times with ATCC1754 PETC medium reformulated to remove all sources of organic carbon (Table 1, ESI†). pH was initially adjusted to 6.0 using NaOH 5.0 M and a methanogen inhibitor was added punctually during the first month. After 67 days of operation, two similar reactors (HT3 and HT4) were inoculated with 18% of the previous ones, 5% of the initial fermentative reactor and 77% of fresh medium (all percentages referred to v/v). Table 2 (ESI)† describes in more detail the operational conditions and inoculation source for each reactor.

2.3. Electrochemical characterization

Preliminary tests were performed in microbial electrolysis cells (MECs) under open/closed circuit and abiotic conditions at different temperatures (25 °C, 37 °C and 50 °C), while the inoculum activity was tested in batch fermentation using 0.1 L penicillin bottles sealed with butyl rubber stoppers and aluminium crimp caps. Software from BioLogic (EC-Lab v10.37) was used to run simultaneous multitechnique electrochemistry routines with a potentiostat, which included chronoamperometry (CA), open circuit voltage (OCV) and cyclic voltammetry (CV). A cathode potential of -0.6 V was fixed for CA whereas its variation was followed during OCV. CV under turnover conditions (in the presence of an electron acceptor) was performed before and after inoculation to qualitatively distinguish between biotic and abiotic performances. Four cycles from -0.2 V to -1 V were performed by imposing a linear scanning potential rate of 1 mV s⁻¹. To represent the results, the

last cycle of every CV is shown. Prior to use, the working electrodes were pre-treated in a 0.5 M solution of HCl and a 0.5 M solution of NaOH for a total of two days, and rinsed with deionized water for an additional day. At the end of the experimental study, the voltage of the reference electrodes was measured to check for any shift that may have occurred during operation.

2.4. Analytical methods and calculations

Samples from the liquid phase were taken twice a week. To maintain a constant chamber volume of 0.22 L, withdrawn liquid during sampling was replaced with freshly prepared medium saturated with CO₂. Measurements for conductivity and pH were performed with an electric conductivity meter (EC-meter basic 30+, Crison, Spain) and a multimeter (MultiMeter 44, Crison, Spain), respectively, which were calibrated to analyse at 50 °C. The concentration of organic compounds (volatile fatty acids and alcohols) in the liquid phase was assessed using an Agilent 7890A gas chromatograph equipped with a DB-FFAP column and a flame ionization detector.

A mixture of CO₂ and H₂ (20 : 80 v/v) (Praxair, Spain) was bubbled into the fermenters, while pure CO₂ (99.9%, Praxair, Spain) was used to feed the four MECs. Gas was sparged for 10 minutes in the cathode chamber every 2–3 days. To quantify gas production in the MECs, the pressure in the headspace of the reactors was measured using a digital pressure sensor (differential pressure gauge, Testo 512, Spain) and gas samples were analysed periodically during experiments by gas chromatography (490 Micro GC system, Agilent Technologies, US). The GC was equipped with two columns: a CP-molesive 5A for CH₄, carbon monoxide (CO), H₂, oxygen (O₂) and nitrogen (N₂) analysis, and a CP-Poraplot U for CO₂ analysis. Both columns were connected to a thermal conductivity detector (TCD).

The concentration of dissolved H₂ and CO₂ in the liquid media was calculated using Henry's law at 50 °C (eqn (1)), where C_i is the solubility of a gas in a particular solvent (mol L⁻¹), H_i is Henry's law constant in mol L⁻¹ atm⁻¹ (0.0007 for H₂ and 0.0195 for CO₂) and $P_{\text{gas } i}$ is the partial pressure of the gas in atm.

$$C_i = H_i P_{\text{gas},i} \quad (1)$$

The coulombic efficiency (CE) for the conversion of current into products was calculated according to the study by Patil *et al.* (2015)⁴¹ (eqn (2)). C_i is the compound i concentration in the liquid phase (mol L⁻¹), n_i is the molar conversion factor (2 and 8 eq. mol⁻¹ for H₂ and acetate, respectively), F is Faraday's constant (96 485 C mol e⁻¹), V_{NCC} is the net liquid volume of the cathode compartment (L), and I is the intensity demand of the system (A).

$$\text{CE}(\%) = \frac{C_i \cdot \sum_i n_i \cdot F \cdot V_{\text{NCC}}}{\int_0^t I \cdot dt} \times 100 \quad (2)$$

Carbon conversion efficiency (CCE) was calculated as the percent variation between the initial and final samples in a

batch as stated in eqn (3). ΔC_{CO_2} is the difference of CO₂ in the gas plus liquid phases from the beginning (immediately after feeding the system) to the end of a batch, and $\Delta C_{\text{products}}$ is the difference of organic products (*i.e.* acetate) between batches.

$$\text{CCE}(\%) = \frac{\Delta C_{\text{CO}_2} - \Delta C_{\text{products}}}{C_{\text{CO}_2 \text{ initial}}} \times 100 \quad (3)$$

2.5. Extraction of DNA and microbial community structure determination

Samples of carbon cloth and bulk liquid for each reactor were taken at different operation times to assess the microbial community composition. Samples were extracted at 133 and 228 days of operation for HT1, 152 and 228 for HT2, 84 and 160 for HT3 and 65 and 160 for HT4. Before DNA extraction, bulk liquid cells were pelleted by centrifugation, whereas carbon cloth samples were used directly. DNA was extracted using a FastDNA® SPIN kit for Soils (MP Biomedicals, USA) following the manufacturer's instructions. The extracts were distributed in aliquots and stored at -20 °C, and the DNA concentration was measured using a Nanodrop™ 1000 spectrophotometer (Thermo Fisher Scientific, USA). The quality of DNA extracts for downstream molecular applications was checked after PCR detection of 16S rRNA using the universal bacterial primers 27F and 1492R.

The hypervariable V4 region of the 16S rRNA gene was amplified using the primers 515F and 806R following the method described by Kozich and Schloss, which was adapted to produce dual-indexed Illumina compatible libraries in a single PCR step.¹⁴ First, PCR was performed using fusion primers with target-specific portions¹⁵ and Fluidigm CS oligos at their 5' ends. Second, PCR targeting the CS oligos was used to add sequences necessary for Illumina sequencing and unique indexes. PCR products were normalized using Invitrogen SequalPrep DNA normalization plates and the pooled samples were sequenced using an Illumina MiSeq flow cell (v2) in a 500-cycle reagent kit (2 × 250 bp paired-end reads). Finally, sequencing was performed at the RTSF Core facilities at the Michigan State University USA (<https://rtsf.natsci.msu.edu/>).

Sequences were filtered for minimum length (>250 nt) and maximum expected errors (<0.25). Paired-end sequences were merged, quality filtered and clustered into OTUs (operational taxonomic units) using USEARCH v9.1.13.¹⁶ They were clustered at the 97% identity using UCLUST,¹⁷ and checked for the presence of chimeras. OTUs containing only one sequence (singletons) were removed. The subsequent analyses were performed with Qiime v1.9.1.¹⁸ Representative OTU sequences were aligned using PyNAST with default parameters against Silva 132 release (April 2018). The same reference database was used to taxonomically classify the representative sequences using UCLUST. Direct BLASTn searches at the NCBI of selected sequences were used when poor identifications with the Silva database were obtained. Sequences presented in this study have been submitted to the GenBank database within the SRA accession number PRJNA557160.

Samples from the reactors' cathode HT1–2 and HT3–4 were taken for SEM imaging after 228 and 160 days of operation, respectively. They were immersed in a 0.1 M cacodylate buffer solution at pH 7.4 with 2.5% (w/v) glutaraldehyde for 4 hours. After immersion, they were washed twice with cacodylate buffer and water, and dehydrated in an ethanol series. Dehydration with graded ethanol followed the temperature steps of 50, 75, 80, 90, 95 and 3 times 100 °C in periods of 20 minutes. The fixed samples were dried with a critical point dryer (model K-850 CPD, Emitech, Germany) and sputtered-coated with a 40 nm gold layer. The coated samples were examined with a SEM (model DSM-960; Zeiss, Germany) at 20 kV. Images were captured digitally using ESPRIT 1.9 BRUKER software (AXS Microanalysis GmbH, Germany). All analyses were performed in the *Serveis Tècnics de Recerca (STR)* at the University of Girona.

3. Results and discussion

3.1. Selection of the operational conditions to reinforce hydrogen production

The effect of cathode potential and temperature on electrochemical H₂ production and energy consumption was first assessed in duplicate to fix optimal working conditions in the H-type reactors. Regarding temperature, the cathode potential was set at –0.8 V, and electrochemical H₂ production was then studied in terms of volumetric load and electric energy consumption (Fig. 1A). The relationship between both parameters for each temperature was found to be linear (R^2 between 0.995 and 1), as other studies also pointed out.¹⁹ The H₂ production rate per unit of energy consumed was higher at 50 °C (218 m³ H₂ per m³ NCC per d) in contrast to that at 37 or 25 °C (124 and 80 m³ H₂ per m³ NCC per d, respectively). Similarly, Chris Van de Goor and co-workers concluded that higher temperatures positively influenced the hydrogen evolution reaction on platinum electrodes by decreasing the overpotential and modifying the activation energy.²⁰

The H₂ production rate at 50 °C was also tested at different potentials in terms of volumetric load and electric energy consumption (Fig. 1B). The results showed a linear correlation between H₂ production and energy consumption (R^2 between 0.982 and 0.997). Higher H₂ production for the same energy consumption was obtained when the cathode potential was fixed at less negative values, in agreement with previous studies.²¹ At –0.4 V, almost no production was observed. At –0.6 V instead, H₂ generation was slower but more electrically efficient compared to that at –0.8 V.

According to the results, the conditions were set as 50 °C and –0.6 V in subsequent experiments to produce H₂ as reducing power for acetate generation. However, a wider temperature and potential range screening could give insight into the most appropriate configuration.

3.2. Long-term operation of thermophilic METs

The start-up time of MEC reactors was reduced to 10 days (Fig. 2) and after 150 days of operation, the accumulated acetic

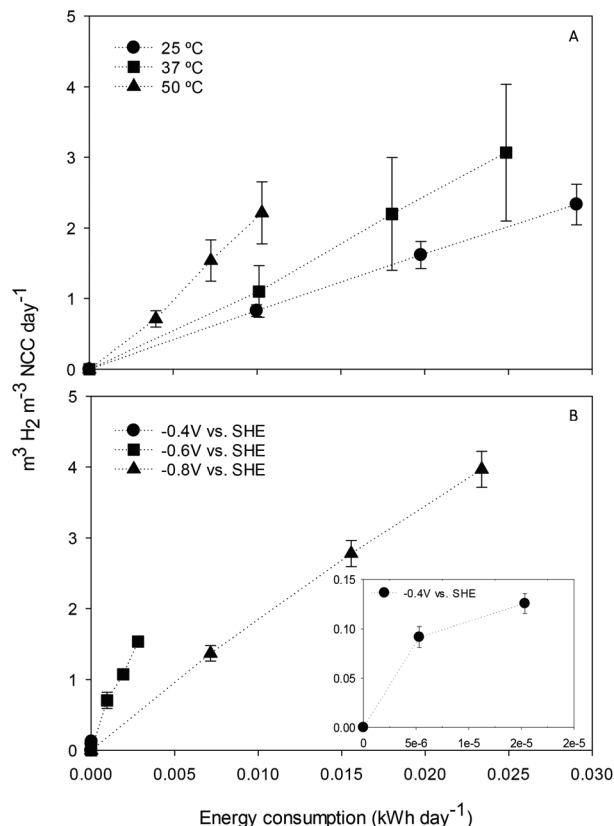


Fig. 1 Electrochemical hydrogen production over electric energy consumption at –0.8 V and different temperatures (A), or 50 °C and different poised cathode potentials (B). The error bars represent the deviation between the two reactors tested.

acid concentration reached 3640 ± 1200 mg L⁻¹ on average, with a maximum production rate of 286 ± 126 mmol acetate per m² per d. Specifically, HT3 achieved the highest concentration and production rate, with a maximum titer of 5250 mg L⁻¹ and 468 mmol acetate per m² per d, respectively.

The number of studies focusing on the bioelectrochemical synthesis of acetate under thermophilic conditions is scarce (Table 3, ESI).[†] Using electricity and CO₂ as the sole carbon source to feed *Moorella thermoautotrophica* at 50 °C, Yu and co-workers achieved an acetate production rate of 58.19 mmol m⁻² d⁻¹.⁴ However, a different study working with the same strain at 60 °C obtained a much lower rate, 3.5 ± 0.3 mmol m⁻² d⁻¹.²² Recently, Song *et al.* (2019b)¹² continuously purged CO₂ with a gas diffuser into a membrane-less reactor. This configuration decreased the internal resistance, which may have helped to obtain a higher acetate titer compared to the present work (10 500 mg L⁻¹). However, at a similar fixed potential (–0.65 V), the maximum product formation velocity was lower (160 mmol acetate per m² per d). One of the main challenges in MEC research is to know how to maintain microbial activity for sustained long-term production.²³ The mixed community of this study could remain active for a long time period (>150 days), which is a reasonable time span to consider thermophilic systems as a reliable oper-

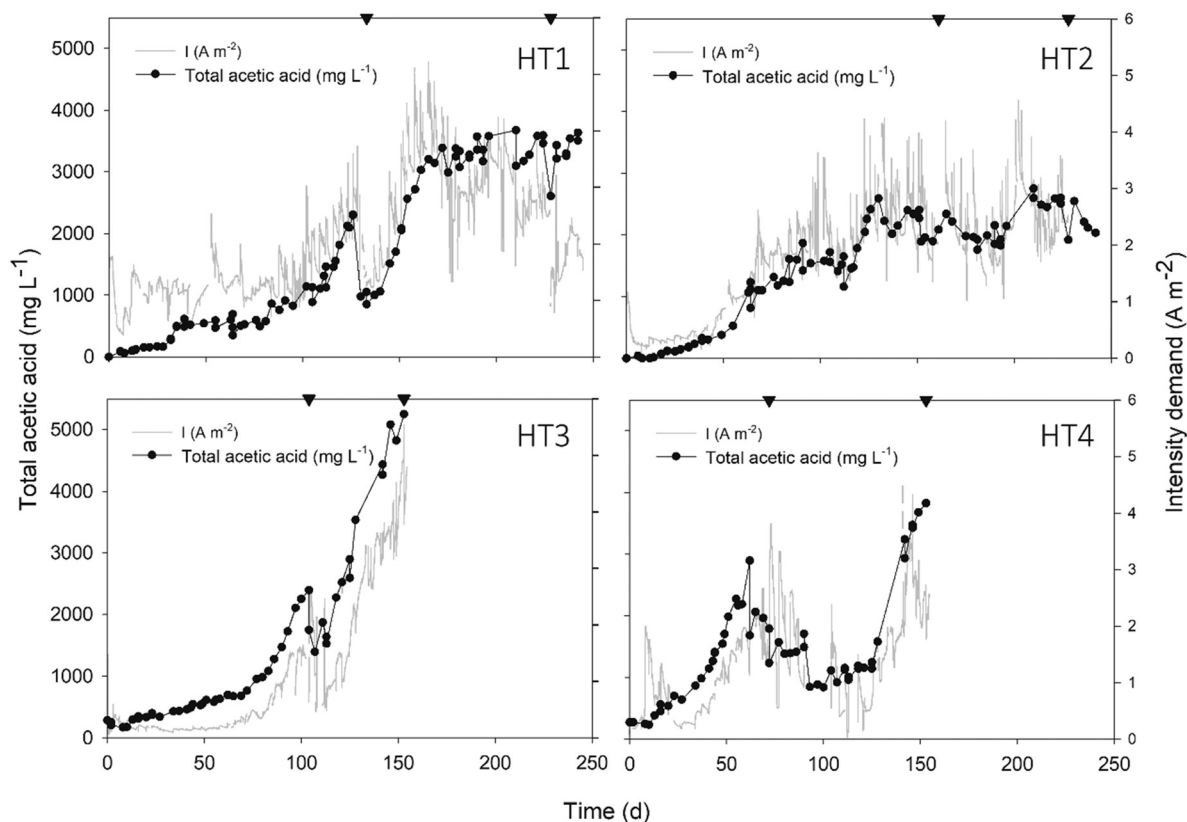


Fig. 2 Total acetic acid concentration (anode + cathode in mg L^{-1}) and intensity demand profiles (A m^{-2}) over time in four different reactors. Acetic acid concentration in the anodic chamber accounted for 20% of the total amount. Sampling points for DNA extraction are indicated by inverted triangles and CO_2 was sparged to feed the system every time a sample was taken.

ation in MEC development. This, together with the fact that biofilms grown at higher temperatures are more electro-chemically active than those grown at lower temperatures,²⁴ is a key starting point to encourage active research in thermophilic METs.

Intensity demand seemed to be related to acetic acid concentration, as the same profiles were observed during the overall study (Fig. 2). This might be explained because as acetate was being accumulated over time, the liquid conductivity increased (see Fig. 1, ESI†) and thus, the internal resistance of the bulk liquid diminished. According to Ohm's law and considering a stable cell potential ($E_{\text{cell}}: -3.1 \pm 0.1$, data not shown), the intensity demand was consequently increased.

More than 80% of the electrons were recovered in the form of H_2 and acetate (Fig. 3). The remaining 20% could be attributed to energy consumed for cell maintenance, oxygen scavenging, or simply lost in the system.²⁵ H_2 mainly explained the whole consumption, while acetate varied depending on the exponential period since part of it could be consumed to fermentatively produce other substances. CH_4 and CO were present in trace amounts ($<0.003\%$ v/v). Ethanol was detected transiently at concentrations below 160 mg L^{-1} , whereas butyric, valeric and propionic acids were found in minor amounts ($<50 \text{ mg L}^{-1}$). On average, one-fourth of the total energy consumed ($24 \pm 8 \text{ kW h}$) was destined to obtain 1 kg of

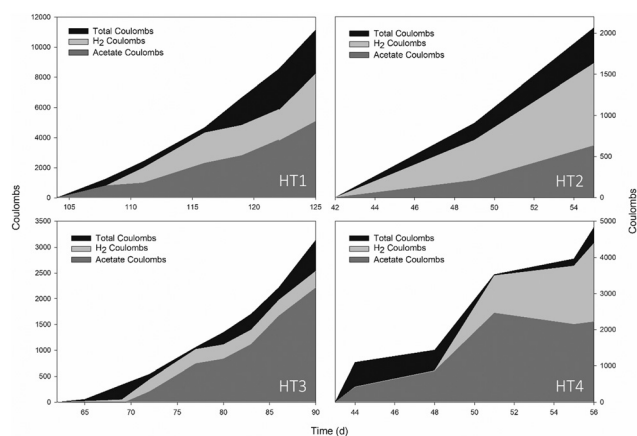


Fig. 3 Distribution of the accumulated coulombs in products compared to total coulombs consumed over time in each reactor. Different intervals have been taken corresponding to the first producing period of each reactor.

acetate while the rest was used for the generation of 1 kg of H_2 ($80 \pm 5 \text{ kW h}$).

CCE fluctuated over time and differed for every feeding interval. Considering that every batch was initiated with approximately 12 mmol of CO_2 (sum of gas and liquid phases),

an average CCE of $45 \pm 16\%$ was obtained for the same producing periods shown in Fig. 3. It means that from the inlet, half of the CO_2 was converted into products, giving an associated carbon ratio from CO_2 to product of 2.22 ± 0.79 mmol C_{CO_2} : mmol $\text{C}_{\text{product}}$ (0.31 ± 0.86 kg of product per kg of CO_2 consumed). A different study for the production of bioplastics obtained a CCE of 73%, in which 0.41 kg of carbon in the form of PHA were generated for every kg of applied carbon as CO_2 .²⁶ The values of the present work are lower, but it must be considered that CO_2 was less available, since the solubility of gases diminishes with increasing temperature. However, with the given data of other thermophilic studies, they cannot be compared to similar systems catalysing comparable end-products. Nevertheless, the low CO_2 solubility at high temperature could be reinforced by using gas diffusion electrodes that enhance mass transport and increase the CCE.³⁹

3.3. Contribution of biofilms to net H_2 production

Elucidating the different operational parameters in METs can give insight into how to steer the system performance. H_2 has been postulated to act as a mediator in redox reactions.¹ Hence, a test to differentiate biotic from pure electrochemical H_2 evolution in the studied MECs was carried out. For this, individual batches considering the time between feeding events were used. The production rate was calculated in each reactor taking into account the H_2 accumulated in the gas plus liquid phases after 4.5 hours. The biotic production was then differentiated from the abiotic considering the H_2 production of the control (Fig. 2a, ESI^\dagger) under the same conditions regarding potential (-0.6 V) and temperature (50 °C) (see section 3.1). Furthermore, to quantify the total bio H_2 formation, the stoichiometric H_2 needed to generate the detected acetate during the same period also had to be considered (Fig. 2c, ESI^\dagger).

During control tests, an abiotic molar rate of 0.77 ± 0.61 mol H_2 per m^2 per d was obtained. This value increased up to 1.25 ± 0.38 mol H_2 per m^2 per d once the reactors were inoculated, and to 8.18 ± 1.51 mol H_2 per m^2 per d when stoichiometric H_2 consumed for acetate generation was contemplated. This means that H_2 production was 10-fold higher in biotic reactors than in the abiotic ones, representing 90.59% of the total production. These values were one order of magnitude above those obtained in other thermophilic studies⁹ even at a less negative fixed potential. They were still low in contrast to those of Ni-based catalysts, although they were similar to those reported in studies that had used stainless steel electrodes.²⁷

Cyclic voltammetry (CV) was performed for abiotic (prior to inoculation) and biotic (42 days after inoculation) conditions, which clearly distinguished the microorganisms' activity (Fig. 4A). With a similar pH (5.86 vs. 5.81, respectively), the intensity demand curve of the biotic system reached 47.5 mA, which compared to the non-inoculated one (8.20 mA) was an indicator of an increase in H_2 production. The presence of redox-active components could not be confirmed in the catho-

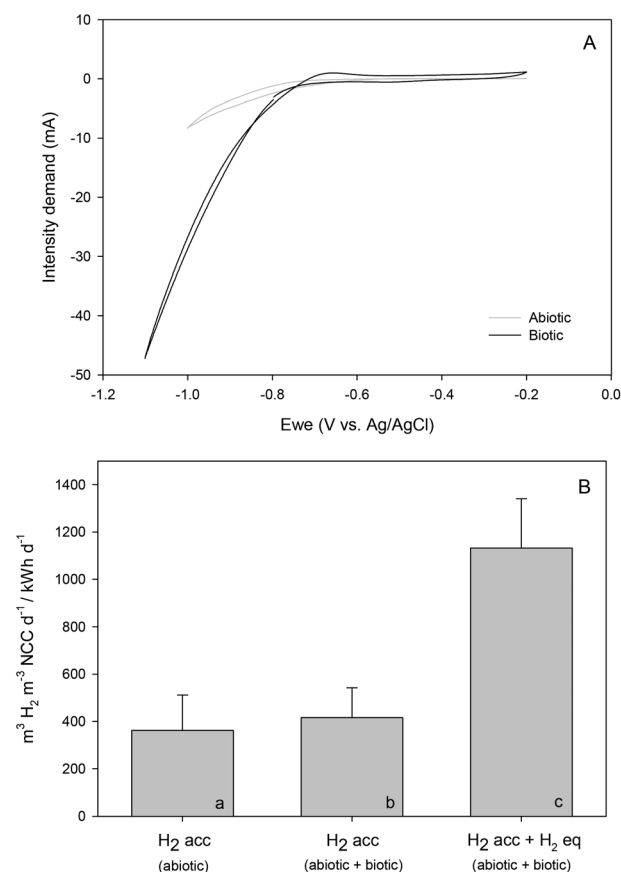


Fig. 4 Comparison between the abiotic and biotic reactors during cyclic voltammetry (A) and H_2 production over the electrical energy consumption test (B) at 50 °C. A distinction has been made between the H_2 accumulation (H_2 acc) in the gas plus liquid phases (a and b) and the H_2 equivalent (H_2 eq.) produced regarding organics concentration in the liquid phase (c).

lyte when microorganisms were not present, with the onset potential of H_2 evolution at around -0.8 V vs. Ag/AgCl.

Meanwhile, a shift to a slightly higher potential of -0.7 V vs. Ag/AgCl was observed when the reaction was bio-catalysed, evidencing hydrogen-mediated production of commodity chemicals.²⁸ These results are clearly shown in Fig. 4B, where the volumetric H_2 rate as a function of electrical energy consumption under abiotic and biotic conditions differed by 70% when considering equivalent H_2 for organics production. The possible role of an enriched electrosynthetic community was also highlighted by other researchers such as LaBelle and co-workers, which was found to lower the H_2 evolution overpotential by 0.25 V.²⁹

3.4. Effects of partial medium replacement on inhibitory mechanisms and acetate productivity

It is well known that regular addition of nutrients into the bulk liquid is necessary to maintain good organic production rates.³⁰ Partial medium replacement has an additional advantage compared to nutrient amendment, which is the dilution of potential inhibitors that may have accumulated during oper-

Table 1 Acetate concentration, production rate, undissociated acetic acid content (HAc), coulombic efficiency (CE), pH and electric conductivity (EC) before and after medium replacement during specific periods in each of the four reactors

Reactor	Before							After						
	Days	Acetate (mM)	Prod. rate (mmol m ⁻² d ⁻¹)	HAc (mM)	CE (%)	pH	EC (mS cm ⁻²)	Days	Acetate (mM)	Prod. rate (mmol m ⁻² d ⁻¹)	HAc (mM)	CE (%)	pH	EC (mS cm ⁻²)
HT1	95–105	19.30	37.00	1.08	54.49	5.74	4.39	105–112	18.00	100.49	0.46	83.09	5.88	10.68
HT2	95–112	27.91	7.90	9.18	30.45	5.53	3.83	112–130	25.95	97.29	3.18	59.53	5.62	9.91
HT3	168–181	65.12	20.18	7.80	12.84	4.83	7.66	183–195	58.22	168.51	7.96	40.17	4.99	6.89
HT4	170–181	49.51	43.15	16.35	30.25	5.21	6.8	183–195	41.50	204.33	2.78	47.78	6.02	8.7

ation. For instance, the accumulation of organic acids and their undissociated forms has been demonstrated to inhibit the metabolic activity of homoacetogens.³¹ In the four thermophilic MECs, we tested the effect of accumulated undissociated acetic acid (HAc) on productivity by substituting part of the cathode compartment with fresh medium in different tests (following the order of reactors, from 15 to 35%).

Every time a part of the medium was replaced, the product formation velocity increased (Table 1). Undissociated HAc seemed to have a minor effect in our systems although estimated concentrations were found in inhibition ranges for homoacetogenic bacteria.³² For instance, similar HAc values before and after medium replacement resulted in an 8-fold increase of acetate production rates in HT3. In other cases, greater productions were found at higher HAc concentrations, (*i.e.* HT4 *vs.* HT1). A second explanation for the observed results was in line with the depletion of an essential component of the medium during batch experiments. In all reactors, acetate production rates increased significantly after medium replacement. The enhancement ranged from roughly 3 times (from 37 to 100 mmol m⁻² d⁻¹ in HT1), to more than 10 times (from 8 to 97 mmol m⁻² d⁻¹ in HT2). In all cases, increments in production rates were concomitant to higher CE. Differently, the substrate (CO₂) was periodically fed during the whole study and it was never entirely consumed, so carbon depletion could also be excluded as a potential factor explaining changes in acetate production.

Further investigation should be focused on the effect of macro and micronutrient depletion as well as the possible excreted inhibitor accumulation.

3.5. Microbial community analysis

At the end of experiments, bacterial cells firmly attached to the cathode surface were clearly visualized in SEM images (Fig. 3, ESI†). Cells appeared to be embedded in a complex matrix, poorly structured in layers, and partly surrounded by tiny particles, most likely ensuring an intimate contact with the electrode surface. The microbial community structure in the four MECs was analysed by barcoded amplicon sequencing of the 16S rRNA gene. Microbial communities in the four reactors were dominated by *Firmicutes* bacteria, accounting for 85–94% in the biofilm and 65–69% in the bulk liquid (Fig. 5). *Proteobacteria* was also present, being more abundant in bulk liquid (26–28%) compared to the biofilm (13–4%). The thermophilic community in both sample types was composed of

the orders *Thermoanaerobacterales*, *Betaproteobacteriales* and *Clostridiales*, the former being the predominant according to relative number of sequences. No methanogenic archaea could be detected in the systems. At the genus level, *Moorella*, *Caloribacterium*, *Desulfotomaculum* and *Tepidiphilus* were the most representative, but at different relative abundances between samples (Fig. 5). Further analysis using BLASTn searches revealed that biocathodes were mainly dominated by *Moorella perchloratireducens* strain An10 (NR 125518.1, 99% sequence similarity) and *Caloribacterium cisternae* strain GL43 (NR 118109.1, 96% sequence similarity).

These results agree with previous analyses of a thermophilic biocathode for H₂ production.⁹ *Moorella thermoacetica* and *M. thermoautotrophica* have been described as electrotroph microorganisms and have been shown to be able to reduce CO₂ to acetate in a wide temperature range (from 25 to 70 °C) in bioelectrochemical systems.²² The sequences found in our systems were more closely related to *M. perchloratireducens* but its putative participation in the electron harvesting process is not known. Except for HT3, relative abundances of *Moorella* related sequences remained at similar values both in liquid and biofilm samples and were sustained through time, posing a reasonable doubt on the participation of this bacterium in electron harvesting in our systems.

In contrast, *Desulfotomaculum* species are considered sulfate-reducing bacteria (SRB). In our systems, they were mainly present in bulk samples and they could probably use sulfate as a terminal electron acceptor to produce reduced hydrogen sulfide (H₂S) when organic substrates were available, but also use CO₂ as the sole carbon source.¹² However, very low amounts of H₂S were found in the liquid media (0.021 ± 0.005 mg L⁻¹). Instead, in CO₂ converting bioelectrochemical systems, SRB such as *Desulfovibrio* and *Desulfobacterium* have been proposed as H₂ producers, electron transfer enhancers and acetate producers.^{33–35} Moreover, they can putatively reduce acetic and butyric acids to the corresponding alcohols or ketones.¹

Differently, in thermophilic microbial fuel cells, Wrighton and co-workers demonstrated the predominance of *Firmicutes* (>50%) in a bioanode community. Those bacteria were electricity-producing members, which used acetate as a carbon source. *Moorella* and *Desulfotomaculum* related sequences were identified as presumably responsible for anode electroactive reactions.³⁶ Similarly, *Caloribacterium* species have been found on bio-anodes, suggesting its participation in electron

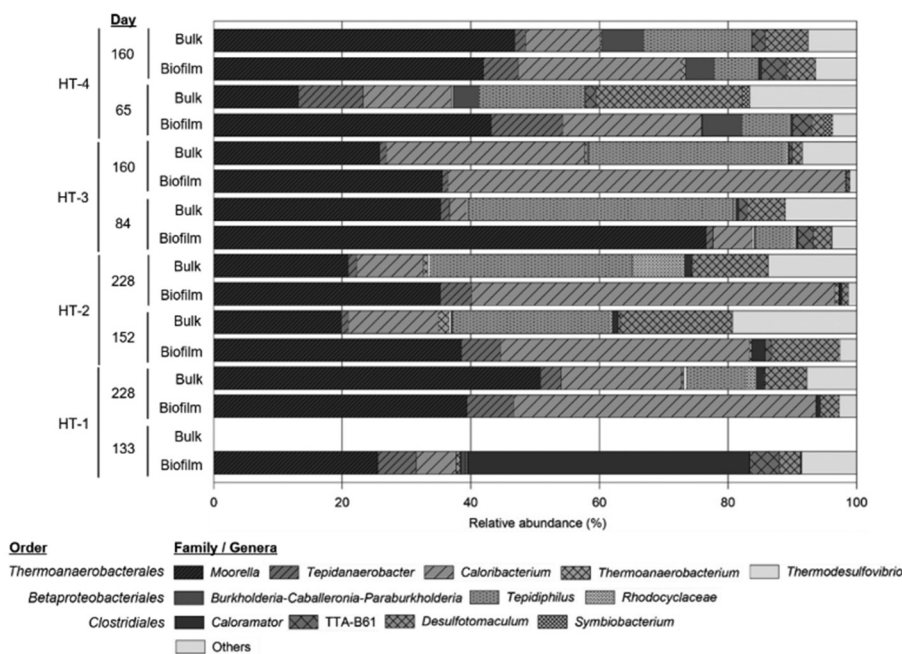


Fig. 5 Microbial community composition in biofilm and bulk liquid samples. The bar chart shows relative abundances of main genera (or families when no further classification could be obtained). Sampling days for each reactor (named HT1–4) are indicated.

transfer.³⁷ In a thermophilic bioreactor, enriched microbial communities revealed a high abundance of both, *Caloribacterium* and *Desulfotomaculum* species when feeding with a synthetic syngas mixture or CO alone. It was proposed that these thermophiles converted the input gas mainly to H₂ and acetate.³⁸

In the mature biofilm (>150 days of constant operation) collected from three out of the four systems analysed in this work, the relative abundance of *Caloribacterium* was higher compared to previous samples. This confirms a selective enrichment of this bacteria on the cathode surface. The latter, together with sustained H₂ evolution and acetate production, suggests the participation of *Caloribacterium* in electrode harvesting. If this could be confirmed by additional experimentation using purified *Caloribacterium* isolates, it would be an additional example of a single species putatively acting as an electrotroph and electrogenic bacterium.

4. Conclusions

This study has reported on the lasting ability of a mixed microbial culture to effectively produce sustained H₂ and acetate under thermophilic conditions. Our results show a reasonable resilience and robustness of the process for a period of over 150 days. An equivalent H₂ formation rate of 8.2 mol H₂ per m² per d was obtained, which exceeded 10 times the abiotic production under the same conditions. Intensity demand profiles were concomitant with acetate generation, providing the power dependence of the system. Approximately, 85% of the electrons consumed were recovered

into products, whose production was resumed in new set-ups shortly after inoculation or medium replacement, indicating a high stability of the microbial community. Micronutrients and enzyme cofactors, but no inhibitory wastes such as accumulated undissociated acids, seemed to have a significant effect on acetate production as observed after repetitive partial replacements of the cathodic electrolyte. Considering the changes of biofilm and bulk liquid microbiomes, the anaerobic sludge from a conventional WWTP turned out to be a suitable inoculum source for thermophilic MEC reactors. *Moorella* and *Caloribacterium* related sequences were found to be the most abundant in the cathode biofilms of the four systems. The obtained results propel research interest to promote the suitable working parameters to obtain higher valuable compounds and fully optimise the performance by integrating carbon capture and utilisation units and replace the required energy for renewable resources.

Conflicts of interest

The authors report no conflicts to declare. The authors alone are responsible for the content and writing of this article.

Acknowledgements

This study has received funding from the European Union's Horizon 2020 research and innovation program under the grant agreement no. 760431. L. R.-A. acknowledges the support from the Catalan Government (2018 FI-B 00347) in the

European FSE program (CCI 2014ES05SFOP007). E. P.-V. is grateful for the Research Training grant from the University of Girona (IFUDG2018/52). S. P. is a Serra Húnter Fellow (UdG-AG-575) and acknowledges the funding from the ICREA Acadèmia award. LEQUIA and IEA have been both recognized as consolidated research groups by the Catalan Government (2017-SGR-1552 and 2017-SGR-548).

References

- 1 Z. J. Ren, X. Huang, H. D. May, L. Lu, Y. Jiang and P. Liang, *Water Res.*, 2019, **149**, 42–55.
- 2 Y. Zhang and I. Angelidaki, *Water Res.*, 2014, **56**, 11–25.
- 3 C. M. Spirito, H. Richter, K. Rabaey, A. J. M. Stams and L. T. Angenent, *Curr. Opin. Biotechnol.*, 2014, **27**, 115–122.
- 4 L. Yu, Y. Yuan, J. Tang and S. Zhou, *Bioelectrochemistry*, 2017, **117**, 23–28.
- 5 B. K. Chaudhary, Final degree thesis, Asian Institute of Technology, 2008.
- 6 A. Hussain, P. Mehta, V. Raghavan, H. Wang, S. R. Guiot and B. Tartakovsky, *Enzyme Microb. Technol.*, 2012, **51**(3), 163–170.
- 7 D. R. Lovley and K. P. Nevin, *Curr. Opin. Biotechnol.*, 2013, **24**(3), 385–390.
- 8 N. Shrestha, G. Chilkoor, B. Vemuri, N. Rathinam, R. K. Sani and V. Gadhamshetty, *Bioresour. Technol.*, 2018, **255**, 318–330.
- 9 Q. Fu, H. Kobayashi, Y. Kuramochi, J. Xu, T. Wakayama, H. Maeda and K. Sato, *Int. J. Hydrogen Energy*, 2013, **38**(35), 15638–15645.
- 10 Q. Fu, Y. Kuramochi, N. Fukushima, H. Maeda, K. Sato and H. Kobayashi, *Environ. Sci. Technol.*, 2015, **49**(2), 1225–1232.
- 11 H.-Y. Yang, B.-L. Bao, J. Liu, Y. Qin, Y.-R. Wang, K.-Z. Su, J.-C. Han and Y. Mu, *Bioelectrochemistry*, 2017, **119**, 180–188.
- 12 H. Song, O. Choi, A. Pandey, Y. G. Kim, J. S. Joo and B.-I. Sang, *Bioresour. Technol.*, 2019, **281**, 474–479.
- 13 D. A. Jadhav, A. D. Chendake, A. Schievano and D. Pant, *Bioresour. Technol.*, 2018, **277**, 148–156.
- 14 J. J. Kozich, S. L. Westcott, N. T. Baxter, S. K. Highlander and P. D. Schloss, *Appl. Environ. Microbiol.*, 2013, **79**(17), 12–20.
- 15 T. Stoeck, D. Bass, M. Nebel, R. Christen, M. D. M. Jones, H.-W. Breiner and T.-A. Richards, *Mol. Ecol.*, 2010, **19**(Suppl 1), 21–31.
- 16 R. C. Edgar and H. Flyvbjerg, *Bioinformatics*, 2015, **31**(21), 3476–3482.
- 17 R. C. Edgar, *Bioinformatics*, 2010, **26**(19), 2460–2461.
- 18 J. G. Caporaso, K. Bittinger, F. D. Bushman, T. Z. DeSantis, G. L. Andersen and R. Knight, *Bioinformatics*, 2010, **26**(2), 266–267.
- 19 P. Batlle-Vilanova, S. Puig, R. Gonzalez-Olmos, A. Vilajeliu-Pons, L. Bañeras, M. D. Balaguer and J. Colprim, *Int. J. Hydrogen Energy*, 2014, **39**(3), 1297–1305.
- 20 C. Van De Goor, Z. Li and G. Mul, Final degree thesis, University of Twente, 2016.
- 21 J. S. Geelhoed and A. J. M. Stams, *Environ. Sci. Technol.*, 2011, **45**(2), 815–820.
- 22 N. Faraghiparapari and K. Zengler, *J. Chem. Technol. Biotechnol.*, 2017, **92**(2), 375–381.
- 23 S. M. T. Raes, L. Jourdin, C. J. N. Buisman and D. P. B. T. B. Strik, *ChemElectroChem*, 2017, **4**(2), 386–395.
- 24 S. A. Patil, F. Harnisch, B. Kapadnis and U. Schröder, *Biosens. Bioelectron.*, 2010, **26**(2), 803–808.
- 25 P. Batlle-Vilanova, R. Ganigue, S. Ramió-Pujol, L. Bañeras, G. Jiménez, M. Hidalgo, M. D. Balaguer, J. Colprim and S. Puig, *Bioelectrochemistry*, 2017, **117**, 57–64.
- 26 T. P. Sciarria, P. Batlle-Vilanova, B. Colombo, B. Scaglia, M. D. Balaguer, J. Colprim, S. Puig and F. Adani, *Green Chem.*, 2018, **20**(17), 4058–4066.
- 27 A. Kundu, J. N. Sahu, G. Redzwan and M. A. Hashim, *Int. J. Hydrogen Energy*, 2013, **38**(4), 1745–1757.
- 28 J. B. A. Arends, S. A. Patil, H. Roume and K. Rabaey, *J. CO2 Util.*, 2017, **20**, 141–149.
- 29 E. V. LaBelle, C. W. Marshall, J. A. Gilbert and H. D. May, *PLoS One*, 2014, **9**(10), 1–10.
- 30 I. Vassilev, P. A. Hernandez, P. Batlle-Vilanova, S. Freguia, J. O. Krömer, J. Keller, P. Ledezma and B. Viridis, *ACS Sustainable Chem. Eng.*, 2017, **6**(7), 8485–8493.
- 31 S. Ramió-Pujol, R. Ganigué, L. Bañeras and J. Colprim, *Bioresour. Technol.*, 2015, **192**, 296–303.
- 32 G. Wang and D. I. C. Wang, *Appl. Environ. Microbiol.*, 1984, **47**(2), 294–298.
- 33 F. Aulenta, L. Catapano, L. Snip, M. Villano and M. Majone, *ChemSusChem*, 2012, **5**(6), 1080–1085.
- 34 Y. Xiang, G. Liu, R. Zhang, Y. Lu and H. Luo, *Bioresour. Technol.*, 2017, **241**, 821–829.
- 35 Z. Zaybak, B. E. Logan and J. M. Pisciotta, *Bioelectrochemistry*, 2018, **123**, 150–155.
- 36 K. C. Wrighton, P. Agbo, F. Warnecke, K. A. Weber, E. L. Brodie, T. Z. DeSantis, P. Hugenholtz, G. L. Andersen and J. D. Coates, *ISME J.*, 2008, **2**(11), 1146–1156.
- 37 H. Wang, L. Lu, D. Mao, Z. Huang, Y. Cui, S. Jin, Y. Zuo and Z. J. Ren, *Chemosphere*, 2019, **235**, 776–784.
- 38 J. I. Alves, A. J. M. Stams, C. M. Plugge, M. Madalena Alves and D. Z. Sousa, *FEMS Microbiol. Ecol.*, 2013, **86**(3), 590–597.
- 39 M. F. Alqahtani, K. P. Katuri, S. Bajracharya, Y. Yu, Z. Lai and P. E. Saikaly, *Adv. Funct. Mater.*, 2018, **28**(43), 1–8.
- 40 M. Dopson, G. Ni and T. H. J. A. Sleutels, *FEMS Microbiol.*, 2016, **40**, 164–181.
- 41 S. A. Patil, S. Gildemyn, D. Pant, K. Zengler, B. E. Logan and K. Rabaey, *Biotechnol. Adv.*, 2015, **33**, 736–744.

Supporting Information

Table 1 (SI). Composition of the medium used in the microbial electrolysis cells

Medium component	(g L ⁻¹)	Trace metal solution	(mg L ⁻¹)	Vitamin solution	(μg L ⁻¹)
KH ₂ PO ₄	0.1	Nitrilotriacetic acid	20.0	Biotin	20.0
NaCl	0.8	MnSO ₄ H ₂ O	10.0	Folic acid	20.0
NH ₄ Cl	1.0	Fe(SO ₄) ₂ (NH ₄) ₂ 6H ₂ O	8.0	Pyridoxine hydrochloride	100.0
MgCl ₂ 6H ₂ O	0.2	CoCl ₂ 6H ₂ O	2.0	Thiamine hydrochloride	50.0
KCl	0.1	ZnSO ₄ 7H ₂ O	0.002	Riboflavin	50.0
CaCl ₂ 2H ₂ O	0.02	CuCl ₂ 2H ₂ O	0.2	Nicotinic acid	50.0
C ₆ H ₁₃ NO ₄ S H ₂ O (MES)	1.95	NiCl ₂ 2H ₂ O	0.2	DL-calcium pantothenate	50.0
Cysteine HCl	0.4	Na ₂ MoO ₄ 2H ₂ O	0.2	Vitamin B12	1.0

Table 2 (SI). Comparison between similar studies working at thermophilic conditions

T (°C)	Inoculum	E _{cat} (V vs. SHE)	Current density (A m ⁻²)	CE (%)	Production rate (mmol m ⁻² d ⁻¹)	Source
55	Thermophilic MFC	-0.8	1.28 ± 0.15	70	H ₂	376.5 ± 73.4 (Fu et al., 2013)
50	<i>M. Thermoautotrophica</i> (DSM 1974)	-0.3	2500 ^a	72 ± 4	CH ₃ COOH	3.48 ± 0.27 (Faraghiparapari and Zengler, 2017)
55	<i>M. thermoautotrophica</i> (DSM 7417)	-0.4	0.63	65	CH ₃ COOH CH ₂ O ₂	63.2 58.2 (Yu et al., 2017)
60	Anaerobic sludge	-0.8	4.94	97	CH ₃ COOH CH ₄	160 380 (Song et al., 2019)
50	Anaerobic sludge	-0.6	5.50 (max) 2.25 ± 0.29	83 ± 3	CH ₃ COOH H ₂	468 4000 This study

^a μMe

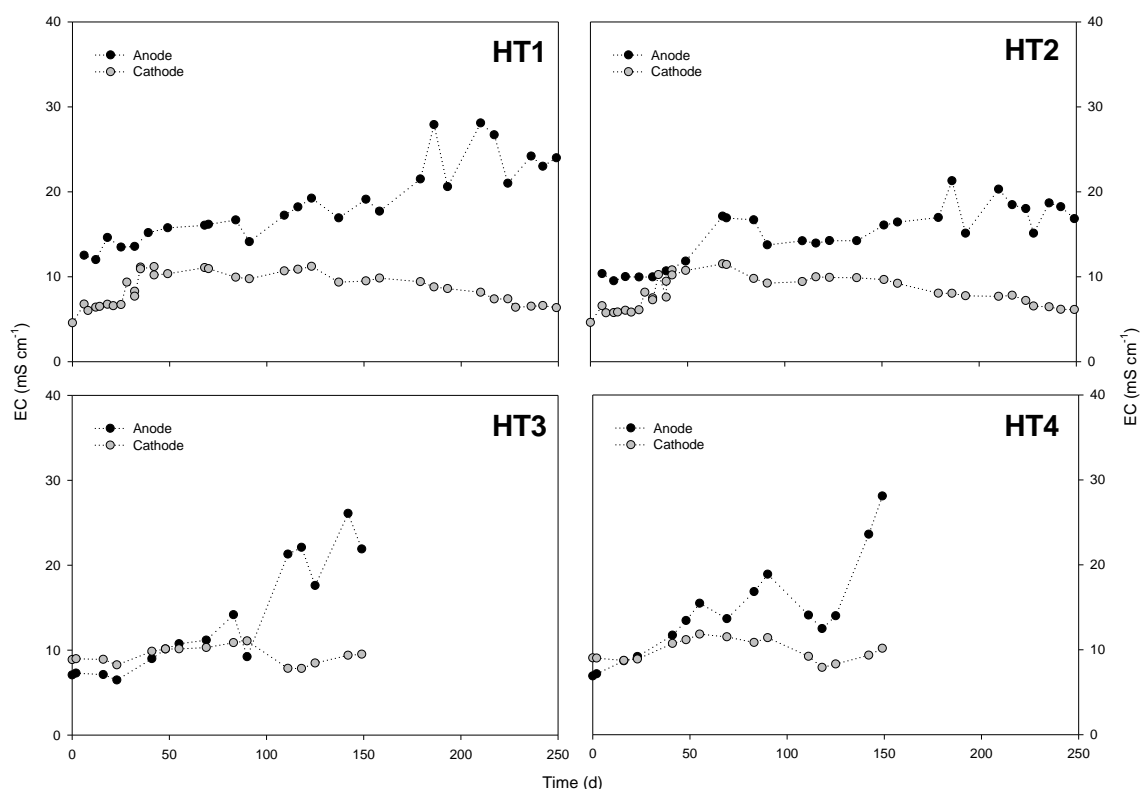


Figure 1 (SI). Electric conductivity (EC) evolution in the anodic and cathodic chambers of each reactor.

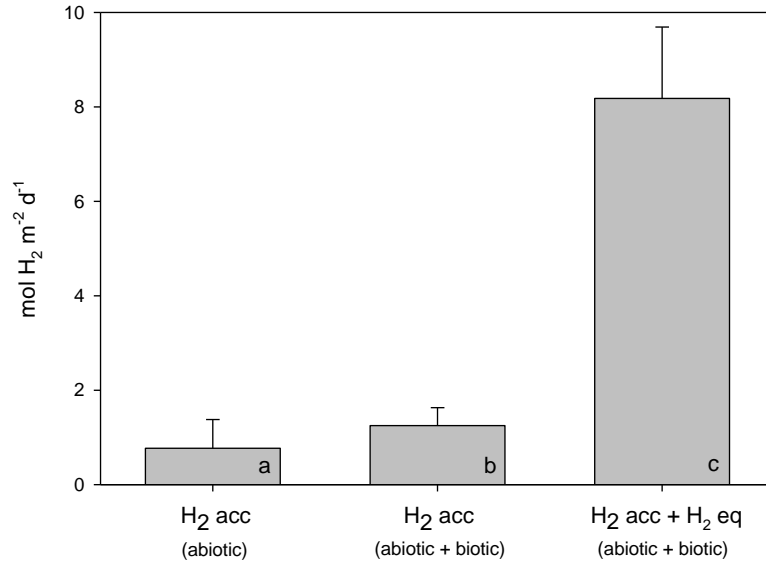


Figure 2 (SI). H₂ production rate comparison between abiotic and biotic systems. A distinction has been made between the H₂ accumulation (H₂ acc) in the gas plus liquid phases (a, b) and the H₂ equivalent (H₂ eq) produced regarding organics concentration in the liquid phase (c).

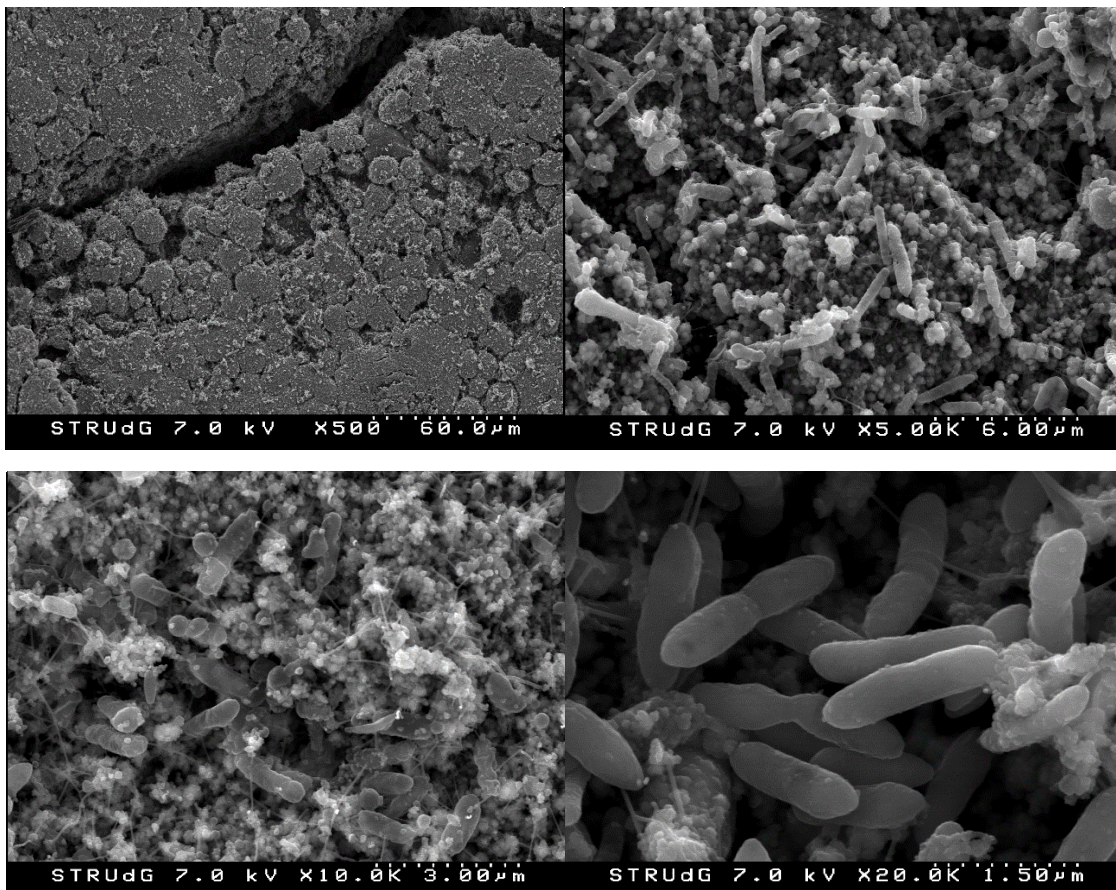


Figure 3 (SI). Scanning electron microscopy of micrographs derived from the four cathode biofilms. Images are seen at different magnifications (from 500 X to 20 000 X).

4.2. Thermophilic bio-electro carbon dioxide recycling harnessing renewable energy surplus

Laura Rovira-Alsina, M. Dolors Balaguer and Sebastià Puig*

LEQUIA. Institute of the Environment, University of Girona. Campus Montilivi,
C/Maria Aurèlia Capmany, 69, E-17003 GironaCatalonia, Spain.

*E-mail: sebastia.puig@udg.edu



Thermophilic bio-electro carbon dioxide recycling harnessing renewable energy surplus

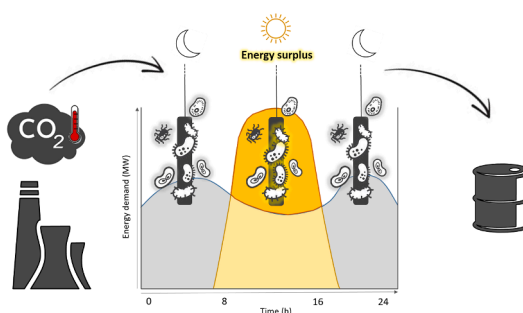
Laura Rovira-Alsina, M. Dolors Balaguer, Sebastià Puig*

LEQUiA, Institute of the Environment, University of Girona, Campus Montilivi, C/Maria Aurèlia Capmany, 69, E-17003 Girona, Catalonia, Spain

HIGHLIGHTS

- Renewable energy surplus can be valorized through microbial electrosynthesis.
- Intermittent power supply conditions may boost the product per energy ratio.
- Enriched thermophilic microbiomes can be highly resilient to fluctuating conditions.
- (Bio)electrochemical processes co-exist with fermentative reactions.

GRAPHICAL ABSTRACT



ARTICLE INFO

Keywords:

Biocatalysis
CO₂ valorisation
Excess energy
Gas fermentation
High temperature

ABSTRACT

Renewable energies will represent an increasing share of the electricity supply, while flue and gasification-derived gases can be a promising CO₂ feedstock with a heat load. In this study, microbial electrosynthesis of organic compounds from CO₂ at high temperature was proposed as an alternative for valorising energy surplus and decarbonizing the economy. The unremitting fluctuation of renewable energy sources was assessed using two bioreactors at 50 °C, under circumstances of continuous and intermittent power supply (ON-OFF; 8–16 h), simulating an off-grid photovoltaic system. Results highlighted that maximum acetate production rate (43.27 g m⁻² d⁻¹) and coulombic efficiency (98%) were achieved by working with an intermittent energy supply, while current density was reduced three times. This boosted the production of acetate per unit of electricity provided up to 138 g kWh⁻¹ and reinforced the robustness of the technology by showing resilience to tolerate perturbations and returning to its initial state.

1. Introduction

Renewable energy has emerged as a progressive step to reach a sustainable energy economy (WEO, 2018). Not only using environmentally friendly energy, but also employing it much more efficiently (Denchak, 2018). However, since these sources are hampered by a

discontinuous output of energy, the problem in balancing supply and demand is still not fully solved (Anvari et al., 2016). 4 out of 27 countries of the European Member States reported a deficit of renewable energy in 2018 (European Environment Agency, 2019), but 10 of them foresaw an expected excess by 2020. As an example, Spain overall surplus was estimated to account for 2,649 ktoe (30,808 MWh), (ECN,

* Corresponding author.

E-mail address: sebastia.puig@udg.edu (S. Puig).

<https://doi.org/10.1016/j.biortech.2020.124423>

Received 29 September 2020; Received in revised form 11 November 2020; Accepted 12 November 2020

Available online 23 November 2020

0960-8524/© 2020 The Authors.

Published by Elsevier Ltd.

This is an open access article under the CC BY-NC-ND license

(<http://creativecommons.org/licenses/by-nc-nd/4.0/>).

2011). Photovoltaic (PV) installations generate a surplus of energy during approximately 8 h per day, coinciding with the solar peak hours (SPH) of this region (Spanish solar radiation data). This becomes more relevant in off-grid systems for isolated locations without reliance on public utilities. Seasonal storage of renewable energy surplus could connect economic and environmental gains by means of a circular and decarbonized economy approach. Hence, there is a need for seeking technologies other than conventional lithium-ion batteries able to collect, transport and convert excess energy (Hu et al., 2017).

Microbial electrosynthesis (MES) has been proposed as a technically feasible near-term technology for carbon dioxide (CO₂) application (Grim et al., 2020; Bian et al., 2020). Recently, Roy et al. (2021) established the first demonstration of microbial electrosynthesis from unpurified industrial CO₂. MES is based on electricity-driven microbial reactions to transform CO₂ from a liability into an asset, while converting excess renewable energy into chemical platforms (Nevin et al., 2010; Rabaey and Rozendal, 2010). Up to now, MES is rooted in the bioH₂-mediated production of organics, mainly acetate (Bian et al., 2020) or short-chain volatile fatty acids (Jourdin et al., 2019; Vassilev et al., 2019). The organics generated could be used as building blocks for other end-products (i.e. bioplastics (Pepè Sciarria et al., 2018)). The production of hydrogen (H₂), either biological or electro-catalytic, plays a key role in H₂-mediated biological reactions as it governs the availability of reducing power and the end-products (Blasco-Gómez et al., 2019; Puig et al., 2017). MES is expected to be an appropriate option for *in-situ* H₂ production and utilization. However, while CO₂ as the sole carbon source is suitable for autotrophic electroactive bacteria acting as catalysts, the intermittency of renewable energy as the only electron donor source could adversely influence the microbial community (Gowrisankaran et al., 2015) and thus, the overall performance of this technology.

Several mesophilic studies have been carried out assuming the use of renewable energy in MES (Ceballos-Escalera et al., 2019; Sánchez et al., 2019; Streeck et al., 2018). Nonetheless, only a few have determined the influence that continuous power supply interruptions could suppose on the stability of the process. Anzola Rojas and co-workers suggested a slight reduction in the production rates, or even shifts in the metabolic pathways that could alter the microbial structure, and provoke the cell death (Anzola Rojas et al., 2018b). They observed a decrease in the concentration of acetic acid during different disconnection time spans (from 4 to 64 h), assuming that it was oxidized back to CO₂ (Anzola Rojas et al., 2018a). Despite, there is a lack of knowledge on the influence of using exclusively the renewable energy surplus, and the prolonged effect of the daily repetition of periods with/without electrical connection at thermophilic conditions (above 40 °C).

Flue and gasification-derived gases have been postulated as a promising feedstock (Liu et al., 2020), containing a high percentage of CO₂ (10–30% v/v) compared to the atmospheric concentration (0.04% v/v). However, the usage of these carbon streams is limited by the high temperature. In our previous study, we demonstrated the ability of a mixed microbial electroactive culture to effectively produce H₂ and acetate from CO₂ mimicking saturated industrial effluent under long-term thermophilic conditions (Rovira-Alsina et al., 2020). The present work assesses the potential integration of thermophilic MES with renewable energy surplus. Two microbial electrolysis cells were operated at 50 °C for the bio-electro CO₂ recycling into organic compounds with repetitive cycles of intermittent power supply (ON-OFF; 8–16 h), simulating off-grid PV systems. H₂, CO₂ and organic compounds productions were monitored over time under conditions of biological stress, which could reflect a wide range of physical responses as a direct effect for homeostasis perturbation, moving forward the development of a robust and resilient microbial community.

2. Materials and methods

2.1. Experimental setups

Two MES systems named R1 and R2 were constructed. They consisted of two identical glass H-type bottles of 0.25 L (Pyrex V-65231 Scharlab, Spain), separated by a cation exchange membrane of 2·10⁻⁴ m² (CMI-1875 T, Membranes international, USA). The cathode consisted of a plain carbon cloth (thickness of 490 μm, surface area of 3·10⁻³; NuVant's Elat LT2400 FuelCellsEtc, USA) connected to a stainless-steel wire. The anode was a 2·10⁻⁶ m³ graphite rod of 0.1 m length and 5·10⁻³ m of diameter (EnViro-cell, Germany). An Ag/AgCl electrode (+0.197 V vs. SHE, model RE-5B, BASI, UK) with an operating temperature range from 0 to 60 °C was placed in the cathodic chamber and used as a reference electrode. Reactors were sealed with butyl rubber caps to prevent gas leakage and keep the headspace volume of each chamber at 0.03 L, while liquid volume accounted for 0.22 L.

Both MES systems were operated in a three-electrode configuration with a potentiostat (BioLogic, Model VSP, France), which controlled the cathode potential at -0.6 V vs. SHE (standard hydrogen electrode) and monitored the current demand over time. All the potentials reported in this work are relative to SHE unless otherwise noted. Prior to use, the working electrodes were pre-treated in a 0.5 M solution of HCl and a 0.5 M of NaOH for a total of two days and rinsed with deionized water for an additional day. At the end of the experimental study, the voltage of the reference electrodes was measured to ensure any shift that may have occurred during operation. The temperature was kept constant at 50 °C using an orbital incubator (SI600 Stuart, UK), and an agitation rate of 80 rpm was fixed to enable mixing and facilitate mass transfer inside the cathodic chambers. The reactors were operated in batch mode and kept in the dark to avoid the growth of phototrophic microorganisms.

2.2. Inoculum

The microbial community was taken from an anaerobic digester working at 37.5 °C of a wastewater treatment plant (WWTP) located in Girona, Spain. A 1:20 dilution with synthetic medium based on ATCC1754 growth medium (Tanner et al., 1993) was incubated in 50 °C fermentative reactors under H₂:CO₂ (80:20 v/v) to promote acetogenesis and microorganisms' adaptation to thermophilic conditions. During this enrichment stage, pH was adjusted to 6.0 and 2-bromoethanesulfonic acid (10 mM) was added to prevent methanogenesis (Jadhav et al., 2018). An additional 1:10 dilution of this inoculum with the reformulated medium to remove all sources of organic carbon, was used to operate the reactors. The microbial community structure was analyzed in previous experiments (Rovira-Alsina et al., 2020), in which *Thermoanaerobacteriales* was the dominant order. At the genus level, *Moorella* and *Caloribacterium* were the most representative. The experiment was carried out during a steady state phase of the both reactors (after 155 days of operation) so that no other variable interfered with the results.

2.3. Monitoring of key operating parameters

BioLogic software (EC-Lab v10.37) was used to alternatively run multi-technique electrochemical routines with the potentiostat, which included closed-circuit operation in chronoamperometry (CA) and open-circuit voltage (OCV). A cathode potential of -0.6 V was fixed for CA whereas its variation was followed during OCV. The general test lasted 5 consecutive weeks. Repetitive cycles of intermittent power supply were performed from week 2 to 4 (both included), while weeks 1 and 5 were used as controls working in CA mode. During weeks 2 to 4, electrical energy was supplied 8 h per day (CA mode), and it was disconnected the next 16 h (OCV mode). In both modes of operation, the cell voltage (E_{cell}) was recorded continuously except at the end of week 3, in which there was a general power outage. Pure CO₂ (99.9%, Praxair, Spain) was used to feed the two MES systems. Gas was sparged for 10 min in the

cathodic chamber once a week to oversaturate the liquid media and renew the headspace, whereas it was added punctually from 1 to 3 times per week to ensure carbon bioavailability. Gas bags (FlexFoil 301.44 Cromlab SL, Spain) were attached in the gas outlet during weekends, whilst during the week, gas pressure was maintained below 4 atm, releasing it to prevent liquid leakages. Samples from the liquid phase were taken from twice to ten times per week depending on the experimental period. The withdrawn liquid during sampling was replaced with freshly prepared medium saturated with CO₂ to maintain constant volumes in both chambers. Finally, 50 mL of fresh medium were added in R2 at day 15 of operation to evaluate the effect of mineral medium replacement. The initial pH of the solution was set at 6.0, but it was not further modified neither with acidic nor basic solutions.

2.4. Analyses and calculations

Conductivity and pH were measured with an electrical conductivity meter (EC-meter basic 30+, Crison, Spain) and a multimeter (Multi-Meter 44, Crison, Spain), respectively. Both devices were calibrated to measure at 50 °C. The concentration of organic compounds (volatile fatty acids and alcohols) in the liquid phase was determined using an Agilent 7890A gas chromatograph equipped with a DB-FFAP column and a flame ionization detector. Gas production was quantified in the MES by measuring the pressure in the headspace of the reactors using a digital pressure sensor (differential pressure gauge, Testo 512, Spain). Gas samples were analyzed periodically during experiments by gas chromatography (490 Micro GC system, Agilent Technologies, US). The GC was equipped with two columns: a CP-molesive 5A for methane (CH₄), carbon monoxide (CO), H₂, oxygen (O₂) and nitrogen (N₂) analysis, and a CP-Poraplot U for CO₂ analysis. The two columns were connected to a thermal conductivity detector (TCD).

The concentrations of dissolved H₂ and CO₂ in the liquid media were calculated using Henry's law at 50 °C (Eq. (1)), where C_i is the solubility of a gas in a particular solvent (mol L⁻¹), H_i is the Henry's law constant in mol L⁻¹ atm⁻¹ (0.0007 for H₂ and 0.0195 for CO₂; values taken from Foust et al. (1959) and recalculated based on the operational temperature using equations from Stumm and Morgan (1996)), and $P_{gas\ i}$ is the partial pressure of the gas in atm.

$$C_i = H_i \cdot A \cdot P_{gas\ i} \quad (1)$$

The coulombic efficiency (CE) for the conversion of current into products (i.e. H₂, acetate, ethanol) was calculated weekly according to Patil et al. (2015) in CA mode (Eq. (2)). C_i is the compound i concentration in the liquid phase (mol L⁻¹), n_i is the molar conversion factor (2, 8 and 18 mol_{eq}⁻¹ for H₂, acetate and ethanol, respectively), F is the Faraday's constant (96485C mol e⁻¹), V_{NCC} is the net liquid volume of the cathode compartment (L), and I the current density of the system (A).

$$CE(\%) = \frac{C_i \cdot A \cdot \sum_i n_i \cdot F \cdot V_{NCC}}{\int_0^t I \cdot A \cdot dt} \cdot 100 \quad (2)$$

Carbon conversion (CC) yield was calculated as the percent variation between the product formed depending on the converted CO₂ as stated in Eq. (3). ΔC_{CO_2} is the difference of CO₂ in the gas plus liquid phases from the beginning (immediately after feeding the system) to the end of a batch, and $\Delta C_{products}$ is the difference of organic products (i.e. acetate) between batches.

$$CC(\%) = \frac{\Delta C_{products}}{\Delta C_{CO_2}} \cdot 100 \quad (3)$$

The optical density (OD) of the bulk liquid was periodically measured to control the growth of the planktonic microbial community with a spectrophotometer (CE 1021, 1000 Series, CECIL Instruments Ltd., UK) at a wavelength of 600 nm. The dry cell weight (DCW) was calculated in g L⁻¹ by interpolating the OD values in an experimental

regression line created using the corresponding mixed inoculum (1 OD = 0.57 g L⁻¹ of DCW).

3. Results and discussion

A detailed monitoring of the main variables has been exposed along the following sections to evaluate the performance of the MES reactors. The results of operating the systems with only the surplus of photovoltaic renewable energy, therefore with repetitive cycles of intermittent power, has been described.

3.1. Current density and products unfolding to switching electrical conditions

Two replicate reactors (R1 and R2) were used to assess an alternative strategy of operation, based on following the daily cycle of sunlight with ON-OFF power supply periods (8 h ON vs. 16 h OFF). Fig. 1 presents the current density and cell voltage profiles of the reactors over time, discerning CA and OCV operation mode. Both reactors followed the same response to the electrical switching conditions. However, the current density of R2 was slightly higher compared to R1. This was linked to a greater increase in electroactivity from week 1, which led to a higher H₂ formation (Fig. 2). During continuous power supply (weeks 1 and 5) the current demand was stable, though peaks of higher intensity were associated to CO₂ feeding points (Batlle-Vilanova et al., 2019) and the accumulation of organics. However, during intermittent disconnection (weeks 2 to 4), shorter spikes could also be related to sudden energy inputs (Zhang et al., 2019). Throughout these weeks, current demand abruptly increased when electricity was connected and progressively decreased along with each CA period. When operated at OCV, the cathode potential rapidly tended to -0.5 V and stabilized in this value until the electric circuit was closed again. Concomitantly, the anode potential decreased up to 0.5 V, giving a theoretical applied cell voltage of 1 V (Fig. 1). The E_{cell} was gradually intensified throughout the weeks as a result of an increase of the ohmic resistance of the system (i.e. sacrificial anode), which came along with a higher current demand, reaching greater levels than when electricity was supplied uninterruptedly (weeks 1 and 5). For instance, maximum values of week 4 were 10.9 A m⁻² for R1 and 13.2 A m⁻² for R2, though in week 5 they decreased until 8.8 and 12.0 A m⁻², respectively.

Fig. 2 presents the evolution of total gas (GP) and H₂ partial pressures (P_{H2}), besides acetate concentrations of both reactors over time. H₂ was continuously produced throughout the experiment, which led to an H₂-mediated production of organics from electricity and CO₂. The first week of the experiment, organic concentrations and H₂ partial pressures were similar between reactors. Operating at CA mode (days -7 to 0), P_{H2} rapidly increased and could barely stabilize at 2 atm until the next batch. This was accompanied by a gradual increase in acetate concentration at a rate of 6.60 ± 0.73 g m⁻² d⁻¹. The following 3 weeks (days 0 to 21), the systems operated at intermittent CA-OCV mode. This slightly affected the gas pressure evolution, which oscillated depending on the electric circuit position (open or closed). However, acetate continued accumulating at a similar rate compared to the first week (8.07 ± 3.67 g m⁻² d⁻¹). Once the continuous electric supply was reestablished (days 21 to 28), the initial behavior of both systems was restored, showing similar H₂ partial pressures and organics profiles as the first week. The maximum acetic acid concentration (6.0 g L⁻¹) was achieved in R1, while H₂ and overall gas pressure turned out to be higher in R2 (maximum of 2.8 and 3.8 atm, respectively). Despite the experiments were carried out under identical operating conditions, a higher bulk density of R1 compared to R2 (0.12 vs. 0.08 g L⁻¹; DCW of Table 1), together with a lower cell voltage (3.9 vs. 8.5 V; Fig. 1), could have promoted a greater production of organic compounds.

Uninterrupted CA mode operation (weeks 1 and 5) usually induced to higher H₂ partial pressures compared to the combination of CA and OCV modes (weeks 2 to 4). Under CA operation, gas pressure increased

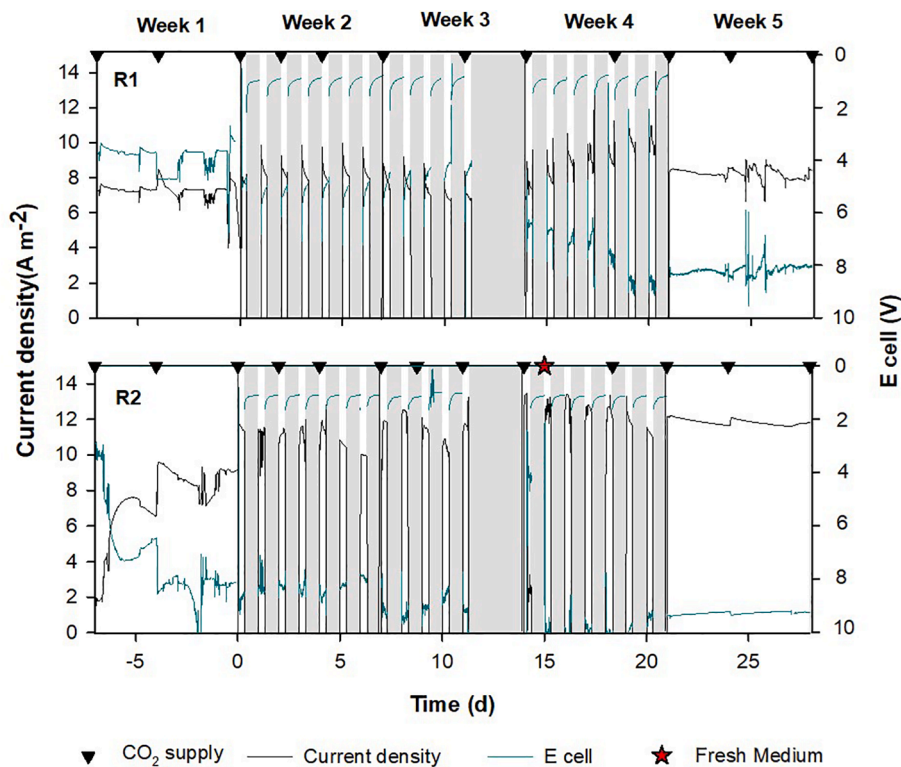


Fig. 1. Current density profiles (black line), and cell potential (Ecell; green line) over time in R1 and R2. White areas represent operation at CA mode, grey areas of OCV mode, black inverted triangles the CO₂ feeding points, red star when fresh medium was added, and vertical black lines separate the 5 weeks in individual batches.

inside the chambers due to H₂ formation, enhancing substrate availability in the liquid phase. Then, H₂ accumulated was consumed at OCV mode through gas fermentation processes, which lowered the gas pressure and the bioavailability as well. The maximum acetate production rate (43.27 g m⁻² d⁻¹) was obtained in R2 after fresh medium addition (week 4). Medium renovation could have played a role in those activities, probably due to nutrients limitation or excreted inhibitors accumulation (Ramíó-Pujol et al., 2015; Rovira-Alsina et al., 2020; Vassilev et al., 2018).

3.2. A synergistic approach from the collected data

Table 1 summarizes and displays the tendency of pH, production rates, current demand, coulombic efficiency (CE) and dry cell weight (DCW) for the two described reactors during the experimental period. pH decreased during repetitive weeks of power disconnection and increased once the electrical connectivity was re-established. It could be associated with the increasing accumulation of acetic acid, though the slight decline in H₂ production due to OCV cycles could also have influenced. Total H₂ production (converted + non-converted H₂) of R1 was higher during weeks 2 to 4 (1.24 ± 0.04 g m⁻² d⁻¹) compared to weeks 1 and 5 (1.08 ± 0.14 g m⁻² d⁻¹), since an increase in current demand contributed to a higher electrochemical H₂ formation. Moreover, higher acetate and ethanol productions were achieved (i.e. 10.81 ± 1.20 vs. 3.60 ± 3.60 g HA m⁻² d⁻¹, respectively), which was related to a lower non-converted rate of H₂ (0.88 ± 0.02 vs. 0.96 ± 0.02 g m⁻² d⁻¹, respectively). R2 followed a similar trend, but maximum H₂ production was attained at stable CA mode (weeks 1 and 5). The CE of both reactors improved operating at intermittent power supply, achieving the utmost value (98% in R1 and 89% in R2) when the highest acetate and H₂ productions were obtained. On the other hand, DCW of both reactors increased during the first week of intermittent energy supply, probably due to an effect of cell detachment. It did not reach atypical values and it

decreased once continuous energy supply was restarted. Switching electrical conditions over a relatively long period (3 weeks) could have threatened the viability of the technology (Zhang et al., 2019). However, current density gradually increased along with the experimental period, sustaining, or even exceeding production rates and conversion efficiencies.

The intermittent polarization effect (simulated using cycles of CA and OCV) was previously studied for harvesting energy from electrochemically active bacteria that usually have interrupted access to electrodes in microbial fuel cell reactors (Guo et al., 2018; Watson and Logan, 2011), even at thermophilic conditions (Carver et al., 2011). Nonetheless, understanding the mechanisms by which bacteria respond to intermittent polarization in MES can be fruitful for future energy-harvesting technologies. Although the number of MES studies in thermophilic conditions is limited and none of them operated under intermittent power supply, the values reported in this study were higher than the production rates published in the literature. Yu and co-workers obtained 3.60 g m⁻² d⁻¹ of acetate using a pure *Moorella thermoautotrophica* strain at 55 °C (Yu et al., 2017). Instead, Song et al. (2019) achieved better results using a gas diffuser in a membrane-less reactor, with a maximum acetate production of 9.61 g m⁻² d⁻¹ at 60 °C. The results of the present work were close to the maximum attained employing the same reactors as in previous tests (Rovira-Alsina et al., 2020), even surpassing acetate production rate (43.27 vs. 28.22 g m⁻² d⁻¹). However, these outcomes are still far from other mesophilic studies such as LaBelle and May (2017) and Jourdin et al. (2015), who obtained an acetate production of 195 and 685 g m⁻² d⁻¹, respectively. Nonetheless, they were working in galvanostatic control (83.3 A m⁻²) and continuous CO₂ addition (25 mL min⁻¹) in the first case, and with a more negative potential (-0.85 V) and periodic bicarbonate addition (from 1 to 4 g L⁻¹) in the second case. Differently, Anzola Rojas and colleagues simulated possible interruptions in the renewable electricity supply by performing variable power cuts (from 4 to 64 h). Acetate

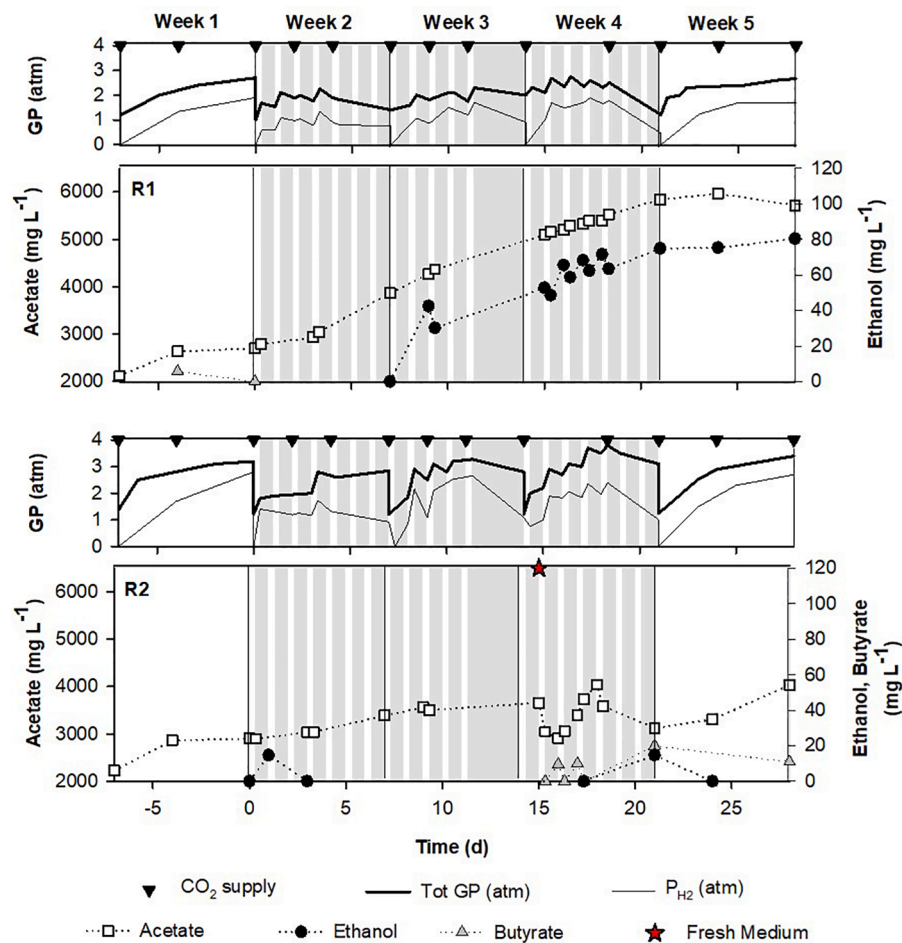


Fig. 2. Total and hydrogen partial pressure (thick and thin black lines), and more relevant organics concentration (acetate: white squares, ethanol: black circles, and butyrate: grey triangles) over time in R1 and R2. White areas represent operation at CA mode, grey areas of OCV mode, black inverted triangles the CO₂ feeding batches, red star when fresh medium was added, and vertical black lines separate the 5 weeks in individual batches.

Table 1

Average pH, absolute production rates of non-converted H₂, total H₂, acetate (HA), ethanol (Et) and butyrate (HB), average current demand, coulombic efficiency (CE) and dry cell weight (DCW) of R1 and R2 during the test. The tendency of each parameter throughout the 5 consecutive weeks is also displayed.

	R1						R2					
	Week 1	Week 2	Week 3	Week 4	Week 5	Tendency	Week 1	Week 2	Week 3	Week 4	Week 5	Tendency
pH	4.3 ± 0.1	4.2 ± 0.1	4.2 ± 0.1	4.1 ± 0.1	4.4 ± 0.0	↘↘↘↘↗	6.2 ± 0.2	6.0 ± 0.3	5.9 ± 0.4	5.4 ± 0.1	5.7 ± 0.1	↘↘↘↘↗
H ₂ (g m ⁻² d ⁻¹)	0.98	0.86	0.90	0.88	0.94	↘↘↘↘↗	1.06	0.98	1.06	1.00	1.02	↘↘↘↘↗
Tot H ₂ (g m ⁻² d ⁻¹)	1.18	1.26	1.26	1.21	0.98	↘↘↘↘↗	1.30	1.15	1.09	1.20	1.28	↘↘↘↘↗
HA (g m ⁻² d ⁻¹)	6.01	12.01	10.81	10.21	1.20	↘↘↘↘↗	7.21	5.40	3.00	43.27	9.61	↘↘↘↘↗
Et (g m ⁻² d ⁻¹)	0.00	0.00	0.49	0.30	0.06	↘↘↘↘↗	0.00	0.00	0.00	0.16	-0.16	↘↘↘↘↗
HB (g m ⁻² d ⁻¹)	-0.06	0.00	0.00	0.00	0.00	↘↘↘↘↗	0.00	0.00	0.00	0.21	-0.09	↘↘↘↘↗
Current (A m ⁻²)	7.2 ± 0.5	8.2 ± 0.8	7.4 ± 0.7	8.9 ± 1.4	8.2 ± 0.3	↘↘↘↘↗	7.5 ± 2.0	10.7 ± 1.6	11.5 ± 0.8	11.1 ± 3.3	11.9 ± 0.2	↘↘↘↘↗
CE (%)	51	98	98	71	20	↘↘↘↘↗	50	72	74	89	68	↘↘↘↘↗
DCW (g L ⁻¹)	0.12	0.15	0.16	0.18	0.15	↘↘↘↘↗	0.08	0.10	0.10	0.14	0.13	↘↘↘↘↗

production rate was decreased up to 77% (from 10.0 to 2.3 g m⁻² d⁻¹) (Anzola Rojas et al., 2018b), and despite its recovery after a period of maximum 16 h, the microbial community behavior had repetitive reversions in producing-consuming acetate for its survival (Anzola Rojas et al., 2018a).

On the contrary, thermophilic microbial electrosynthesis turned out

to be a good approach to valorise renewable energy surplus converting it into organic chemicals. Our study demonstrated the capability to keep a constant production of acetate at similar rates even when electricity was deprived. The cell voltage of both reactors was increased working in discontinuous energy input (Fig. 1), which could have influenced the current demand, H₂ titer and production rates. Nevertheless, the

generation of organic compounds could be sustained throughout the experimental period (Fig. 2). Although consecutive cycles of intermittent power supply had an impact on the catalytic H₂ production, a high current density and gas pressure led to an efficient acetate production.

3.3. The tie between production slopes and reactions stoichiometry

Fig. 3 presents the evolution of pH, CO₂ and products over the week 4 of the study in R1 and R2. H₂ was produced in CA mode, but it was consumed in parallel together with CO₂ for acetate production, since under the applied potential, both reactions were thermodynamically feasible. Otherwise, fermentation processes dominated the consumption of H₂ to produce more acetate at OCV mode. Acetate production rate was lower under OCV operation, which fitted with ethanol and/or butyrate apparition. The mass balance estimated that approximately 70% of the acetate was used to produce ethanol through solventogenesis reaction, whereas butyrate could be generated through chain elongation of ethanol, or directly from acetate, H₂ and H⁺ (Ganigué et al., 2015).

In R1, ethanol production was detected during OCV operation at a rate of $1.30 \pm 0.47 \text{ g m}^{-2} \text{ d}^{-1}$, whereas it was consumed at a similar velocity during CA operation ($-1.40 \pm 0.39 \text{ g m}^{-2} \text{ d}^{-1}$). Meanwhile, ethanol was not detected in R2, but butyrate appeared ($1.07 \pm 0.03 \text{ g m}^{-2} \text{ d}^{-1}$) and disappeared ($-2.18 \pm 0.081 \text{ g m}^{-2} \text{ d}^{-1}$) during OCV and CA mode, respectively. The absence of ethanol does not imply a lack of its production, as it could have been produced and instantaneously used for butyrate synthesis (Raes et al., 2017). Under CA conditions, protons migrated from the anodic to the cathodic chamber to achieve electron neutrality (Matemadombo et al., 2016), while under OCV operation, there was still a proton diffusion, but the electron circuit transfer was cut. In concordance, pH had repetitive oscillations between cycles mainly related to the H⁺ reduction during CA mode and the unceasing acetate accumulation along OCV mode. Although the slopes of H₂ and CO₂ evolution were similar among reactors, pH and the organics (acetate, ethanol and butyrate) production velocity of R1 were lower than R2. pH of R1 was closer to acetic acid pK_a at 50 °C (pK_a 4.1) which together with a high acetate concentration, favoured the shift from acetogenesis to solventogenesis (Blasco-Gómez et al., 2019), accumulating ethanol and reversing the pH tendency. Instead, pH of R2 was kept above 5. This factor together with a higher concentration of H₂ could have derived to acetate consumption for butyrate production, which was accompanied by a gradual increase in pH (Fig. 3).

Overall, carbon conversion (CC) yield from CO₂ to product for each reactor was roughly 2.3-fold higher under the span time of power supply

Table 2

Average carbon conversion yield (CC) and coulombic efficiencies (CE) for R1 and R2 considering periods of power supply (CA) and disconnection (OCV).

	CC yield (%)		CE (%)			
	CA	OCV	CA		CA-OCV (batch)	
			H _{Ac}	H ₂	H _{Ac}	H ₂
R1	49 ± 10	20 ± 8	80 ± 5	46 ± 36	162 ± 29	56 ± 7
R2	66 ± 14	29 ± 9	46 ± 32	73 ± 24	20 ± 14	40 ± 3

(CA), coinciding with more acetate production compared to OCV mode (Table 2). About 100% of the electrons were recovered into final products when considering total H₂ production (converted + non-converted H₂), albeit R2 transformed less amount of H₂ into acetate.

3.4. Energy per product trade-off

One of the fundamental points in any catalytic system is the energy demand. Fig. 4 presents the amount of product based on the energy supplied over time. The weekly H₂ and acetate productions per unit of electrical consumption (E) were compared operating at continuous CA (weeks 1 and 5) and intermittent CA-OCV mode (weeks 2 to 4). In general, there was a gradual and concomitant growth in the ratio of product vs. energy (HA or H₂:E) within reactors. It increased over time once the cycles of intermittency begun, but it decreased when permanent electrical connectivity was re-established. That encompassed up to 138.12 g HA kWh⁻¹ and 20.72 g H₂ kWh⁻¹ in R1, a 18-fold higher HA:E and 7-fold higher H₂:E compared to continuous CA operation. A similar behavior was detected in R2, although the ratios were smaller as a result of lower DCW and acetate production; plus higher cell voltage and current density (Fig. 1 and Table 1).

This relationship cannot be compared to other thermophilic studies due to lack of data. However, at mesophilic conditions and CA mode, Arends et al. (2017) detailed a specific energy input per kilogram of acetic acid produced during batch processes of 29 kWh, which would be equivalent to 34.53 g HA kWh⁻¹. On the other side, Jeremiase et al. (2010) reported an electrical energy input of 2.6 kWh per m⁻³ of H₂ formation using a Ni foam cathode, which considering the ideal gas law under normal conditions, would be equivalent to 32.02 g H₂ kWh⁻¹. Both values are within the range obtained in our experiment, though working intermittently at CA-OCV mode, the utmost HA:E proportion could exceed the previous results.

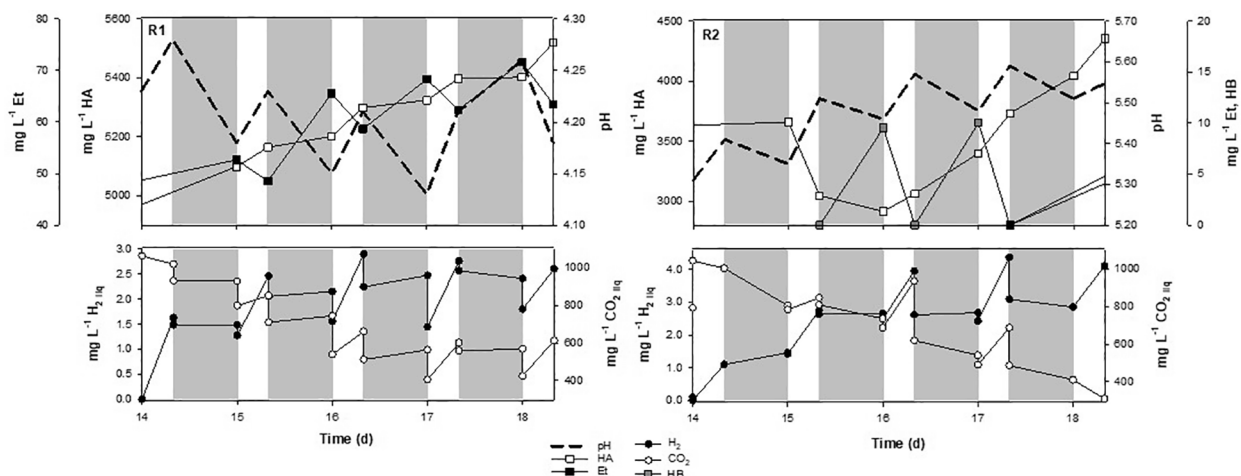


Fig. 3. Evolution of H⁺ (dashed lines), ethanol (black squares), acetic acid (white squares), butyric acid (grey squares), H₂ (black circles) and CO₂ (white circles) concentrations in liquid media of R1 and R2 over the week 4 of the study. White areas represent operation at CA mode and grey areas of OCV mode. CO₂ was supplied at day 14 by oversaturating the liquid media.

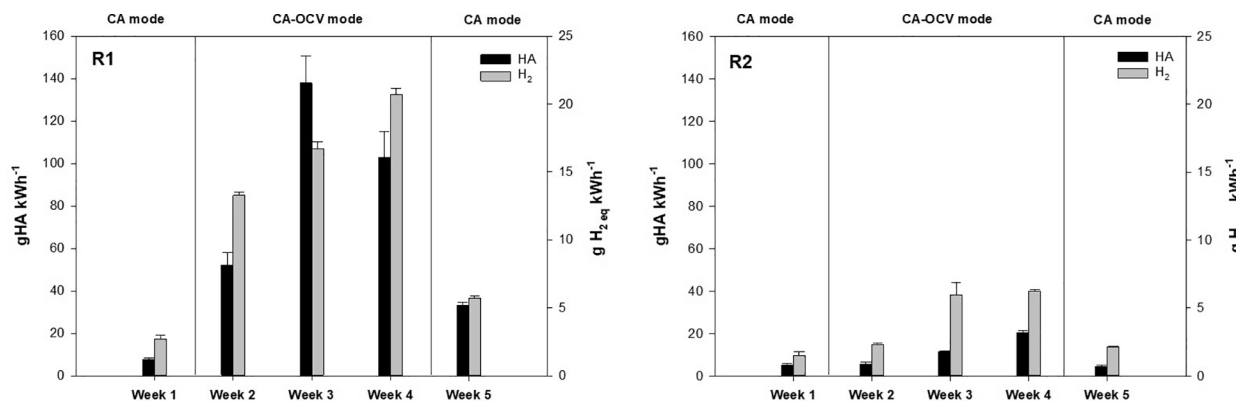


Fig. 4. Acetic acid (g HA) and H₂ (g H₂ eq) per unit of electrical energy consumption (kWh⁻¹) in each week of the analyzed period of R1 and R2.

3.5. Implications

This technology can contribute to improve the environmental pillar of sustainability and move towards a decarbonized economy by using renewable energy and CO₂ as feedstocks. 0.115 ± 0.022 kWh d⁻¹ were consumed on average during the weeks before and after the assay took place (CA mode) whereas only the half, 0.056 ± 0.004 kWh d⁻¹, was required during power interruptions (CA-OCV mode) due to switching electric conditions. Although working on a laboratory scale, the total energy consumed (0.13 kWh) by R1 and R2 during the entire study (5 weeks), could save 13.31 L of natural gas, while considering the absorbed CO₂, and a CO₂ factor in Spain of 404 g kWh⁻¹ (Solar edge, 2019), 53 g of CO₂ were avoided while 3 g were absorbed. This is equivalent to the amount of CO₂ that $1.6 \cdot 10^{-3}$ trees would have consumed, or differently, if applying a tree planted factor of 0.00135 trees kWh⁻¹ (used in Spain), it would be equivalent to grow $1.8 \cdot 10^{-4}$ trees.

These are negligible values compared to the huge amount of energy distributed and CO₂ emitted worldwide. However, what must be considered is the impact that this technology can have if it is scaled-up to revenue excess energy and accomplish the European Union target of achieving a net-zero carbon economy by 2050 (United Nations, 2015). In order to buffer the fluctuations of naturally flowing energy, a proper strategy for storing and utilizing energy is required, and we have proposed a way to improve the efficiency of organics production from CO₂ by using intermittent power operation. However, additional experiments under different operational conditions (i.e. variable configurations and temperatures) are needed to support this premise. Increasing evidence indicates that the technology may be improved by controlling key parameters such as pH, CO₂ and H₂ through on-line probes that would allow real time monitoring for an efficient control of the process. Recently, a reactor for solar energy utilization was set up through the combination of different devices to effectively meet the demands on-site (Koike et al., 2020). In the present study, isolating H₂ and acetate productions from the organics evolution in a two-step process would allow an effective control of the main operational conditions (Ganigué et al., 2016) and therefore, the magnification of the overall productivity.

4. Conclusions

Renewable energy surplus could be valorised through thermophilic bioelectrochemical acetate production while contributing to decrease CO₂ emissions. The intermittent power connection intensified the organic compounds production: current density supplied ratio, keeping similar rates compared to continuous power operation. Bio-electro reduction of CO₂ occurred in CA mode, whereas carboxylates fermentation dominated in OCV mode. Furthermore, acetate production never ceased, as sufficient reducing power and carbon source (H₂ and CO₂, respectively) were bioavailable in any of the applied conditions. The

outcomes underscore that storing the oversupply electricity across daily cycles is a feasible challenge for the versatile MES platform.

Declaration of Competing Interest

The authors declare that they have no known competing financial interests or personal relationships that could have appeared to influence the work reported in this paper.

Acknowledgements

This work was supported by the European Union's Horizon 2020 research and innovation program under the grant agreement No 760431 (BioRECO₂VER). L.R-A acknowledges the support by the Catalan Government (2018 FI-B 00347) in the European FSE program (CCI 2014ES05SFOP007). S.P is a Serra Húnter Fellow (UdG-AG-575) and acknowledges the funding from the ICREA Academia award. LEQUIA has been recognized as consolidated research groups by the Catalan Government (2017-SGR-1552).

Appendix A. Supplementary data

Supplementary data to this article can be found online at <https://doi.org/10.1016/j.biortech.2020.124423>.

References

- Anvari, M., Lohmann, G., Wächter, M., Milan, P., Lorenz, E., Heinemann, D., Tabar, M.R., Peinke, J., 2016. Short term fluctuations of wind and solar power systems. *New J. Phys.* 18 <https://doi.org/10.1088/1367-2630/18/6/063027>.
- Anzola Rojas, M. del P., Mateos, R., Sotres, A., Zaiat, M., Gonzalez, E.R., Escapa, A., De Wever, H., Pant, D., 2018a. Microbial electrosynthesis (MES) from CO₂ is resilient to fluctuations in renewable energy supply. *Energy Convers. Manag.* 177, 272–279. <https://doi.org/10.1016/j.enconman.2018.09.064>.
- Anzola Rojas, M. del P., Zaiat, M., Rafael, E., Wever, H. De, 2018b. Effect of the electric supply interruption on a microbial electrosynthesis system converting inorganic carbon into acetate. *Bioresour. Technol.* 266, 203–210. <https://doi.org/10.1016/j.biortech.2018.06.074>.
- Arends, J.B.A., Patil, S.A., Roume, H., Rabaey, K., 2017. Continuous long-term electricity-driven bioproduction of carboxylates and isopropanol from CO₂ with a mixed microbial community. *J. CO₂ Util.* 20, 141–149. <https://doi.org/10.1016/j.jcou.2017.04.014>.
- Battle-Vilanova, P., Rovira-Alsina, L., Puig, S., Balaguer, M.D., Icaran, P., Monsalvo, V. M., Rogalla, F., Colprim, J., 2019. Biogas upgrading, CO₂ valorisation and economic reevaluation of bioelectrochemical systems through anodic chlorine production in the framework of wastewater treatment plants. *Sci. Total Environ.* 690, 352–360. <https://doi.org/10.1016/j.scitotenv.2019.06.361>.
- Bian, B., Bajracharya, S., Xu, J., Pant, D., Saikaly, P.E., 2020. Microbial electrosynthesis from CO₂: Challenges, opportunities and perspectives in the context of circular bioeconomy. *Bioresour. Technol.* 302, 122863 <https://doi.org/10.1016/j.biortech.2020.122863>.
- Blasco-Gómez, R., Ramió-Pujol, S., Baneras, L., Colprim, J., Balaguer, M.D., Puig, S., 2019. Unravelling the factors that influence the bio-electrorecycling of carbon dioxide towards biofuels. *Green Chem.* 21, 684–691. <https://doi.org/10.1039/C8GC03417F>.

- Carver, S.M., Vuoriranta, P., Tuovinen, O.H., 2011. A thermophilic microbial fuel cell design. *J. Power Sources* 196, 3757–3760. <https://doi.org/10.1016/j.jpowsour.2010.12.088>.
- Ceballos-Escalera, A., Molognoni, D., Bosch-Jimenez, P., Shahparasti, M., Bouchakour, S., Luna, A., Guisasaola, A., Borrás, E., Della Pirriera, M., 2019. Bioelectrochemical systems for energy storage: A scaled-up power-to-gas approach. *Appl. Energy* 260, 114138. <https://doi.org/10.1016/j.apenergy.2019.114138>.
- Denchak, M., 2018. Fossil Fuels: The Dirty Facts. URL <https://www.nrdc.org/stories/fossil-fuels-dirty-facts> (accessed 9.24.19).
- Energy research Centre of the Netherlands, 2011. Cost-Efficient and Sustainable Deployment of Renewable Energy Sources towards the 20% Target by 2020, and beyond.
- European Environment Agency Share of renewable energy in gross final energy consumption in Europe <https://www.eea.europa.eu/data-and-maps/indicators/renewable-gross-final-energy-consumption-4/assessment-4> 2019 accessed 5.6.20.
- Foust, A.S., Wenzel, L.A., Maus, L., Andersen, L.B., 1959. *Principles of Unit Operations*. Wiley Int. Ed. 369–400.
- Ganigué, R., Puig, S., Batlle-Vilanova, P., Balaguer, M.D., Colprim, J., 2015. Microbial electrosynthesis of butyrate from carbon dioxide. *Chem. Commun.* 51, 3235–3238. <https://doi.org/10.1039/c4cc10121a>.
- Ganigué, R., Sánchez-Paredes, P., Bañeras, L., Colprim, J., 2016. Low fermentation pH is a trigger to alcohol production, but a killer to chain elongation. *Front. Microbiol.* 7, 1–11. <https://doi.org/10.3389/fmicb.2016.00702>.
- Gowrisankaran, G., Reynolds, S.S., Samano, M., 2015. Intermittency and the value of renewable energy. *J. Chem. Inf. Model.* 53, 1689–1699. <https://doi.org/10.1017/CBO9781107415324.004>.
- Grim, R.G., Huang, Z., Guarnieri, M.T., Ferrell, J.R., Tao, L., Schaidle, J.A., 2020. Transforming the carbon economy: challenges and opportunities in the convergence of low-cost electricity and reductive CO₂ utilization. *Energy Environ. Sci.* 13, 472–494. <https://doi.org/10.1039/c9ee02410g>.
- Guo, F., Babauta, J.T., Beyenal, H., 2018. Impact of intermittent polarization on electrode-respiring *Geobacter sulfurreducens* biofilms. *J. Power Sources* 406, 96–101. <https://doi.org/10.1016/j.jpowsour.2018.10.053>.
- Hu, X., Zou, C., Zhang, C., Li, Y., 2017. Technological developments in batteries: a survey of principal roles, types, and management needs. *IEEE Power Energy Mag.* 15, 20–31. <https://doi.org/10.1109/MPE.2017.2708812>.
- Jadhav, D.A., Chendake, A.D., Schievano, A., Pant, D., 2018. Suppressing methanogens and enriching electrogens in bioelectrochemical systems. *Bioresour. Technol.* <https://doi.org/10.1016/j.biortech.2018.12.098>.
- Jeremiasse, A.W., Hamelers, H.V.M., Saakes, M., Buisman, C.J.N., 2010. Ni foam cathode enables high volumetric H₂ production in a microbial electrolysis cell. *Int. J. Hydrogen Energy* 35, 12716–12723. <https://doi.org/10.1016/j.ijhydene.2010.08.131>.
- Jourdin, L., Grieger, T., Monetti, J., Flexer, V., Freguia, S., Lu, Y., Chen, J., Romano, M., Wallace, G.G., Keller, J., 2015. High acetic acid production rate obtained by microbial electrosynthesis from carbon dioxide. *Environ. Sci. Technol.* 49, 13566–13574. <https://doi.org/10.1021/acs.est.5b03821>.
- Jourdin, L., Winkelhorst, M., Rawls, B., Buisman, C.J.N., Strik, D.P.B.T.B., 2019. Enhanced selectivity to butyrate and caproate above acetate in continuous bioelectrochemical chain elongation from CO₂: Steering with CO₂ loading rate and hydraulic retention time. *Bioresour. Technol. Reports* 7, 100284. <https://doi.org/10.1016/j.biteb.2019.100284>.
- Koike, K., Fujii, K., Kawano, T., Wada, S., 2020. Bio-mimic energy storage system with solar light conversion to hydrogen by combination of photovoltaic devices and electrochemical cells inspired by the antenna-associated photosystem II. *Plant Signal. Behav.* 00 <https://doi.org/10.1080/15592324.2020.1723946>.
- LaBelle, E.V., May, H.D., 2017. Energy efficiency and productivity enhancement of microbial electrosynthesis of acetate. *Front. Microbiol.* 8, 1–9. <https://doi.org/10.3389/fmicb.2017.00756>.
- Liu, Z., Wang, K., Chen, Y., Tan, T., Nielsen, J., 2020. Third-generation biorefineries as the means to produce fuels and chemicals from CO₂. *Nat. Catal.* 3 <https://doi.org/10.1038/s41929-019-0421-5>.
- Matemadombo, F., Puig, S., Ganigué, R., Ramírez-García, R., Batlle-Vilanova, P., Balaguer, M., Colprim, J., 2016. Modelling the simultaneous production and separation of acetic acid from CO₂ using an anion exchange membrane microbial electrosynthesis system. *Chem. Technol. Biotechnol.* 92, 1211–1217. <https://doi.org/10.1002/jctb.5110>.
- Nevin, K.P., Woodard, T.L., Franks, A.E., 2010. *Microbial Electrosynthesis: Feeding Microbes Electricity To Convert Carbon Dioxide and Water to Multicarbon Extracellular Organic*. *Am. Soc. Microbiol.* 1, 1–4. <https://doi.org/10.1128/mBio.00103-10.Editor>.
- Patil, S.A., Gildemyn, S., Pant, D., Zengler, K., Logan, B.E., Rabaey, K., 2015. A logical data representation framework for electricity-driven bioproduction processes. *Biotechnol. Adv.* 33, 736–744. <https://doi.org/10.1016/j.biotechadv.2015.03.002>.
- Pepe Sciarria, T., Batlle-Vilanova, P., Colombo, B., Scaglia, Barbara, Balaguer, M.D., Colprim, J., Puig, S., Adani, Fabrizio, 2018. Bio-electrorecycling of carbon dioxide into bioplastics. *Green Chem.* <https://doi.org/10.1039/C8GC01771A>.
- Puig, S., Ganigué, R., Batlle-Vilanova, P., Balaguer, M.D., Bañeras, L., Colprim, J., 2017. Tracking bio-hydrogen-mediated production of commodity chemicals from carbon dioxide and renewable electricity. *Bioresour. Technol.* 228, 201–209. <https://doi.org/10.1016/j.biortech.2016.12.035>.
- Rabaey, K., Rozendal, R.A., 2010. Microbial electrosynthesis - Revisiting the electrical route for microbial production. *Nat. Rev. Microbiol.* 8, 706–716. <https://doi.org/10.1038/nrmicro2422>.
- Raes, S.M.T., Jourdin, L., Buisman, C.J.N., Strik, D.P.B.T.B., 2017. Continuous long-term bioelectrochemical chain elongation to butyrate. *ChemElectroChem* 4, 386–395. <https://doi.org/10.1002/celec.201600587>.
- Ramió-Pujol, S., Ganigué, R., Bañeras, L., Colprim, J., 2015. Incubation at 25°C prevents acid crash and enhances alcohol production in *Clostridium carboxidivorans* P7. *Bioresour. Technol.* 192, 296–303. <https://doi.org/10.1016/j.biortech.2015.05.077>.
- Rovira-Alsina, L., Perona-Vico, E., Bañeras, L., Colprim, J., Balaguer, M.D., Puig, S., 2020. Thermophilic bio-electro CO₂ recycling into organic compounds. *Green Chem.* 22, 2947–2955. <https://doi.org/10.1039/d0gc00320d>.
- Roy, M., Yadav, R., Chiranjeevi, P., Patil, S.A., 2021. Direct utilization of industrial carbon dioxide with low impurities for acetate production via microbial electrosynthesis. *Bioresour. Technol.* 320, 124289 <https://doi.org/10.1016/j.biortech.2020.124289>.
- Sánchez, O.G., Birdja, Y.Y., Bulut, M., Vaes, J., Breugelmans, T., Pant, D., 2019. Recent advances in industrial CO₂ electroreduction. *Opin. Green Sustain. Chem. Curr.* <https://doi.org/10.1016/j.cogsc.2019.01.005>.
- Solar edge, 2019. Technical Note – Monitoring Platform Environmental Benefits Calculation.
- Song, H., Choi, O., Pandey, A., Kim, Y.G., Joo, J.S., Sang, B.I., 2019. Simultaneous production of methane and acetate by thermophilic mixed culture from carbon dioxide in bioelectrochemical system. *Bioresour. Technol.* 281, 474–479. <https://doi.org/10.1016/j.biortech.2019.02.115>.
- Spanish solar radiation data. URL <http://www.adrase.com/en/> (accessed 10.3.19).
- Streeck, J., Hank, C., Neuner, M., Gil-Carrera, L., Kokko, M., Pauliuk, S., Schaadt, A., Kerzenmacher, S., White, R.J., 2018. Bio-electrochemical conversion of industrial wastewater combined with downstream methanol synthesis – an economic- and life cycle assessment. *Green Chem.* 00, 1–3. <https://doi.org/10.1039/C8GC00543E>.
- Stumm, W., Morgan, J.J., 1996. *Aquatic chemistry – chemical equilibria and rates in natural waters*. *Environ. Sci. Technol.*
- Tanner, R.S., Miller, L.M., Yang, D., 1993. *Clostridium ljungdahlii* sp. nov., an acetogenic species in clostridial rRNA homology group I. *Int. J. Syst. Bacteriol.* 43, 232–236. <https://doi.org/10.1099/00207713-43-2-232>.
- United Nations, 2015. Paris agreement.
- Vassilev, I., Hernandez, P.A., Batlle-Vilanova, P., Freguia, S., Krömer, J.O., Keller, J., Ledezma, P., Virdis, B., 2018. Microbial electrosynthesis of isobutyric, butyric, caproic acids, and corresponding alcohols from carbon dioxide. *ACS Sustain. Chem. Eng.* 6, 8485–8493. <https://doi.org/10.1021/acscuschemeng.8b00739>.
- Vassilev, I., Kracke, F., Freguia, S., Keller, J., Krömer, J.O., Ledezma, P., Virdis, B., 2019. Microbial electrosynthesis system with dual biocathode arrangement for simultaneous acetogenesis, solventogenesis and carbon chain elongation. *Chem. Commun.* 55, 4351–4354. <https://doi.org/10.1039/c9cc00208a>.
- Watson, W.J., Logan, B.E., 2011. Analysis of polarization methods for elimination of power overshoot in microbial fuel cells. *Electrochem. Commun.* 13, 54–56. <https://doi.org/10.1016/j.elecom.2010.11.011>.
- WEO, 2018. The gold standard of energy analysis. accessed 9.24.19. <https://www.iea.org/weo2018/>.
- Yu, L., Yuan, Y., Tang, J., Zhou, S., 2017. Thermophilic *Moorella thermoautotrophica*-immobilized cathode enhanced microbial electrosynthesis of acetate and formate from CO₂. *Bioelectrochemistry* 117, 23–28. <https://doi.org/10.1016/j.bioelechem.2017.05.001>.
- Zhang, X., Rabaey, K., PrévotEAU, A., 2019. Reversible effects of periodic polarization on anodic electroactive biofilms. *ChemElectroChem* 6, 1921–1925. <https://doi.org/10.1002/celec.201900228>.

Supporting Information

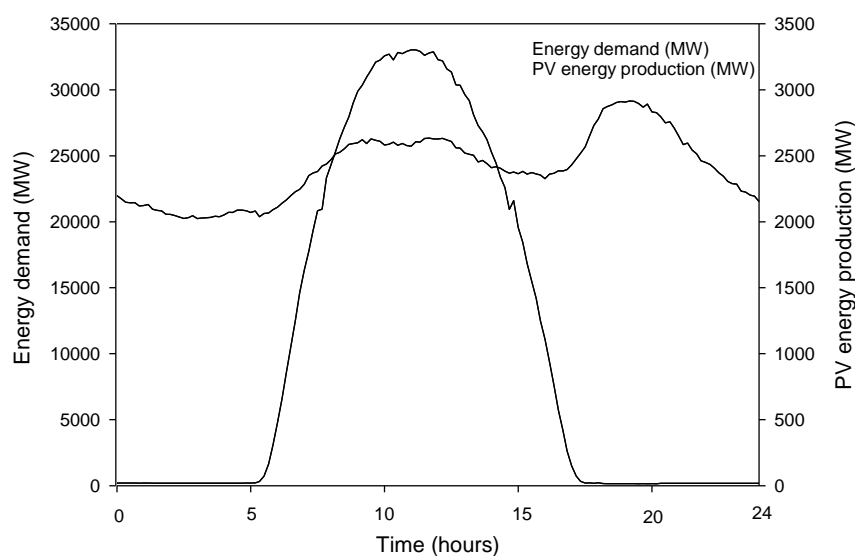


Figure S1. Electrical energy demand (light grey) and photovoltaic (PV) energy generation (dark grey) on March 24th of 2019 (Spain).

Table S1. Composition of the medium used in the microbial electrolysis cells

Medium component	(g L ⁻¹)	Trace metal solution	(mg L ⁻¹)	Vitamin solution	(μg L ⁻¹)
KH ₂ PO ₄	0.1	Nitrilotriacetic acid	20.0	Biotin	20.0
NaCl	0.8	MnSO ₄ H ₂ O	10.0	Folic acid	20.0
NH ₄ Cl	1.0	Fe(SO ₄) ₂ (NH ₄) ₂ 6H ₂ O	8.0	Pyridoxine hydrochloride	100.0
MgCl ₂ 6H ₂ O	0.2	CoCl ₂ 6H ₂ O	2.0	Thiamine hydrochloride	50.0
KCl	0.1	ZnSO ₄ 7H ₂ O	0.002	Riboflavin	50.0
CaCl ₂ 2H ₂ O	0.02	CuCl ₂ 2H ₂ O	0.2	Nicotinic acid	50.0
C ₆ H ₁₃ NO ₄ S H ₂ O (MES)	1.95	NiCl ₂ 2H ₂ O	0.2	DL-calcium pantothenate	50.0
Cysteine HCl	0.4	Na ₂ MoO ₄ 2H ₂ O	0.2	Vitamin B12	1.0

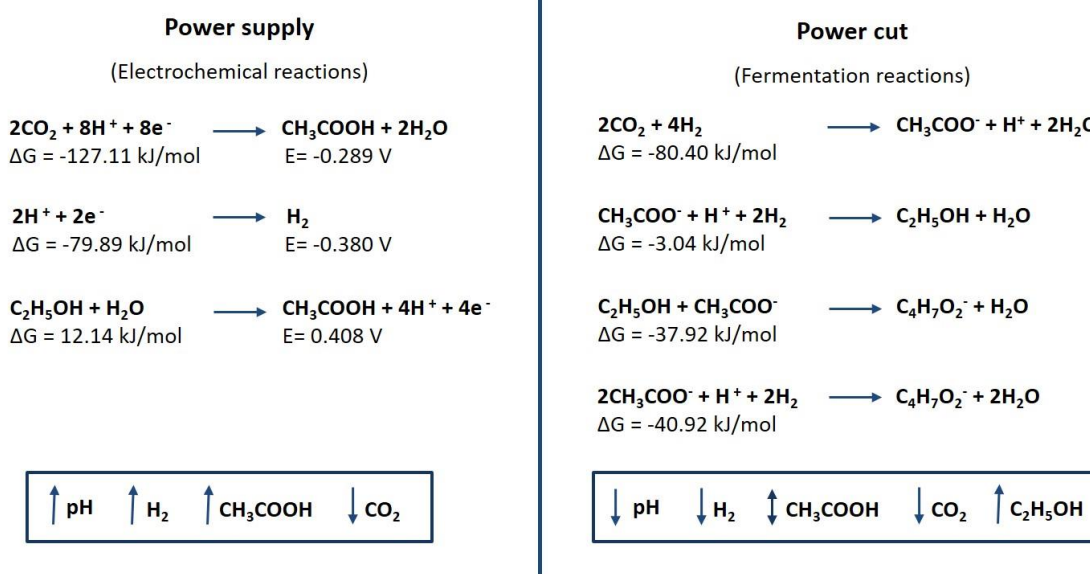


Figure S2. Electrochemical and fermentation reactions during power supply and power cuts. Conditions used for the thermochemical parameters calculations: $T = 323 \text{ K}$, $\text{pH} = 7$, $P_{\text{H}_2} = 1$ and activities = 1. Units of potential values: V vs. SHE. The effect in chemical properties and products fluctuation is given in a blue box.

Table S2. Concentration of CO_2 , H_2 , H^+ , acetic acid (HA), ethanol and butyric acid in liquid media of R1 and R2 during power supply (CA) and disconnection (OCV) of week 4 of the study.

R1	CO_2	H_2	pH d^{-1}	HA	Et	R2	CO_2	H_2	pH d^{-1}	HA	HB
	$(\text{mg L}^{-1} \text{d}^{-1})$	$(\text{mg L}^{-1} \text{d}^{-1})$		$(\text{mg L}^{-1} \text{d}^{-1})$	$(\text{mg L}^{-1} \text{d}^{-1})$		$(\text{mg L}^{-1} \text{d}^{-1})$	$(\text{mg L}^{-1} \text{d}^{-1})$		$(\text{mg L}^{-1} \text{d}^{-1})$	$(\text{mg L}^{-1} \text{d}^{-1})$
ON	510.5 ± 123.2	4.2 ± 0.6	$0.18 \pm 0,04$	240.2 ± 51.0	-19.1 ± 5.3	ON	514.9 ± 290.5	4.8 ± 1.0	0.36 ± 0.08	514.9 ± 290.5	-29.7 ± 1.1
OFF	$35.2 \pm 35,2$	0.0 ± 0.2	$-0.13 \pm 0,02$	33.0 ± 24.0	17.7 ± 6.4	OFF	-114.4 ± 4.4	0.0 ± 0.2	-0.10 ± 0.03	114.4 ± 4.4	14.5 ± 0.4



Figure S3. Reactors assembly and configuration in the orbital incubator.

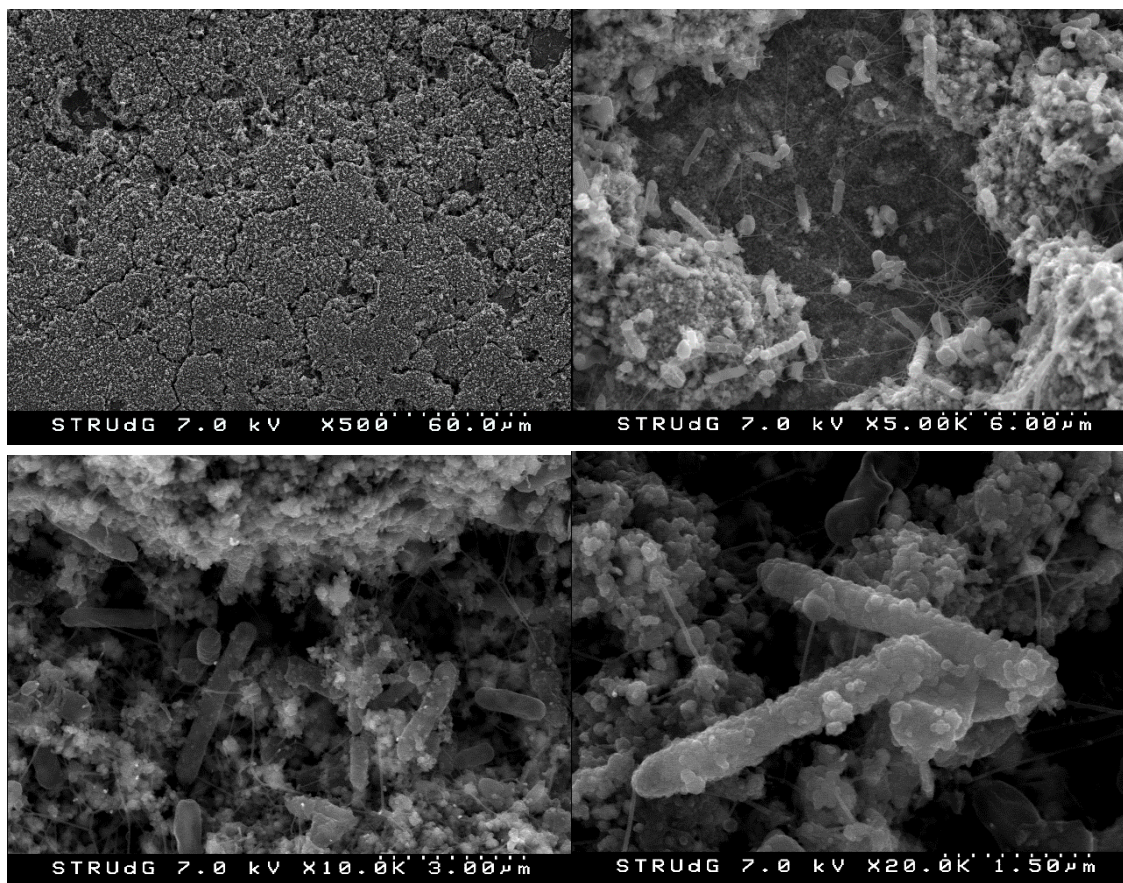


Figure S4. Scanning electron microscopy of micrographs derived from the cathode biofilms before the experiments started. Images are seen at different magnifications (from 500 X to 20 000 X).

4.3. Thermodynamic approach to foresee experimental CO₂ reduction to organic compounds

Laura Rovira-Alsina, Meritxell Romans-Casas, M. Dolors Balaguer and Sebastià Puig*

LEQUIA. Institute of the Environment, University of Girona. Campus Montilivi,
C/Maria Aurèlia Capmany, 69, E-17003 GironaCatalonia, Spain.

*E-mail: sebastia.puig@udg.edu



Thermodynamic approach to foresee experimental CO₂ reduction to organic compounds

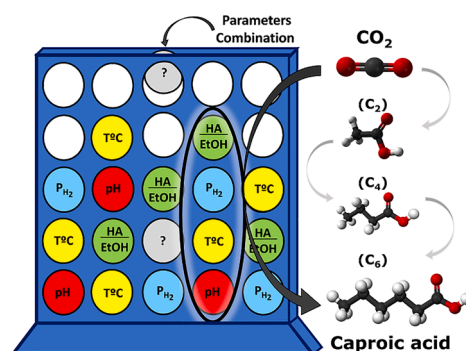
Laura Rovira-Alsina¹, Meritxell Romans-Casas¹, M. Dolors Balaguer, Sebastià Puig^{*}

LEQUIA, Institute of the Environment, University of Girona, Campus Montilivi, C/Maria Aurèlia Capmany, 69, E-17003 Girona, Catalonia, Spain

HIGHLIGHTS

- The potential procurement of elongated compounds from CO₂ was studied and tested.
- The thermodynamic analysis revealed ethanol was the bottleneck for chain elongation.
- Experimental tests allowed fine-tuning of the operating conditions.
- The integration of thermodynamics and biology intensified caproic acid production.
- The highest caproic acid titer (>11 g L⁻¹) was obtained from simple substrates.

GRAPHICAL ABSTRACT



ARTICLE INFO

Keywords:
 Anaerobic fermentation
 Carboxylate platform
 Chain elongation
 CO₂ valorization
 Open culture

ABSTRACT

Anaerobic gas fermentation is a promising approach to transform carbon dioxide (CO₂) into chemical building blocks. However, the main operational conditions to enhance the process and its selectivity are still unknown. The main objective of this study was to trigger chain elongation from a joint perspective of thermodynamic and experimental assessment. Thermodynamics revealed that acetic acid formation was the most spontaneous reaction, followed by n-caproic and n-butyric acids, while the doorway for alcohols production was bounded by the selected conditions. Best parameters combinations were applied in three 0.12 L fermenters. Experimentally, n-caproic acid formation was boosted at pH 7, 37 °C, Acetate:Ethanol mass ratio of 1:3 and low H₂ partial pressure. Though these conditions did not match with those required to produce their main substrates, the unification of both perspectives yielded the highest n-caproic acid concentration (>11 g L⁻¹) so far from simple substrates, accounting for 77 % of the total products.

1. Introduction

CO₂ can be reused as a substrate for energy, fuels and chemicals formation through different approaches. Gas fermentation (GF) is a well-

known technology able to perform the recycling of CO₂ (Agler et al., 2011) into chemical building blocks using microorganisms as catalysts (Dürre and Eikmanns, 2015). Acetic acid (HA), a short-chain carboxylic acid (SCCA), is one of the most produced compounds which can be

* Corresponding author.

E-mail address: sebastia.puig@udg.edu (S. Puig).

¹ These authors contributed equally.

<https://doi.org/10.1016/j.biortech.2022.127181>

Received 23 March 2022; Received in revised form 12 April 2022; Accepted 14 April 2022

Available online 18 April 2022

0960-8524/© 2022 The Authors. Published by Elsevier Ltd. This is an open access article under the CC BY-NC-ND license (<http://creativecommons.org/licenses/by-nc-nd/4.0/>).

further valorised through its reduction into elongated compounds, the so-called medium-chain carboxylic acids (MCCAs, compounds from six to twelve carbons). Chain elongation is included in the carboxylate platform, set out as a second fermentation process (Agler et al., 2011) and its feasibility has been already proven (Angenent et al., 2016; Candry and Ganigué, 2021). It involves the cyclic addition of two carbon molecules to the compound-chain through the reverse β -oxidation pathway, in which an electron donor (i.e. ethanol) and an electron acceptor (i.e. an organic compound itself) are interconnected through electron transfer mechanisms (Cavalcante et al., 2017). Although pure cultures were initially employed and largely investigated, it was later demonstrated that open cultures are advantageous due to their robust and resilient communities, and their increased production rates owing to their synergistic behaviour (Pinto et al., 2021; Paquete et al., 2022). This brings the technology closer to environmental conditions and its utilization has been proven to be both, cost and energy more efficient (Pinto et al., 2021).

Elongated organic compounds have broad applications such as pharmaceutical and chemical industries (Angenent et al., 2016). MCCA produced through fermentative reduction are attractive assets since they are considered suitable energy carriers avoiding the use of fossil sources at low yields (Cavalcante et al., 2017). For instance, n-butyric acid (C_4) can be employed to produce fuels (i.e. butyl or ethyl butyrate), to manufacture plastics and as a flavouring agent (Dessi et al., 2021). In respect of n-caproic acid (C_6), it has been thoroughly investigated due to its multiple applications as an antimicrobial agent, additive for animal feed and as a potential precursor for biofuels production (Dessi et al., 2021). In addition, its current market price is circa 3.7 \$/kg, followed by other organics such as alcohols, but far much higher than other acids as acetic or propionic (Wood et al., 2021).

The formations of n-butyric (HB) and n-caproic (HC) acids have been largely studied from a broad range of substrates. Elongations from HA into HB and HC using ethanol (EtOH) as electron donor have been reported before (Romans-Casas et al., 2021). Grootsholten and colleagues (2013) compared HC production rates with and without EtOH addition from HA. Recently, the feasibility of chain elongation reactions was assessed for different fermentation pathways and reactants proportion, highlighting that higher concentrations of HB benefitted HC production (Wang et al., 2020). However, there are still many gaps in knowledge, specially related to unravelling the optimum working conditions to trigger a selective formation of one specific compound starting from CO_2 . Therefore, the main challenges that hinder a competitive and efficient production remain to be overcome.

Thermodynamics deals with the relationship between different forms of energy and its conversion. It is variable, depends on many factors and involves a large number of molecules interacting intricately (Hanselmann, 1991). However, when the system reaches equilibrium, it can be described in a simpler approach that can give valuable information related to energy processes. The present study developed a thermodynamic based-model to elucidate the appropriate conditions to favour chain elongation reactions. The model was focused on the combination of four parameters: pH, temperature (T), substrates ratio and compounds titers. A set of parameters identified as optimal was subsequently tested experimentally to beat the limited knowledge of the co-effect of working conditions and biology, given that thermodynamics is conditioned by the kinetics and enzymatic capabilities of each microorganism. Fermentative tests from CO_2 were carried out adding hydrogen (H_2), HA and EtOH that can be obtained from a bioelectrochemical system (BES) (Vassilev et al., 2022), as substrates.

2. Materials and methods

2.1. Thermodynamic analysis

A thermodynamic based-model was built considering the main gas fermentation and chain elongation reactions. They were equated

stoichiometrically and the standard Gibbs free energy (ΔG°) of the main reactions was calculated and compared with the literature (Table 1). The standard Gibbs free energies of formation ($\Delta_f G^\circ$) and the standard enthalpies of formation ($\Delta_f H^\circ$) were extracted from Amend and Shock (2001), Alberty (2001) and the CRC Handbook of Chemistry and Physics (Lide and Baysinger, 2004). The carboxylate chain length was limited to six carbon atoms, as with longer chain compounds the addition of electrons bonded with each additional step in the β -reverse oxidation is smaller (Lambrecht et al., 2019).

The $\Delta G_{T_s}^\circ$ of each reaction was corrected considering the temperature, ionic strength, pH and species' concentrations. The corrected Gibbs free energy of reactions at different temperatures ($\Delta G_{(T)}$ 25, 37 and 50 °C) was calculated using the Helmholtz equation (Eq. (1)) where standard temperature (T_s) was 298.15 K and $\Delta H_{T_s}^\circ$ was calculated using the standard enthalpy of formation values of each compound taken from Kleerebezem and Van Loosdrecht (2010).

$$\Delta G_{(T)} = \Delta G_{T_s}^\circ \frac{T}{T_s} + \Delta H_{T_s}^\circ \frac{T_s - T}{T_s} \quad (1)$$

The effect of the ionic strength was calculated based on the extended Debye-Hückel equation (Eq. (2)) where $\Delta G_{T(I)}$ is the corrected Gibbs free energy, x_i is the stoichiometry coefficient of each specie, $RT\alpha = 9.20483 \cdot 10^{-3} T - 1.28467 \cdot 10^{-5} T^2 + 4.95199 \cdot 10^{-8} T^3$, $N_{H,i}$ is the number of hydrogen atoms in the substance i , Z_i is the charge number of each specie, $B = 1.5 \text{ kg}^{1/2} \text{ mol}^{-1/2}$ (empirical constant from Goldberg and Tewari, 1991) and I is the ionic strength of the solution.

$$\Delta G_{T(I)} = \Delta G_T + \left(\sum_r x_i \frac{RT\alpha (Z_i^2 - N_{H,i}) I^2}{1 + B I^{1/2}} \right) \quad (2)$$

The range of concentrations studied was selected considering the

Table 1

Standard Gibbs free energy (ΔG°) change for gas fermentation and chain elongation reactions. For chain elongation reaction with ethanol oxidation, the overall coupled reaction is shown and used for the calculations below.

Reaction	ΔG_{25}° (kJ mol ⁻¹)	Source
Gas fermentation		
R1 Hydrogenotrophic acetogenesis $4H_2 + 2CO_2 \rightarrow CH_3COO^- + H^+ + 2H_2O$	-94.96	(Spirito et al., 2014)
R2 Hydrogenotrophic solventogenesis $6H_2 + 2CO_2 \rightarrow CH_3CH_2OH + 3H_2O$	-105.00	(Baleeiro et al., 2019)
Chain elongation		
R3 Acetate reduction to ethanol with H_2 $CH_3COO^- + H^+ + 2H_2 \rightarrow CH_3CH_2OH + H_2O$	-10.50	(Spirito et al., 2014)
R4 Ethanol-acetate elongation to n-butyrate $6CH_3CH_2OH + 4CH_3COO^- \rightarrow 5CH_3(CH_2)_2COO^- + H^+ + 2H_2 + 4H_2O$	-28.75	(Wang et al., 2020)
R5 Ethanol-butyrate elongation to n-caproate $6CH_3CH_2OH + 5CH_3(CH_2)_2COO^- \rightarrow 5CH_3(CH_2)_4COO^- + CH_3COO^- + H^+ + 2H_2 + 4H_2O$	-36.7	(Spirito et al., 2014)
R6 Hydrogenotrophic acetate elongation to n-butyrate $2H_2 + 2 CH_3COO^- + H^+ \rightarrow CH_3(CH_2)_2COO^- + 2H_2O$	-48.20	(Baleeiro et al., 2019)
R7 Ethanol-acetate elongation to n-caproate $12CH_3CH_2OH + 3CH_3COO^- \rightarrow 5CH_3(CH_2)_4COO^- + 2H^+ + 4H_2 + 8H_2O$	-57.60	(Wang et al., 2020)
R8 n-butyrate elongation to n-butanol $CH_3(CH_2)_2COO^- + H^+ + 2H_2 \rightarrow CH_3(CH_2)_3OH + H_2O$	-6.46	(Agler et al., 2011)*
R9 n-caproate elongation to n-hexanol $CH_3(CH_2)_4COO^- + H^+ + 2H_2 \rightarrow CH_3(CH_2)_5OH + H_2O$	-10.33	(Agler et al., 2011)*

ΔG° activities equal to 1 and pH 7.

* Recalculated from ΔG values at 37 °C.

average concentration of ions in previous experiments. The Eq. (3) was used to calculate the three different molal ionic strengths (0.07, 0.09 and 0.11 b) used for further calculations, in which c_i is the molal concentration of the ion i (mol kg⁻¹) and z_i is the charge number of that ion.

$$I = \frac{1}{2} \sum_{i=1} c_i z_i^2 \quad (3)$$

The pH and the activities of products and substrates in the medium were corrected by adapting the Nernst equation (Eq. (4)), in which R is the gas constant (8.31 J K⁻¹ mol⁻¹), T is the chosen temperature (25, 37 or 50 °C in K), $[i]$ denotes the activities of reactants and products of a general reaction $aA + bB \leftrightarrow cC + dD$ and xH is the stoichiometric coefficient of H⁺ (Gildemyn et al., 2017), which is positive when it is on the reactants side, and negative when it is on the products side. The corrected Gibbs free energy ($\Delta G_{T,I(pH,T)}$) is shortened as $\Delta G'$.

$$\Delta G' = \Delta G_{T,I} + RT \ln \Pi - \ominus RT \ln \left(\left[\frac{10^{-\text{pH}}}{10^{-7}} \right]^{xH} \right) \quad \Pi = \frac{[C]^c [D]^d}{[A]^a [B]^b} \quad (4)$$

Assuming that the system is dilute, the calculations were simplified by estimating the activities as molar concentrations (M), which ranged from 0.001 to 0.210 M. Regarding gaseous components, the concentration in the liquid phase was estimated considering the H₂ partial pressure (which ranged from 0.25 to 1.75 atm) and Henry's law (Eq. (5)), where C_i is the solubility of a gas component (i) in a particular solvent (mol L⁻¹), H_i is Henry's law constant in mol L⁻¹ atm⁻¹ and P_i is the partial pressure of the gas component (i) in atm.

$$C_i = H_i \cdot P_i \quad (5)$$

Then, the division of the corrected Gibbs free energy by the electron transfer events (Ne) in each reaction ($\Delta G \text{ Ne}^{-1}$) was calculated to indirectly evidence the competitiveness of the different reaction pathways according to Wu et al. (2018). By mixing variables and conditions of the model, several situations were depicted, but not all the data were presented to ease the understanding of the results.

2.2. Inoculum, experimental setup, and operational conditions

An enriched mixed culture that previously showed the ability to trigger chain elongation (Blasco-Gómez et al., 2021) was used to validate the outputs from the thermodynamic model. Three main fermentative tests (F1 to F3) operated under the best set of conditions to prompt HC formation were tested. They consisted of 0.12 L serum bottles, with 0.05 L of the liquid phase and 0.07 L of headspace. Each fermenter was filled with a modified ATCC1754 PETC medium (see supplementary material) and inoculated with a 20 % (v/v) of the culture. Three consecutive washes with the same fresh media were conducted to remove all organic carbon sources coming from the raw culture. The pH of the medium was initially fixed to 6.0 and later adjusted depending on the experimental conditions. All bottles were hermetically closed with rubber stoppers and aluminium caps.

Operational conditions were established at the beginning of each experimental test and corresponded (for F1) to the ones unravelled as optimal by the thermodynamic model for HC formation. However, F2 and F3 were performed under compromise conditions to consider biological factors. Control tests (PF 1 – PF 6) were performed to check the model results for both HA and EtOH production and its accuracy in a real scenario. The temperature was maintained constant at either 25 °C (room temperature control), 37 °C (Advanced Programmable Heated Circulator thermostat bath, AP28H200A1, Spain) or 50 °C (SI600 orbital incubator, Stuart, UK). pH was set at 5.0, 6.0 or 7.0, and adjusted throughout the operational period by adding 1 M sodium hydroxide or 1 M hydrochloric acid when required. The used acetic acid to ethanol mass ratio (HA:EtOH) was 1:3 in tests where those substrates were employed, corresponding to 1 g L⁻¹ and 3 g L⁻¹ of HA and EtOH, respectively. The ratio was selected to favour the selectivity of HC formation (Wu et al.,

2022). All fermenters were kept in agitation to promote mass transfer and under the darkness to avoid photosynthetic growth. They were sparged with a gas mixture of CO₂:H₂ (20:80 % v/v, Praxair, Spain) twice a week, leading to an overpressure of 1 bar to keep an anaerobic environment rich in carbon and reducing power. However, F3 was once a week fed with pure CO₂ (99.9 %, Praxair, Spain), alternating the feeding regime with the CO₂:H₂ mixture to study the effect of different H₂ partial pressures. All tests were conducted in duplicate.

2.3. Analyses and calculations

Gas- and liquid-phase samples were taken once or twice a week to track the evolution of the main reactions. To maintain a steady volume, withdrawn liquid volume was replaced by fresh medium and pH was restored when needed. Electrical conductivity and pH were measured with an electrical conductivity meter (EC-meter basic 30+, Crison, Spain) and a multimeter (MultiMeter 44, Crison, Spain), respectively. The concentration of volatile fatty acids and alcohols in the liquid phase was determined using an Agilent 7890A gas chromatograph equipped with a DB-FFAP column and a flame ionization detector. The optical density (OD) was periodically measured in absorbance units (AU) to control the growth of the microbial community with a spectrophotometer (CE 1021, 1000 Series, CECIL Instruments Ltd., UK) at a wavelength of 600 nm. The dry cell weight (DCW) was calculated by performing a regression line with the total suspended solids (TSS) of different volumes of the inoculum (1 OD = 565.75 mg L⁻¹). Gas samples were analysed by gas chromatography (490 Micro GC system, Agilent Technologies, US). The Micro GC was equipped with two columns: a CP-molesive 5A for methane (CH₄), carbon monoxide (CO), H₂, oxygen (O₂) and nitrogen (N₂) analysis, and a CP-Poraplot U for CO₂ analysis, connected to a thermal conductivity detector (TCD).

Gas pressure profiles were quantified by measuring the pressure in the headspace of the fermenters using a digital pressure sensor (differential pressure gauge, Testo 512, Spain). The concentrations of dissolved H₂ and CO₂ in the liquid media were calculated using Henry's law (Eq. (5)).

3. Results and discussion

Given the current interest generated by bio-CO₂ recycling technologies and the production of MCCAs, the present work aimed to produce elongated compounds, as HC, under the most suitable conditions. To obtain a C₆ elongated product from H₂ and CO₂ as the only substrates, a succession of several reactions was required. First, a thermodynamic model was developed to study each reaction individually and to investigate whether these conditions allowed the production of several intermediates up to HC in concomitance. Then, these conditions were tested experimentally to shed light on how the enzymatic capabilities of the biocatalyst and the kinetics of the reaction affected this approach.

3.1. Prospects for chain elongation from CO₂ step by step

HC production from CO₂ is performed through a series of cascade reactions. The spontaneity of those reactions is given by the Gibbs free energy, though its standard value is influenced by environmental conditions. First, the ΔG_{25}^0 values for each intermediate reaction were corrected by temperature and ionic strength ($\Delta G_{T,I}$) and represented under different scenarios (see supplementary material). None of these variables substantially modified the spontaneity of the reactions, although the temperature had a linear effect ($R^2 > 0.999$) increasing the ΔG values between 0.23 and 0.59 kJ mol⁻¹ per 1 °C depending on each reaction. HA was by difference the most thermodynamically favoured compound followed by HC and HB, EtOH, n-hexanol (HexOH) and n-butanol (ButOH). Otherwise, the ratio of the corrected $\Delta G_{T,I}$ to the number of electrons transferred in each reaction ($\Delta G_{T,I} \text{ Ne}^{-1}$) was calculated to indirectly point out the competitiveness between pathways

(Wu et al., 2018). $\Delta G_{T,I} \text{ Ne}^{-1}$ ratios of most of the chain elongation reactions were close to each other except for HA formation (see [supplementary material](#)), indicating that the competition between them was noticeable, as their relative differences diminished. Moreover, the order of the $\Delta G_{T,I} \text{ Ne}^{-1}$ profiles changed with respect to $\Delta G_{T,I}$ ones, with HB being more spontaneous than HC and increasing the distance between EtOH and HexOH profiles. Given that any redox reaction tends to equilibrium, it was expected that the spontaneity would also be modified by the species concentration. Hence, the effect of changing pH and concentrations of reactants and products was also considered to correct the Gibbs free energy of each reaction ($\Delta G_{T,I(pH,r)}$), from now on simplified as $\Delta G'$.

The production of HA from CO_2 and H_2 was inspected as the first step of the chain reaction. Fig. 1 represents the $\Delta G'$ variation under different conditions of temperature, pH, substrate ratio of employed gases and product concentration when following the hydrogenotrophic HA formation (Table 1, R1). The major spontaneity turned out to occur at 25 °C, pH 7 and high hydrogen partial pressure (P_{H_2}). Higher ratios of $P_{\text{H}_2} : P_{\text{CO}_2}$ (3:1 and 1:1) enhanced the reaction compared to lower ratios (1:3), pointing out the great importance of H_2 , assumed to be the electron donor of the reaction. Conversely, a rise in HA concentration considerably decreased the negative $\Delta G'$ values, while the effect of pH was even more remarkable (lower $\Delta G'$ values when less H^+ accumulated on the product side). HA formation was favourable for all the conditions tested, though threshold conditions where a shift in the spontaneity occurred (positive $\Delta G'$ values) were calculated by the model: 50 °C, pH 5, low P_{H_2} and CO_2 availability (<0.023 M). Considering HA is one of the

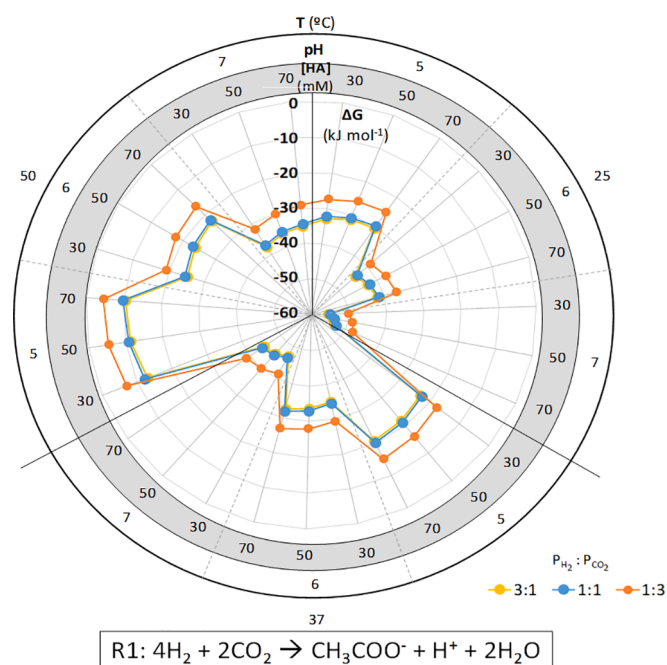


Fig. 1. Gibbs free energy variation ($\Delta G'$) for hydrogenotrophic acetic acid (HA) formation. Different conditions of pH, temperature (T; °C), substrates ratios (P_{H_2} and P_{CO_2} ; H_2 and CO_2 partial pressures respectively, in atm) and product concentration ([HA] in mM) were tested.

main substrates for the production of longer-chain carboxylates (Ange-ment et al., 2016), the conditions favoring its formation should be heeded throughout the process.

Two different reactions were studied concerning EtOH formation, either by employing H_2 and CO_2 as substrates or through HA conversion (Fig. 2). $\Delta G'$ values for hydrogenotrophic EtOH production (Fig. 2A) were lower compared to EtOH formation through HA reduction (Fig. 2B). This matches with the literature (Baleeiro et al., 2019; Spirito et al., 2014), but after considering the concentration of reactants and products, none of them were spontaneous for any of the parameters tested ($\Delta G' > 0$), differing from the standard ones (Table 1, R2 and R3).

According to the previously reported by other authors, EtOH is usually the bottleneck of chain elongation, since it is the main compound required as an electron donor. Even though $\Delta G'$ values were positive, the most favourable conditions for EtOH were similar to HA formation (25 °C and high P_{H_2}), though pH 5 decreased $\Delta G'$ values compared to pH 7. Concerning reaction R2, an EtOH concentration under 10^{-3} M was necessary to shift the $\Delta G'$ to negative values while for reaction R3 it was not possible until EtOH reached concentrations below 10^{-8} M. Nevertheless, at 50 °C $\Delta G'$ values could never surpass the spontaneity line.

Since HC is thought to be produced through the intermediate formation of HB, it was also inspected from different substrates: HA plus EtOH (Fig. 3A) and H_2 plus HA (Fig. 3B). The first reaction studied (Table 1, R4) was thermodynamically feasible under all considered conditions, being the best combination 25 °C, pH 7 and 1:3 HA:EtOH mass ratio. In this case, the pH and HB accumulation were revealed to be the most important parameters for its spontaneity, crossing the limit under $\text{pH} < 5$ and $[\text{HB}] > 1$ M. The second reaction (Table 1, R6) was not spontaneous provably due to the low solubility of H_2 that limits its bioavailability in the liquid phase, though as stated by Liu et al. (2016), low pH slightly diminished $\Delta G'$ values. Besides, the developed model predicted that under low temperature (25 °C), high H_2 :HA ratios (1:50), low amounts of HB ($< 10^{-6}$ M) and high amounts of substrates ($[\text{H}_2] > 0.02$ M and $[\text{HA}] > 0.1$ M), the hydrogenotrophic HB formation could also become spontaneous.

Coinciding with the literature (Spirito et al., 2014; Wang et al., 2020), HC production was propitious under both studied situations (Fig. 4). The same working conditions (25 °C, pH 7 and high EtOH concentration) thermodynamically prosper both reactions (Table 1, R5 and R7), favouring its formation over intermediates as HB. However, the product accumulation had more impact compared to the previous reaction for HB production, and a lower amount (0.45 M) of HC was enough to switch its spontaneity. HC from HB and EtOH (Fig. 4A) was less favourable than with HA and EtOH (Fig. 4B). Those results oppose what is claimed in previous studies (Cavalcante et al., 2017) but it can be attributed to the ATP needed for EtOH oxidation in the overall coupled reaction (Wang et al., 2020). Nonetheless, when HB and EtOH worked as substrates (Table 1, R5), the effect of temperature was lower (0.4 $\Delta G'$ units per °C) compared to when HA and EtOH were used (Table 1, R7), in which $\Delta G'$ values increased 0.8 units per degree. Furthermore, reactions R4, R5 and R7 (Table 1) should be considered as H_2 is on the product side, so unlike the rest of the reactions, high P_{H_2} negatively affects their spontaneity. Nevertheless, ButOH and HexOH (see [supplementary material](#)), whose emergence would decrease the selectivity of the process, were not thermodynamically feasible. High reducing power was needed for both to favour their production (Agler et al., 2011), though the concentration of their corresponding acids (HB and HC,

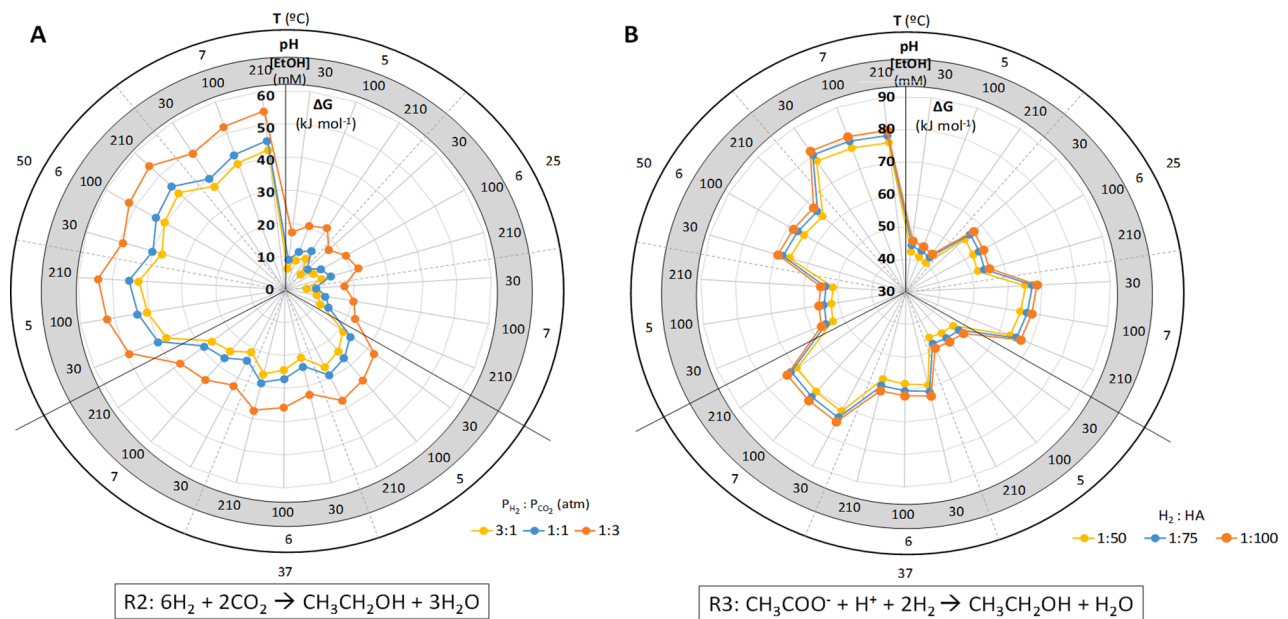


Fig. 2. Gibbs free energy variation ($\Delta G'$) for hydrogenotrophic ethanol (EtOH) formation (A) and acetic acid (HA) conversion to ethanol (B). Different conditions of pH, temperature (T; °C), substrates ratios (P_{H_2} and P_{CO_2} ; H_2 and CO_2 partial pressures respectively, in atm, or HA and H_2 in M) and product concentration ([EtOH] in mM) were tested.

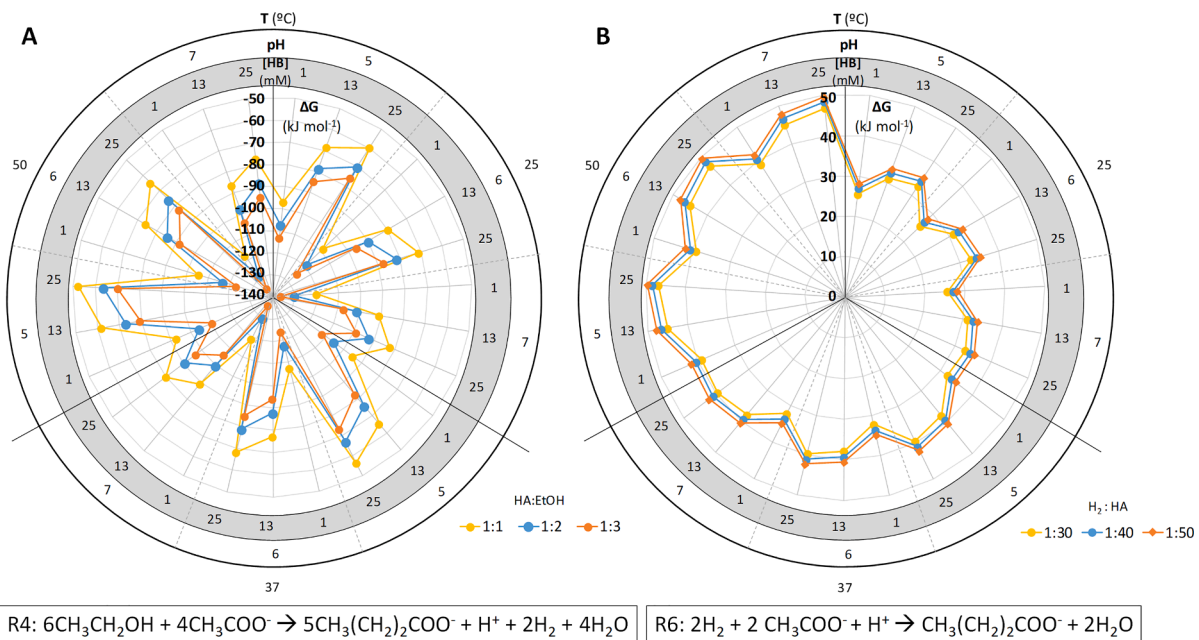


Fig. 3. Gibbs free energy variation ($\Delta G'$) for n-butyric acid (HB) production from HA and EtOH (A) or HA and H_2 (B). Different conditions of pH, temperature (T; °C), substrate ratios in molar (M) units, and product concentration ([HB] in mM) were tested.

respectively) turned out to be more pivotal than the accumulation of H_2 . Besides low temperature (25 °C), low pH (5) boosted the two reactions (Table 1, R8 and R9) since an acidic pH favors the direction of the reactions to move towards the product side to reach equilibrium. Even though $\Delta G'$ values were positive, under the same studied conditions HexOH formation was slightly more reinforced compared to ButOH. However, their thermodynamic behavior among variables followed the same trend. Obtained results are consistent with previously reported

data (Agler et al., 2011).

Altogether, after considering the working conditions, the modified Gibbs free energies were less favourable compared to the standard ones. The ionic strength of the solution had the lowest influence on the spontaneity of the reactions. On the other hand, the low solubility of the gases was the most decisive factor when these were used as substrates, for which HA was the only thermodynamically favourable compound from H_2 and CO_2 (Table 2). All studied reactions were enhanced at low

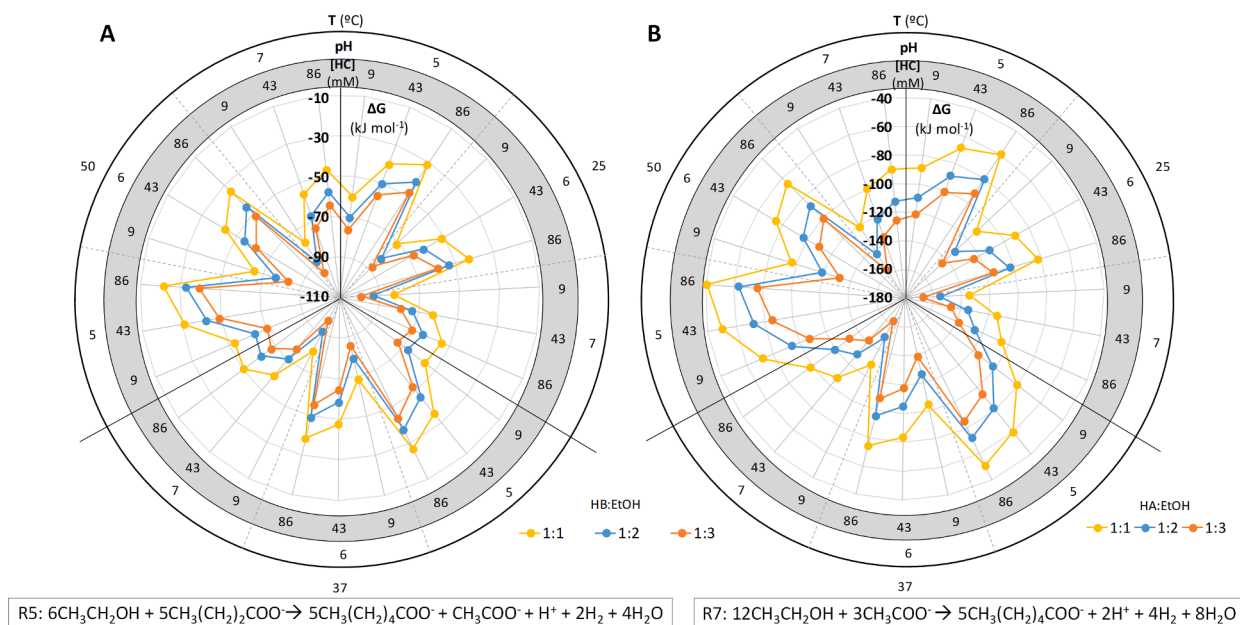


Fig. 4. Evolution of Gibbs free energy ($\Delta G'$) for n-caproic acid (HC) formation from EtOH and HB (A) or HA (B). Different conditions of pH, temperature (T ; $^{\circ}\text{C}$), substrate ratios (M) and product concentration ([HC] in mM) were tested.

Table 2

Compilation of the thermodynamic analysis outputs for the formation of each compound. Spontaneous reactions are colored in green, while non-spontaneous ones are colored in red.

Compound	Energy requirements			Optimal thermodynamic conditions		
				pH	T ($^{\circ}\text{C}$)	Substrate
Acetic acid	$\text{H}_2 + \text{CO}_2$	(R 1)	Spontaneous	7	25	High P_{H_2}
Ethanol	$\text{H}_2 + \text{CO}_2$	(R 2)	Requires Energy	5	25	High P_{H_2}
	$\text{H}_2 + \text{HA}$	(R 3)				High HA
n-Butyric acid	$\text{HA} + \text{EtOH}$	(R 4)	Spontaneous	7	25	High EtOH
	$\text{HA} + \text{H}_2$	(R 6)	Requires energy	5	25	High P_{H_2}
n-Caproic acid	$\text{HB} + \text{EtOH}$	(R 5)	Spontaneous	7	25	High EtOH
	$\text{HA} + \text{EtOH}$	(R 7)				High EtOH
n-Butanol		(R 8)	Requires energy	5	25	High HB
n-Hexanol		(R 9)	Requires energy	5	25	High HC

temperatures (like standard conditions), possibly due to their negative enthalpy increase in the range studied, since an increase in temperature caused an increase in $\Delta G'$, reducing the spontaneity. Theoretically, 25 $^{\circ}\text{C}$, pH 7 and high EtOH availability were aligned for the successive CO_2 elongation to HC. However, EtOH formation constituted a limitation for this purpose and the recalculated $\Delta G'$ values at different operational conditions are only theoretical, which means that there is no guarantee for microbial reactions to occur. In real systems, especially those in which biocatalysts are employed, many other factors as energy losses due to product inhibition and counter ion transport, genome, proteome and reaction kinetics that influence the microbial activity are involved (Korth and Harnisch, 2019). Yet, if the circumstances are given and the reactions take place, it should occur under the best thermodynamic conditions. Therefore, the set of parameters disentangled as optimal for HC formation was experimentally tested and evaluated.

3.2. Experimental tests to validate the thermodynamic outputs

HA and EtOH were needed as the main substrates to achieve the biological production of HC from CO_2 . Different pHs (5, 6, 7) and temperatures (25, 37, 50 $^{\circ}\text{C}$) were tested with the purpose to validate the results of the thermodynamic model (see supplementary material). HA was produced under any of the applied conditions, while EtOH was not.

In natural systems, $\Delta G'$ of at least -20 kJ mol^{-1} is required to consider a reaction as spontaneous (Smeaton and Van Cappellen, 2018). High temperatures may increase the rate of reactions but at the same time, they may exclude some microbial cultures from the game (Rovira-Alsina et al., 2020). Thus, a compromise between thermodynamics, kinetics, and biology (pH 7, 50 $^{\circ}\text{C}$ and high P_{H_2}) turned out to be the best combination for a fast HA generation (see supplementary material). On the contrary, EtOH formation has been reported as a constraint for these systems (Bian et al., 2020). Even though its production was also tested under 37 $^{\circ}\text{C}$ to favour microbial activity (Ghysels et al., 2021), no EtOH was obtained either from H_2 and CO_2 or from H_2 and HA (see supplementary material). However, other studies stated the ability to produce EtOH using different technologies and substrates (Blasco-Gómez et al., 2019), eventually using the route proposed by de Leeuw and co-workers (2021). Since in the present scenario only HA was obtained (see supplementary material), EtOH was externally supplied in the following experiments.

Two fermenters were operated in duplicate for HC formation under the best thermodynamic conditions (pH 7, 25 $^{\circ}\text{C}$, HA:EtOH of 1 to 3 g L^{-1}) and sparged with a gas mixture of $\text{CO}_2:\text{H}_2$ (20:80 v/v) under 1 bar of overpressure (Fig. 5, F1) to keep an anaerobic atmosphere and the continuous HA generation. During the first 15 days of operation, no production was registered but the optical density linearly increased,

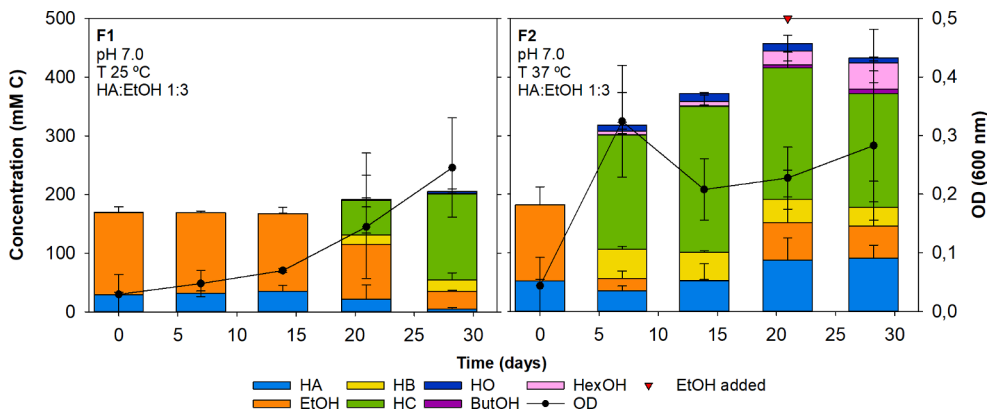


Fig. 5. Evolution of carbon compounds in the first (F1) and second (F2) fermentative tests. F1 was operated under the most suitable conditions unraveled by the thermodynamic model to trigger caproic acid production. F2 was performed with the aim to optimize chain elongation considering biological factors. HA: acetic acid, EtOH: ethanol, HB: n-butyric acid, HC: n-caproic acid, ButOH: n-butanol, HexOH: n-hexanol and OD: optical density. The red inverted triangle points out extra ethanol addition.

which could be attributed to microbial growth. After that period, elongated compounds were obtained concomitantly with a higher increase in OD. HC was the main product, with a maximum concentration of 146.16 ± 1.73 mM C and a corresponding production rate of 12.45 ± 11.26 mM C d^{-1} (80.40 ± 53.42 mmol C g DCW $^{-1}$ d^{-1}). Besides, HB was also observed, reaching a maximum concentration of 19.38 ± 11.98 mM C and a peak production rate of 2.28 ± 0.41 mM C d^{-1} (27.81 ± 15.11 mmol C g DCW $^{-1}$ d^{-1}). Other compounds such as ButOH and HexOH were also present at the end of the test, but the sum of their concentrations was below 5 mM C. Based on the stoichiometry of the proposed reactions to accomplish HC production (Table 1, R4 and R5 or R7) and considering that EtOH is the only compound that was consumed but not produced, 2.4 mol were the minimum amount required to obtain 1 mol of HC. Considering an initial and final concentration of 86 and 15 mM of EtOH respectively, the maximum theoretical HC that could be produced in this test was 29 mM (176 mM C), meaning that only 30 mM C remained unconverted in the form of other compounds.

However, a set of conditions was sought to optimize HC production rates that were not only thermodynamically favourable but also closer to the biological complexity of these systems. Therefore, a second test at 37 °C was carried out in duplicate (Fig. 5, F2). Selected conditions corresponded to the optimum temperature for microbial activity and the second-best model output. During the first 7 days of operation, most of

the EtOH was consumed to produce HB and HC, while it was fully consumed after 14 days, so 130 mM C extra of EtOH were supplied. It must be noted that by increasing the temperature the carbon build-up was enhanced. It is likely that as the thermodynamic model disclosed, the shortage of EtOH together with the high availability of HB and HC may have caused a shift in the metabolic pathways for the formation of these acids to the solventogenesis of their corresponding alcohols, decreasing the selectivity of the final spectrum. Even though they were not thermodynamically feasible, small amounts of ButOH and HexOH appeared to be produced thereafter. It has also been reported in previous studies, indicating that few microorganisms have the ability to trigger these reactions, possibly employing energy obtained in other simultaneous reactions (Pinto et al., 2021). The maximum concentrations of organic substances reached were as follows: 50.11 ± 4.77 mM C of HB, 253.25 ± 13.82 mM C of HC, 7.74 ± 10.95 of ButOH and 46.35 ± 55.00 mM C of HexOH. Other compounds accounted for <10 mM C. Nonetheless, HC was the main compound obtained at a maximum production rate of 25.08 ± 7.08 mM C d^{-1} (137.05 ± 1.71 mmol C g DCW $^{-1}$ d^{-1}) and with a selectivity of 67 %. The results matched with expectations as operating under higher temperatures, higher production rates were anticipated (Rovira-Alsina et al., 2020). Here, considering an available concentration of 260 mM C of EtOH (initial plus added) and a non-converted concentration of 55 mM C, 256 mM C of HC could

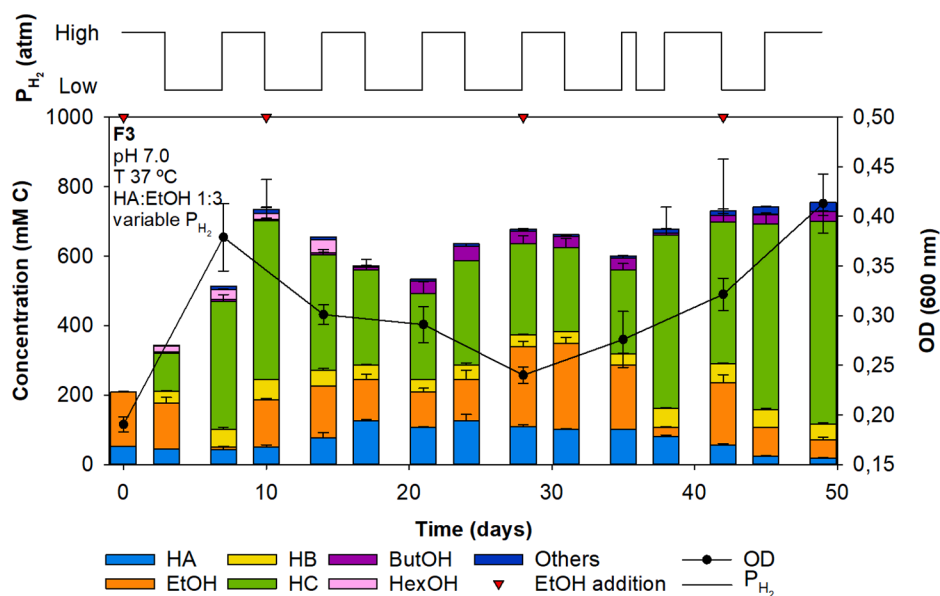


Fig. 6. Evolution of carbon compounds in the third fermentative test (F3) working under the same operational conditions as F2 but periodically varying the H₂ partial pressure. HA: acetic acid, EtOH: ethanol, HB: n-butyric acid, HC: n-caproic acid, ButOH: n-butanol, HexOH: n-hexanol, OD: optical density, P_{H₂}: hydrogen partial pressure. Inverted triangles indicate external ethanol addition.

theoretically have been produced. However, the maximum was reached halfway through the test (day 15) and part of the HC was oxidized back to shorter compounds or converted to HexOH.

Following the results of the thermodynamic model, high P_{H_2} was expected to favour the formation of HA (Table 2) while low partial pressures were of interest to obtain HB and HC. Successive chain elongation steps consume and decrease the H_2 concentration. Therefore, it was periodically added in the system sparged together with CO_2 in previous tests to maintain available reducing power and a balanced microbial community composition (Paquete et al., 2022). Here, an additional test (Fig. 6) was performed under the same conditions as F2 with the only difference of the periodic modification of the P_{H_2} (from 0.60 to 1.80 atm) to optimize all the stages required for the elongation of HA and EtOH to HC. However, a certain amount was always kept in the system since its presence is a major selective factor in the microbial community.

Variable P_{H_2} could have accelerated the process since a similar concentration of HC as at the end of test F2 was obtained in <10 days. The maximum concentration and production rate of HC were 583.52 ± 17.82 mM C (11.30 ± 0.35 g L⁻¹) and 95.53 ± 3.19 mM C d⁻¹ (1.85 ± 0.12 g L⁻¹ d⁻¹, 565.96 ± 163.12 mmol C g DCW⁻¹ d⁻¹) respectively, substantially higher than those of F2, while there was less residual HB. These results are in the range with the theoretical (maximum of 593 mM C of HC) and competitive with those achieved when performing in-line extraction (Kucek et al., 2016), as HB can act as an intermediate in favour of the formation of HC. In addition, some HA was accumulated over time, putatively both by its hydrogenotrophic formation and by the oxidation of EtOH, also necessary to address chain elongation (De Leeuw et al., 2019) but in lower amounts. This test evidenced that the highest HC yields were related to low P_{H_2} (days 8, 38 and 44), while the cases where this was not applicable can be attributed to a punctual decrease in pH due to the high microbial activity and the consequent accumulation of acids, that may have caused the solventogenesis of HB and HC into their respective alcohols (ButOH and HexOH, i.e. days 13 and 21). Nevertheless, HC was the main compound accounting for over 77 % of the total carbon at the end of the experiment, which represented an increase in selectivity of 10 % compared to the previous test (F2). The optical density followed a similar trend to F2, with a remarkable growth early on of the experiment, which was then presumably limited due to the lack of EtOH (day 8). Despite this, it was able to rebound to the maximum values acquired so far (>0.4 AU) together with the maximum HC production for this study.

3.3. Implications of the developed approach

The theoretical best operational conditions using the thermodynamic-based model were assessed experimentally (see supplementary material). HA formation was thermodynamically feasible under any given conditions and it was experimentally validated, although temperature ruled out the best theoretical scenario due to its impact on reaction rates. Keeping a high P_{H_2} was crucial since a thermodynamic bottleneck may exist at low P_{H_2} , where hydrogenotrophic acetogenesis can be reversible (Ni et al., 2011). On the other hand, EtOH production was not feasible probably due to not all acetogens are capable to couple EtOH formation with net ATP gain (Candry et al., 2020). Finally, the parameters for the formation of HC matched except for the optimal temperature. 37 °C resulted to be better than 25 °C, as higher temperatures enhance the kinetics of the reactions, but as indicated by Spirito et al. (2014), 50 °C was fatal for biological chain elongation, hypothesizing enzyme inactivation. Therefore, temperature adequacy is of vital importance to enhance the desired reactions and ultimately produce elongated organic compounds.

Some authors suggested that concentrations of HC higher than 7.5 mM can have inhibitory effects on microbiological communities (Wu et al., 2020). Despite this, the concentration reached in the present study clearly exceeded this threshold, reaching concentrations >10 times

higher (97 mM) without compromising its production. This discrepancy could be attributable to pH, which modifies the equilibrium between the dissociated and undissociated forms and to strain-specific inhibition thresholds, as postulated by Ramió-Pujol and co-workers (2015). Furthermore, a kinetic and thermodynamic modeling analysis (González-Cabaleiro et al., 2013) suggested that direct conversion of HA to MCCA by H_2 was very unlikely to be attainable even under high P_{H_2} . Here, direct HC from H_2 and CO_2 could not be experimentally achieved (see supplementary material). Though, the indirect generation via sequential pathways in a single reactor may also be slowed down by the different conditions required for HA formation, the kinetics of which depends mainly on the soluble gas.

Overall, chain elongation reactions represented favorable thermodynamics for all carboxylates despite alcohols, usually with a lower energy gain when H_2 was present. Experimentally, the best configuration to obtain HC could be the formation of its main substrates and its subsequent elongation in two separate steps (Romans-Casas et al., 2021). The integration of the knowledge obtained through the model and its inference to perform experimental tests helped to define and apply the most favorable conditions for each reaction, thus obtaining the highest concentration of HC so far from simple compounds. Besides, this approach provides insights on the importance of merging key factors to study biological processes and consider them as a complex network of constantly changing interactions.

4. Conclusions

The present work addresses some concerns for the screening of operating parameters in chain elongation processes. Thermophilic conditions reinforced HA formation, EtOH production was the limiting step and longer carbon compounds were only obtained at mid temperatures. Particularly, HC was boosted under 37 °C, pH 7 and 1:3 (HA:EtOH) ratio, especially with intermittently P_{H_2} decrease. This study enlightens the differences between thermodynamic projections and experimental results, which enabled to optimize the working parameters and to obtain the highest HC concentration from single substrates. However, given the intrinsic characteristics of each compound, further investigation is required to maximize the target-product selectivity.

Declaration of Competing Interest

The authors declare that they have no known competing financial interests or personal relationships that could have appeared to influence the work reported in this paper.

Acknowledgments

The authors acknowledge funding from the Spanish Ministry of Science and Innovation (PLEC2021-007802). LEQUIA (<http://www.lequia.udg.edu/>) has been recognized as a consolidated research group by the Catalan Government (2017-SGR-1552). L.R.-A. acknowledge the support by the Catalan Government (2018 FI-B 00347) in the European FSE program (CCI 2014ES05SFOP007). M.R.-C. is grateful for the support of the Spanish Government (FPU20/01362). S.P. is a Serra Hunter Fellow (UdG-AG-575) and acknowledges the funding from the ICREA Academia award. Open Access funding provided thanks to the CRUE-CSIC agreement with Elsevier.

Appendix A. Supplementary data

Supplementary data to this article can be found online at <https://doi.org/10.1016/j.biortech.2022.127181>.

References

- Agler, M.T., Wrenn, B.A., Zinder, S.H., Angenent, L.T., 2011. Waste to bioproduct conversion with undefined mixed cultures: The carboxylate platform. *Trends Biotechnol.* 29 (2), 70–78. <https://doi.org/10.1016/j.tibtech.2010.11.006>.
- Alberty, R.A., 2001. Effect of temperature on standard transformed Gibbs energies of formation of reactants at specified pH and ionic strength and apparent equilibrium constants of biochemical reactions. *J. Phys. Chem. B* 105 (32), 7865–7870. <https://doi.org/10.1021/jp011308v>.
- Amend, J.P., Shock, E.L., 2001. Energetics of overall metabolic reactions of thermophilic and hyperthermophilic Archaea and Bacteria. *FEMS Microbiol. Rev.* 25 (2), 175–243. [https://doi.org/10.1016/S0168-6445\(00\)00062-0](https://doi.org/10.1016/S0168-6445(00)00062-0).
- Angenent, L.T., Richter, H., Buckel, W., Spirito, C.M., Steinbusch, K.J.J., Plugge, C.M., Strik, D.P.B.T.B., Grootsholten, T.I.M., Buisman, C.J.N., Hamelers, H.V.M., 2016. Chain Elongation with Reactor Microbiomes. *Open-Cult. Biotechnol. Produce Biochem.* 50 (6), 2796–2810. <https://doi.org/10.1021/acs.est.5b04847>.
- Baleeiro, F.C.F., Kleinstueber, S., Neumann, A., Sträuber, H., 2019. Syngas-aided anaerobic fermentation for medium-chain carboxylate and alcohol production: the case for microbial communities. *Appl. Microbiol. Biotechnol.* 103 (21–22), 8689–8709. <https://doi.org/10.1007/s00253-019-10086-9>.
- Bian, B., Bajracharya, S., Xu, J., Pant, D., Saikaly, P.E., 2020. Microbial Electrosynthesis from CO₂: Challenges, opportunities and perspectives in the context of circular bioeconomy. *Bioresour. Technol.* 302, 122863. <https://doi.org/10.1016/j.biortech.2020.122863>.
- Blasco-Gómez, R., Ramió-Pujol, S., Bañeras, L., Colprim, J., Balaguer, M.D., Puig, S., 2019. Unravelling the factors that influence the bio-electrorecycling of carbon dioxide towards biofuels. *Green Chem.* 21, 684–691. <https://doi.org/10.1039/c8gc03417f>.
- Blasco-Gómez, R., Romans-Casas, M., Bolognesi, S., Perona-Vico, E., Colprim, J., Bañeras, L., Balaguer, M.D., Puig, S., 2021. Steering bio-electro recycling of carbon dioxide towards target compounds through novel inoculation and feeding strategies. *J. Environ. Chem. Eng.* 9 (4), 105549. <https://doi.org/10.1016/j.jece.2021.105549>.
- Candry, P., Ganigué, R., 2021. Chain elongators, friends, and foes. *Curr. Opin. Biotechnol.* 67, 99–110. <https://doi.org/10.1016/j.copbio.2021.01.005>.
- Candry, P., Huang, S., Carvajal-Arroyo, J.M., Rabaey, K., Ganigüe, R., 2020. Enrichment and characterisation of ethanol chain elongating communities from natural and engineered environments. *Sci. Rep.* 10 (3682), 1–10. <https://doi.org/10.1038/s41598-020-60052-z>.
- Cavalcante, W.d.A., Leitão, R.C., Gehring, T.A., Angenent, L.T., Santaella, S.T., 2017. Anaerobic fermentation for n-caproic acid production: A review. *Process Biochem.* 54, 106–119.
- de Leeuw, K.D., Ahrens, T., Buisman, C.J.N., Strik, D.P.B.T.B., 2021. Open Culture Ethanol-Based Chain Elongation to Form Medium Chain Branched Carboxylates and Alcohols. *Front. Bioeng. Biotechnol.* 9 (697439), 2296–4185. <https://doi.org/10.3389/fbioe.2021.697439>.
- de Leeuw, K.D., Buisman, C.J.N., Strik, D.P.B.T.B., 2019. Branched Medium Chain Fatty Acids: Iso-Caproate Formation from Iso-Butyrate Broadens the Product Spectrum for Microbial Chain Elongation. *Environ. Sci. Technol.* 53 (13), 7704–7713. <https://doi.org/10.1021/acs.est.8b07256>.
- Dessi, P., Rovira-Alsina, L., Sánchez, C., Dinesh, G.K., Tong, W., Chatterjee, P., Tedesco, M., Farràs, P., Hamelers, H.M.V., Puig, S., 2021. Microbial electrosynthesis: Towards sustainable biorefineries for production of green chemicals from CO₂ emissions. *Biotechnol. Adv.* 46, 107675. <https://doi.org/10.1016/j.biortechadv.2020.107675>.
- Dürre, P., Eikmanns, B.J., 2015. C1-carbon sources for chemical fuel production by microbial gas fermentation. *Curr. Opin. Biotechnol.* 35, 63–72. <https://doi.org/10.1016/j.copbio.2015.03.008>.
- Ghysels, S., Buffel, S., Rabaey, K., Ronsse, F., Ganigué, R., 2021. Biochar and activated carbon enhance ethanol conversion and selectivity to caproic acid by *Clostridium kluyveri*. *Bioresour. Technol.* 319, 124236. <https://doi.org/10.1016/j.biortech.2020.124236>.
- Gildemyn, S., Rozendal, R.A., Rabaey, K., 2017. A Gibbs Free Energy-Based Assessment of Microbial Electrocatalysis. *Trends Biotechnol.* 35 (5), 393–406. <https://doi.org/10.1016/j.tibtech.2017.02.005>.
- Goldberg, R.N., Tewari, Y.B., 1991. Thermodynamics of the disproportionation of adenosine 5'-diphosphate to adenosine 5'-triphosphate and adenosine 5'-monophosphate. I. Equilibrium model. *Biophys. Chem.* 40 (3), 241–261. [https://doi.org/10.1016/0301-4622\(91\)80024-L](https://doi.org/10.1016/0301-4622(91)80024-L).
- González-Cabaleiro, R., Lema, J.M., Rodríguez, J., Kleerebezem, R., 2013. Linking thermodynamics and kinetics to assess pathway reversibility in anaerobic bioprocesses. *Energy Environ. Sci.* 6 (12), 3780–3789. <https://doi.org/10.1039/c3ee42754d>.
- Grootsholten, T.I.M., Steinbusch, K.J.J., Hamelers, H.V.M., Buisman, C.J.N., 2013. Chain elongation of acetate and ethanol in an upflow anaerobic filter for high rate MCFA production. *Bioresour. Technol.* 135, 440–445. <https://doi.org/10.1016/j.biortech.2012.10.165>.
- Hanselmann, K.W., 1991. Microbial energetics applied to waste repositories. *Experientia* 47, 645–687. <https://doi.org/10.1007/BF01958816>.
- Kleerebezem, R., Van Loosdrecht, M.C.M., 2010. A generalized method for thermodynamic state analysis of environmental systems. *Crit. Rev. Environ. Sci. Technol.* 40 (1), 1–54. <https://doi.org/10.1080/10643380802000974>.
- Korth, B., Harnisch, F., 2019. Modeling microbial electrosynthesis. *Adv. Biochem. Eng. Biotechnol.* 167, 273–325. https://doi.org/10.1007/10_2017_35.
- Kucek, L.A., Nguyen, M., Angenent, L.T., 2016. Conversion of L-lactate into n-caproate by a continuously fed reactor microbiome. *Water Res.* 93, 163–171. <https://doi.org/10.1016/j.watres.2016.02.018>.
- Lambrecht, J., Cichocki, N., Schattenberg, F., Kleinstueber, S., Harms, H., Müller, S., Sträuber, H., 2019. Key sub-community dynamics of medium-chain carboxylate production. *Microb. Cell Fact.* 18 (92), 1–18. <https://doi.org/10.1186/s12934-019-1143-8>.
- Lide, D.R., Baysinger, G., 2004. CRC handbook of chemistry and physics: a ready-reference book of chemical and physical data, 41-4368–41-4368 Choice Rev. Online 41 (8). <https://doi.org/10.5860/choice.41-4368>.
- Liu, Y., Lü, F., Shao, L., He, P., 2016. Alcohol-to-acid ratio and substrate concentration affect product structure in chain elongation reactions initiated by unacclimatized inoculum. *Bioresour. Technol.* 218, 1140–1150. <https://doi.org/10.1016/j.biortech.2016.07.067>.
- Ni, B.J., Liu, H., Nie, Y.Q., Zeng, R.J., Du, G.C., Chen, J., Yu, H.Q., 2011. Coupling glucose fermentation and homoacetogenesis for elevated acetate production: Experimental and mathematical approaches. *Biotechnol. Bioeng.* 108 (2), 345–353. <https://doi.org/10.1002/bit.22908>.
- Paquete, C.M., Rosenbaum, M.A., Bañeras, L., Rotaru, A.E., Puig, S., 2022. Let's chat: Communication between electroactive microorganisms. *Bioresour. Technol.* 347, 126705. <https://doi.org/10.1016/j.biortech.2022.126705>.
- Pinto, T., Flores-Alsina, X., Gernaey, K.V., Junicke, H., 2021. Alone or together? A review on pure and mixed microbial cultures for butanol production. *Renew. Sustain. Energy Rev.* 147, 111244. <https://doi.org/10.1016/j.rser.2021.111244>.
- Ramió-Pujol, S., Ganigué, R., Bañeras, L., Colprim, J., 2015. Incubation at 25°C prevents acid crash and enhances alcohol production in *Clostridium carboxidivorans* P7. *Bioresour. Technol.* 192, 296–303. <https://doi.org/10.1016/j.biortech.2015.05.077>.
- Romans-Casas, M., Blasco-Gómez, R., Colprim, J., Balaguer, M.D., Puig, S., 2021. Bio-electro CO₂ recycling platform based on two separated steps. *J. Environ. Chem. Eng.* 9 (5), 105909. <https://doi.org/10.1016/j.jece.2021.105909>.
- Rovira-Alsina, L., Perona-Vico, E., Bañeras, L., Colprim, J., Balaguer, M.D., Puig, S., 2020. Thermophilic bio-electro CO₂ recycling into organic compounds. *Green Chem.* 22 (9), 2947–2955. https://doi.org/10.1007/978-3-540-74382-8_4.
- Smeaton, C.M., Van Cappellen, P., 2018. Gibbs Energy Dynamic Yield Method (GEDYM): Predicting microbial growth yields under energy-limiting conditions. *Geochim. Cosmochim. Acta* 241, 1–16. <https://doi.org/10.1016/j.gca.2018.08.023>.
- Spirito, C.M., Richter, H., Rabaey, K., Stams, A.J.M., Angenent, L.T., 2014. Chain elongation in anaerobic reactor microbiomes to recover resources from waste. *Curr. Opin. Biotechnol.* 27, 115–122. <https://doi.org/10.1016/j.copbio.2014.01.003>.
- Vassilev, I., Dessi, P., Puig, S., Kokko, M., 2022. Cathodic biofilms – A prerequisite for microbial electrosynthesis. *Bioresour. Technol.* 348, 126788. <https://doi.org/10.1016/j.biortech.2022.126788>.
- Wang, Q., Zhang, P., Bao, S., Liang, J., Wu, Y., Chen, N., Wang, S., Cai, Y., 2020. Chain elongation performances with anaerobic fermentation liquid from sewage sludge with high total solid as electron acceptor. *Bioresour. Technol.* 306, 123188. <https://doi.org/10.1016/j.biortech.2020.123188>.
- Wood, J.C., Grové, J., Marcellin, E., Heffernan, J.K., Hu, S., Yuan, Z., Virdis, B., 2021. Strategies to improve viability of a circular carbon bioeconomy—A techno-economic review of microbial electrosynthesis and gas fermentation. *Water Res.* 201, 117306. <https://doi.org/10.1016/j.watres.2021.117306>.
- Wu, Q., Guo, W., Bao, X., Meng, X., Yin, R., Du, J., Zheng, H., Feng, X., Luo, H., Ren, N., 2018. Upgrading liquor-making wastewater into medium chain fatty acid: Insights into co-electron donors, key microflora, and energy harvest. *Water Res.* 145, 650–659. <https://doi.org/10.1016/j.watres.2018.08.046>.
- Wu, Q., Ren, W., Guo, W., Ren, N., 2022. Effect of substrate structure on medium chain fatty acids production and reactor microbiome. *Environ. Res.* 204 (A), 111947. <https://doi.org/10.1016/j.envres.2021.111947>.
- Wu, S.-L., Sun, J., Xueming, C., Wei, W., Song, L., Dai, X., Ni, B.-J., 2020. Unveiling the mechanisms of medium-chain fatty acid production from waste activated sludge alkaline fermentation liquor through physiological, thermodynamic and metagenomic investigations. *Water Res.* 169, 115218. <https://doi.org/10.1016/j.watres.2019.115218>.

Supporting Information

Table S1. Composition of the medium used (salts, trace metals and vitamins).

Medium compounds	(g L ⁻¹)	Trace metal solution	(mg L ⁻¹)	Vitamin solution	(µg L ⁻¹)
NH ₄ Cl	1.0	Nitrilotriacetic acid	20.0	Biotin	20.0
KCl	0.1	MnSO ₄ · H ₂ O	10.0	Folic acid	20.0
MgCl ₂ · 6H ₂ O	0.2	Fe(SO ₄) ₂ (NH ₄) ₂ · 6H ₂ O	8.0	Pyridoxine hydrochloride	100.0
NaCl	0.8	CoCl ₂ · 6H ₂ O	2.0	Thiamine hydrochloride	50.0
KH ₂ PO ₄	0.1	ZnSO ₄ · 7H ₂ O	0.002	Riboflavin	50.0
CaCl ₂ · 2H ₂ O	0.02	CuCl ₂ · 2H ₂ O	0.2	Nicotinic acid	50.0
C ₆ H ₁₃ NO ₄ S · H ₂ O (MES)	1.95	NiCl ₂ · 2H ₂ O	0.2	DL-calcium pantothenate	50.0
Cysteine-HCl	0.4	Na ₂ MoO ₄ · 2H ₂ O	0.2	Vitamin B12	1.0

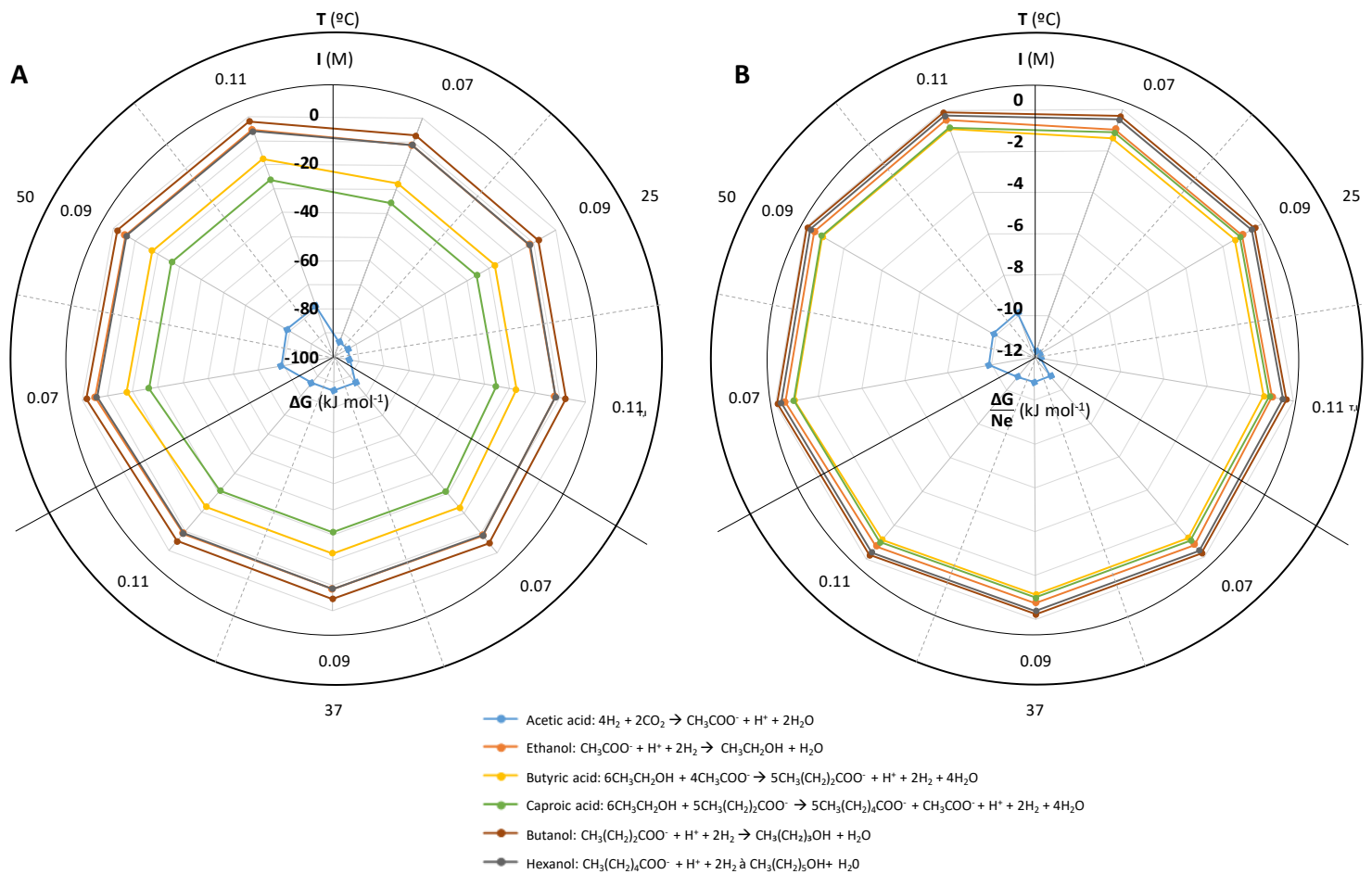


Figure S1. Gibbs free energy ($\Delta G_{T,I}$) evolution (A) and changes in ΔG to the numbers of electron transfer (Ne) in each reaction (B) for different compounds production under variable temperature (25, 37, 50 $^{\circ}\text{C}$) and ionic strength (0.02, 0.04, 0.06 M). The reactions taken into account are displayed below the graphs.

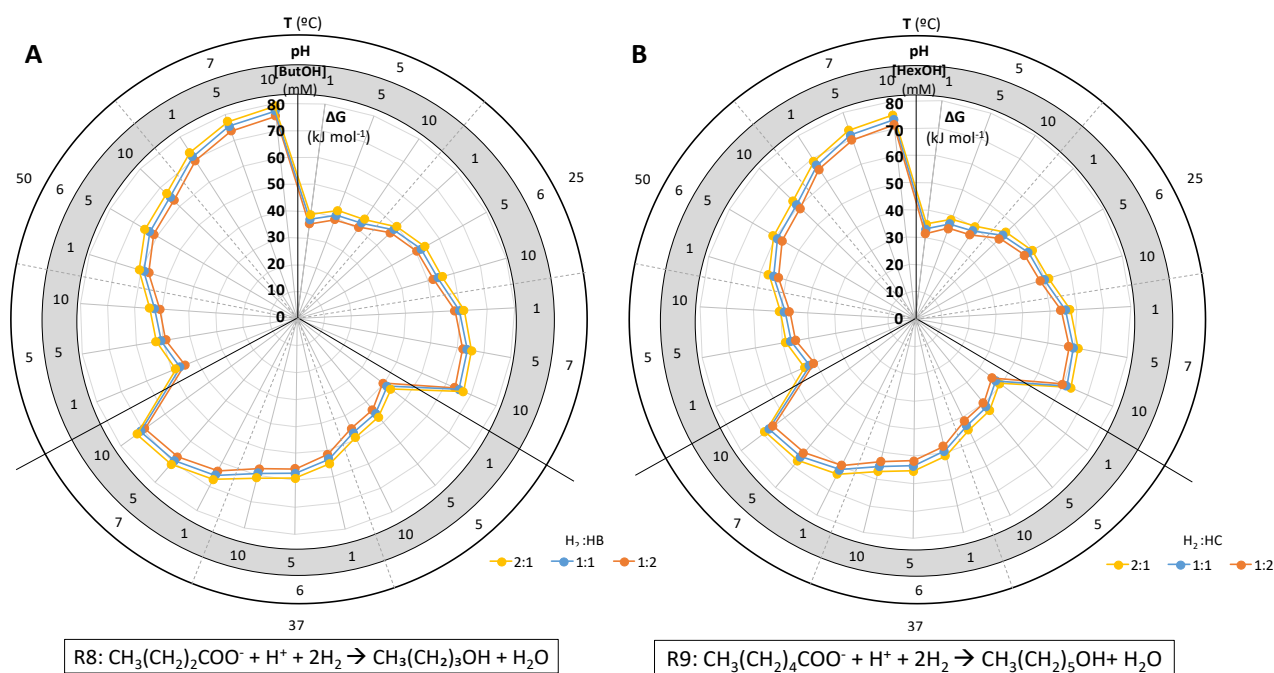


Figure S2. Evolution of modified Gibbs free energy ($\Delta G'$) for n-butanol (ButOH, A) and n-hexanol (HexOH, B) formation. The combination of various conditions of pH, temperature (T; °C), pH, substrate ratios in M and products concentration in mM were studied.

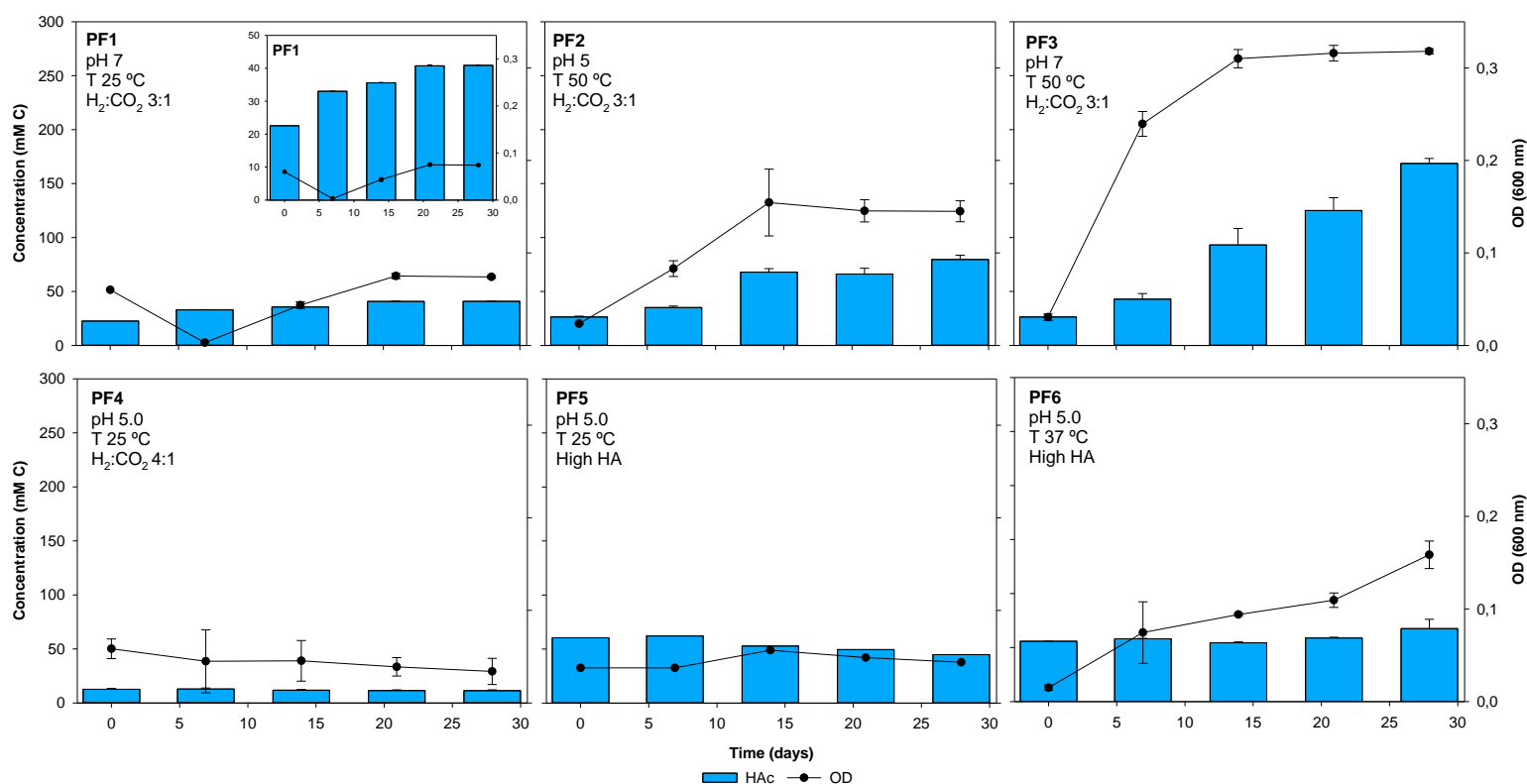


Figure S3. Previous fermentative tests (PF1 to 6). Tests PF1 to PF3 aimed to acetic acid (HA) production. PF1 performed under the set of conditions unraveled as the optimal one by the model (pH 7, 25 °C and high $H_2:CO_2$ ratio). PF2 was performed at the same conditions except for temperature, which was 50 °C. PF3 was performed at pH 7 and 37 °C. Tests PF4 to PF6 focused on ethanol production. PF4 was carried out under the thermodynamics best conditions (pH 5, 25 °C and high $H_2:CO_2$). PF5 was executed at the same conditions except for HA, which in this case was highly available. PF6 was operated at pH 5, 37 °C and high HA availability.

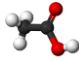
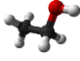
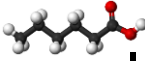
Best conditions	Acetic acid 			Ethanol 			Caproic acid 		
	pH	T [°]	Subs.	pH	T [°]	Subs.	pH	T [°]	Subs.
Thermodynamically	7.0	25 °C	High P_{H_2}	Not spontaneous under tested conditions			7.0	25 °C	Low P_{H_2}
Experimentally	7.0	50 °C	High P_{H_2}	-	-	-	7.0	37 °C	Low P_{H_2}

Figure S4. Summary and comparison of the outputs of the present study for the formation of acetic acid, ethanol and n-caproic acid, from the thermodynamic and experimental points of view. Green boxes indicate matching conditions whilst orange boxes the mismatching ones. Non-colored ones denote non-spontaneous reactions.

4.4. Transition roadmap for thermophilic CO₂ microbial electrosynthesis: from lab to pilot plant

Laura Rovira-Alsina, M. Dolors Balaguer and Sebastià Puig*

LEQUIA. Institute of the Environment, University of Girona. Campus Montilivi,
C/Maria Aurèlia Capmany, 69, E-17003 GironaCatalonia, Spain.

*E-mail: sebastia.puig@udg.edu

Transition roadmap for thermophilic CO₂ microbial electrosynthesis: from lab to pilot plant

Laura Rovira-Alsina, M. Dolors Balaguer, Sebastià Puig*

LEQUIA. Institute of the Environment.

University of Girona. Campus Montilivi. C/Maria Aurèlia Capmany, 69, E-17003 Girona, Catalonia, Spain.

*Corresponding author: Sebastià Puig E-mail address: sebastia.puig@udg.edu

Abstract

Think twice, act wise. This study attempts to tackle at a glance the main challenges for scaling-up the thermophilic bioelectrochemical conversion of CO₂ into acetate. First, real gaseous emissions were tested with mixed microbial consortia, which were found to have no substantial influence on production rates (difference of 2.5 %). Then, a bench-scale system (TRL 4-5) was designed and launched to control key operational variables. Under 50 °C and a fixed current of 1.3 A m⁻², CO₂ was reduced at a rate of 2.21 kg CO₂ kg⁻¹ acetate, while the electricity consumption per kg of acetate produced was 2.07 kWh kg⁻¹, the most efficient value so far. The results suggested that this system can harness renewable energy surplus and be operated under intermittent power supply. The right balance between maximising current densities without compromising biocompatibility with catalysts will determine the transition from laboratory scale towards its implementation in the market.

Keywords

Acetate production; Carbon conversion; Exhaust / Flue gas; Galvanostatic control; Power to Product ratio

1. Introduction

If carbon dioxide (CO₂) were made visible, perhaps we might be able to see the magnitude of the challenge and start working on real solutions to mitigate it. Yet, given that it is invisible, it seems that the solutions implemented often are too. Although politics is the most powerful force, all those who are truly concerned about the situation have to strive to represent a majority that will push for substantial changes. Microbial electrosynthesis (MES) of organic compounds from CO₂ is a strong alternative for capturing and storing this greenhouse gas (GHG) in the long term (Bian et al., 2020). It allows the production of value-added compounds from harmful waste without the need to use scarce and environmentally unfriendly raw materials that can trigger conflicts between politically unstable countries (Bajracharya, 2016). However, this technology is still at low technology readiness levels (TRLs) (Virdis et al., 2022), and still needs multiple-steps to scale up and reach a competitive position in the market (Fruehauf et al., 2020). Many efforts have been devoted to deciphering the metabolic pathways responsible for the reduction of CO₂ to different compounds such as methane (Van Eerten-jansen et al., 2012), ethanol (Romans-Casas et al., 2021), butyrate (Batlle-Vilanova et al., 2017), caproate (Jourdin et al., 2018), among others (Vassilev, 2019), depending on the microbial culture and operational conditions used. Nevertheless, the most ancient metabolism for CO₂ fixation is the Wood-Ljungdahl pathway, in which hydrogen (H₂) is used as an electron donor and CO₂ as an electron acceptor to obtain acetate (HA) (Schuchmann and Müller, 2014). This is a platform compound with lower economic value compared to others (Jourdin et al., 2020), but with a huge potential to be used as a precursor for different products such as plastics, dyes, inks, pesticides, rubbers, detergents and pharmaceuticals (Verbeeck, 2014). Today, the technology needs to get closer to industrial deployment moving out of the laboratory and start using affordable materials for the scale-up, treating gaseous effluents, and operating at conditions similar to where it could be implemented (Christodoulou et al., 2017). Even though most of the studies are carried out under mesophilic conditions, the possibility of operating these systems at higher temperatures (> 50 °C) to exploit the residual heat from CO₂ point emissions (e.g. cement plants) has proven to be an effective approach to reduce microbial competition and thus, increase the selectivity of the final product (Rovira-Alsina et al., 2020). The different reactions that can occur depending on the biological catalyst used (Von Stockar et al., 2006) and the operational parameters (Angenent et al., 2016) have also been studied from a thermodynamic perspective. Again, granted a simple and scalable design for industrial application, the most thermodynamically favourable compound to be obtained in any of the usual combinations of variables is HA (Rovira-Alsina et al., 2022). On the other hand, given that these systems require an electrical input to drive the thermodynamically unfavourable reactions (Rabaey and Rozendal, 2010), their integration with renewables is the most viable option. Some studies rely on the transition of the public grid to increase the share of energy from

renewables (Dessi et al., 2020), but the use of MES to store excess energy when it exceeds demand is also an attractive option to be considered (Rovira-Alsina et al., 2021; Su and Ajo-Franklin, 2019).

Therefore, studies using real off-gases are needed to assess how microbial consortia would adapt to an impure CO₂ effluent and how this would affect production rates and overall performance. In this sense, the transition to higher TRLs will require implementing a digital transformation to help monitor, control and operate in the most efficient, sustainable and competitive way the MES systems. The present study aimed at testing a real CO₂ stream for its thermophilic bioelectro-conversion to HA and applying all the background knowledge to design and start up for the first time, a fully automated bench-scale system.

2. Materials and methods

2.1. Inoculum and growth media

The microbial community was taken from an anaerobic digester working at 37.5 °C of a wastewater treatment plant (WWTP) located in Girona, Spain. A 1:20 dilution with a synthetic solution based on ATCC1754 growth medium (Tanner et al., 1993) was incubated in 50 °C fermentative reactors under H₂:CO₂ (80:20 v/v) to promote acetogenesis and microorganisms' adaptation to thermophilic conditions. During this enrichment stage, pH was adjusted to 6 and 2-bromoethanesulfonic acid (10 mM) was added to prevent methanogenesis (Jadhav et al., 2018). Two additional 1:20 dilutions of this inoculum with the reformulated medium to remove all sources of organic carbon were performed before inoculating the reactors. All the experiments were carried out with the same adapted inoculum after an initial growth period of at least 30 days.

2.2. Batch tests with real off-gas supply. Set-up and operation

Two MES systems named HT1 and HT2 were constructed for real CO₂ testing. They consisted of two identical glass H-type bottles (Pyrex V-65231 Scharlab, Spain), separated by a cation exchange membrane of 2·10⁻⁴ m² (CMI-1875 T, Membranes International, USA). The cathode consisted of a plain carbon cloth (thickness of 490 μm, working area of 3.0·10⁻³ m² for HT1 and of 1.2·10⁻³ m² for R2; NuVant's Elat LT2400 FuelCellsEtc, USA) connected to a stainless-steel wire. The anode was a 2·10⁻⁶ m³ graphite rod of 0.1 m in length and 5·10⁻³ m in diameter (EnViro-cell, Germany). An Ag/AgCl electrode (+0.197 V vs. SHE (standard hydrogen electrode), model RE-5B, BASI, UK) with an operating temperature range from 0 to 60 °C was placed in the cathodic chamber and used as a reference electrode. Reactors were sealed with butyl rubber caps to prevent gas leakage and keep the headspace volume of each chamber at 0.03 L (for HT1) and 0.01 L (for HT2), while the liquid volume accounted for 0.22 L in HT1 and 0.09 L in HT2. Both MES systems were operated in a three-electrode configuration

with a potentiostat (BioLogic, Model VSP, France), which controlled the cathode potential at -0.8 V vs. SHE and monitored the current demand over time. All the potentials reported in this work are relative to SHE unless otherwise noted. Before use, the working electrodes were pre-treated in a 0.5 M solution of HCl and 0.5 M of NaOH for a total of two days and rinsed with deionized water for an additional day. At the end of the experimental study, the voltage of the reference electrodes was measured to ensure any shift that may have occurred during operation. The temperature was kept constant at 50 °C and an agitation rate of 80 rpm was fixed using a magnetic stirrer (Agimatic-ED-C; Scharlab, Spain) to enable mixing and facilitate mass transfer inside the cathodic chambers. All reactors were operated in batch mode and kept in the dark to avoid the growth of phototrophic microorganisms.

Either pure CO_2 (99.9 %, Praxair, Spain) or real CO_2 off-gas coming from an industrial relevant gas emitter (main components: 74 % nitrogen (N_2), 14 % CO_2 and 12 % oxygen (O_2)) was sparged for 10 min in the cathodic chamber twice a week to oversaturate the liquid media and renew the headspace. Additionally, it was added or removed punctually from 1 to 5 times per week to ensure a gas pressure between 1 and 2 atm. Samples from the liquid phase were taken before bubbling and the withdrawn liquid was replaced with a freshly prepared medium to maintain constant volumes in both chambers. The initial pH was set at 6 , and it was modified with a basic solution (NaOH 1 M) when required. Electric conductivity (EC) and pH were measured with an EC meter (basic 30+, Crison, Spain) and a multimeter (MultiMeter 44, Crison, Spain), respectively. The optical density (OD) of the bulk liquid was also measured to control the growth of the planktonic microbial community with a spectrophotometer (Thermo Fisher Scientific, USA) at a wavelength of 600 nm. Gas pressure in the headspace of the reactors was measured using a digital pressure sensor (differential pressure gauge, Testo 512, Spain).

2.3. Pilot plant: Instrumentalisation, set-up and operation

A fully equipped bench-scale bioelectrochemical system was designed and set up for dynamic control of the operational variables using pure CO_2 (99.9% , Praxair, Spain) as feed. The pH (easySense pH 32; Mettler Toledo, Spain), EC (easySense Cond 77; Mettler Toledo, Spain), pressure (PA3526; ifm, Spain), temperature and dissolved CO_2 (InPro® 5000(i); Mettler Toledo, Spain), H_2 (H2100 microsensor; UniSense, Denmark) and O_2 (easySense O_2 21; Mettler Toledo, Spain) content were monitored by in-line probes in the recirculation loop using a continuous stirred probe holder (HYCC, EEUU) (**Figure 1A**). They were controlled by actuator pumps and a multi-transmitter (Multi-parameter Transmitter M200; Mettler Toledo, Spain) that supplied the required component on demand through a remote access tool (EasyAccess 2.0) and an operation interface software (cMT Viewer). An Ag/AgCl reference electrode was placed also in the recirculation loop for proper electrochemical control. Liquid CO_2 concentration was kept between a maximum range from 600 to 1200 mg L^{-1} by using a magneto-inductive flowmeter (SM4100; ifm, Spain) installed and connected to a gas bottle (99.9 % CO_2) to keep the set point. An

ON/OFF pH control system pumped HCl or NaOH 5M solutions using electromagnetic diaphragm dosing pumps (DOSATec PCO; Dosatron, Spain) to the medium when required, maintaining a pH range between 4.5 and 7.0. Gas flow meters (Digital Flow Switch PF2M721; SMC, Spain) were installed in the inlet and outlet of the circuit to quantify the CO₂ conversion and H₂ production rates. The pilot plant installation was assessed with two different reactor configurations, though all were operated in batch mode and kept in the dark to avoid the growth of phototrophic microorganisms.

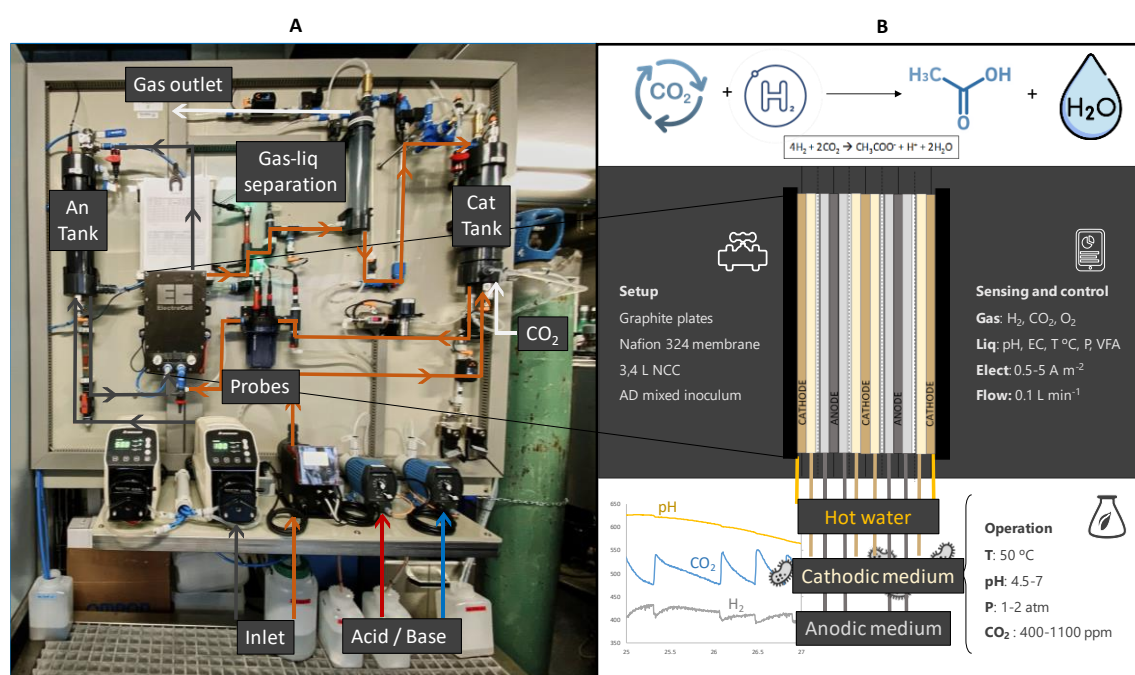


Figure 1. Picture of the bench-scale system equipped with the monitoring and control devices (A) and diagram of the set-up and operation of the ECell reactor (B).

Two Electro MP Cells (ECell model 1735; ElectroCell A/S, Denmark) were constructed consisting of two stainless steel end plates, compacting two types of electrolyte distributor racks (PVDF frame sets) that separated up to two anodic compartments from three cathodic ones by cationic exchange membranes (Nafion N324) (**Figure 1B**). 1mm EPDM rubber gaskets were placed between the PVDF frame sets to avoid leaks. The electrodes consisted of graphite plates (SIGRAFINE® R8710; FuelCellStore). Three of them could function as working electrodes (4 operative faces; working area of 0.04 m²) and the two rest could serve as counter electrodes (4 operative faces; working area of 0.04 m²). The ECells were operated under galvanostatic (GA) control through a programmable logic controller (Haiwell PLC - H02PW, China) connected to a power supply unit (MQR120-24F; Mibbo, China), fixing the cathodic current and tracking the cell voltage evolution over time. The cathodic and anodic compartments of the ECell accounted for 0.4 L each, and the medium was injected in parallel from the bottom to the top of the cell, following a cross-flow. The total volume of the cathodic circuit amounted to 3.5 L, while the

anodic one comprised 2.5 L, keeping 0.1 L for the headspace. The current of the working electrode was fixed from 0.5 to 5 A m⁻² and the temperature at 50 °C using a circulation ultra-thermostat (Digit-cool 3001373; Selecta, Spain) and a thermal heating mat (Lerway, Spain). Good mixing conditions were assured with a micro-pump (85376; MicroPump, USA) that recirculated the medium at a flow rate of 0.1 L min⁻¹.

A flat plate (FP) reactor was additionally constructed consisting of two methacrylate compartments of 0.185 L each separated by a cationic exchange membrane (CMI-1875T, Membranes international, USA) of 0.008 m² (4.4 cm width and 18.8 cm length). The anode consisted of 0.013 m² (4.3 cm width and 15 cm length) of commercial carbon cloth (Thickness 490 μm; NuVant's ELAT, LT2400W, FuelCellsEtc, USA) connected to a carbon rod (0.45 cm diameter and 4.4 cm of length, Mersen Iberica, Spain) and the same, a 0.013 m² carbon cloth in contact to a carbon rod was used as a cathode electrode. The reactor was operated under GA control fixing the cathodic current at 5 A m⁻² and the same temperature and mixing conditions as in the ECells were applied for this set-up.

To assess the performance of reactors, gas samples were daily taken to check and recalibrate the dissolved gas sensors, while liquid samples were taken from 2 to 7 days per week, depending on the experiment, for the quantification of volatile fatty acids. At the end of each test, 80 % and 100 % of the cathodic and anodic media, respectively, were drained and replaced with fresh medium to start the following one.

2.4. Analyses and calculations

The concentration of organic compounds (volatile fatty acids and alcohols) in the liquid phase was determined using an Agilent 7890A gas chromatograph equipped with a DB-FFAP column and a flame ionization detector. Gas samples were analysed by gas chromatography (490 Micro GC system, Agilent Technologies, US) equipped with two columns: a CP-molesive 5A for methane (CH₄), carbon monoxide (CO), H₂, O₂ and N₂ analysis, and a CP-Poraplot U for CO₂ analysis. The two columns were connected to a thermal conductivity detector (TCD).

In HT reactors, the concentrations of dissolved H₂, CO₂ and O₂ in the liquid media were calculated using Henry's law at 50 °C (Equation 1), where C_i is the solubility of a gas in a particular solvent (mol L⁻¹), H_i is the Henry's law constant in mol L⁻¹ atm⁻¹ (0.0007 for H₂, 0.0195 for CO₂ and 0.0009 for O₂) and $P_{gas\ i}$ is the partial pressure of the gas in atm.

$$C_i = H_i P_{gas\ i} \quad \text{Equation 1}$$

The coulombic efficiency (CE) for the conversion of the current into products (i.e. H₂, HA, O₂) was calculated according to Patil et al. (2015) (Equation 2), where C_i is the compound i concentration in the

liquid phase ($\text{mol C}_i \text{ L}^{-1}$), n_i is the molar conversion factor (2, 8 and 4 moleq^{-1} for H_2 , HA and O_2 , respectively), F is the Faraday's constant ($96485 \text{ C mol e}^{-1}$), V_{NCC} is the net liquid volume of the cathode compartment (L), and I the intensity demand of the system (A).

$$CE (\%) = \frac{C_i \cdot \sum_i n_i \cdot F \cdot V_{NCC}}{\int_0^t I \cdot dt} \cdot 100$$

Equation 2

3. Results and discussion

3.1. Microbial electrosynthesis of acetate using real off-gases

Two HT reactors were operated during a 100-days experimental period. Both HTs behaved similarly in terms of gas composition and HA production, although HT2 had lower production rates, probably related to the smaller surface area of the cathode electrode (Patil et al., 2015). They were fed with synthetic gas (100 % CO_2) twice a week from day 0 to day 53, and then replaced with real off-gas (14 % CO_2 and 12 % O_2) for the rest of the trial (**Figure 2**). HA was produced from day 1, maintaining similar rates until day 28, which caused a decrease in pH from 6.4 to 4.5, when its concentration stopped increasing due to nutrient limitation (Rovira-Alsina et al., 2020). OD also dropped, probably because the cells adhered to the electrode until HA production ceased, leading to an accumulation of H_2 in the headspace which elevated the gas pressure, pH and also OD. On day 42, a new batch was started by exchanging part of the liquid for fresh medium, which further increased the pH and decreased the OD. HA production was restarted and the change of gas supply (from synthetic to real gas) did not seem to affect its production, which remained at a similar slope (81 vs. 79 $\text{mg L}^{-1} \text{ d}^{-1}$) until day 75, before a new batch was performed. During this period, the percentage of CO_2 in the headspace decreased an 86 % while O_2 was a 12 % higher than before, balancing the ratios between the two gases, while some of the H_2 produced accumulated again in the gas phase together with N_2 , that not being used, was the most abundant compound (around 80 %). As the HA concentration increased, the pH decreased again and, interestingly, the OD rose from 0.2 to 0.7 units due to the eventual development of a mixed microbial community with O_2 scavengers, acetogens and methanogens that when pH was above 6, produced up to 23 % of CH_4 . The latter could be inhibited by a single addition of 1 g L^{-1} of 2-bromoethanesulfonic acid.

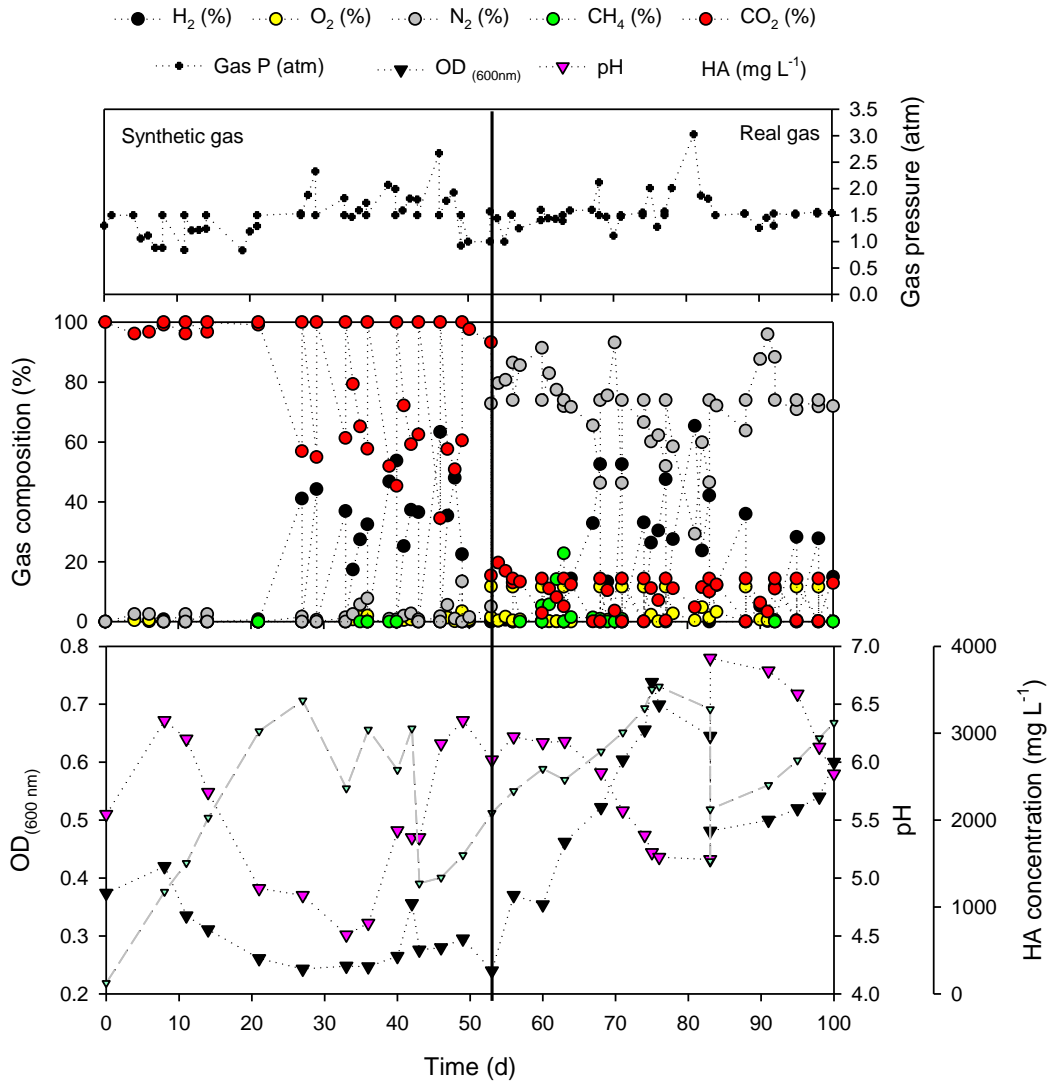


Figure 2. Variation of the gas and liquid phases of the HT1 reactor over time. OD: Optical Density at 600 nm; HA: Acetate. The vertical black line separates the period of synthetic CO₂ feed from the period with real off-gas addition.

A more detailed analysis of specific production periods (**Table 1**) showed that during the synthetic gas feed, all the CO₂ supplied and H₂ produced were devoted to HA production, reaching a CE_{HA} between 80 and 100 %. The intensity demand remained constant at 1.8 A m⁻² and OD values decreased. Even though the maximum HA production rate (10.4 g m⁻² d⁻¹) was obtained during the first period after inoculation (from day 0 to 28), the switch to real gas feeding did not change the production slope, which in that period (from day 42 to 53) was about 6 g m⁻² d⁻¹. However, the composition of the gas varied, reducing the CO₂ partial pressure from 1.2 to 0.5 atm and, conversely, increasing the O₂ partial pressure to 0.4 atm. The change in the gas feeding decreased the intensity demand until, after a period of adjustment, it gradually started to increase, reaching up to 0.5 A m⁻² more than before, but the direction of the electrons was split, giving a CE_{HA} of 45 % and a CE_{H₂} of 25 %, while only some of the electrons

were used for O₂ reduction (<3 %). Yet, HA production yielded a higher rate (8.4 g m⁻² d⁻¹) and OD increased, suggesting that most of the O₂ was consumed by microorganisms in the bulk liquid rather than being electrochemically reduced.

Table 1. Acetate (HA) production rate (g m⁻² d⁻¹), optical density (OD_{600nm}) variation (u d⁻¹), gases (CO₂ and O₂) partial pressures (atm), coulombic efficiencies (CE % of HA, H₂ and total) and average intensity demand (A m⁻²) of HT1 during production periods using synthetic (from day 41 to 53) and real off-gas feed (from day 53 to 75).

	Synthetic gas	Real off-gas
HA production rate (g m ⁻² d ⁻¹)	5.94 ± 1.78	5.79 ± 0.12
OD _{600nm} (u d ⁻¹)	-0.012 ± 0.010	0.023 ± 0.010
P _{CO₂} (atm)	1.2 ± 0.3	0.5 ± 0.2
P _{O₂} (atm)	0.01 ± 0.01	0.40 ± 0.20
CE _{HA} (%)	90 ± 10	45 ± 5
CE _{H₂} (%)	5 ± 2	25 ± 5
CE _{tot} (%)	95 ± 5	73 ± 6
Intensity demand (A m ⁻²)	1.8 ± 0.1	2.3 ± 0.3

The presence of O₂ in the real off-gas (12 %) was expected to have an impact either by increasing the intensity demand for O₂ reduction or by decreasing HA production. However, the results showed that the use of untreated gas was not detrimental to the microbial community nor HA production. After saturation, O₂ was normally depleted within one day, while CO₂ was consumed progressively over three days, until it was completely exhausted. If a minimum of CO₂ could have been maintained in the system through a more frequent gas supply, production rates would probably have been higher. The maximum HA production rates (10.4 and 8.4 g m⁻² d⁻¹ for synthetic and real CO₂, respectively) and the CE obtained (100 % and 79 %) are among the results of most MES studies reported so far with similar carbon materials and fixed potentials (Mateos et al., 2019; Song et al., 2019; Yang et al., 2021). To our knowledge, this is the first study operating with real gases and thermophilic conditions for more than 1 month, and these reactors continue running and producing at similar rates. The only study that also used industrial CO₂ for acetate production *via* MES (Roy et al., 2021) obtained lower cumulative HA concentration (1.8 g L⁻¹) but a higher production rate (65 g m⁻² d⁻¹). However, the used off-gas was obtained from a brewery industry containing mainly CO₂ (97.9 % of CO₂, 1.7 % of N₂ and 0.4 % of O₂), being much purer compared to the off-gas tested in the present study.

3.2. Galvanostatic control adjustment for efficient energy use

Previous tests under similar conditions (50 °C, open culture, carbon-based electrodes and CO₂ feed; Rovira-Alsina et al., 2020; Rovira-Alsina et al., 2021) had been carried out by fixing the cathodic potential. The potentiostatic control may be useful in narrowing down the electron transfer

mechanisms possibly involved and may lead to the formation of a more energy-efficient microbial community. However, when thinking about scaling up the technology, constant current (GA control) may allow better control of production rates and selectivity, as it is less sensitive to local changes (e.g. pH) and the electron flow can be controlled to stoichiometrically match the CO₂ supply rate (Molenaar et al., 2017).

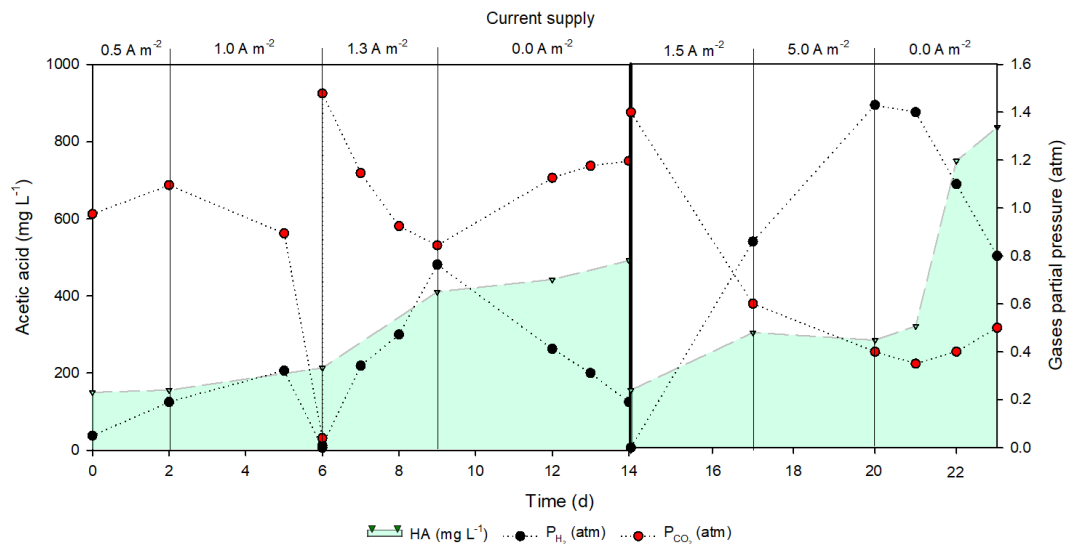


Figure 3. Acetate (HA) accumulation (mg L^{-1}) and gas partial pressures (atm) of H₂ and CO₂ over time in the ECell at different current densities. The vertical black line indicates two batch-periods.

The ECells were inoculated and operated for 15 days to start up the reactor and condition the microbial biomass to the new configuration. Several short tests were consecutively performed at different fixed intensities ranging from 0.5 to 5.0 A m⁻² (**Figure 3**). At 0.5 A m⁻², there was almost no HA production and the low power consumption accounted for H₂ production. At 1.0 A m⁻², part of the CO₂ was consumed for HA generation, but the increased electrical input was not proportional compared to the amount required at 1.3 A m⁻² for the improved HA production rate (1.23 vs. 5.59 g m⁻² d⁻¹) (**Table 2**). Subsequently, the current supply was cut off and the remaining H₂ was almost entirely consumed to produce more HA, albeit at a slower rate (1.39 g m⁻² d⁻¹). At this point, a new batch was started at 1.5 A m⁻² in which a lower HA production rate was obtained (4.25 g m⁻² d⁻¹) compared to at 1.3 A m⁻² while more unused H₂ accumulated in the medium. Increasing the current to 5.0 A m⁻² resulted in a significant change in power consumption (an order of magnitude (Wh d⁻¹) higher compared to any other condition), but this was not followed by a higher HA production, rather only by a larger accumulation of H₂ (P_{H₂} up to 1.43 atm). In addition, the colour of the medium turned completely black and small particles were detected which caused clogging problems in the tube circuit. Again, the electrical supply was cut off and, remarkably, HA production restarted, reaching the fastest production rate (36.64 g m⁻² d⁻¹) of the whole study, while the H₂ content decreased lowering the total gas pressure (from 1.8 to

1.3 atm). This indicated that at 5 A m⁻², biomass might have been inhibited but remained in a latent state, being able to resume metabolism when conditions turned favourable.

Table 2. Fixed current supply (A m⁻²), acetate (HA) production rate (g m⁻² d⁻¹), energy (E) consumption (Wh d⁻¹) and energy per acetate ratio (E:HA) in kWh kg⁻¹ over different current densities and reactors set-ups. HT: H-type cells used in previous thermophilic tests; with continuous (Rovira-Alsina et al., 2020) and intermittent (Rovira-Alsina et al., 2021) electric supply.

Current density I (A m ⁻²)	Acetate production HA (g m ⁻² d ⁻¹)	Energy consumption E (Wh d ⁻¹)	Energy per Acetate ratio E:HA (kWh kg ⁻¹)
0.5	0.24	0.57	59.03
1	1.23	1.74	35.54
1.3	5.59	2.23	9.97
1.5	4.25	2.80	16.49
5	0.00	17.41	-
3 (HT)	28.10	8.74	24.00
10 (HT On-Off)	43.27	0.94	7.25

The energy per acetate ratio (E:HA) turned out to be maximised at 1.3 A m⁻² (**Table 2**), and it was close to the value obtained working under an interrupted power supply. These results are in line with the proposal to operate such systems intermittently by following the fluctuations of renewable energy to produce H₂ when there is excess electricity and convert it into HA when there are no natural resources to generate it.

3.3. CO₂ reduction to HA at pilot scale

With the ultimate goal of operating the ECell at 50 °C with real off-gas feed and interrupted power supply, it was first operated in the pilot plant set-up under controlled conditions. This assumed a minimum pH of 4.5, a synthetic CO₂ dissolved content between 750 and 850 mg L⁻¹, a total pressure below 2 atm, and a continuous power supply of 1.3 A m⁻² (**Figure 4**).

During an experimental period of 40 days, HA was produced at a rate of 5.07 g m⁻² d⁻¹, with a maximum production peak of 24.18 g m⁻² d⁻¹ (between days 12 and 15). The produced H₂ was probably consumed, as the average concentration in the liquid remained low (0.21 ± 0.10 mg L⁻¹), although this could be due to the frequent supply of CO₂, which displaced part of the H₂. CO₂ was added and consumed cyclically, exceeding the lower limit of the marked threshold every approximately half day, while pH profiles had longer cycles, requiring the addition of base (NaOH 5M) every 2-3 days. Setting a current density at 1.3 A m⁻², resulted in low cumulative energy consumption (0.06 kWh d⁻¹), internal resistance (0.1 Ω cm⁻²), and cell voltage (between 1.7 V), which translated into a low E:HA ratio (7.39 kWh kg⁻¹ HA) if the whole trial is taken into account, and the lowest ratio obtained so far when focusing only on the peak

production period ($2.07 \text{ kWh kg}^{-1} \text{ HA}$). This value is lower than the observed for HA formation both, by working with the HT configuration at intermittent energy supply (**Table 2**) and by commercial methanol carbonylation, which requires $3.53 \text{ kWh kg}^{-1} \text{ HA}$ (Althaus et al., 2007). When compared to other bioelectrosynthesis studies under mesophilic conditions, the difference can be up to 2 orders of magnitude (Arends et al., 2017; Jourdin et al., 2018; Sciarria et al., 2018). On the other hand, CO_2 was consumed at a rate of $182 \pm 17 \text{ mg L}^{-1} \text{ d}^{-1}$ during the period of maximum production, while the average for the whole trial decreased to $130 \pm 40 \text{ mg L}^{-1} \text{ d}^{-1}$. Considering also the mean production rate, this implies a CO_2 to HA ratio of $2.21 \text{ kg CO}_2 \text{ kg HA}^{-1}$. Stoichiometrically, 1.47 kg of CO_2 are needed for the generation of one kg of HA, meaning that part of this CO_2 was also used for microbial growth and maintenance.

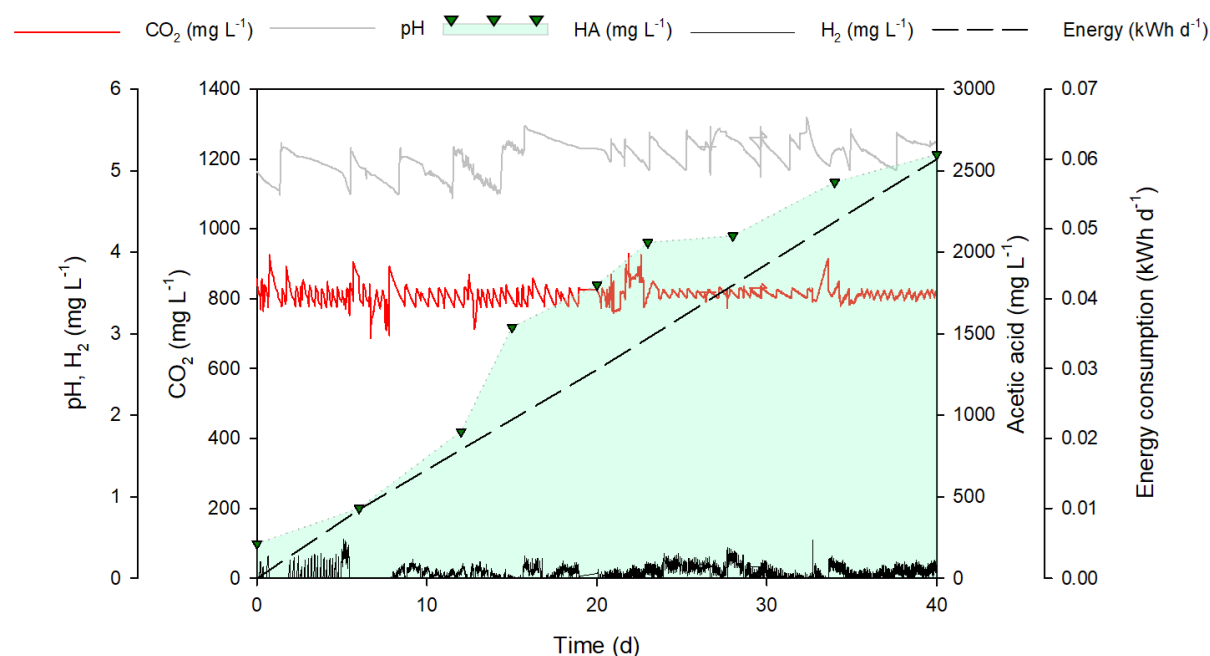


Figure 4. Acetate (HA) accumulation (mg L^{-1}), pH, H_2 and CO_2 concentration (mg L^{-1}) and power consumption (kWh d^{-1}) over time in ECell reactors using the bench-scale configuration. pH range was controlled between 4.5 and 5.5, CO_2 concentration between 750 and 850 mg L^{-1} , and the total pressure could not exceed 2.1 atm .

Theoretically, if considering the stoichiometric H_2 needed to reach the maximum HA production obtained in previous studies ($28 \text{ g m}^{-2} \text{ d}^{-1}$) with the HT configuration (Rovira-Alsina et al., 2020), a fixed current of 7.5 A m^{-2} would be required working under continuous power supply, while this value would decrease to 2.5 A m^{-2} if intermittent power supply (Rovira-Alsina et al., 2021) could be applied. Therefore, the configuration of the ECell in the pilot plant resulted in a very good performance in terms of energy utilisation and control of operational variables, as the production rate obtained was the maximum according to stoichiometry, using less energy than with other set-ups. However, $24 \text{ g m}^{-2} \text{ d}^{-1}$

is still far below the value ($4100 \text{ g m}^{-2} \text{ d}^{-1}$) set for industrial commercialisation (Gadkari et al., 2022). Considering that low amounts of H_2 were detected, the system should operate with a higher current supply, but this seemed to be limited by the decomposition of the material due to the combined effect of temperature and electron flow.

3.4. Considerations to be addressed for scaling up the technology

The pilot plant proved to be sensitive in its response to the output signals, keeping the operating set points at the desired value or fluctuating the working range when necessary for intelligent management of the processing data. However, the synergy between cause-effect response is as important as the quality of the base components for the scale-up of the technology. In this respect, the reactor material and its layout are key factors to be taken into account.

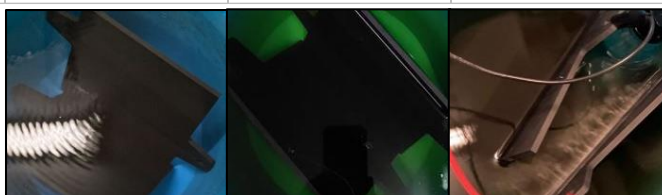
3.4.1. Electrode material

Even though the ECell was found to be a good electrolyser for H_2 production and the composition of the electrodes was supposed to be pure graphite, the relatively high temperature and current densities seemed to cause a release of substances that could affect the viability of the biomass and hamper the yield. For this reason, a quick quantitative test was conducted with only the electrodes in the synthetic medium to determine the impact that working under these conditions could have on the overall performance (**Table 3**).

The values of OD, pH, EC and sulphur content with the graphite plates in the medium were in the usual range for synthetic media. When the temperature ($50 \text{ }^\circ\text{C}$) was applied, all variables increased slightly, while the colour of the solution turned green. When a current of 1.3 A m^{-2} was applied, a physicochemical perturbation occurred, which increased OD, EC and sulphur more than 18, 2 and 4 times respectively, compared to the initial values, whereas the colour of the solution changed to a dark black. This indicates that in addition to the temperature, the flow of electrons between the electrodes modified their state, causing them to deteriorate. Apart from sulphur that can be very toxic to microorganisms, these graphite plates may contain other impurities that can affect the microbial community. Hence, a compromise had to be found between low current densities and energy-efficient HA production for this particular case.

Table 3. Optical density (OD_{600nm}), pH, electric conductivity (EC) in $mS\ cm^{-1}$ and sulphur content ($mg\ L^{-1}$) in the abiotic medium with the electrodes submerged, with the addition of temperature ($50\ ^\circ C$), and also with power supply ($1.3\ A\ m^{-2}$).

	Medium	Medium at $50\ ^\circ C$	Medium at $50\ ^\circ C$ and $1.3\ A\ m^{-2}$
$OD_{(600nm)}$	0.003	0.008	0.059
pH	5.5	5.4	2.04
EC ($mS\ cm^{-1}$)	5.33	6.37	12.24
Sulphur ($mg\ L^{-1}$)	30	48	129



Graphite is suitable for use as an electrochemical electrode, as it has good electrical conductivity properties, is biocompatible, and the material is still abundant and relatively cheap (Kamal et al., 2020). However, under these operating conditions, it turned out not to be the best choice. Therefore, other materials such as carbon cloth or carbon felt that have proven to be efficient for microbial electrosynthesis (Zhang et al., 2013) even at high temperatures (Yu et al., 2017), should be tested with the bench-scale configuration.

3.4.2. Internal resistances

The selection of the electrode material is an essential part of the performance of MES. The anode material governs the electrochemical oxidation of the substrates and the subsequent electron transfer to the cathode. Similarly, a good cathode material should reduce the cell potential and enhance the H_2 evolution reaction (Park et al., 2022). However, the distribution of internal resistances in most microbial electrolysis cells remains unclear, making it difficult to optimise and scale up the technology. Varying electrode spacing, inducing fluid movement between electrodes and adjusting the electrode surface area ratio are some strategies that can balance the internal resistance distribution (Miller et al., 2019).

Different reactor configurations with various electrode materials were tested in the bench-scale set-up. The FP reactor using carbon cloth in contact with a graphite rod working as a cathode resulted in feasible operation at higher current densities ($5A\ m^{-2}$) (Figure 5). However, the decomposition of the graphite increased the internal resistance of the system (from 0.6 to $4.8\ \Omega\ cm^{-2}$), exceeding the threshold value of the cell voltage ($5\ V$) and hindering its operation. Although the bio-viability of the system was not compromised, the stability was affected. If a stainless steel wire had been used instead of the graphite rod, the stability would probably have been improved (Blasco-Gómez et al., 2021) but

neither HA production ($11.28 \text{ g m}^{-2} \text{ d}^{-1}$) nor the relative production to energy consumption ($36.87 \text{ kWh kg}^{-1}$) seemed to be enhanced compared to the ECell set-up.

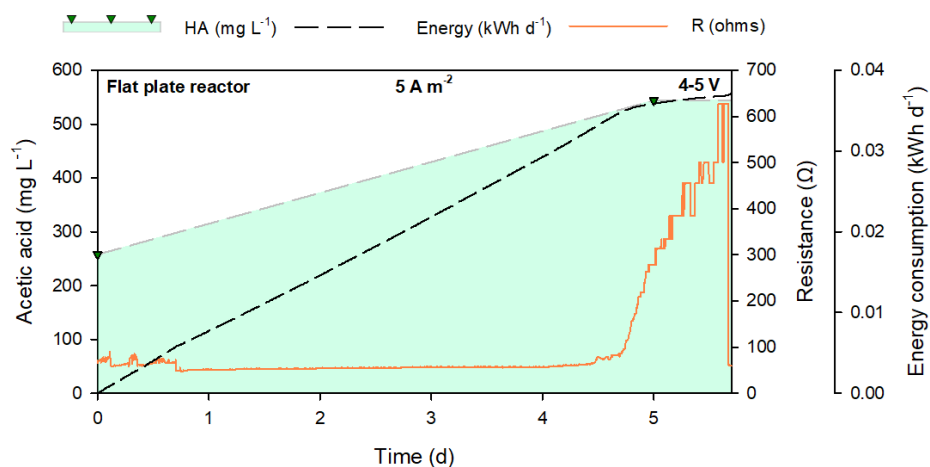


Figure 5. Acetate (HA) accumulation (mg L^{-1}), ohmic resistance (Ω) and power consumption (kWh d^{-1}) over time in the flat plate reactor with a fixed current supply of 5 A m^{-2} .

These results proved that although the purchased reactor design is suitable for scaling up, more configurations, materials and operating conditions still need to be tested to find a proper bioreactor that promotes microbe-material interactions and good gas-liquid mass transfer for efficient HA production. Despite advances in electrode materials research, modifications and cheaper novel alternatives are needed to improve MES performance and overcome the challenges for practical purposes. The design and operation of the bench-scale system were successful in terms of response sensitivity and operational variability. Yet, the results call for intensive investigation of a biocompatible reactor design capable of supplying reducing energy *in situ* without compromising the long-term durability of the biocatalyst. In particular, it is essential to test the MES designs developed on a pilot scale under digitalised control of variables, with an intermittent power supply to increase the product/energy ratio and to apply real off-gases to bring the technology closer to real application.

4. Conclusions

Real exhaust gases were tested at a laboratory scale and the results showed no substantial impact on HA production yields (difference of 2.5 %). Setting the current supply of the ECell reactor at 1.3 A m^{-2} resulted to be the best compromise between energy consumed per product obtained (2.07 kWh kg^{-1} HA), the most competitive ratio obtained so far. The limiting H_2 content suggested that higher electric current should be applied to obtain more competitive production rates. However, this requires a

combined approach considering biological, electrochemical and economic aspects, always with the ultimate goal of reducing significant amounts of CO₂.

Declaration of Competing Interest

The authors declare that they have no known competing financial interests or personal relationships that could have appeared to influence the work reported in this paper.

Acknowledgements

The authors acknowledge funding from the Spanish Ministry of Science and Innovation (PLEC2021-007802). LEQUIA (<http://www.lequia.udg.edu/>) has been recognized as a consolidated research group by the Catalan Government (2017-SGR-1552). L.R.-A. acknowledge the support by the Catalan Government (2018 FI-B 00347) in the European FSE program (CCI 2014ES05SFOP007). S.P is a Serra Hunter Fellow (UdG-AG-575) and acknowledges the funding from the ICREA Academia award.

References

- Althaus H.-J., Chudacoff M., Hischier R., Jungbluth N., Osses M. and Primas A. (2007) Life Cycle Inventories of Chemicals. ecoinvent report No. 8, v2.0. EMPA Dübendorf, Swiss Centre for Life Cycle Inventories, Dübendorf, CH, from www.ecoinvent.org.
- Angenent, L.T., Richter, H., Buckel, W., Spirito, C.M., Steinbusch, K.J.J., Plugge, C.M., Strik, D.P.B.T.B., Grootscholten, T.I.M., Buisman, C.J.N., Hamelers, H.V.M., 2016. Chain Elongation with Reactor Microbiomes: Open-Culture Biotechnology to Produce Biochemicals. *Environ. Sci. Technol.* 50, 2796–2810. <https://doi.org/10.1021/acs.est.5b04847>
- Arends, J.B.A., Patil, S.A., Roume, H., Rabaey, K., 2017. Continuous long-term electricity-driven bioproduction of carboxylates and isopropanol from CO₂ with a mixed microbial community. *J. CO₂ Util.* 20, 141–149. <https://doi.org/10.1016/j.jcou.2017.04.014>
- Bajracharya, S., 2016. Microbial Electrosynthesis of Biochemicals. Wageningen University. <https://doi.org/10.18174/385426>
- Batlle-Vilanova, P., Ganigué, R., Ramió-Pujol, S., Bañeras, L., Jiménez, G., Hidalgo, M., Balaguer, M.D., Colprim, J., Puig, S., 2017. Microbial electrosynthesis of butyrate from carbon dioxide: Production and extraction. *Bioelectrochemistry* 117, 57–64. <https://doi.org/10.1016/j.bioelechem.2017.06.004>

Bian, B., Bajracharya, S., Xu, J., Pant, D., Saikaly, P.E., 2020. Microbial electrosynthesis from CO₂: Challenges, opportunities and perspectives in the context of circular bioeconomy. *Bioresour. Technol.* 302, 122863. <https://doi.org/10.1016/j.biortech.2020.122863>

Blasco-Gómez, R., Romans-casas, M., Bolognesi, S., Perona-vico, E., Colprim, J., Balaguer, M.D., Puig, S., 2021. Steering bio-electro recycling of carbon dioxide towards target compounds through novel inoculation and feeding strategies. *J. Environ. Chem. Eng.* 9, 105549. <https://doi.org/10.1016/j.jece.2021.105549>

Christodoulou, X., Okoroafor, T., Parry, S., Velasquez-Orta, S.B., 2017. The use of carbon dioxide in microbial electrosynthesis: Advancements, sustainability and economic feasibility. *J. CO₂ Util.* 18, 390–399. <https://doi.org/10.1016/j.jcou.2017.01.027>

Dessì, P., Rovira-Alsina, L., Sánchez, C., Dinesh, G.K., Tong, W., Chatterjee, P., Tedesco, M., Farràs, P., Hamelers, H.M.V., Puig, S., 2020. Microbial electrosynthesis: Towards sustainable biorefineries for production of green chemicals from CO₂ emissions. *Biotechnol. Adv.* 107675. <https://doi.org/10.1016/j.biotechadv.2020.107675>

Fruehauf, H.M., Enzmann, F., Harnisch, F., Ulber, R., Holtmann, D., 2020. Microbial Electrosynthesis – An Inventory on Technology Readiness Level and Performance of Different Process Variants. *Biotechnol. J.* 2000066, 2000066. <https://doi.org/10.1002/biot.202000066>

Gadkari, S., Haji Mirza Beigi, B., Aryal, N., Sadhukhan, J., 2022. Microbial electrosynthesis : is it sustainable for bioproduction of acetic acid ? *RSC Adv.* 9921–9932. <https://doi.org/10.1039/d1ra00920f>

Jourdin, L., Raes, S.M.T., Buisman, C.J.N., Strik, D.P.B.T.B., 2018. Critical biofilm growth throughout unmodified carbon felts allows continuous bioelectrochemical chain elongation from CO₂ up to caproate at high current density. *Front. Energy Res.* 6. <https://doi.org/10.3389/fenrg.2018.00007>

Jourdin, L., Sousa, J., Stralen, N. van, Strik, D.P.B.T.B., 2020. Techno-economic assessment of microbial electrosynthesis from CO₂ and/or organics: An interdisciplinary roadmap towards future research and application. *Appl. Energy* 279. <https://doi.org/10.1016/j.apenergy.2020.115775>

Kamal, A.S., Othman, R., Jabarullah, N.H., 2020. Preparation and synthesis of synthetic graphite from biomass waste: A review. *Syst. Rev. Pharm.* 11, 881–894.

Mateos, R., Sotres, A., Alonso, R.M., Morán, A., Escapa, A., 2019. Enhanced CO₂ Conversion to Acetate through Microbial Electrosynthesis (MES) by Continuous Headspace Gas Recirculation. *Energies.*

- Miller, A., Singh, L., Wang, L., Liu, H., 2019. Linking internal resistance with design and operation decisions in microbial electrolysis cells. *Environ. Int.* 126, 611–618.
<https://doi.org/10.1016/j.envint.2019.02.056>
- Molenaar, S.D., Saha, P., Mol, A.R., Sleutels, T.H.J.A., ter Heijne, A., Buisman, C.J.N., 2017. Competition between methanogens and acetogens in biocathodes: A comparison between potentiostatic and galvanostatic control. *Int. J. Mol. Sci.* 18. <https://doi.org/10.3390/ijms18010204>
- Park, S.G., Rajesh, P.P., Sim, Y.U., Jadhav, D.A., Noori, M.T., Kim, D.H., Al-Qaradawi, S.Y., Yang, E., Jang, J.K., Chae, K.J., 2022. Addressing scale-up challenges and enhancement in performance of hydrogen-producing microbial electrolysis cell through electrode modifications. *Energy Reports* 8, 2726–2746.
<https://doi.org/10.1016/j.egyr.2022.01.198>
- Patil, S.A., Gildemyn, S., Pant, D., Zengler, K., Logan, B.E., Rabaey, K., 2015. A logical data representation framework for electricity-driven bioproduction processes. *Biotechnol. Adv.* 33, 736–744. <https://doi.org/10.1016/j.biotechadv.2015.03.002>
- Pepè Sciarria, T., Batlle-Vilanova, P., Colombo, B., Scaglia, B., Balaguer, M.D., Colprim, J., Puig, S., Adani, F., 2018. Bio-electrorecycling of carbon dioxide into bioplastics. *Green Chem.* 20, 4058–4066.
<https://doi.org/10.1039/c8gc01771a>
- Rabaey, K., Rozendal, R.A., 2010. Microbial electrosynthesis - Revisiting the electrical route for microbial production. *Nat. Rev. Microbiol.* 8, 706–716. <https://doi.org/10.1038/nrmicro2422>
- Romans-Casas, M., Blasco-Gómez, R., Colprim, J., Balaguer, M.D., Puig, S., 2021. Bio-electro CO₂ recycling platform based on two separated steps. *J. Environ. Chem. Eng.* 9, 105909.
<https://doi.org/10.1016/j.jece.2021.105909>
- Rovira-Alsina, L., Balaguer, M.D., Puig, S., 2021. Thermophilic bio-electro carbon dioxide recycling harnessing renewable energy surplus. *Bioresour. Technol.* 321.
<https://doi.org/10.1016/j.biortech.2020.124423>
- Rovira-Alsina, L., Perona-Vico, E., Bañeras, L., Colprim, J., Balaguer, M.D., Puig, S., 2020. Thermophilic bio-electro CO₂ recycling into organic compounds. *Green Chem.* 22, 2947–2955.
<https://doi.org/10.1039/d0gc00320d>
- Rovira-Alsina, L., Romans-Casas, M., Balaguer, M.D., Puig, S., 2022. Thermodynamic approach to foresee experimental CO₂ reduction to organic compounds. *Bioresour. Technol.* 354.
<https://doi.org/10.1016/j.biortech.2022.127181>
- Roy, M., Yadav, R., Chiranjeevi, P., Patil, S.A., 2021. Direct utilization of industrial carbon dioxide with

low impurities for acetate production via microbial electrosynthesis. *Bioresour. Technol.* 320, 124289. <https://doi.org/10.1016/j.biortech.2020.124289>

Schuchmann, K., Müller, V., 2014. Autotrophy at the thermodynamic limit of life: A model for energy conservation in acetogenic bacteria. *Nat. Rev. Microbiol.* 12, 809–821. <https://doi.org/10.1038/nrmicro3365>

Song, H., Choi, O., Pandey, A., Kim, Y.G., Joo, J.S., Sang, B.I., 2019. Simultaneous production of methane and acetate by thermophilic mixed culture from carbon dioxide in bioelectrochemical system. *Bioresour. Technol.* 281, 474–479. <https://doi.org/10.1016/j.biortech.2019.02.115>

Su, L., Ajo-Franklin, C.M., 2019. Reaching full potential: bioelectrochemical systems for storing renewable energy in chemical bonds. *Curr. Opin. Biotechnol.* 57, 66–72. <https://doi.org/10.1016/j.copbio.2019.01.018>

Tanner, R.S., Miller, L.M., Yang, D., 1993. *Clostridium ljungdahlii* sp. nov., an acetogenic species in clostridial rRNA homology group I. *Int. J. Syst. Bacteriol.* 43, 232–236. <https://doi.org/10.1099/00207713-43-2-232>

Van Eerten-jansen, M.C.A.A., Heijne, A. Ter, Buisman, C.J.N., Hamelers, H.V.M., 2012. Microbial electrolysis cells for production of methane from CO₂ : long-term performance and perspectives. *Int. J. energy Res.* 809–819. <https://doi.org/10.1002/er>

Vassilev, I., 2019. Microbial electrosynthesis: Anode-and cathode-driven bioproduction of chemicals and biofuels. <https://doi.org/10.14264/uql.2019.39>

Verbeeck, K., 2014. Combined Synthesis and Extraction of Acetate From CO₂ Using Microbial Electrosynthesis. *Gent*.

Viridis, B., Hoelzle, R., Marchetti, A., Boto, S.T., Rosenbaum, M.A., Blasco-Gómez, R., Puig, S., Freguia, S., Villano, M., 2022. Electro-fermentation: Sustainable bioproductions steered by electricity. *Biotechnol. Adv.* 59, 107950. <https://doi.org/10.1016/j.biotechadv.2022.107950>

Von Stockar, U., Maskow, T., Liu, J., Marison, I.W., Patiño, R., 2006. Thermodynamics of microbial growth and metabolism: An analysis of the current situation. *J. Biotechnol.* 121, 517–533. <https://doi.org/10.1016/j.jbiotec.2005.08.012>

Yang, H.Y., Hou, N.N., Wang, Y.X., Liu, J., He, C.S., Wang, Y.R., Li, W.H., Mu, Y., 2021. Mixed-culture biocathodes for acetate production from CO₂ reduction in the microbial electrosynthesis: Impact of temperature. *Sci. Total Environ.* 790, 148128. <https://doi.org/10.1016/j.scitotenv.2021.148128>

Yu, L., Yuan, Y., Tang, J., Zhou, S., 2017. Thermophilic *Moorella thermoautotrophica*-immobilized cathode enhanced microbial electrosynthesis of acetate and formate from CO₂. *Bioelectrochemistry* 117, 23–28. <https://doi.org/10.1016/j.bioelechem.2017.05.001>

Zhang, T., Nie, H., Bain, T.S., Lu, H., Cui, M., Snoeyenbos-West, O.L., Franks, A.E., Nevin, K.P., Russell, T.P., Lovley, D.R., 2013. Improved cathode materials for microbial electrosynthesis. *Energy Environ. Sci.* 6, 217–224. <https://doi.org/10.1039/c2ee23350a>

Chapter 5. Discussion



5. General discussion

The research described in this PhD thesis addressed the bioelectro-recycling of CO₂ from the laboratory to the pilot scale including its assessment with real industrial off-gases. Fundamental studies were necessary to have a solid base to work on. However, moving away from the core to consider the real situation from a global perspective was necessary to remain in the right direction and not get side-tracked by the knowledge that is sometimes not applicable. This discussion chapter aims at summarising, relate and contrast all the results obtained with recent literature and proposing a roadmap for the future.

5.1. Current state of the art of HA production from CO₂

From the first proof of concept of microbial CO₂ reduction on a cathode, peak HA concentrations and production rates increased rapidly up to 13.5 g L⁻¹ (Gildemyn et al., 2015) and 685 g m⁻² d⁻¹ (Jourdin et al., 2015b) in a decade (**Table 4**). However, there has been no substantial increase after 2015 onwards and, recalling the required threshold of 4100 g HA m⁻² d⁻¹ of Gadkari et al. (2022), these values remain too low for an industrially relevant process (PrévotEAU et al., 2020). Meanwhile, very little effort has been put into **thermophilic** research even though it has the potential for waste heat recovery from real exhaust gases, presumably because the technology is still at low TRLs (3-5). The few studies conducted at high temperatures (≥ 50 °C) resulted in low production rates (< 10 g m⁻² d⁻¹), though the applied potentials were also noticeably lower compared to mesophilic studies (**Table 4**). Yu et al. (2017) obtained 2.8-fold higher HA production rates at 55 °C compared to at 25 °C. Faraghiparapari and Zengler (2016) achieved 55 % higher HA titers at 60 °C compared to at 50 °C with *Moorella thermoautotrophica* as a pure culture. In that study, the concentration of HA and CE achieved remained lower (59 % and 15 %, respectively) compared to other trials with mesophilic cultures of *Sporomusa ovata*. Yang et al. (2021) obtained denser biofilms using a mixed microbial culture and 41 % higher HA concentration at 25 and 35 °C compared to at 55 and 70 °C. However, the results obtained in the present PhD thesis were in between the HA concentrations and production rates achieved by other authors working under mesophilic conditions. It is worthy to highlight that the thermophilic operation also helped to avoid diversification of the final products, while many mesophilic studies employing mixed cultures had co-production of other compounds such as ethanol, butyrate, or caproate, among others (Anwer et al., 2021; Arends et al., 2017; Bajracharya et al., 2016; Jourdin et al., 2018; Vassilev et al., 2018). If chemical knowledge, especially reaction kinetics and organic chemistry, were combined with biological knowledge, substantial improvements in the synthesis of target compounds could be achieved (Bourne, 2003). In this sense, more thermophilic studies should focus on heat utilisation and reaction kinetics enhancement.

Table 4. Comparison of the state of the art of microbial electrosynthesis of acetate from CO₂ using enriched mixed consortia. In many cases, concentration and production rates have been calculated according to the data provided by the authors.

Cathode	Area (m ²)	Reactor	T (°C)	E vs. SHE (V)	I (A m ⁻²)	Conc. (g L ⁻¹)	Rate (g m ⁻² d ⁻¹)	CE (%)	Comments	Reference
Graphite plates	0.0036	H-Cells	60	-0.30	--	0.02	0.21	79	Different temperatures and <i>Moorella</i> strains tested.	Faraghiparapari and Zengler, 2016
Carbon cloth with carbon nanoparticles	0.0147	H-Cells	55	-0.40	0.063	0.44	3.80	65	Formate co-production using <i>Moorella</i> strains	Yu et al., 2017
Carbon disk	0.0081	Single chamber	60	-0.65	4.9	10.50	9.61	97	Methane co-production	Song et al., 2019
Carbon cloth	0.0030	H-Cells	50	-0.60	11.0	6	43.27	89	Intermittent energy supply	This PhD thesis
Stainless steel	0.0100	Three-chamber	21	-1.14	50.0	13.5	24.30	73	Galvanostatic control	Gildemyn et al., 2015
RVC* foam (EPD*-3D)	0.0037	Two-chamber	35	-0.85	102.0	11	685.0 ^c	100	High product specificity	Jourdin et al., 2015
GDE*	0.0010	Circular-shaped flow cell	30	-0.90	20.0	2.5	36.6	35	Ethanol and butyrate co-production	Bajracharya et al., 2016
Carbon felt	0.0100	Two-chamber	30	-1.40	5.0	6.4	21.0	63	Galvanostatic control; butyrate and isopropanol co-production	Arends et al., 2017
rGO* on carbon felt	0.0050	Two chamber	25	-0.85	4.9	7.1	9.5	77	Graphene oxide on cathode surface	Song et al., 2017
RVC foam	0.0048	Modular scalable design	25	-0.80	83.3	3.6	195.0 ^d	35	Galvanostatic control and continuous media flow	LaBelle and May, 2017
Graphite granules	0.0152	Glass vessel	35	-0.80	9.0	4.9	9.5	44	Other carboxylates and alcohols co-production	Vassilev et al., 2018
Carbon felt with GAC*	0.0050 ^a	H-Cells	25	-0.85	4.1	3.92	7.8	65	Fluidized granular bed	Dong et al., 2018
Graphite felt	0.0067	H-Cells	--	-0.80	2.4	0.62	10.0	74	Electric supply interruption	Del Pilar Anzola Rojas et al., 2018
Carbon felt	0.0100	Three-chamber	21	-1.30	5.0	4.2	76.0	28	Galvanostatic control; <i>in-situ</i> extraction	Verbeeck et al., 2018
3-layers carbon felt	0.0020 ^b	Two-chamber	32	-0.85	175.0	8.6	376.0 ^c	88	Butyrate and caproate co-production	Jourdin et al., 2018
Graphite felt	0.0176	Two-chamber	25	-0.80	2.1	1.96	6.7	79	Continuous headspace gas recirculation	Mateos et al., 2019
Modified carbon felt	0.0025	Two-chamber	25	-0.85	5.6	13.74	26.9	73	Perovskite-based multifunctional cathode	Tian et al., 2020
EPD-3D	6.1 cm ² cm ⁻³	Two-chamber	35	-0.85	6.3	1.18 kg m ⁻²	42.4	100	Comparison of different cathode materials	Flexer and Jourdin, 2020
Carbon felt	0.0449	H-Cells	25	-0.90	0.3	0.53	0.6	45	Different temperatures tested	Yang et al., 2021
Mo2C7N-doped 3D loofah sponge	0.0018	H-Cells	25	-0.85	15.0	6.08	167.0 ^c	68	Comparison with carbon felt	Huang et al., 2021
TiO2 on carbon felt	0.0004	Two-chamber	27	-0.90	7.3	8.86	269.0 ^d	73	Comparison of different cathode materials	Das et al., 2021
Carbon paper coated with MV-PANI	0.0014	H-Cells	--	-0.80	14.8	4.42	207.0 ^d	74	Comparison of different cathode materials; ethanol co-production	Anwer et al., 2021
Nickel foam coated with carbon nanotubes	0.0035	Two-chamber	30	-0.60	2.8	0.90	2.8	91	Different delivery and CO2 flow rates; methane co-production	Bian et al., 2021

RVC: Reticulated Vitreous Carbon; EPD: Electrophoretic Deposition Technique; rGO: Graphene Oxide; GDE: Gas Diffusion Electrode; GAC: Granular Activated Carbon; a: considering only the carbon felt area; b: projected area/0.012 of total area; c: only considering the projected surface area; d: calculated with the given projected surface area

On the other hand, thin autotrophic **biofilms** of a few micrometres are often developed in MES due to limited C and energy uptake (Vassilev et al., 2022). Increasing the electrode surface area (Flexer and Jourdin, 2020), creating a positive surface charge (Das et al., 2021), enhancing hydrophilicity (Tian et al., 2020) and conductivity (Thatikayala and Min, 2021) have proven effective in increasing biofilm

formation. However, excessive thick biofilms on the cathodes could result in mass transfer limitations, restricting the availability of nutrients, CO₂ and reducing equivalents, so a trade-off between microbial enrichment and abundance must be sought. The highest current densities, CEs and production rates were achieved in **3D structured cathode electrodes** hosting relatively thick (5-10 μm) active biofilms (Claassens et al., 2019). A Mo₂C/N-doped 3D loofah sponge cathode obtained 167 g m⁻² d⁻¹, 2.5 times more HA production than with carbon felt (Huang et al., 2021). A similar production rate (195 g m⁻² d⁻¹) was attained with RVC foam, where electron limitation was reduced by galvanostatic control at a current intensity of 83.3 A m⁻², between 5-6 times higher (LaBelle and May, 2017). Differently, polymer-based redox mediators were used to modify electrodes to enrich biofilm formation and reduce the internal resistance of the system, achieving 1.3 times higher production of HA (207 g m⁻² d⁻¹) compared to plain carbon paper electrodes (Anwer et al., 2021). Better bacterial attachment and more production of H₂ were also observed when using TiO₂ on carbon felt, achieving 2.14-fold higher production rates of HA (269 g m⁻² d⁻¹) in comparison with a MES operated with no cathode catalyst (Das et al., 2021). Nevertheless, Jourdin et al. (2018) demonstrated a continuous, biofilm-driven HA production on unmodified carbon felt electrodes, getting a 1.2 cm-deep biofilm, high current density (175 A m⁻²) and production rate (376 g m⁻² d⁻¹).

5.1.1. Acetate production relative to energy consumption

Normalising current densities and production rates as a function of electrode surface area is not always straightforward. It should be noted that some studies consider only the projected surface area, which is the surface of the electrode facing the membrane, always smaller than the working surface area (the total surface available for bacterial growth and electron uptake). This can be easily calculated when working with simple cathodes (e.g. carbon cloth), but very difficult when working with 3D electrodes. Moreover, as the major cost of the technology is given by electricity, the needle in the haystack would be to consider the amount of product obtained (in this case HA) per unit of electricity consumed, or otherwise, the **energy required for the production of 1 kg of product (Figure 12)**.

The studies with carbon cathodes have not yet succeeded in exceeding the production rate of 100 g HA m⁻² d⁻¹, while the use of different cathodic materials such as RVC foam has led to higher yields but also larger energy consumptions. Considering proton exchange membrane (PEM) and alkaline electrolyzers (Carmo et al., 2013; Shiva Kumar and Himabindu, 2019) to produce the equivalent H₂ required, or HA production *via* methanol carbonylation (Althaus et al., 2007), the results of the present PhD thesis are competitive in terms of energy consumption, but none of the current MES studies come close to the **threshold production rate of 4100 g m⁻² d⁻¹** to make it an economically feasible process (Gadkari et al., 2022). Graphite electrodes (Romans-Casas et al., 2021) seem to require less energy input per kg of HA

compared to other materials, but production rates (normalized by the working area) were also lower compared to other studies. Stainless steel material did not seem to reinforce production rates (Gildemyn et al., 2015) compared to C-based electrodes, whereas on some occasions carbon cloth resulted in high energy consumption provably because of product diversification (Pepè Sciarria et al., 2018). Thus, it is necessary to increase product selectivity by using the electrons efficiently to maximise the target product.

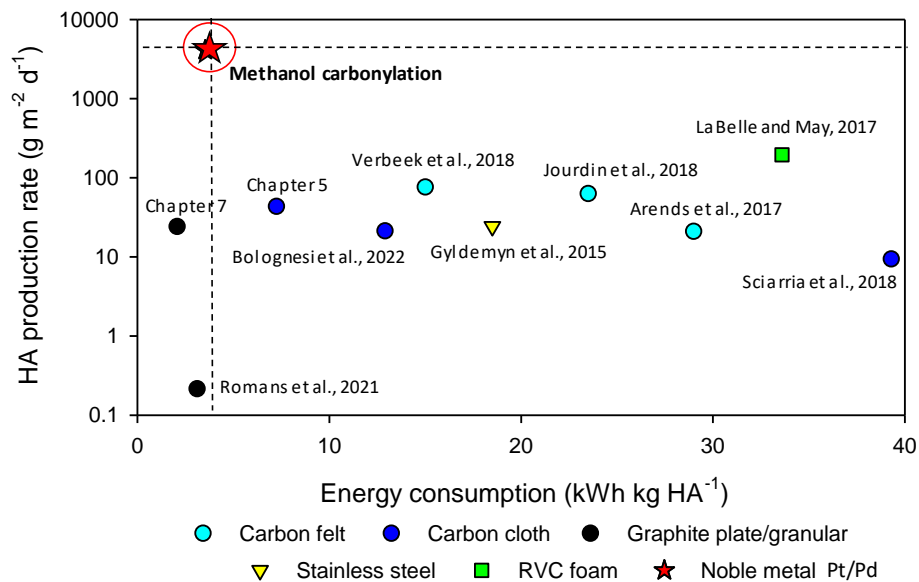


Figure 12. Acetic acid (HA) production rate vs. energy consumption of microbial electro-synthesis studies from CO₂ using different electrodes. The energy consumption *via* methanol carbonylation (3.5 kWh kg⁻¹) and the theoretical production threshold of 4100 g m⁻² d⁻¹ were considered targets to be attained for MECs implementation.

It is of vital importance to operate at high volumetric production rates for an industrial process, thus MECs need to increase current densities. However, it is questionable whether H₂ can be produced with high energy efficiencies when using conventional bacterial growth media as an electrolyte due to the low conductivity (typically < 10 mS cm⁻¹). This is another constraint to be solved, as high **ohmic resistances** (> 100 Ω cm⁻²) (Borole and Lewis, 2017) are obtained compared to less than 0.1 Ω cm⁻² in PEM electrolyzers that have conductivities above 200 mS cm⁻¹ (Carmo et al., 2013). In the set-ups used for this PhD thesis, the resistance was determined by the impedance spectroscopy method and was found to be below 0.5 Ω cm⁻² in the pilot plant, while for the HTs reactors it was expected to be much higher, though it could not be calculated as the carbon cloth and graphite rod connections generated disturbances in the measurement. High ohmic resistances result in **current densities** for MES typically under **20 A m⁻²**, which is well below those measured in abiotic electrolyzers (> 1000 A m⁻²) for CO₂ electro-reduction (De Luna et al., 2019), or in commercial PEM electrolyzers (up to 20000 A m⁻²) for H₂

production (Schmidt et al., 2017). On the other hand, PrévotEAU et al. (2020) calculated that to combine current densities relevant for HA production with acceptable energy efficiencies (90 %) and considering an electricity cost of 0.03 € kWh⁻¹, it would be necessary to decrease the specific resistance by at least one or two orders of magnitude. Hence, this would have to be addressed with new designs to lower the cell voltage by reducing the distance between electrodes and using optimised materials to shorten the energy requirement of the system, which is not an easy endeavour.

5.2. Perspectives for MES evolution to higher technology readiness levels (TRLs)

In the last decade, different MES technologies have been described based on biofilms or soluble mediators, EF, secondary MES, or even hybrid systems offering a range of process performances and TRLs up to 7 (system prototype demonstration in operational environment) (Fruehauf et al., 2020). In general, TRL 6 (technology demonstrated in relevant environment) is considered the “launch pad” for the transition from research to industrial implementation and commercialisation, although at the moment it is only achieved when combining bioelectrochemical conversion in hybrid systems (Haas et al., 2018). Despite the research efforts and advances in design, materials and performance, CO₂-based MES still are at low TRLs, as they suffer from a lack of adequate scale-up procedures and **limited surface-to-volume ratios**. Enzmann et al. (2019) suggested that scaling up to 10-100 L working volume prototypes should be based on modular designs that account for the distance between electrodes to minimise electrical resistance and intensify current densities.

Another constraint limiting the scale-up is the multiple **metabolic platforms** of the micro-organisms. Assuming an unrestricted supply of electron donor (H₂) and acceptor (CO₂), the overall rate of MES conversion would be proportional to the amount of biocatalyst (Kantzow et al., 2015). However, robust and resilient electroactive biofilms are difficult to achieve. When the electron transfer is mediated through H₂ (most common case), acetogens gain 0.3 to 1.0 mol of ATP per mol of HA produced. Yet, CO₂ reduction and H₂ oxidation can be coupled with an electron-transport phosphorylation module, making it possible to gain additional ATP and live beyond the thermodynamic edge of life (Katsyv and Müller, 2020). Nevertheless, the growth rate of an acetogenic cathodic biofilm was calculated to be 0.12 d⁻¹ based on computational modelling (Cabau-Peinado et al., 2021), which is at least 1 order of magnitude lower than for heterotrophs such as *Escherichia coli* (Gibson et al., 2018).

Besides the active surface area of the cathode, the **limited CO₂ solubilisation** remains a big challenge for MES. Gas diffusion electrodes have been proposed to partially solve this issue (Bajracharya et al., 2016), also promoting the biofilm development on the electrode surface and resulting in an HA production rate of 37 g m⁻² d⁻¹ (**Table 4**). Jourdin et al. (2018) developed a flow-through system to increase the

contact between the biocatalyst, electrolyte and C source, promoting the formation of a thick and heterogeneous biofilm, enabling high current densities (175 A m^{-2}) and high HA production rates ($376 \text{ g m}^{-2} \text{ d}^{-1}$). They observed that a thicker biofilm was developed under continuous operation, which was predicted to be due to a constant replenishment of nutrients, product removal and washing out of planktonic cells (Cabau-Peinado et al., 2021). More recently, a biofilm with *S. ovata* cells embedded in the cathode formed by 3D-bioprinting (Krige et al., 2021) resulted in a decrease of the start-up time to 40 h and an HA production rate of $104 \text{ g m}^{-2} \text{ d}^{-1}$, one order of magnitude higher than typical *S. ovata* production rates in HT cells, and 2-3 fold higher than reactors using specialized cathodes. In the present PhD thesis, the biofilms were characterised morphologically by scanning electron microscopy and phylogenetically by sequencing, but no thick biofilms were observed on the carbon cloth surfaces. Even though the optimisation of MES relies on a better understanding of electro-active biofilms, these methods do not provide quick results, are invasive, and destroy partially or totally the MES cells. An alternative would be online monitoring and quantification of biofilms by visual techniques (Pereira et al., 2022). It has rarely been used on cathode electrodes (Hackbarth et al., 2020), though it would be pivotal to improve the start-up of MES reactors and the growth of active biofilms.

Biofilms should adapt to the **dynamic conditions** of MES operation such as variable CO_2 feeding supply, pH gradients, intermittent power and different P_{H_2} (Vassilev et al., 2022). Nevertheless, poor information is available on the effect of oxygen diffusion and hydrodynamics on biofilm generation and temperature, which also influence the biofilm development. Velvizhi et al. (2022) proved that an enriched biocatalyst could adapt its nature based on the operational conditions, reaching higher production rates when applying a potential of -0.8 V vs. SHE compared to fermentation or open-circuit voltage conditions. If a well-structured biofilm and the faradaic efficiency were stable, the cell voltage would be inversely proportional to the energy efficiency and proportional to the cost of electrical energy per amount of electro-generated product (Dessi et al., 2020). However, whereas the putative mechanisms of DET have not yet been elucidated, it is increasingly accepted that under cathodic potentials below -0.4 V vs. SHE , indirect electron transfer *via* H_2 has led to the most relevant production rates (Blanchet et al., 2015; Kracke et al., 2019). Low current densities seem not to be limited by an intrinsic maximum value to biofilm performance but are rather a consequence of the rapid increase of cell voltage. Despite, even if much higher current densities were reached to approach competitiveness, they would also induce other challenges, such as limiting CO_2 mass transfer, high alkalinity gradients and considerable H_2 bubble formation on the cathode surface (PrévotEAU et al., 2020).

Since electricity has been identified as the most important operating cost, computing this is necessary for the **economic viability** of MES (Christodoulou et al., 2017; Jourdin et al., 2020). In an economic assessment for HA production from CO_2 , both production and investment costs using MES were

estimated to be high compared to commercial production through methanol carbonylation or direct ethane oxidation (Christodoulou and Velasquez-orta, 2016). However, the integration of **MES with AF** was projected to have the potential to reduce CO₂ release, double production rates and decrease investment costs by 9 %, setting production costs to market-competitive values. The anode material was found to be the second most important expense, while cell voltage, CE and current density also had a significant impact on both capital and operating costs (Jourdin et al., 2020). This study showed that the only likely way to achieve cost-effectiveness targets was to increase selectivity towards caproate, with an electron share of at least 36 %. However, it was concluded that MES and electrochemical CO₂ reduction are two distinct processes targeting separate markets, but that they can benefit from each other if further cooperation is fostered.

5.2.1. Moving towards a digital transformation

A virtual representation of these systems, supported by **digital data**, would help to understand the past, observe the present and predict the future, thus contributing to decision making (**Figure 13**). By being able to identify potential challenges, improvements can be implemented and future operations can be anticipated based on envisioned designs, simulations and real-time data collection. That was the aim of the pilot plant presented in chapter 4.4. Visualise the design before creating the physical prototype to improve performance and reduce the environmental impact, lower costs and increase the CE efficiency of the results. Data collection was leveraged to drive intelligent workflows, design for faster and smarter decision-making and real-time response to system disruptions. The defined control system consisted of a process variable basis divided into indicator devices giving informative signals (e.g. inlet flow rate, outlet H₂ and O₂ content, conductivity of the medium), or control signals (e.g. inlet pH and CO₂, temperature, pressure) which, depending on the set range, acted on control devices (e.g. acid/base dosing pumps, CO₂ supply, temperature controller flow, overpressure valves). This made it possible to work on different combinations of parameters and to record continuously the response signals immediately after any change, without the need to delay the next adjustments.

Nonetheless, while many organisations have undertaken a digital transformation in response to a single competitive threat or market change, the goal of a digital transition is better conceived as building a technical and operational platform to evolve and adapt to an ever-changing environment. It is also a change that requires an ongoing challenge to the status quo, experimenting and **becoming comfortable with failure**.

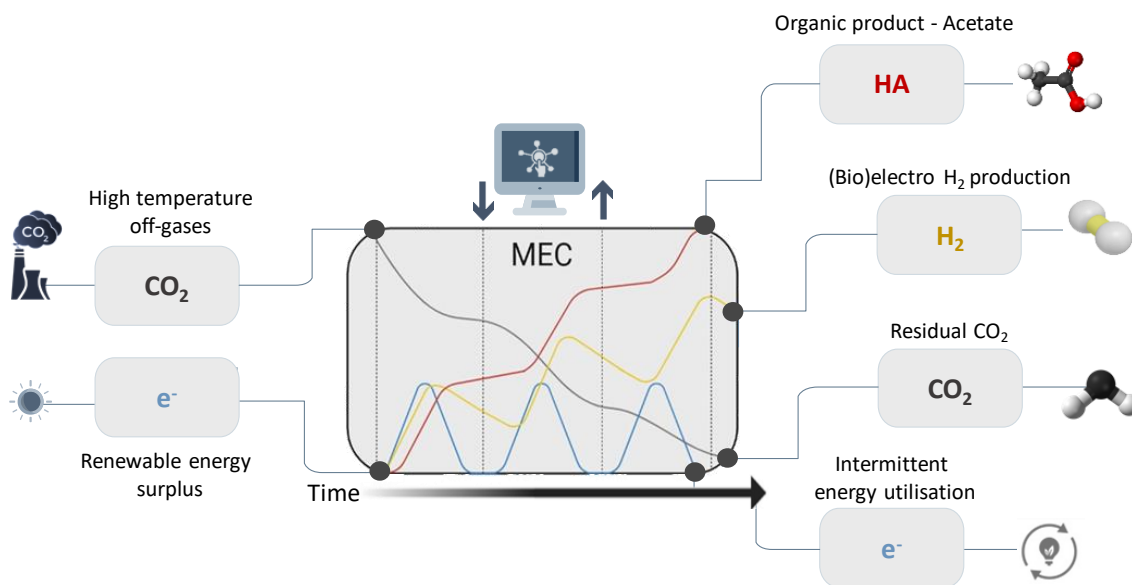


Figure 13. Schematic proposal for the digitalisation of microbial acetate electro-synthesis from renewable energy surplus and CO₂. While electricity input is intermittent, acetate (HA) and CO₂ are produced and consumed continuously at different rates, depending on the availability of H₂. H₂ is produced when electricity is available and consumed when it is not, combining electrochemical and anaerobic fermentation processes.

5.3. MES as a sustainable energy battery

This PhD thesis assessed different scenarios for HA production concluding that even if the productivity of MES could be increased to match the highest space-time yield reported for acetogenic bacteria (**148 g L⁻¹ d⁻¹**) in a continuous gas fermenter fed with H₂ and CO₂, the environmental impact would still be significantly higher than that produced by fossil-based processes (Gadkari et al., 2022). On the other hand, when considering other technologies such as sludge-to-biochar, MES suffers from lower cost-effectiveness in the **capture of CO₂** (Pahunang et al., 2021). But, when compared to other conventional mechanisms to **store renewable energy**, it offers a potential alternative that has not been much envisioned and besides, converts CO₂ into useful products.

Batteries and similar devices accept and store chemical energy for later conversion to electrical energy. It was estimated that the use of batteries instead of other technologies, such as combined cycle gas turbines, could reduce GHG emissions by up to 87 %, corresponding to 1.98 MT CO₂ eq. for an optimal supply in 2035 (Chowdhury et al., 2020). Yet, batteries degrade over time, with a lifetime of about 10-20 years, depending on how they are operated with the corresponding environmental implications (i.e. their chemicals soak into the soil and contaminate water). To maintain a reliable and constant storage

capacity as batteries deteriorate, large-scale battery plants will require continuous installation and replacement of batteries in stages. In comparison, MES can be seen as a potential device that accepts, stores and converts electrical energy on demand into a useful product with chemical energy. In this case, the degradation of MECs is close to zero, as biomass is self-regenerating and, with proper maintenance, peak production could be maintained indefinitely (Jourdin et al., 2015a). In addition, batteries have risk issues related to thermal runaway, which can lead to explosions and fires if safety measures are not implemented, whereas, in MES, H₂ used as reducing power is produced and consumed *in-situ*, avoiding safety risks related to transport and storage of this inflammable gas.

On the other hand, both batteries and MES require a relatively small portion of land and are likely to be sited very close to the energy demand or generation locations, with little environmental impact. However, the effects of batteries on soil and water are more related to their disposal at the end of their useful life, and to the extraction of resources to produce new batteries. Lead-acid and lithium-ion batteries use common materials such as plastic and steel, but also chemicals and minerals such as lead, lithium, graphite, nickel and cobalt, which are finite resources. In contrast, MES offers the possibility to operate by reusing water from WWTPs and C electrodes that are not harmful to the environment. However, cationic exchange membranes contain negatively charged sulfonate or phosphonate, or carboxyl fixed groups and selectively transfer cations that could have an impact on eutrophication in natural water bodies (Pismenskaya et al., 2022). Determining the ultimate sustainability of the resources and materials required for both technologies needs consideration of the full life cycle and supply chain, as well as end-of-life issues such as recycling, disposal or decommissioning (Chowdhury et al., 2020).

Globally, increasing levels of renewable energy will drive a greener grid. It is clear to foresee the sustainability benefits of using storage to further promote the decarbonisation of the grid through increased uptake of renewables. However, storage solutions that enable more renewables must also be sustainable, not only in the use phase but also up and downstream. At this early stage of development of both technologies, comprehensive life cycle analysis is limited by the diversity of materials and multiple operating scenarios. While battery production is being perfected, alternatives such as graphene supercapacitors that instead of holding electricity in the form of chemical potential, store it in an electric field, are being considered. The addition of graphene creates strong, lightweight supercapacitors. However, most of the recent work in this field has focused on increasing energy density towards the range of thin-film batteries, and it will be a challenge in the coming years to increase the power density to hold a charge for longer (Velasco et al., 2021). In this sense, MES could be used as “batteries” that are both practical and environmentally friendly to store green electricity for

a long time with the possibility of obtaining energy-valuable products through chain elongation processes (Steinbusch et al., 2011).

5.3.1. Challenging options and prospects

To date, the economic viability of MES is still hampered by factors such as the energy consumption, low titer and low selectivity of the products obtained, which ultimately pose a challenge for downstream recovery and purification steps. In this context, the results chapters showed a targeted transition of these systems from the initial utilisation of waste heat from CO₂ emissions, towards the restricted use of surplus renewable energy and the study of optimal operating variables for the selection of a product, to the use of real off-gases and digitalised pilot plant scale implementation (Figure 14). This represents an innovative approach, based on the use of a polarised electrode interface to harness both, natural resources and CO₂ emissions to store energy in the form of a chemical product. In addition, the amount of CO₂ uptaken as feedstock for HA production was more than doubled (2.21 kg CO₂ kg HA⁻¹) compared to the value found by Otto et al. (2015) in a study to identify CO₂ utilisation reactions with the most potential for further exploration and technology development.

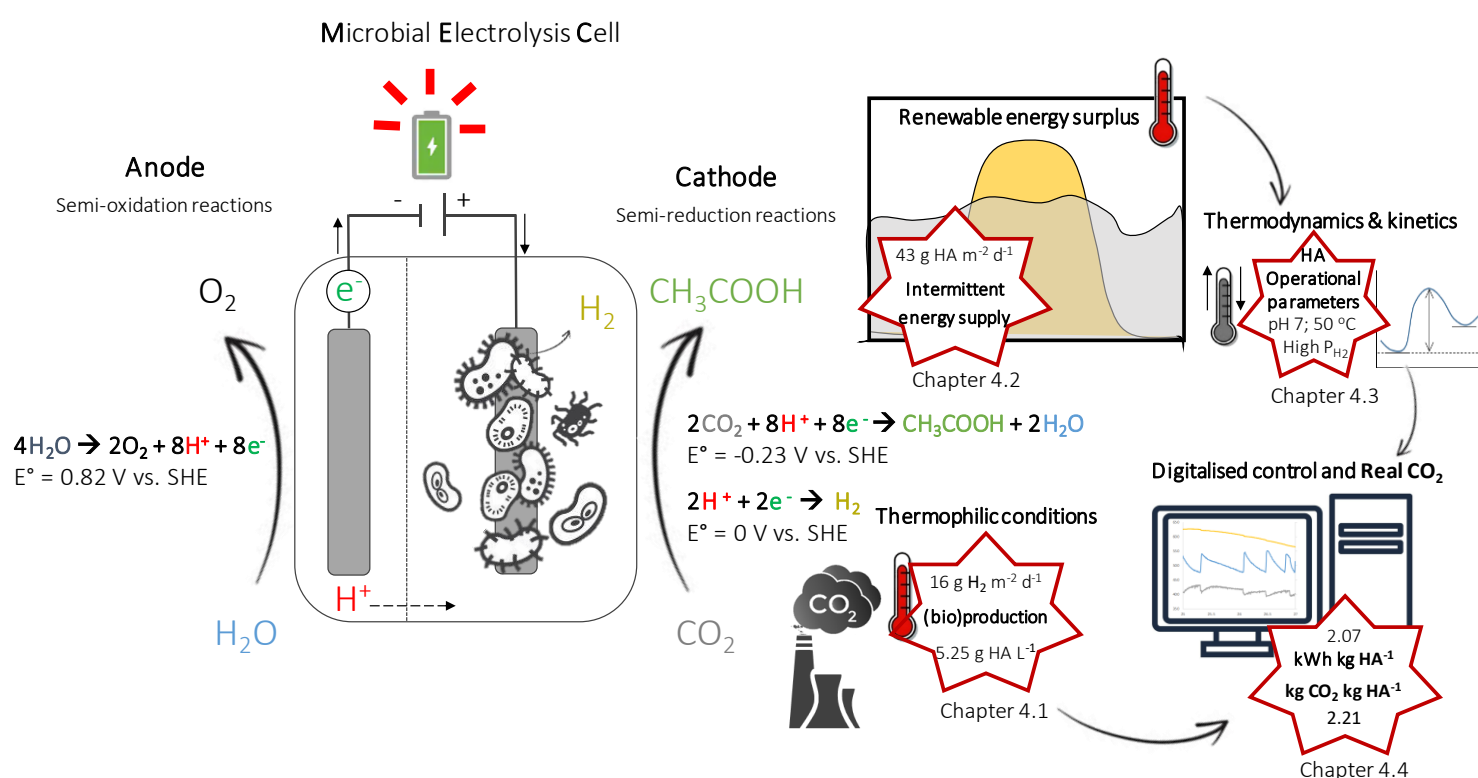


Figure 14. Summarising outline including the roadmap from the objectives set to the results achieved.

Different **carbon capture technologies** have been proposed to be coupled with relevant CO₂ sources (e.g. WWTPs) to increase cost-effectiveness and obtain value-added products (Pahunang et al., 2021). Such coupling or even replacement has emerged as an economically viable option (Lu et al., 2018), promising an internal rate of return of 63 % that can even be increased through C credits and further research to reduce the capital cost of construction. In addition, fiscal incentives for CO₂ capture and storage are among the key policy recommendations in the European Gas Regulatory Forum (IOGP, 2019), closing the price of permits in the EU C market last Friday 24th of June 2022 at an all-time high of over 96 euros per tonne. Thus, MES can be part of a solution that not only stores energy, but also avoids CO₂ emissions and integrates into the wastewater treatment cycle.

If focusing on **solar energy (Figure 15)**, several integrated systems have been developed that harness intermittent sunlight through photo-induced reactions instead of using electricity generated *via* photovoltaics (PV). However, all are at TRLs between 3-4 so extra efforts are needed to make them efficient, safe, robust and economically viable. Although some components used in these technologies are expensive (PV panels and catalysts), if high energy efficiencies could be reached, it would have the potential to produce valuable compounds at a low cost. Yet, the thermodynamic limitation was already analysed in 1961 by Shockley and Queisser, resulting in maximum conversion efficiency of 33 % using a band gap of 1.1-1.4 V vs. SHE in a single junction device. These conversion efficiencies can be increased to 45 % by minimising the excess voltage in a multi-junction or tandem solar cell (Jia et al., 2016), but this results in higher material and processing costs (Inganäs and Sundström, 2016). To become competitive with fossil fuel-derived feedstocks, electrical-to-chemical conversion efficiencies need to reach at least 60 %, and renewable electricity prices need to fall below 0.04 € kWh⁻¹ (De Luna et al., 2019), a value from which we are moving further away from every day.

Regardless of the considerable economic barriers within the complex, established, and highly connected petrochemical industry, some of the **technical challenges** that also remain to be solved are (i) improving light harvesting while understanding the interfacial electron/energy transfer process, (ii) finding simple solutions to concentrate and utilise CO₂ from off-gases and the atmosphere, (iii) developing more stable (bio)electrocatalysts and photocatalysts for CO₂ reduction, and (iv) developing industrially viable recovery methods for less abundant elements (EuCheMS, 2016). However, researchers have been trying to develop artificial photosynthesis for more than a century (Ciamician, 1912), revealing the complex challenge of mimicking the most important photo-biochemical process on Earth, and even if the current design and operational constraints were overcome, the question remains whether the greatest limitation may be biological.

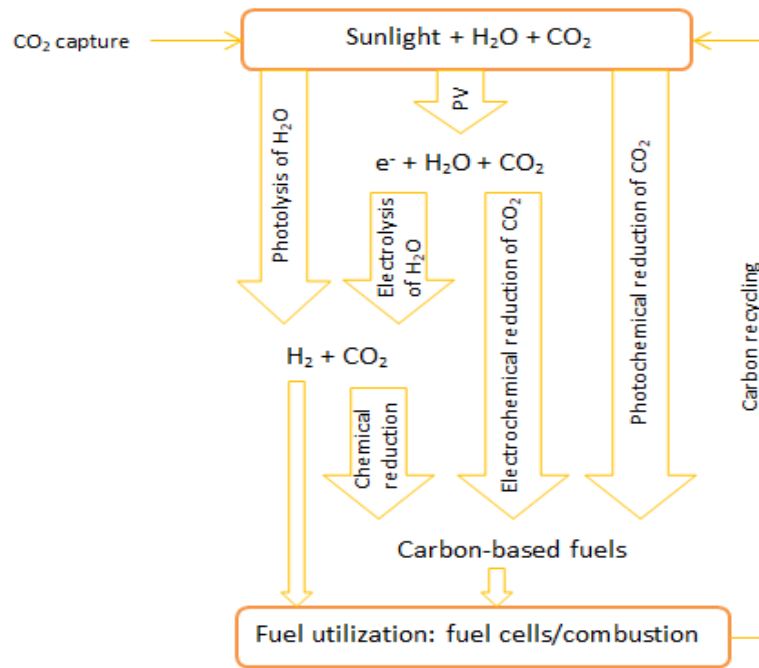


Figure 15. Options for solar-driven chemical processes

From a long-term perspective, these systems should provide a basis for remotely distributed zones, progressively enabling the substitution of fossil fuels as the main chemical and energy sources, and breaking the current monopoly of markets dominated by a few countries that trigger a huge geopolitical impact. Lithium batteries currently offer the most practical solution for storing energy and are set to remain an integral part of the power supply for a considerable time to come. But, in the coming years and with further refinement, MES is expected to offer a real alternative that will help to change our relationship with renewables. Whether in electricity generation, storage or power transformation, the expectation is that one day, every stage of the energy pathway will be **100 % green**.

Chapter 6. Conclusions



6. Conclusions

Time is running out for unprecedented changes in the way we work and live if we want to continue working and living in today's world. This means we must avoid involution and instead, embrace revolution. Initiatives are being taken to minimise carbon emissions and the impacts of climate change, but strong action is needed to enable a meaningful transformation.

This PhD thesis sought to address the challenges of moving toward scaling up MES systems **to convert recalcitrant CO₂ off-gasses into a useful product (i.e. HA)**. Among much to be done, improving production rates and selectivity of the final products, and minimising the energy input, seem to be the main restraints hindering the scaling up of the technology. Especially, if carbon-based materials and open cultures are used, which in turn makes the technology more sustainable. However, microbial electrosynthesis has demonstrated its potential to contribute to a decarbonised and more sustainable energy development. In particular, the following improvements were achieved in this PhD thesis:

- The thermophilic operation (50 °C) helped to decrease competition between metabolic pathways, giving an advantage to acetogens for HA production with high selectivity (over 95 %), and providing a promising CO₂ conversion to acetate ratio (2.2 kg CO₂ kg HA⁻¹).
- By exploiting the surplus of renewable energy, it was possible to couple bioelectrochemical H₂ production with fermentative HA generation, alternating periods with and without power supply. It reduced electricity consumption by three times and even improved HA production rates (43 g m⁻² d⁻¹) obtained until then, which reduced the ratio of energy per product by 18-fold compared to normal operation with continuous electric supply (7 vs. 130 kWh kg HA⁻¹).
- The thermodynamic model was a useful tool for the efficient use of resources according to the operational conditions. The formation of acetic acid proved to be the most spontaneous in all conditions tested, being the only compound obtained at 50 °C. Yet, it was not the fastest, as at 37 °C caproic acid yielded a higher production rate. This underlines that the reactions kinetics, as well as the biological constraints, are critical aspects that also have to be taken into account.
- Real off-gases did not seem to hamper the productivity of an open culture, which was able to operate in the long term with similar performance (2.5 % decrease in HA production rate) despite the low CO₂ (14 %) and high O₂ (12 %) content compared to synthetic gas (100 % CO₂).
- The utilisation of an optimised design for process control by means of variables including pH, dissolved gases, pressure and temperature, led to an efficient thermophilic reduction of CO₂ to HA. Low ohmic resistances (40 Ω cm⁻²) were obtained and the best product per energy ratio was achieved so far (483 g kWh⁻¹), even compared to conventional HA production *via* methanol carbonylation (286 g kWh⁻¹).

6.1. Outlook

One of the most promising projections is to integrate MES with AF in a scenario where both technologies have scope for development, such as WWTPs. However, even if the selectivity and energy targets could be met, the main limitation to achieving sufficiently high production rates will be difficult to overcome. Despite the availability of nutrients, absence of inhibitors, adequate physico-chemical parameters and mixing, the exponential growth and production rates that electrotrophs can achieve are lower than that of heterotrophs, and the values of heterotrophs cannot be compared to those of chemical catalysts. It must be said that the C source also differs. The C-H bond of organic compounds has lower energy than the C-O bond in CO₂, making CO₂ more stable and less reactive than other organic compounds.

In this sense, there is perhaps an opportunity to change the perspective from which we approach the targets. Instead of envisaging the MES as an industrial process for the massive generation of products, the potential for reducing the C footprint and storing renewable energy, albeit in chemical form, should be promoted. It is a matter of refocusing purposes and revalorising results. Using the knowledge acquired so far to scale up a technology that goes hand in hand with others to ensure a sustainable and climate-neutral future.

Providing a reliable and sufficient supply of energy for the long-term development of our planet with future generations in mind requires focused and dedicated research, together with large integrated approaches, aided by adequate funding and active industry collaboration. However, before addressing the technical, financial or regulatory boundaries, we must resolve the limits we impose on ourselves and start working together, transforming what we believe to be individual achievements into multidisciplinary solutions, with broad expertise and a useful outcome.

Chapter 7. References



7. References

- Althaus, H., Chudacoff, M., Hirschier, R., Jungbluth, N., Osses, M., Primas, A., Hellweg, S., 2007. Life cycle inventories of chemicals., in: Ecoinvent. pp. 1–957.
- Ambler, J.R., Logan, B.E., 2011. Evaluation of stainless steel cathodes and a bicarbonate buffer for hydrogen production in microbial electrolysis cells using a new method for measuring gas production. *Int. J. Hydrogen Energy* 36, 160–166.
<https://doi.org/10.1016/j.ijhydene.2010.09.044>
- Anwer, A.H., Khan, N., Khan, M.D., Shakeel, S., Khan, M.Z., 2021. Redox mediators as cathode catalyst to boost the microbial electro-synthesis of biofuel product from carbon dioxide. *Fuel* 302, 121124. <https://doi.org/10.1016/j.fuel.2021.121124>
- Arends, J.B.A., Patil, S.A., Roume, H., Rabaey, K., 2017. Continuous long-term electricity-driven bioproduction of carboxylates and isopropanol from CO₂ with a mixed microbial community. *J. CO₂ Util.* 20, 141–149. <https://doi.org/10.1016/j.jcou.2017.04.014>
- Arends, J.B.A., Verstraete, W., 2012. 100 years of microbial electricity production: Three concepts for the future. *Microb. Biotechnol.* 5, 333–346. <https://doi.org/10.1111/j.1751-7915.2011.00302.x>
- Aulenta, F., Catapano, L., Snip, L., Villano, M., Majone, M., 2012. Linking bacterial metabolism to graphite cathodes: electrochemical insights into the H₂-producing capability of *Desulfovibrio* sp. *ChemSusChem* 5, 1080–5. <https://doi.org/10.1002/cssc.201100720>
- Bajracharya, S., 2016. *Microbial Electrosynthesis of Biochemicals*. Wageningen University.
<https://doi.org/10.18174/385426>
- Bajracharya, S., Ter Heijne, A., Dominguez Benetton, X., Vanbroekhoven, K., Buisman, C.J.N., Strik, D.P.B.T.B., Pant, D., 2015. Carbon dioxide reduction by mixed and pure cultures in microbial electrosynthesis using an assembly of graphite felt and stainless steel as a cathode. *Bioresour. Technol.* 195, 14–24. <https://doi.org/10.1016/j.biortech.2015.05.081>
- Bajracharya, S., Vanbroekhoven, K., Buisman, C.J.N., Pant, D., Strik, D.P.B.T.B., 2016. Application of gas diffusion biocathode in microbial electrosynthesis from carbon dioxide. *Environ. Sci. Pollut. Res.* 23, 22292–22308. <https://doi.org/10.1007/s11356-016-7196-x>
- Bard, A.J., Parsons, R., Jordan, J., 1985. *Standard potentials in aqueous solution*, IUPAC. ed. CRC Press.
- Barker, D.J., Turner, S.A., Napier-Moore, P.A., Clark, M., Davison, J.E., 2009. CO₂ Capture in the Cement Industry. *Energy Procedia* 1, 87–94. <https://doi.org/10.1016/j.egypro.2009.01.014>
- Battle-Vilanova, P., 2016. Bioelectrochemical transformation of carbon dioxide to target compounds through microbial electrosynthesis.
- Battle-Vilanova, P., Puig, S., Gonzalez-Olmos, R., Balaguer, M.D., Colprim, J., 2016. Continuous acetate

- production through microbial electrosynthesis from CO₂ with microbial mixed culture. *J. Chem. Technol. Biotechnol.* 91, 921–927. <https://doi.org/10.1002/jctb.4657>
- Batlle-Vilanova, P., Rovira-Alsina, L., Puig, S., Balaguer, M.D., Icaran, P., Monsalvo, V.M., Rogalla, F., Colprim, J., 2019. Biogas upgrading, CO₂ valorisation and economic revaluation of bioelectrochemical systems through anodic chlorine production in the framework of wastewater treatment plants. *Sci. Total Environ.* 690, 352–360. <https://doi.org/10.1016/j.scitotenv.2019.06.361>
- Bian, B., Bajracharya, S., Xu, J., Pant, D., Saikaly, P.E., 2020. Microbial electrosynthesis from CO₂: Challenges, opportunities and perspectives in the context of circular bioeconomy. *Bioresour. Technol.* 302, 122863. <https://doi.org/10.1016/j.biortech.2020.122863>
- Blanc, P., Zafar, M., Levy, J., Gupta, P., 2020. Five Steps to Energy Storage. *Innovation Insights Brief 2020*. World Energy Council. 62.
- Blanchet, E., Duquenne, F., Rafrafi, Y., Etcheverry, L., Erable, B., Bergel, A., 2015. Importance of the hydrogen route in up-scaling electrosynthesis for microbial CO₂ reduction. *Energy Environ. Sci.* 8, 3731–3744. <https://doi.org/10.1039/c5ee03088a>
- Blasco-Gómez, R., 2020. Steering CO₂ bio-electrorecycling into valuable compounds through inline monitoring of key operational parameters.
- Blasco-Gómez, R., Batlle-Vilanova, P., Villano, M., Balaguer, M.D., Colprim, J., Puig, S., 2017. On the edge of research and technological application: A critical review of electromethanogenesis. *Int. J. Mol. Sci.* 18, 1–32. <https://doi.org/10.3390/ijms18040874>
- Bolognesi, S., 2021. Microbial electrochemical technologies for biofuels and bioenergy production.
- Borole, A.P., Lewis, A.J., 2017. Proton transfer in microbial electrolysis cells. *Sustain. Energy Fuels* 1, 725–736. <https://doi.org/10.1039/c7se00034k>
- Bourne, J.R., 2003. Mixing and the selectivity of chemical reactions. *Org. Process Res. Dev.* 7, 471–508. <https://doi.org/10.1021/op020074q>
- Breznak, J.A., Switzer, J.M., 1986. Acetate synthesis from H₂ plus CO₂ by termite gut microbes. *Appl. Environ. Microbiol.* 52, 623–630. <https://doi.org/10.1128/aem.52.4.623-630.1986>
- Bui, M., Adjiman, C.S., Bardow, A., Anthony, E.J., Boston, A., Brown, S., Fennell, P.S., Fuss, S., Galindo, A., Hackett, L.A., Hallett, J.P., Herzog, H.J., Jackson, G., Kemper, J., Krevor, S., Wilcox, J., Dowell, N. Mac, 2018. Carbon capture and storage (CCS): the way forward. *Energy Environ. Sci.* 11. <https://doi.org/10.1039/c7ee02342a>
- C2ES, 2022. Carbon Capture | Center for Climate and Energy Solutions [WWW Document]. URL <https://www.c2es.org/content/carbon-capture/>
- Cabau-Peinado, O., Straathof, A.J.J., Jourdin, L., 2021. A General Model for Biofilm-Driven Microbial

- Electrosynthesis of Carboxylates From CO₂. *Front. Microbiol.* 12, 1–17.
<https://doi.org/10.3389/fmicb.2021.669218>
- Call, D.F., Merrill, M.D., Logan, B.E., 2009. High surface area stainless steel brushes as cathodes in microbial electrolysis cells. *Environ. Sci. Technol.* 43, 2179–2183.
<https://doi.org/10.1021/es803074x>
- Carmo, M., Fritz, D.L., Mergel, J., Stolten, D., 2013. A comprehensive review on PEM water electrolysis. *Int. J. Hydrogen Energy* 38, 4901–4934.
<https://doi.org/10.1016/j.ijhydene.2013.01.151>
- Chandrasekhar, K., Naresh Kumar, A., Kumar, G., Kim, D.H., Song, Y.C., Kim, S.H., 2021. Electro-fermentation for biofuels and biochemicals production: Current status and future directions. *Bioresour. Technol.* 323, 124598. <https://doi.org/10.1016/j.biortech.2020.124598>
- Chen, W., Liu, Z., Li, Y., Xing, X., Liao, Q., Zhu, X., 2021. Improved electricity generation, coulombic efficiency and microbial community structure of microbial fuel cells using sodium citrate as an effective additive. *J. Power Sources* 482. <https://doi.org/10.1016/j.jpowsour.2020.228947>
- Cheng, S., Logan, B.E., 2011. High hydrogen production rate of microbial electrolysis cell (MEC) with reduced electrode spacing. *Bioresour. Technol.* 102, 3571–3574.
<https://doi.org/10.1016/j.biortech.2010.10.025>
- Cheng, S., Logan, B.E., 2007. Sustainable and efficient biohydrogen production via electrohydrogenesis. *Proc. Natl. Acad. Sci.* 104, 18871–18873.
<https://doi.org/10.1073/pnas.0706379104>
- Chowdhury, J.I., Balta-Ozkan, N., Goglio, P., Hu, Y., Varga, L., McCabe, L., 2020. Techno-environmental analysis of battery storage for grid level energy services. *Renew. Sustain. Energy Rev.* 131, 110018. <https://doi.org/10.1016/j.rser.2020.110018>
- Christodoulou, X., Okoroafor, T., Parry, S., Velasquez-orta, S.B., 2017. The use of carbon dioxide in microbial electrosynthesis : Advancements , sustainability and economic feasibility. *Biochem. Pharmacol.* 18, 390–399. <https://doi.org/10.1016/j.jcou.2017.01.027>
- Christodoulou, X., Velasquez-orta, S.B., 2016. Microbial Electrosynthesis and Anaerobic Fermentation: An Economic Evaluation for Acetic Acid Production from CO₂ and CO.
<https://doi.org/10.1021/acs.est.6b02101>
- Ciamician, G., 1912. The photochemistry of the future. *Science* (80-.). XXXVI, 926.
- Claassens, N.J., Cotton, C.A.R., Kopljar, D., Bar-Even, A., 2019. Making quantitative sense of electromicrobial production. *Nat. Catal.* 2, 437–447.
<https://doi.org/10.1038/s41929-019-0272-0>
- Clauwaert, P., Tolêdo, R., van der Ha, D., Crab, R., Verstraete, W., Hu, H., Udert, K.M., Rabaey, K.,

2008. Combining biocatalyzed electrolysis with anaerobic digestion. *Water Sci. Technol.* 57, 575–579. <https://doi.org/10.2166/wst.2008.084>
- CO2 Value Europe, 2022. Solutions to decrease net CO2 emissions [WWW Document]. URL <https://co2value.eu/our-projects/>
- Collet, C., Schwitzguébel, J.P., Péringer, P., 2003. Improvement of acetate production from lactose by growing *Clostridium thermolacticum* in mixed batch culture. *J. Appl. Microbiol.* 95, 824–831. <https://doi.org/10.1046/j.1365-2672.2003.02060.x>
- Cozzi, L., Gould, T., 2021. *World Energy Outlook 2021*. IEA 1–386.
- Cusick, R.D., Bryan, B., Parker, D.S., Merrill, M.D., Mehanna, M., Kiely, P.D., Liu, G., Logan, B.E., 2011. Performance of a pilot-scale continuous flow microbial electrolysis cell fed winery wastewater. *Appl. Microbiol. Biotechnol.* 89, 2053–2063. <https://doi.org/10.1007/s00253-011-3130-9>
- Das, Sovik, Das, Swati, Ghangrekar, M.M., 2021. Application of TiO₂ and Rh as cathode catalyst to boost the microbial electrosynthesis of organic compounds through CO₂ sequestration. *Process Biochem.* 101, 237–246. <https://doi.org/10.1016/j.procbio.2020.11.017>
- De Luna, P., Hahn, C., Higgins, D., Jaffer, S.A., Jaramillo, T.F., Sargent, E.H., 2019. What would it take for renewably powered electrosynthesis to displace petrochemical processes? *Science* (80-.). 364. <https://doi.org/10.1126/science.aav3506>
- Demedziuk, S., 2018. The New Dimension of War – the Ukraine Conflict. *Secur. Def. Q.* 1, 91–109. <https://doi.org/10.5604/01.3001.0010.8473>
- Desloover, J., Arends, J.B.A., Hennebel, T., Rabaey, K., 2012. Operational and technical considerations for microbial electrosynthesis. *Biochem. Soc. Trans.* 40, 1233–1238. <https://doi.org/10.1042/bst20120111>
- Dessi, P., Rovira-Alsina, L., Sánchez, C., Dinesh, G.K., Tong, W., Chatterjee, P., Tedesco, M., Farràs, P., Hamelers, H.M.V., Puig, S., 2020. Microbial electrosynthesis: Towards sustainable biorefineries for production of green chemicals from CO₂ emissions. *Biotechnol. Adv.* 107675. <https://doi.org/10.1016/j.biotechadv.2020.107675>
- Dong, Y., Qu, Y., He, W., Du, Y., Liu, J., Han, X., Feng, Y., 2015. A 90-liter stackable baffled microbial fuel cell for brewery wastewater treatment based on energy self-sufficient mode. *Bioresour. Technol.* 195, 66–72. <https://doi.org/10.1016/j.biortech.2015.06.026>
- Dopson, M., Ni, G., Sleutels, T.H.J.A., 2016. Possibilities for extremophilic microorganisms in microbial electrochemical systems. *FEMS Microbiol. Rev.* 40, 164–181. <https://doi.org/10.1093/femsre/fuv044>
- ECHEMI, 2022. Acetic acid Price and Market Analysis [WWW Document]. URL <https://www.echemi.com/productsInformation/tempid160628000977-acetic-acid.html>

- EEX, 2022. Spot market data - powernext [WWW Document]. URL <https://www.powernext.com/spot-market-data>
- ElMekawy, A., Hegab, H.M., Mohanakrishna, G., Elbaz, A.F., Bulut, M., Pant, D., 2016. Technological advances in CO₂ conversion electro-biorefinery: A step toward commercialization. *Bioresour. Technol.* <https://doi.org/10.1016/j.biortech.2016.03.023>
- Emerson, D.F., Woolston, B.M., Liu, N., Donnelly, M., Currie, D.H., Stephanopoulos, G., 2018. Enhancing hydrogen-dependent growth of and carbon dioxide fixation by *Clostridium ljungdahlii* through nitrate supplementation. *Biotechnol. Bioeng.* 116, 294–306. <https://doi.org/10.1002/bit.26847>
- Enzmann, F., Mayer, F., Stöckl, M., Mangold, K.M., Hommel, R., Holtmann, D., 2019. Transferring bioelectrochemical processes from H-cells to a scalable bubble column reactor. *Chem. Eng. Sci.* 193, 133–143. <https://doi.org/10.1016/j.ces.2018.08.056>
- EuCheMS, 2016. Solar driven chemistry 1–5. <https://doi.org/10.1331/JAPhA.2011.11513>
- Faraghiparapari, N., Zengler, K., 2016. Production of organics from CO₂ by microbial electrosynthesis (MES) at high temperature. *J. Chem. Technol. Biotechnol.* 92, 375–381. <https://doi.org/10.1002/jctb.5015>
- Feng, Y., He, W., Liu, J., Wang, X., Qu, Y., Ren, N., 2014. A horizontal plug flow and stackable pilot microbial fuel cell for municipal wastewater treatment. *Bioresour. Technol.* 156, 132–138. <https://doi.org/10.1016/j.biortech.2013.12.104>
- Flexer, V., Jourdin, L., 2020. Purposely Designed Hierarchical Porous Electrodes for High Rate Microbial Electrosynthesis of Acetate from Carbon Dioxide. *Acc. Chem. Res.* 53, 311–321.
- Foglia, D., Wukovits, W., Friedl, A., De Vrije, T., Claassen, P.A.M., 2011. Fermentative hydrogen production: Influence of application of mesophilic and thermophilic bacteria on mass and energy balances. *Chem. Eng. Trans.* 25, 815–820. <https://doi.org/10.3303/CET1125136>
- Fruehauf, H.M., Enzmann, F., Harnisch, F., Ulber, R., Holtmann, D., 2020. Microbial Electrosynthesis – An Inventory on Technology Readiness Level and Performance of Different Process Variants. *Biotechnol. J.* 2000066, 2000066. <https://doi.org/10.1002/biot.202000066>
- Fu, Q., 2013. A Study on Thermophilic Bioelectrochemical Systems for CO₂-to-Methane Conversion Technology.
- Fu, Q., Kobayashi, H., Kawaguchi, H., Vilcaez, J., Wakayama, T., Maeda, H., Sato, K., 2013a. Electrochemical and phylogenetic analyses of current-generating microorganisms in a thermophilic microbial fuel cell. *J. Biosci. Bioeng.* 115, 268–271. <https://doi.org/10.1016/j.jbiosc.2012.10.007>
- Fu, Q., Kobayashi, H., Kuramochi, Y., Xu, J., Wakayama, T., Maeda, H., Sato, K., 2013b.

- Bioelectrochemical analyses of a thermophilic biocathode catalyzing sustainable hydrogen production. *Int. J. Hydrogen Energy* 38, 15638–15645.
<https://doi.org/10.1016/j.ijhydene.2013.04.116>
- Gadkari, S., Haji Mirza Beigi, B., Aryal, N., Sadhukhan, J., 2022. Microbial electrosynthesis : is it sustainable for bioproduction of acetic acid ? *RSC Adv.* 9921–9932.
<https://doi.org/10.1039/d1ra00920f>
- Gavilanes, J., Noori, M.T., Min, B., 2019. Enhancing bio-alcohol production from volatile fatty acids by suppressing methanogenic activity in single chamber microbial electrosynthesis cells (SCMECs). *Bioresour. Technol. Reports* 7, 100292. <https://doi.org/10.1016/j.biteb.2019.100292>
- GCDL, 2022. Renewable Energy - Our World in Data [WWW Document]. URL
<https://ourworldindata.org/renewable-energy>
- Gibson, B., Wilson, D.J., Feil, E., Eyre-Walker, A., 2018. The distribution of bacterial doublingtimes in the wild. *Proc. B* 285, 20180789. <https://doi.org/http://dx.doi.org/10.1098/rspb.2018.0789>
- Gildemyn, S., Verbeeck, K., Slabbinck, R., Andersen, S.J., PrévotEAU, A., Rabaey, K., 2015. Integrated production, extraction, and concentration of acetic acid from CO₂ through microbial electrosynthesis. *Environ. Sci. Technol. Lett.* 2, 325–328.
<https://doi.org/10.1021/acs.estlett.5b00212>
- Gorby, Y.A., Yanina, S., McLean, J.S., Rosso, K.M., Moyles, D., Dohnalkova, A., Beveridge, T.J., Chang, I.S., Kim, B.H., Kim, K.S., Culley, D.E., Reed, S.B., Romine, M.F., Saffarini, D.A., Hill, E.A., Shi, L., Elias, D.A., Kennedy, D.W., Pinchuk, G., Watanabe, K., Ishii, S., Logan, B., Nealsen, K.H., Fredrickson, J.K., 2006. Electrically conductive bacterial nanowires produced by *Shewanella oneidensis* strain MR-1 and other microorganisms. *Proc. Natl. Acad. Sci. U. S. A.* 103, 11358–11363. <https://doi.org/10.1073/pnas.0604517103>
- Gregory, K.B., Bond, D.R., Lovley, D.R., 2004. Graphite electrodes as electron donors for anaerobic respiration. *Environ. Microbiol.* 6, 596–604. <https://doi.org/10.1111/j.1462-2920.2004.00593.x>
- Grim, R.G., Huang, Z., Guarnieri, M.T., Ferrell, J.R., Tao, L., Schaidle, J.A., 2020. Transforming the carbon economy: challenges and opportunities in the convergence of low-cost electricity and reductive CO₂ utilization . *Energy Environ. Sci.* 13, 472–494.
<https://doi.org/10.1039/c9ee02410g>
- Groth, T., Shinde, V., Meade, R., Kefalas, P., 2019. THE LIMITS TO RENEWABLE ENERGY.
- Ha, P.T., Lee, T.K., Rittmann, B.E., Park, J., Chang, I.S., 2012. Treatment of alcohol distillery wastewater using a bacteroidetes-dominant thermophilic microbial fuel cell. *Environ. Sci. Technol.* 46, 3022–3030. <https://doi.org/10.1021/es203861v>
- Haas, T., Krause, R., Weber, R., Demler, M., Schmid, G., 2018. Technical photosynthesis involving CO₂

electrolysis and fermentation. *Nat. Catal.* 1, 32–39. <https://doi.org/10.1038/s41929-017-0005-1>

Hackbarth, M., Jung, T., Reiner, J.E., Gescher, J., Horn, H., Hille-Reichel, A., Wagner, M., 2020. Monitoring and quantification of bioelectrochemical *Kyrpidia spormannii* biofilm development in a novel flow cell setup. *Chem. Eng. J.* 390. <https://doi.org/10.1016/j.cej.2020.124604>

Hasyim, R., Imai, T., Reungsang, A., O-Thong, S., 2011. Extreme-thermophilic biohydrogen production by an anaerobic heat treated digested sewage sludge culture. *Int. J. Hydrogen Energy* 36, 8727–8734. <https://doi.org/10.1016/j.ijhydene.2010.06.079>

Hausfather, Z., Moore, F.C., 2022. Commitments could limit warming to below 2 °C. *Nature* 604.

Hernández-Fernández, F.J., Pérez De Los Ríos, A., Salar-García, M.J., Ortiz-Martínez, V.M., Lozano-Blanco, L.J., Godínez, C., Tomás-Alonso, F., Quesada-Medina, J., 2015. Recent progress and perspectives in microbial fuel cells for bioenergy generation and wastewater treatment. *Fuel Process. Technol.* 138, 284–297. <https://doi.org/10.1016/j.fuproc.2015.05.022>

Hodges, A., Hoang, A.L., Tsekouras, G., Wagner, K., Lee, C.Y., Swiegers, G.F., Wallace, G.G., 2022. A high-performance capillary-fed electrolysis cell promises more cost-competitive renewable hydrogen. *Nat. Commun.* 13, 1–11. <https://doi.org/10.1038/s41467-022-28953-x>

Huang, H., Wang, H., Huang, Q., Song, T. shun, Xie, J., 2021. Mo₂C/N-doped 3D loofah sponge cathode promotes microbial electrosynthesis from carbon dioxide. *Int. J. Hydrogen Energy* 46, 20325–20337. <https://doi.org/10.1016/j.ijhydene.2021.03.165>

Hussain, A., Mehta, P., Raghavan, V., Wang, H., Guiot, S.R., Tartakovsky, B., 2012. The performance of a thermophilic microbial fuel cell fed with synthesis gas. *Enzyme Microb. Technol.* 51, 163–170. <https://doi.org/10.1016/j.enzmictec.2012.05.008>

IEA, 2022. Electricity Market Report. Int. Energy Agency.

Inganäs, O., Sundström, V., 2016. Solar energy for electricity and fuels. *Ambio* 45, 15–23. <https://doi.org/10.1007/s13280-015-0729-6>

IOGP, 2019. The potential for CCS and CCU in Europe. Rep. to thirty Second Meet. Eur. Gas Regul. Forum 5-6 June 2019. 1–47.

IPCC, 2021. Climate Change 2021. Phys. Sci. Basis. Contrib. Work. Gr. 1 to Sixth Assess. Rep. Intergov. Panel Clim. Chang. In Press.

Jia, J., Seitz, L.C., Benck, J.D., Huo, Y., Chen, Y., Ng, J.W.D., Bilir, T., Harris, J.S., Jaramillo, T.F., 2016. Solar water splitting by photovoltaic-electrolysis with a solar-to-hydrogen efficiency over 30%. *Nat. Commun.* 7, 13237. <https://doi.org/10.1038/ncomms13237>

Jiang, Y., May, H.D., Lu, L., Liang, P., Huang, X., Ren, Z.J., 2019. Carbon dioxide and organic waste valorization by microbial electrosynthesis and electro-fermentation. *Water Res.* 149, 42–55. <https://doi.org/10.1016/j.watres.2018.10.092>

- Jiang, Y., Su, M., Zhang, Y., Zhan, G., Tao, Y., Li, D., 2013. Bioelectrochemical systems for simultaneously production of methane and acetate from carbon dioxide at relatively high rate. *Int. J. Hydrogen Energy* 38, 3497–3502. <https://doi.org/10.1016/j.ijhydene.2012.12.107>
- Jourdin, L., 2015. Microbial electrosynthesis from carbon dioxide: performance enhancement and elucidation of mechanisms.
- Jourdin, L., Freguia, S., Donose, B.C., Chen, J., Wallace, G.G., Flexer, V., 2014. A novel carbon nanotube modified scaffold as an efficient biocathode material for improved microbial electrosynthesis 13093–13102. <https://doi.org/10.1039/c4ta03101f>
- Jourdin, L., Freguia, S., Donose, B.C., Keller, J., 2015a. Autotrophic hydrogen-producing biofilm growth sustained by a cathode as the sole electron and energy source. *Bioelectrochemistry* 102, 56–63. <https://doi.org/10.1016/j.bioelechem.2014.12.001>
- Jourdin, L., Grieger, T., Monetti, J., Flexer, V., Freguia, S., Lu, Y., Chen, J., Romano, M., Wallace, G.G., Keller, J., 2015b. High Acetic Acid Production Rate Obtained by Microbial Electrosynthesis from Carbon Dioxide. *Environ. Sci. Technol.* 49, 13566–13574. <https://doi.org/10.1021/acs.est.5b03821>
- Jourdin, L., Raes, S.M.T., Buisman, C.J.N., Strik, D.P.B.T.B., 2018. Critical Biofilm Growth throughout Unmodified Carbon Felts Allows Continuous Bioelectrochemical Chain Elongation from CO₂ up to Caproate at High Current Density. *Front. Energy Res.* 6, 1–15. <https://doi.org/10.3389/fenrg.2018.00007>
- Jourdin, L., Sousa, J., Stralen, N. van, Strik, D.P.B.T.B., 2020. Techno-economic assessment of microbial electrosynthesis from CO₂ and/or organics: An interdisciplinary roadmap towards future research and application. *Appl. Energy* 279. <https://doi.org/10.1016/j.apenergy.2020.115775>
- Kadier, A., Simayi, Y., Abdeshahian, P., Azman, N.F., Chandrasekhar, K., Kalil, M.S., 2016. A comprehensive review of microbial electrolysis cells (MEC) reactor designs and configurations for sustainable hydrogen gas production. *Alexandria Eng. J.* 55, 427–443. <https://doi.org/10.1016/j.aej.2015.10.008>
- Kantzow, C., Mayer, A., Weuster-Botz, D., 2015. Continuous gas fermentation by *Acetobacterium woodii* in a submerged membrane reactor with full cell retention. *J. Biotechnol.* 212, 11–18. <https://doi.org/10.1016/j.jbiotec.2015.07.020>
- Karadag, D., Puhakka, J.A., 2010. Effect of changing temperature on anaerobic hydrogen production and microbial community composition in an open-mixed culture bioreactor. *Int. J. Hydrogen Energy* 35, 10954–10959. <https://doi.org/10.1016/j.ijhydene.2010.07.070>
- Katsyv, A., Müller, V., 2020. Overcoming Energetic Barriers in Acetogenic C₁ Conversion. *Front. Bioeng. Biotechnol.* 8. <https://doi.org/10.3389/fbioe.2020.621166>

- Korth, B., Harnisch, F., 2019. Modeling microbial electrosynthesis. *Adv. Biochem. Eng. Biotechnol.* 167, 273–325. https://doi.org/10.1007/10_2017_35
- Korth, B., Maskow, T., Picioreanu, C., Harnisch, F., 2016. The microbial electrochemical Peltier heat: An energetic burden and engineering chance for primary microbial electrochemical technologies. *Energy Environ. Sci.* 9, 2539–2544. <https://doi.org/10.1039/c6ee01428c>
- Kracke, F., Wong, A.B., Maegaard, K., Deutzmann, J.S., Hubert, M.A., Hahn, C., Jaramillo, T.F., Spormann, A.M., 2019. Robust and biocompatible catalysts for efficient hydrogen-driven microbial electrosynthesis. *Commun. Chem.* 2, 1–9. <https://doi.org/10.1038/s42004-019-0145-0>
- Krige, A., Rova, U., Christakopoulos, P., 2021. 3D bioprinting on cathodes in microbial electrosynthesis for increased acetate production rate using *Sporomusa ovata*. *J. Environ. Chem. Eng.* 9, 106189. <https://doi.org/10.1016/j.jece.2021.106189>
- LaBelle, E. V., May, H.D., 2017. Energy efficiency and productivity enhancement of microbial electrosynthesis of acetate. *Front. Microbiol.* 8, 1–9. <https://doi.org/10.3389/fmicb.2017.00756>
- Larsen, H., Petersen, S., 2016. Future options for energy technologies.
- Liang, P., Duan, R., Jiang, Y., Zhang, X., Qiu, Y., Huang, X., 2018. One-year operation of 1000-L modularized microbial fuel cell for municipal wastewater treatment. *Water Res.* 141, 1–8. <https://doi.org/10.1016/J.WATRES.2018.04.066>
- Liu, Y., 2007. Overview of some theoretical approaches for derivation of the Monod equation. *Appl. Microbiol. Biotechnol.* 73, 1241–1250. <https://doi.org/10.1007/s00253-006-0717-7>
- Llirós, M., Casamayor, E.O., Borrego, C., 2008. High archaeal richness in the water column of a freshwater sulfurous karstic lake along an interannual study. *FEMS Microbiol. Ecol.* 66, 331–342. <https://doi.org/10.1111/j.1574-6941.2008.00583.x>
- Logan, B.E., Hamelers, B., Rozendal, R., Schröder, U., Keller, J., Freguia, S., Aeltermann, P., Verstraete, W., Rabaey, K., 2006. Microbial fuel cells: Methodology and technology. *Environ. Sci. Technol.* 40, 5181–5192. <https://doi.org/10.1021/es0605016>
- López-Gutiérrez, J.C., Henry, S., Hallet, S., Martin-Laurent, F., Catroux, G., Philippot, L., 2004. Quantification of a novel group of nitrate-reducing bacteria in the environment by real-time PCR. *J. Microbiol. Methods* 57, 399–407. <https://doi.org/10.1016/j.mimet.2004.02.009>
- Lovley, D.R., 2011. Live wires: Direct extracellular electron exchange for bioenergy and the bioremediation of energy-related contamination. *Energy Environ. Sci.* 4, 4896–4906. <https://doi.org/10.1039/c1ee02229f>
- Lu, L., Guest, J.S., Peters, C.A., Zhu, X., Rau, G.H., Ren, Z.J., 2018. Wastewater treatment for carbon capture and utilization. *Nat. Sustain.* 1, 750–758. <https://doi.org/10.1038/s41893-018-0187-9>
- Lu, L., Ren, Z.J., 2016. Microbial electrolysis cells for waste biorefinery : A state of the art review.

- Bioresour. Technol. 215, 254–264. <https://doi.org/10.1016/j.biortech.2016.03.034>
- Maggi, F., Fiona, F.H., Riley, W.J., 2018. The Thermodynamic Links between Substrate, Enzyme, and Microbial Dynamics in Michaelis–Menten–Monod Kinetics. *Int. J. Chem. Kinet.* 50, 343–356. <https://doi.org/10.1002/kin.21163>
- Marshall, C.W., May, H.D., 2009. Electrochemical evidence of direct electrode reduction by a thermophilic Gram-positive bacterium, *Thermincola ferriacetica*. *Energy Environ. Sci.* 2, 699. <https://doi.org/10.1039/b823237g>
- Marshall, C.W., Ross, D.E., Fichot, E.B., Norman, R.S., May, H.D., 2012. Electrosynthesis of commodity chemicals by an autotrophic microbial community. *Appl. Environ. Microbiol.* 78, 8412–8420. <https://doi.org/10.1128/AEM.02401-12>
- Marsili, E., Baron, D.B., Shikhare, I.D., Coursolle, D., Gralnick, J.A., Bond, D.R., 2008. *Shewanella* secretes flavins that mediate extracellular electron transfer. *Proc. Natl. Acad. Sci. U. S. A.* 105, 3968–3973. <https://doi.org/10.1073/pnas.0710525105>
- Martin, W.F., 2012. Hydrogen, metals, bifurcating electrons, and proton gradients: The early evolution of biological energy conservation. *FEBS Lett.* 586, 485–493. <https://doi.org/10.1016/j.febslet.2011.09.031>
- Mateos, R., 2018. Contributions towards practical application of microbial electrosynthesis.
- May, H.D., Evans, P.J., LaBelle, E. V., 2016. The bioelectrosynthesis of acetate. *Curr. Opin. Biotechnol.* 42, 225–233. <https://doi.org/10.1016/j.copbio.2016.09.004>
- Mikulčić, H., Vujanović, M., Fidaros, D.K., Priesching, P., Minić, I., Tatschl, R., Duić, N., Stefanović, G., 2012. The application of CFD modelling to support the reduction of CO₂ emissions in cement industry. *Energy* 45, 464–473. <https://doi.org/10.1016/j.energy.2012.04.030>
- Min, S., Jiang, Y., Li, D., 2013. Production of acetate from carbon dioxide in bioelectrochemical systems based on autotrophic mixed culture. *J. Microbiol. Biotechnol.* 23, 1140–1146. <https://doi.org/10.4014/jmb.1304.04039>
- Monod, J., 1949. The growth of bacterial cultures. *Annu. Rev. M* 3, 371–394.
- Muñoz-Aguilar, R., Molognoni, D., Bosch-Jimenez, P., Borràs, E., Della Pirriera, M., Luna, Á., 2018. Design, Operation, Modeling and Grid Integration of Power-to-Gas Bioelectrochemical Systems. *Energies* 11, 1947. <https://doi.org/10.3390/en11081947>
- Nevin, K.P., Hensley, S.A., Franks, A.E., Summers, Z.M., Ou, J., Woodard, T.L., Snoeyenbos-West, O.L., Lovley, D.R., 2011. Electrosynthesis of organic compounds from carbon dioxide is catalyzed by a diversity of acetogenic microorganisms. *Appl. Environ. Microbiol.* 77, 2882–2886. <https://doi.org/10.1128/AEM.02642-10>
- Nevin, K.P., Woodard, T.L., Franks, A.E., 2010. *Microbial Electrosynthesis : Feeding Microbes*

- Electricity To Convert Carbon Dioxide and Water to Multicarbon Extracellular Organic. *Am. Soc. Microbiol.* 1, 1–4. <https://doi.org/10.1128/mBio.00103-10>. Editor
- NOAA, 2022. Global Monitoring Laboratory - Carbon Cycle Greenhouse Gases [WWW Document]. URL <https://gml.noaa.gov/ccgg/trends/monthly.html>
- Nolan, D.P., 2017. Classified Area Pump Installations. *Fire Pump Arrange. Ind. Facil.* 161–167. <https://doi.org/10.1016/b978-0-12-813043-8.00012-9>
- Osset-Álvarez, M., Rovira-Alsina, L., Pous, N., Blasco-Gómez, R., Colprim, J., Balaguer, M.D., Puig, S., 2019. Niches for bioelectrochemical systems on the recovery of water, carbon and nitrogen in wastewater treatment plants. *Biomass and Bioenergy* 130. <https://doi.org/10.1016/j.biombioe.2019.105380>
- Otto, A., Grube, T., Schiebahn, S., Stolten, D., 2015. Closing the loop: Captured CO₂ as a feedstock in the chemical industry. *Energy Environ. Sci.* 8, 3283–3297. <https://doi.org/10.1039/c5ee02591e>
- Pahunang, R.R., Buonerba, A., Senatore, V., Oliva, G., Ouda, M., Zarra, T., Muñoz, R., Puig, S., Ballesteros, F.C., Li, C.W., Hasan, S.W., Belgiorno, V., Naddeo, V., 2021. Advances in technological control of greenhouse gas emissions from wastewater in the context of circular economy. *Sci. Total Environ.* 792, 148479. <https://doi.org/10.1016/j.scitotenv.2021.148479>
- Paquete, C.M., Rosenbaum, M.A., Bañeras, L., Rotaru, A.-E., Puig, S., 2022. Let's chat: Communication between electroactive microorganisms. *Bioresour. Technol.* 347, 126705. <https://doi.org/10.1016/j.biortech.2022.126705>
- Patil, S.A., Arends, J.B.A., Vanwonterghem, I., Van Meerbergen, J., Guo, K., Tyson, G.W., Rabaey, K., 2015. Selective Enrichment Establishes a Stable Performing Community for Microbial Electrosynthesis of Acetate from CO₂. *Environ. Sci. Technol.* 49, 8833–8843. <https://doi.org/10.1021/es506149d>
- Patil, S.A., Hägerhäll, C., Gorton, L., 2012. Electron transfer mechanisms between microorganisms and electrodes in bioelectrochemical systems. *Bioanal. Rev.* 1, 71–129. https://doi.org/10.1007/11663_2013_2
- Pepè Sciarria, T., Batlle-Vilanova, P., Colombo, B., Scaglia, B., Balaguer, M.D., Colprim, J., Puig, S., Adani, F., 2018. Bio-electrorecycling of carbon dioxide into bioplastics. *Green Chem.* 20, 4058–4066. <https://doi.org/10.1039/c8gc01771a>
- Pereira, J., de Nooy, S., Sleutels, T., ter Heijne, A., 2022. Opportunities for visual techniques to determine characteristics and limitations of electro-active biofilms. *Biotechnol. Adv.* 107549. <https://doi.org/10.1016/j.biotechadv.2022.108011>
- Perona-Vico, E., 2021. Importance of hydrogen-mediated mechanisms for microbial electrosynthesis : regulation at the molecular level.

- Pismenskaya, N., Tsygurina, K., Nikonenko, V., 2022. Recovery of Nutrients from Residual Streams Using Ion-Exchange Membranes: Current State, Bottlenecks, Fundamentals and Innovations. *Membranes (Basel)*. 12. <https://doi.org/10.3390/membranes12050497>
- Poston, J.M., Kuratomi, K., Stadtman, E.R., 1966. The Conversion of Carbon Dioxide to Acetate. *J. Biol. Chem.* 241, 4209–4216. [https://doi.org/10.1016/s0021-9258\(18\)99771-1](https://doi.org/10.1016/s0021-9258(18)99771-1)
- Potter, M.C., 1911. Electrical Effects Accompanying the Decomposition of Organic Compounds. *R. Soc.* 84, 260–276.
- PrévotEAU, A., Carvajal-Arroyo, J.M., Ganigué, R., Rabaey, K., 2020. Microbial electrosynthesis from CO₂: forever a promise? *Curr. Opin. Biotechnol.* 62, 48–57. <https://doi.org/10.1016/j.copbio.2019.08.014>
- Puig, S., Ganigué, R., Batlle-Vilanova, P., Balaguer, M.D., Bañeras, L., Colprim, J., 2017. Tracking biohydrogen-mediated production of commodity chemicals from carbon dioxide and renewable electricity. *Bioresour. Technol.* 228, 201–209. <https://doi.org/10.1016/j.biortech.2016.12.035>
- Rabaey, K., Boon, N., Höfte, M., Verstraete, W., 2005. Microbial phenazine production enhances electron transfer in biofuel cells. *Environ. Sci. Technol.* 39, 3401–3408. <https://doi.org/10.1021/es048563o>
- Rabaey, K., Rozendal, R.A., 2010. Microbial electrosynthesis - Revisiting the electrical route for microbial production. *Nat. Rev. Microbiol.* 8, 706–716. <https://doi.org/10.1038/nrmicro2422>
- Ritchie, H., Roser, M., 2020. Energy production and consumption. *Our World Data*.
- Romans-Casas, M., Blasco-Gómez, R., Colprim, J., Balaguer, M.D., Puig, S., 2021. Bio-electro CO₂ recycling platform based on two separated steps. *J. Environ. Chem. Eng.* 9, 105909. <https://doi.org/10.1016/j.jece.2021.105909>
- Rosenbaum, M., Aulenta, F., Villano, M., Angenent, L.T., 2011. Cathodes as electron donors for microbial metabolism: which extracellular electron transfer mechanisms are involved? *Bioresour. Technol.* 102, 324–333. <https://doi.org/10.1016/j.biortech.2010.07.008>
- Rossi, R., Jones, D., Myung, J., Zikmund, E., Yang, W., Alvarez, Y., Pant, D., Evans, P.J., Page, M.A., Cropek, D.M., Logan, B.E., 2019. Evaluating a multi-panel air cathode through electrochemical and biotic tests. *Water Res.* 148, 51–59. <https://doi.org/10.1016/j.watres.2018.10.022>
- Rotaru, A., Yee, M.O., Musat, F., 2021. Microbes trading electricity in consortia of environmental and biotechnological significance. *Curr. Opin. Biotechnol.* 67, 119–129. <https://doi.org/10.1016/j.copbio.2021.01.014>
- Rozendal, R.A., Jeremiasse, A.W., Hamelers, H.V.M., Buisman, C.J.N., 2008. Hydrogen Production with a Microbial Biocathode. *Environmental Microbiol.* 42, 629–634.
- Sadhukhan, J., Lloyd, J.R., Scott, K., Premier, G.C., Yu, E.H., Curtis, T., Head, I.M., 2016. A critical review

- of integration analysis of microbial electrosynthesis (MES) systems with waste biorefineries for the production of biofuel and chemical from reuse of CO₂. *Renew. Sustain. Energy Rev.* 56, 116–132. <https://doi.org/10.1016/j.rser.2015.11.015>
- Samdariya, N., Sharma, Ar., Shukla, R., 2021. Impact of Cement Plant on Rural Economy : A Review. *Shodh Drishti* 12.
- Santoro, C., Babanova, S., Cristiani, P., Artyushkova, K., Atanassov, P., Bergel, A., Bretschger, O., Brown, R.K., Carpenter, K., Colombo, A., Cortese, R., Erable, B., Harnisch, F., Kodali, M., Phadke, S., Riedl, S., Rosa, L.F.M., Schröder, U., 2021. How Comparable are Microbial Electrochemical Systems around the Globe? An Electrochemical and Microbiological Cross-Laboratory Study. *ChemSusChem* 14, 2313–2330. <https://doi.org/10.1002/cssc.202100294>
- Schievano, A., Puig, S., Pant, D., 2019. Recent advances in microbial synthesis from CO₂ and other gaseous streams. *Front. Energy Res.*
- Schmidt, O., Gambhir, A., Staffell, I., Hawkes, A., Nelson, J., Few, S., 2017. Future cost and performance of water electrolysis: An expert elicitation study. *Int. J. Hydrogen Energy* 42, 30470–30492. <https://doi.org/10.1016/j.ijhydene.2017.10.045>
- Schröder, U., Harnisch, F., Angenent, L.T., 2015. Microbial electrochemistry and technology: terminology and classification. *Energy Environ. Sci.* 8, 513–519. <https://doi.org/10.1039/C4EE03359K>
- Shiva Kumar, S., Himabindu, V., 2019. Hydrogen production by PEM water electrolysis – A review. *Mater. Sci. Energy Technol.* 2, 442–454. <https://doi.org/10.1016/j.mset.2019.03.002>
- Shockley, W., Queisser, H.J., 1961. Detailed balance limit of efficiency of p-n junction solar cells. *J. Appl. Phys.* 32, 510–519. <https://doi.org/10.1063/1.1736034>
- Shrestha, N., Chilkoor, G., Vemuri, B., Rathinam, N., Sani, R.K., Gadhamshetty, V., 2018. Extremophiles for microbial-electrochemistry applications: A critical review. *Bioresour. Technol.* 255, 318–330. <https://doi.org/10.1016/j.biortech.2018.01.151>
- Sleutels, T.H.J.A., Darus, L., Hamelers, H.V.M., Buisman, C.J.N., 2011. Effect of operational parameters on Coulombic efficiency in bioelectrochemical systems. *Bioresour. Technol.* 102, 11172–11176. <https://doi.org/10.1016/j.biortech.2011.09.078>
- Steinbusch, K.J.J., Hamelers, H.V.M., Plugge, C.M., Buisman, C.J.N., 2011. Biological formation of caproate and caprylate from acetate: Fuel and chemical production from low grade biomass. *Energy Environ. Sci.* 4, 216–224. <https://doi.org/10.1039/c0ee00282h>
- Stoll, K.I., Herbig, S., Zwick, M., Boukis, N., Sauer, J., Neumann, A., Oswald, F., 2018. Fermentation of H₂ and CO₂ with *Clostridium ljungdahlii* at elevated process pressure - first experimental results. *Chem. Eng. Trans.* 64, 151–156. <https://doi.org/10.3303/CET1864026>

- Talabardon, M., Schwitzguébel, J.P., Péringer, P., 2000a. Anaerobic thermophilic fermentation for acetic acid production from milk permeate. *J. Biotechnol.* 76, 83–92.
[https://doi.org/10.1016/S0168-1656\(99\)00180-7](https://doi.org/10.1016/S0168-1656(99)00180-7)
- Talabardon, M., Schwitzguébel, J.P., Péringer, P., Yang, S.T., 2000b. Acetic acid production from lactose by an anaerobic thermophilic coculture immobilized in a fibrous-bed bioreactor. *Biotechnol. Prog.* 16, 1008–1017. <https://doi.org/10.1021/bp0001157>
- Thatikayala, D., Min, B., 2021. Copper ferrite supported reduced graphene oxide as cathode materials to enhance microbial electrosynthesis of volatile fatty acids from CO₂. *Sci. Total Environ.* 768, 144477. <https://doi.org/10.1016/j.scitotenv.2020.144477>
- Tian, S., He, J., Huang, H., Song, T.S., Wu, X., Xie, J., Zhou, W., 2020. Perovskite-Based Multifunctional Cathode with Simultaneous Supplementation of Substrates and Electrons for Enhanced Microbial Electrosynthesis of Organics. *ACS Appl. Mater. Interfaces* 12, 30449–30456.
<https://doi.org/10.1021/acscami.0c07910>
- United Nations, 2022. THE 17 GOALS | Sustainable Development [WWW Document]. URL <https://sdgs.un.org/goals>
- United Nations, 2015. Paris agreement.
- United Nations, 1998. Kyoto protocol to the united nations framework Convention on climate change. *United Nations Fram. Conv. Clim. Chang.* 1–21. <https://doi.org/10.51663/pnz.58.2.07>
- United Nations, 1992. United Nations Framework Convention on Climate Change United Nations. *United Nations Fram. Conv. Clim. Chang.* 1–33.
- Van Eerten-Jansen, M.C.A.A., Ter Heijne, A., Grootcholten, T.I.M., Steinbusch, K.J.J., Sleutels, T.H.J.A., Hamelers, H.V.M., Buisman, C.J.N., 2013. Bioelectrochemical Production of Caproate and Caprylate from Acetate by Mixed Cultures. *ACS Sustain. Chem. Eng.* 1, 1069–1069.
<https://doi.org/10.1021/sc400143v>
- van Geem, K.M., Galvita, V. V., Marin, G.B., 2019. Making chemicals with electricity. *Science (80-)*. 364, 734–735. <https://doi.org/10.1126/SCIENCE.AAX5179>
- Vassilev, I., 2019. Microbial electrosynthesis: Anode-and cathode-driven bioproduction of chemicals and biofuels. <https://doi.org/10.14264/uql.2019.39>
- Vassilev, I., Dessì, P., Puig, S., Kokko, M., 2022. Cathodic biofilms - A prerequisite for microbial electrosynthesis. *Bioresour. Technol.* 126788. <https://doi.org/10.1016/j.biortech.2022.126788>
- Vassilev, I., Hernandez, P.A., Batlle-Vilanova, P., Freguia, S., Krömer, J.O., Keller, J., Ledezma, P., Virdis, B., 2018. Microbial Electrosynthesis of Isobutyric , Butyric , Caproic acids and corresponding Alcohols from Carbon dioxide. *ACS Sustain. Chem. Eng.* 6, 8485–8493.
<https://doi.org/10.1021/acssuschemeng.8b00739>

- Vassilev, I., Kracke, F., Freguia, S., Keller, J., Krömer, J.O., Ledezma, P., Viridis, B., 2019. Microbial electrosynthesis system with dual biocathode arrangement for simultaneous acetogenesis, solventogenesis and carbon chain elongation. *Chem. Commun.* 55, 4351–4354.
<https://doi.org/10.1039/c9cc00208a>
- Velasco, A., Ryu, Y.K., Boscá, A., Ladrón-De-Guevara, A., Hunt, E., Zuo, J., Pedrós, J., Calle, F., Martínez, J., 2021. Recent trends in graphene supercapacitors: From large area to microsupercapacitors. *Sustain. Energy Fuels* 5, 1235–1254. <https://doi.org/10.1039/d0se01849j>
- Velvizhi, G., Sarkar, O., Rovira-Alsina, L., Puig, S., Mohan, S.V., 2022. Conversion of carbon dioxide to value added products through anaerobic fermentation and electro fermentation: A comparative approach. *Int. J. Hydrogen Energy.* <https://doi.org/10.1016/j.ijhydene.2021.12.205>
- Vilajeliu-Pons, A., Puig, S., Salcedo-Dávila, I., Balaguer, M.D., Colprim, J., 2017. Long-term assessment of six-stacked scaled-up MFCs treating swine manure with different electrode materials. *Environ. Sci. Water Res. Technol.* 3, 947–959. <https://doi.org/10.1039/c7ew00079k>
- Viridis, B., Hoelzle, R., Marchetti, A., Boto, S.T., Rosenbaum, M.A., Blasco-Gómez, R., Puig, S., Freguia, S., Villano, M., 2022. Electro-fermentation: Sustainable bioproductions steered by electricity. *Biotechnol. Adv.* 59, 107950. <https://doi.org/10.1016/j.biotechadv.2022.107950>
- Von Stockar, U., Maskow, T., Liu, J., Marison, I.W., Patiño, R., 2006. Thermodynamics of microbial growth and metabolism: An analysis of the current situation. *J. Biotechnol.* 121, 517–533.
<https://doi.org/10.1016/j.jbiotec.2005.08.012>
- Wood, J.C., Grové, J., Marcellin, E., Heffernan, J.K., Hu, S., Yuan, Z., Viridis, B., 2021. Strategies to improve viability of a circular carbon bioeconomy-A techno-economic review of microbial electrosynthesis and gas fermentation. *Water Res.* 201, 117306.
<https://doi.org/10.1016/j.watres.2021.117306>
- Wrighton, K.C., Agbo, P., Warnecke, F., Weber, K.A., Brodie, E.L., DeSantis, T.Z., Hugenholtz, P., Andersen, G.L., Coates, J.D., 2008. A novel ecological role of the Firmicutes identified in thermophilic microbial fuel cells. *ISME J.* 2, 1146–1156. <https://doi.org/10.1038/ismej.2008.48>
- Yang, H.Y., Hou, N.N., Wang, Y.X., Liu, J., He, C.S., Wang, Y.R., Li, W.H., Mu, Y., 2021. Mixed-culture biocathodes for acetate production from CO₂ reduction in the microbial electrosynthesis: Impact of temperature. *Sci. Total Environ.* 790, 148128.
<https://doi.org/10.1016/j.scitotenv.2021.148128>
- Ying, Z., Chen, H., He, Z., Hu, Y., Huang, Z., Gao, J., Wang, X., Ye, J., Zhao, J., Zhang, S., Chen, J., 2022. Redox mediator-regulated microbial electrolysis cell to boost coulombic efficiency and degradation activity during gaseous chlorobenzene abatement. *J. Power Sources* 528.
<https://doi.org/10.1016/j.jpowsour.2022.231214>

- Yu, L., Yuan, Y., Tang, J., Zhou, S., 2017. Thermophilic *Moorella thermoautotrophica*-immobilized cathode enhanced microbial electrosynthesis of acetate and formate from CO₂. *Bioelectrochemistry* 117, 23–28. <https://doi.org/10.1016/j.bioelechem.2017.05.001>
- Zamora, P., Georgieva, T., Ter Heijne, A., Sleutels, T.H.J.A., Jeremiassen, A.W., Saakes, M., Buisman, C.J.N., Kuntke, P., 2017. Ammonia recovery from urine in a scaled-up Microbial Electrolysis Cell. *J. Power Sources* 356, 491–499. <https://doi.org/10.1016/j.jpowsour.2017.02.089>
- Zeppilli, M., Paiano, P., Torres, C., Pant, D., 2021. A critical evaluation of the pH split and associated effects in bioelectrochemical processes. *Chem. Eng. J.* 422, 130155. <https://doi.org/10.1016/j.cej.2021.130155>
- Zhang, T., Nie, H., Bain, T.S., Lu, H., Cui, M., Snoeyenbos-West, O.L., Franks, A.E., Nevin, K.P., Russell, T.P., Lovley, D.R., 2013. Improved cathode materials for microbial electrosynthesis. *Energy Environ. Sci.* 6, 217–224. <https://doi.org/10.1039/c2ee23350a>